



EXPERIMENTAL AND PREDICTED SOLUBILITIES OF 3,4-DIMETHOXYBENZOIC ACID IN SELECT ORGANIC SOLVENTS OF VARYING POLARITY AND HYDROGEN-BONDING CHARACTER

Kaci R. Bowen^[a], Timothy W. Stephens^[a], Helen Lu^[a], Kalpana Satish^[a], Danyang Shan^[a], William E. Acree, Jr.^{[a]*} and Michael H. Abraham^[b]

Keywords: 3,4-dimethoxybenzoic acid solubility, alcohol solvents, alkyl acetate solvents, alkoxyalcohol solvents, solute descriptors.

Experimental solubilities are reported for 3,4-dimethoxybenzoic acid dissolved in 16 alcohol, 5 alkyl alkanoate, 5 alkoxyalcohol and 6 ether solvents. The measured solubility data were correlated with the Abraham solvation parameter model. Mathematical expressions based on the Abraham model predicted the observed molar solubilities to within 0.083 log units.

* Corresponding Author

Fax: 940-565-4318.

E-Mail: acree@unt.edu.

[a] Department of Chemistry, 1155 Union Circle Drive #305070, University of North Texas, Denton, TX 76203-5017 (USA).

[b] Department of Chemistry, University College London, 20 Gordon Street, London, WC1H 0AJ (UK).

Introduction

Solubility is one of the more important physicochemical properties of crystalline organic compounds as it plays such an important role in many manufacturing processes, including solvent selection for organic syntheses, for chemical separations by two-phase extractions involving either an aqueous-organic or a biphasic organic solvent system, and for purifications by recrystallizations. For organic syntheses one must select a suitable reaction solvent that can not only dissolve the starting reagent materials, but also can be removed easily after the chemical reaction is complete. Product isolation and purification can be accomplished by evaporation in the case of a volatile solvent media, or by filtration if the reaction product is crystalline. Recrystallization and extraction can be performed to remove undesired reaction by-products and excess reactants. Considerable attention has been afforded in recent years to measuring the solubility of crystalline organic compounds in organic solvents, and to developing mathematical expressions to predict the solubility behavior of various classes of organic compounds.

This study continues our systematic examination of the solubility behavior of substituted benzoic acids in organic solvents of varying polarity and hydrogen-bonding character. Substituted benzoic acids are of particular interest to us because several of the derivatives exhibit therapeutic properties. For example, acetylsalicylic acid (aspirin) is an “over-the-counter” non-steroidal anti-inflammatory drug (NSAID) taken orally to reduce fever and to relieve minor muscle pains and aches. 2-Hydroxybenzoic acid, the main

metabolite of acetylsalicylic acid, is an ingredient in skin care products for the treatment of acne, psoriasis and warts. Previous studies of reported solubility data for benzoic acid¹, 2-acetylsalicylic acid², 4-aminobenzoic acid³, 2-chloro-5-nitrobenzoic acid⁴, 3-chlorobenzoic acid⁵, 4-chlorobenzoic acid⁶, 4-chloro-3-nitrobenzoic acid⁴, 3,4-dichlorobenzoic acid⁷, 3,5-dinitrobenzoic acid⁸, 3,5-dinitro-2-methylbenzoic acid⁹, 2-hydroxybenzoic acid¹⁰, 2-methoxybenzoic acid¹¹, 4-methoxybenzoic acid¹¹, 2-methylbenzoic acid¹², 3-methylbenzoic acid⁶, 3-nitrobenzoic acid¹³, and 4-nitrobenzoic acid¹⁴ in various organic solvents. In the current study solubilities of 3,4-dimethoxybenzoic acid (also called veratric acid) were measured at 25 °C in several alcohol, alkyl alkanoate, alkoxyalcohol, 2-alkanone and ether solvents of varying polarity and hydrogen-bonding characteristics. The measured solubility data is correlated using the Abraham solvation parameter model.

Experimental

Chemicals: 3,4-Dimethoxybenzoic acid (Acros Organics, 99+ %) and water (Aldrich, HPLC Grade) were used as received. The purity of 3,4-dimethoxybenzoic acid was 99.8 % (±0.2 %) as determined by nonaqueous titration with a freshly standardized sodium methoxide solution to the thymol blue endpoint according to the method of Fritz and Lisicki¹⁵, except that benzene was replaced with toluene. Methyl acetate (Aldrich, 99.5 %, anhydrous), ethyl acetate (Aldrich, 99.8 %, anhydrous), propyl acetate (Aldrich, 99.5 %), butyl acetate (Aldrich, 99.7 %), pentyl acetate (Aldrich, 99 %), methyl butyrate (Aldrich, 99 %), propylene carbonate (Aldrich, 99+ %, anhydrous), diethyl ether (Aldrich, 99+ %, anhydrous), diisopropyl ether (Aldrich, 99 %, anhydrous), dibutyl ether (Acros Organics, 99+ %), 1,4-dioxane (Aldrich, 99.8 %, anhydrous), tetrahydrofuran (Aldrich, 99.9 %, anhydrous), methanol (Aldrich, 99.8 %, anhydrous), ethanol (Aaper Alcohol and Chemical Company,

absolute), 1-propanol (Aldrich, 99+ %, anhydrous), 1-butanol (Aldrich, HPLC, 99.8+ %), 1-pentanol (Aldrich, 99+ %), 1-hexanol (Alfa Aesar, 99+ %), 1-heptanol (Alfa Aesar, 99+ %), 1-octanol (Aldrich, 99+ %, anhydrous), 1-decanol (Alfa Aesar, 99+ %), 2-propanol (Aldrich, 99+ %, anhydrous), 2-butanol (Aldrich, 99+ %, anhydrous), 2-methyl-1-propanol (Aldrich, 99+ %, anhydrous), 2-methyl-2-propanol (Arco Chemical Company, 99+ %), 3-methyl-1-butanol (Aldrich, 99 %, anhydrous), 2-pentanol (Acros Organics, 99+ %), 2-methyl-1-butanol (Aldrich, 99 %), 4-methyl-2-pentanol (Acros Organics, 99+ %), 2-methyl-1-pentanol (Aldrich, 99 %), 2-propanone (Aldrich, HPLC, 99.9 %), 2-butanone (Aldrich, HPLC, 99.7 %), 2-ethoxyethanol (Aldrich, 99 %), 2-isopropoxyethanol (Aldrich, 99 %), 2-butoxyethanol (Acros Organics, 99 %), and 3-methoxy-1-butanol (Aldrich, 99 %) were stored over molecular sieves and distilled shortly before use. Gas chromatographic analysis showed the organic solvent purities to be at least 99.7 mole percent.

Method: Excess solute and solvent were placed in sealed amber glass bottles and allowed to equilibrate in a constant temperature water bath at 25.0 ± 0.1 °C for at least 72 hours (often longer) with periodic agitation. After equilibration, the samples stood unagitated for several hours in the constant temperature bath to allow any finely dispersed solid particles to settle to the bottom of the container. Attainment of equilibrium was verified both by repetitive measurements the following day (or sometimes after two days) and by approaching equilibrium from supersaturation by pre-equilibrating the solutions at a slightly higher temperature. Undissolved material from several containers were removed and analyzed to ensure that the equilibrium solid phase was indeed pure crystalline 3,4-dimethoxybenzoic acid. Melting point temperatures of the undissolved residues were identical that of recrystallized 3,4-dimethoxybenzoic acid.

Aliquots of saturated 3,4-dimethoxybenzoic acid solutions were transferred through a coarse filter into a tared volumetric flask to determine the mass of sample analyzed and diluted quantitatively with 2-propanol for spectrophotometric analysis at 286 nm on a Milton Roy Spectronic 1001 Plus. 2-Propanone and 2-butanone exhibited significant absorbances at the analysis wavelength, and it was necessary to remove the both solvents by evaporation at 60 °C prior to dilution with 2-propanol. Concentrations of the dilute solutions were determined from a Beer-Lambert law absorbance versus concentration working curve for nine standard solutions. The calculated molar absorptivity of the standard solutions varied slightly with concentration, $\epsilon \approx 4,700 \text{ L mol}^{-1} \text{ cm}^{-1}$ to $\epsilon \approx 4,900 \text{ L mol}^{-1} \text{ cm}^{-1}$, over the concentration range from $9.76 \times 10^{-5} \text{ M}$ to $3.25 \times 10^{-4} \text{ M}$.

Experimental molar concentrations were converted to (mass/mass) solubility fractions by multiplying by the molar mass of 3,4-dimethoxybenzoic acid, volume(s) of volumetric flask(s) used and any dilutions required to place the measured absorbances on the Beer-Lambert law absorbance versus concentration working curve, and then dividing by the mass of the saturated solution analyzed. Mole fraction solubilities were computed from solubility

mass fractions using the molar masses of the solute and solvent. Experimental 3,4-dimethoxybenzoic acid mole fraction solubilities, X_S^{exp} , are listed in Table 1 for the 36 organic solvents studied. Numerical values represent the average of between four and eight independent determinations, and were reproducible to within ± 2 %. Published literature values of Li and coworkers¹⁶ are reported in the last column of Table 1. Literature values were measured using a dynamic method with laser monitoring to determine the temperature at which the suspended solid particles completely dissolved. The experimental uncertainty in the published solubility data is ± 4 %. Examination of the numerical entries in Table 1 reveals that for the eight solvents for which independent literature values are available, our observed mole fraction solubilities are in good agreement with the published solubility data. Differences in experimental methodologies and chemical purities can lead to differences of a few percent between values determined by two different research groups.

Table 1. Experimental 3,4-dimethoxybenzoic acid mole fraction solubilities, X_S^{exp} , in selected organic solvents at 25 °C.

Organic Solvent	X_S^{exp}	X_S^{exp}
Methanol	0.00764	
Ethanol	0.00720	0.00753 ¹⁶
1-Propanol	0.00643	0.00635 ¹⁶
1-Butanol	0.00625	0.00570 ¹⁶
1-Pentanol	0.00615	
1-Hexanol	0.00615	
1-Heptanol	0.00617	
1-Octanol	0.00616	
1-Decanol	0.00577	
2-Propanol	0.00618	0.00606 ¹⁶
2-Butanol	0.00651	
2-Methyl-1-propanol	0.00450	0.00413 ¹⁶
2-Methyl-2-propanol	0.00945	
3-Methyl-1-butanol	0.00560	
2-Methyl-1-butanol	0.00541	
2-Pentanol	0.00593	
4-Methyl-2-pentanol	0.00646	
2-Methyl-1-pentanol	0.00573	
Methyl acetate	0.00854	0.00802 ¹⁶
Ethyl acetate	0.00813	0.00723 ¹⁶
Propyl acetate	0.00682	
Butyl acetate	0.00660	
Pentyl acetate	0.00654	
Methyl butyrate	0.00678	
Propylene carbonate	0.00799	
Diethyl ether	0.00313	
Diisopropyl ether	0.00143	
Dibutyl ether	0.00112	
1,4-Dioxane	0.02897	
Tetrahydrofuran	0.03937	
Propanone	0.01177	
Butanone	0.01206	0.01200 ¹⁶
2-Ethoxyethanol	0.03037	
2-Isopropoxyethanol	0.02335	
2-Butoxyethanol	0.01485	
3-Methoxy-1-butanol	0.02547	

As part of the experimental measurements we did determine the solubility of 3,4-dimethoxybenzoic acid in water at 25 °C which is needed for the Abraham model correlations. The molar solubility of 3,4-dimethoxybenzoic acid in water is $C_w^{\text{sat}} = 0.00320$ M. One drop of hydrochloric acid was added to prevent ionization.

Results and Discussion

Abraham Model: During the past 20 years there have been numerous methods developed for predicting the solubility of crystalline nonelectrolyte compounds in organic solvents based on empirical and semi-empirical quantitative structure – property relationships (QSPR) for which the basic underlying solute-solvent molecular interactions are not always clearly defined. While such QSPR treatments may show some descriptive/predictive ability, they often require large experimental data sets for training purposes, and both the inputted solute parameters/properties and calculated equation coefficients encode no useful chemical information. The approach that we have taken in recent years in describing the solubility is based on the Abraham solvation parameter model¹⁷⁻¹⁹ which contains a realistic description of how solute and solvent molecules are believed to interact in solution. The basic Abraham model is based on two linear free energy relationships (LFERs) that quantify solute transfer between two phases. The first LFER quantifies solute transfer between two condensed phases:¹⁷⁻¹⁹

$$\log (SR \text{ or } P) = c_p + e_p E + s_p S + a_p A + b_p B + v_p V \quad (1)$$

and the second LFER describes solute transfer from the gas phase:¹⁷⁻¹⁹

$$\log (GSR \text{ or } K) = c_k + e_k E + s_k S + a_k A + b_k B + l_k L \quad (2)$$

where

P is the water-to-organic solvent partition coefficient or alkane-to-polar organic solvent partition coefficient, and

K is the gas-to-organic solvent partition.

For solubility predictions, the Abraham model uses the solubility ratio which is given by the ratio of the molar solubilities of the solute in the organic solvent, C_s^{sat} , and in water, C_w^{sat} (*i.e.*, $SR = C_s^{\text{sat}}/C_w^{\text{sat}}$). The gas phase solubility ratio is similarly calculated as the molar solubility in the organic solvent divided by the solute gas phase concentration (*i.e.*, $GSR = C_s^{\text{sat}}/C_G$), the latter value calculable from the solute vapor pressure above the solid at the solution temperature.

The independent variables in Eqns. 1 and 2 are the Abraham solute descriptors defined as follows: E represents

the solute excess molar refraction (in units of $\text{cm}^3 \text{mol}^{-1}/10$), S denotes to the solute dipolarity/polarizability, A and B quantify the overall solute hydrogen bond acidity and basicity, V is the solute's McGowan characteristic molecular volume (in units of $\text{cm}^3 \text{mol}^{-1}/100$) and L corresponds the logarithm of the gas-to-hexadecane partition coefficient measured at 298 K. The lower case regression coefficients and constants (c_p , e_p , s_p , a_p , b_p , v_p , c_k , e_k , s_k , a_k , b_k and l_k) in Eqns. 1 and 2 represent the complimentary condensed phase property and serve to characterize the specific condensed phase system under consideration. Solute descriptors when combined with the respective equation coefficients describe the contributions that each type of solute-solvent interaction makes to the overall solute transfer process. For example, the $a_p \cdot A$ and $a_l \cdot A$ terms in Eqns. 1 and 2 describe the hydrogen-bonding interactions between the H-bond donor sites on the solute and the H-bond acceptor sites on the solvent, while the $b_p \cdot B$ and $b_l \cdot B$ terms involve interactions between the solute H-bond acceptor sites and solvent H-bond donor sites.

The equation coefficients for all of the transfer processes considered in the present study are tabulated in Table 2. A more complete list of equation coefficients can be found elsewhere.¹⁹ The actual numerical values of the equation coefficients may differ slightly from values used in our much earlier publications. The coefficients are periodically revised when additional experimental data become available. Except for the practical “wet” water-to-1-octanol and water-to-diethyl ether partition coefficients (first two entries in Table 2), all of the listed transfer processes pertain to the “dry” anhydrous organic solvent. The “dry” equation coefficients are more applicable for solubility predictions as the condensed phase is not saturated with water as would be the case with the two “wet” partitioning processes.

Abraham Model Predictions: The predictive application of the Abraham model is relatively straightforward given that we have an existing set of preliminary solute descriptors for 3,4-dimethoxybenzoic acid ($E = 0.890$, $S = 1.570$, $A = 0.580$, $B = 0.760$, $V = 1.3309$, and $L = 6.670$) based on measured water-to-diethyl ether, water-to-octanol, gas-to-diethyl ether and gas-to-octanol practical partition coefficient data and calculated fragment group values.^{20,21} The numerical values of the existing solute descriptors are inserted into the sets of $\log SR$ correlations and $\log GSR$ correlations constructed from the equation coefficients given in Table 1. The predicted $\log SR$ values are then converted into 3,4-dimethoxybenzoic acid molar solubilities in the different organic solvents, C_s^{sat} , (more specifically into the logarithms of the molar solubilities, $\log C_s^{\text{sat}}$) using a value of $\log C_w^{\text{sat}} = -2.495$, which is based on our measured molar solubility of unionized 3,4-dimethoxybenzoic acid of $C_w^{\text{sat}} = 0.00320$. Similarly, the predicted $\log GSR$ values are converted into $\log C_s^{\text{sat}}$ values using a value of $\log C_s = -10.765$.

For comparison purposes, the measured molar fraction solubilities, X_s^{exp} , in Table 1 were converted to molar solubilities by dividing X_s^{exp} , by the ideal molar volume of the saturated solution (*i.e.*, $C_s^{\text{exp}} \approx X_s^{\text{exp}} / [X_s^{\text{exp}} \cdot V_{\text{solute}} + (1 - X_s^{\text{exp}}) \cdot V_{\text{solvent}}]$).

Table 2. Coefficients in Eqn. (1) and Eqn. (2) for various Processes^a

Process/solvent	<i>c</i>	<i>e</i>	<i>s</i>	<i>a</i>	<i>b</i>	<i>v/l</i>
A. Water to solvent: Eqn. (1)						
1-Octanol (wet)	0.088	0.562	-1.054	0.034	-3.460	3.814
Diethyl ether (wet)	0.248	0.561	-1.016	-0.226	-4.553	4.075
Methanol (dry)	0.276	0.334	-0.714	0.243	-3.320	3.549
Ethanol (dry)	0.222	0.471	-1.035	0.326	-3.596	3.857
1-Propanol (dry)	0.139	0.405	-1.029	0.247	-3.767	3.986
2-Propanol (dry)	0.099	0.344	-1.049	0.406	-3.827	4.033
1-Butanol (dry)	0.165	0.401	-1.011	0.056	-3.958	4.044
1-Pentanol (dry)	0.150	0.536	-1.229	0.141	-3.864	4.077
1-Hexanol (dry)	0.115	0.492	-1.164	0.054	-3.978	4.131
1-Heptanol (dry)	0.035	0.398	-1.063	0.002	-4.342	4.317
1-Octanol (dry)	-0.034	0.489	-1.044	-0.024	-4.235	4.218
1-Decanol (dry)	-0.058	0.616	-1.319	0.026	-4.153	4.279
2-Butanol (dry)	0.127	0.253	-0.976	0.158	-3.882	4.114
2-Methyl-1-propanol (dry)	0.188	0.354	-1.127	0.016	-3.568	3.986
2-Methyl-2-propanol (dry)	0.211	0.171	-0.947	0.331	-4.085	4.109
3-Methyl-1-butanol (dry)	0.073	0.360	-1.273	0.090	-3.770	4.273
2-Pentanol (dry)	0.115	0.455	-1.331	0.206	-3.745	4.201
Diethyl ether (dry)	0.350	0.358	-0.820	-0.588	-4.956	4.350
1,4-Dioxane (dry)	0.123	0.347	-0.033	-0.582	-4.810	4.110
Tetrahydrofuran (dry)	0.223	0.363	-0.384	-0.238	-4.932	4.450
Propanone	0.313	0.312	-0.121	-0.608	-4.753	3.942
Butanone	0.246	0.256	-0.080	-0.767	-4.855	4.148
Methyl acetate (dry)	0.351	0.223	-0.150	-1.035	-4.527	3.972
Ethyl acetate (dry)	0.328	0.369	-0.446	-0.700	-4.904	4.150
Propyl acetate (dry) ^b	0.288	0.363	-0.474	-0.784	-4.939	4.216
Butyl acetate (dry)	0.248	0.356	-0.501	-0.867	-4.973	4.281
Propylene carbonate (dry)	0.004	0.168	0.504	-1.283	-4.407	3.421
(Gas to water)	-0.994	0.577	2.549	3.813	4.841	-0.869
B. Gas to solvent: Eqn. (2)						
1-Octanol (wet)	-0.198	0.002	0.709	3.519	1.429	0.858
Diethyl ether (wet)	0.206	-0.169	0.873	3.402	0.000	0.882
Methanol (dry)	-0.039	-0.338	1.317	3.826	1.396	0.773
Ethanol (dry)	0.017	-0.232	0.867	3.894	1.192	0.846
1-Propanol (dry)	-0.042	-0.246	0.749	3.888	1.076	0.874
2-Propanol (dry)	-0.048	-0.324	0.713	4.036	1.055	0.884
1-Butanol (dry)	-0.004	-0.285	0.768	3.705	0.879	0.890
1-Pentanol (dry)	-0.002	-0.161	0.535	3.778	0.960	0.900
1-Hexanol (dry)	-0.014	-0.205	0.583	3.621	0.891	0.913
1-Heptanol (dry)	-0.056	-0.216	0.554	3.596	0.803	0.933
1-Octanol (dry)	-0.147	-0.214	0.561	3.507	0.749	0.943
1-Decanol (dry)	-0.139	-0.090	0.356	3.547	0.727	0.958
2-Butanol (dry)	-0.034	-0.387	0.719	3.736	1.088	0.905
2-Methyl-1-propanol (dry)	-0.003	-0.357	0.699	3.595	1.247	0.881
2-Methyl-2-propanol (dry)	-0.053	-0.443	0.699	4.026	0.882	0.907
3-Methyl-1-butanol (dry)	-0.052	-0.430	0.628	3.661	0.932	0.937
2-Pentanol (dry)	-0.031	-0.325	0.496	3.792	1.024	0.934
Diethyl ether (dry)	0.288	-0.347	0.904	2.937	0.000	0.963
1,4-Dioxane (dry)	-0.034	-0.389	1.724	2.989	0.000	0.922
Tetrahydrofuran	0.193	-0.391	1.244	3.256	0.000	0.994
Propanone	0.127	-0.387	1.733	3.060	0.000	0.866
Butanone	0.112	-0.474	1.671	2.878	0.000	0.916
Methyl acetate (dry)	0.134	-0.477	1.749	2.678	0.000	0.876
Ethyl acetate (dry)	0.182	-0.352	1.316	2.891	0.000	0.916
Propyl acetate (dry) ^b	0.165	-0.383	1.264	2.757	0.000	0.935
Butyl acetate (dry)	0.147	-0.414	1.212	2.623	0.000	0.954
Propylene carbonate (dry)	-0.356	-0.413	2.587	2.207	0.455	0.719
(Gas to water)	-1.271	0.822	2.743	3.904	4.814	-0.213

^a The dependent variable is $\log SR$ and $\log GSR$ for all of the correlations, except for 1-octanol (wet) and diethyl ether (wet) where the practical water-to-1-octanol and water-to-diethyl ether partition coefficient was used. ^bThe equation coefficients for propyl acetate are estimated as the average of the coefficients for ethyl acetate and butyl acetate.

The molar volume of the hypothetical subcooled liquid 3,4-dimethoxybenzoic acid, $V_{\text{solute}}=143.8 \text{ cm}^3 \text{ mol}^{-1}$, was estimated as the molar volume of benzoic acid ($V_{\text{benzoic acid}}=104.4 \text{ cm}^3 \text{ mol}^{-1}$) plus two times the molar volume of methoxybenzene ($V_{\text{methoxybenzene}} = 109.1 \text{ cm}^3 \text{ mol}^{-1}$) minus two times the molar volume of benzene ($V_{\text{benzene}} = 89.4 \text{ cm}^3 \text{ mol}^{-1}$). Any errors resulting from the

estimation of 3,4-dimethoxybenzoic acid's hypothetical subcooled liquid molar volume, V_{Solute} , or the ideal molar volume approximation will have negligible effect of the calculated $C_{\text{S}}^{\text{exp}}$ values because 3,4-dimethoxybenzoic acid is not overly soluble in many of the solvents considered. From a mathematical standpoint, the $X_{\text{S}}^{\text{exp}} \cdot V_{\text{Solute}}$ term contributes very little to the molar volumes of the saturated solutions.

Table 3. Comparison Between Observed and Back-Calculated Molar Solubilities of 3,4-Dimethoxybenzoic Acid Based Upon Eqn. (1) and Eqn. (2), and Existing Molecular Solute Descriptors^a

Solvent	Equation (1)				Equation (2)		
	$\log C_{\text{S}}^{\text{exp}}$	$\log(C_{\text{S}}/C_{\text{W}})^{\text{exp}}$	$\log(C_{\text{S}}/C_{\text{W}})^{\text{calc}}$	$\log C_{\text{S}}^{\text{calc}}$	$\log(C_{\text{S}}/C_{\text{G}})^{\text{exp}}$	$\log(C_{\text{S}}/C_{\text{G}})^{\text{pred}}$	$\log C_{\text{S}}^{\text{pred}}$
1-Octanol (wet)		1.480 ^b	1.400 ^b		9.750 ^b	9.767 ^b	
Diethyl ether (wet)		0.880 ^b	0.984 ^b		9.150 ^b	9.282 ^b	
Methanol (dry)	-0.735	1.760	1.793	-0.702	10.030	10.164	-0.601
Ethanol (dry)	-0.916	1.579	1.606	-0.889	9.849	9.979	-0.786
1-Propanol (dry)	-1.070	1.425	1.469	-1.026	9.695	9.817	-0.948
2-Propanol (dry)	-1.097	1.398	1.453	-1.042	9.668	9.822	-0.943
1-Butanol (dry)	-1.169	1.326	1.341	-1.154	9.596	9.701	-1.064
1-Pentanol (dry)	-1.267	1.228	1.269	-1.226	9.498	9.619	-1.146
1-Hexanol (dry)	-1.309	1.186	1.231	-1.264	9.456	9.586	-1.179
1-Heptanol (dry)	-1.362	1.133	1.167	-1.328	9.403	9.541	-1.224
1-Octanol (dry)	-1.410	1.085	1.143	-1.352	9.355	9.436	-1.329
1-Decanol (dry)	-1.501	0.994	0.973	-1.522	9.264	9.339	-1.426
2-Butanol (dry)	-1.154	1.341	1.436	-1.059	9.611	9.781	-0.984
2-Methyl-1-propanol (dry)	-1.315	1.180	1.336	-1.159	9.450	9.686	-1.079
2-Methyl-2-propanol (dry)	-1.001	1.494	1.432	-1.063	9.764	9.811	-0.954
3-Methyl-1-butanol (dry)	-1.293	1.202	1.269	-1.226	9.472	9.633	-1.132
2-Pentanol (dry)	-1.267	1.228	1.295	-1.200	9.498	9.666	-1.099
Diethyl ether (dry)	-1.525	0.970	1.124	-1.371	9.240	9.417	-1.348
1,4-Dioxane (dry)	-0.480	2.015	1.841	-0.654	10.285	10.161	-0.604
Tetrahydrofuran (dry)	-0.328	2.167	1.954	-0.541	10.437	10.281	-0.484
Propanone (dry)	-0.803	1.692	1.682	-0.813	9.962	10.054	-0.711
Butanone (dry)	-0.879	1.616	1.734	-0.761	9.886	10.093	-0.672
Methyl acetate (dry)	-0.973	1.522	1.559	-0.936	9.792	9.852	-0.913
Ethyl acetate (dry)	-1.085	1.410	1.346	-1.149	9.680	9.721	-1.044
Propyl acetate (dry)	-1.229	1.266	1.271	-1.224	9.536	9.644	-1.121
Butyl acetate (dry)	-1.303	1.192	1.194	-1.301	9.462	9.566	-1.199
Propylene carbonate (dry)	-1.029	1.466	1.404	-1.091	9.736	9.644	-1.121
Gas-to-Water		8.270	8.256			8.270	8.269

^a Numerical values of the descriptors used in these calculations are: $E=0.890$, $S=1.570$, $A=0.580$, $B=0.760$, $V=1.3309$ and $L=6.670$.

^b Practical partition coefficient.

Examination of the numerical entries in Table 3 reveals that our existing solute descriptors provide a very reasonable estimation of the solubility behavior of 3,4-dimethoxybenzoic acid in diethyl ether, tetrahydrofuran, 1,4-dioxane, and in 15 alcohol and four alkyl acetate solvents. Standard deviations between predicted and observed values were 0.091 and 0.134 log units for Eqns. 1 and 2, respectively. The prediction of the practical water-to-diethyl ether partition coefficient ($\log P_{\text{exp}} = 0.8822$) and water-to-1-octanol partition coefficient ($\log P_{\text{exp}} = 1.4822$) is included in the standard deviation for Eqn. 1. A predictive error of ± 0.13 log units corresponds to approximately a

35 % error in estimating the molar solubility. Standard deviations of 0.091 and 0.134 log units are comparable to the standard deviations associated with the transfer coefficients for the individual solvents, which for most solvents fell in the range of ± 0.12 to ± 0.20 log units.

Equation coefficients are available for only 25 of the 36 organic solvents studied. 3,4-Dimethoxybenzoic acid solubilities were measured in solvents like 2-ethoxyethanol, 2-isopropoxyethanol, 2-butoxyethanol, 3-methoxy-1-butanol, 2-methyl-1-butanol, 2-methyl-1-pentanol, 4-methyl-2-pentanol, pentyl acetate and diisopropyl ether so that we

would have more experimental data to use in subsequent studies to generate solute transfer correlation equations for additional organic solvents. Predictions were not made for dibutyl ether because past studies suggest that carboxylic acids exhibit significant dimerization in this particular

solvent, in which case the measured solubility would represent the sum of the molar concentration of monomeric solute plus twice the molar concentration of the carboxylic acid dimer. Our existing solute descriptors pertain to the monomeric form of 3,4-dimethoxybenzoic acid.

Table 4. Comparison between observed and back-calculated molar solubilities of 3,4-dimethoxybenzoic acid based upon Eqn. (1) and Eqn. (2), and revised molecular solute descriptors^a

Solvent	log C_S^{exp}	log $(C_S/C_W)^{exp}$	Equation (1)		log $(C_S/C_G)^{exp}$	Equation (2)	
			log $(C_S/C_W)^{calc}$	log C_S^{calc}		log $(C_S/C_G)^{calc}$	log C_S^{calc}
1-Octanol (wet)		1.480 ^b	1.371		9.927	9.843	
Diethyl ether (wet)		0.880 ^b	0.967		9.327	9.371	
Methanol (dry)	-0.735	1.760	1.774	-0.721	10.207	10.257	-0.685
Ethanol (dry)	-0.916	1.579	1.571	-0.924	10.026	10.050	-0.892
1-Propanol (dry)	-1.070	1.425	1.433	-1.062	9.872	9.881	-1.061
2-Propanol (dry)	-1.097	1.398	1.410	-1.085	9.845	9.878	-1.064
1-Butanol (dry)	-1.169	1.326	1.309	-1.186	9.772	9.769	-1.173
1-Pentanol (dry)	-1.267	1.228	1.226	-1.269	9.675	9.675	-1.267
1-Hexanol (dry)	-1.309	1.186	1.193	-1.302	9.633	9.646	-1.296
1-Heptanol (dry)	-1.362	1.133	1.133	-1.362	9.580	9.601	-1.341
1-Octanol (dry)	-1.410	1.085	1.116	-1.379	9.532	9.499	-1.443
1-Decanol (dry)	-1.501	0.994	0.932	-1.563	9.441	9.395	-1.547
2-Butanol (dry)	-1.154	1.341	1.396	-1.099	9.788	9.838	-1.104
2-Methyl-1-propanol (dry)	-1.315	1.180	1.291	-1.204	9.627	9.742	-1.200
2-Methyl-2-propanol (dry)	-1.001	1.494	1.389	-1.106	9.941	9.862	-1.080
3-Methyl-1-butanol (dry)	-1.293	1.202	1.313	-1.182	9.649	9.684	-1.258
2-Pentanol (dry)	-1.267	1.228	1.239	-1.256	9.675	9.712	-1.230
Diethyl ether (dry)	-1.525	0.970	1.117	-1.378	9.417	9.499	-1.443
1,4-Dioxane (dry)	-0.480	2.015	1.887	-0.608	10.462	10.307	-0.635
Tetrahydrofuran (dry)	-0.328	2.167	1.975	-0.520	10.613	10.396	-0.546
Propanone (dry)	-0.803	1.692	1.723	-0.772	10.139	10.198	-0.744
Butanone (dry)	-0.879	1.616	1.777	-0.718	10.063	10.232	-0.710
Methyl acetate (dry)	-0.973	1.522	1.596	-0.899	9.968	9.996	-0.946
Ethyl acetate (dry)	-1.085	1.410	1.367	-1.128	9.857	9.841	-1.101
Propyl acetate (dry)	-1.229	1.266	1.290	-1.205	9.713	9.760	-1.182
Butyl acetate (dry)	-1.303	1.192	1.212	-1.283	9.639	9.679	-1.263
Propylene carbonate (dry)	-1.029	1.466	1.489	-1.006	9.913	9.961	-0.981
Gas-to-Water		8.447	8.420		8.447	8.446	

^a Numerical values of the descriptors used in these calculations are: $E = 0.950$, $S = 1.646$, $A = 0.570$, $B = 0.755$, $V = 1.3309$ and $L = 6.746$.

^b Practical partition coefficient.

Revision of Solute Descriptor Values: The existing values that we have for 3,4-dimethoxybenzoic acid do provide very good predictions for the observed solubility behaviour of the compound in alcohol, alkyl acetate and ether solvents. The values were based on only two experimental practical partition coefficients; however, and it is desirable to have values based on a database having greater chemical diversity. One of the criticisms that models of this type often encounter is that one must not make predictions outside of the chemical space used in determining the solute descriptors and/or equation coefficients. We can address this concern now since experimental data are available for updating the solute descriptors, and there is no reason for us not to perform the few additional calculations to update the numerical values. Combining the two sets of LFERs, log (SR or P) and log

(GSR or K) correlations, we have a total of 54 mathematical equations. The characteristic McGowan volume of 3,4-dimethoxybenzoic acid is known, $V = 1.3309$, from the summation of the individual atomic sizes less a contribution for each bond in the molecule.²³ The E solute descriptor is $E = 0.950$, which is slightly larger than the estimate used several years ago when our preliminary solute descriptors were initially calculated. The set of 54 equations were then solved using Microsoft “Solver” to yield the numerical values of the four remaining solute descriptors that best described the log (SR or P) and log (GSR or K) values. The updated set of molecular solute descriptors are $E = 0.950$, $S = 1.646$, $A = 0.570$, $B = 0.755$, $V = 1.3309$, and $L = 6.746$; and the vapor phase concentration was log $C_G = -10.942$. The updated solute descriptors differ very slightly from our previous values. This is to be expected as our existing

solute descriptors did provide a very good mathematical description of the observed solubility behavior of 3,4-dimethoxybenzoic acid in the alcohol, alkyl acetate, and ether solvents. The updated solute descriptors reproduce the experimental log (*SR* or *P*) and log (*GSR* or *K*) values to within an overall standard deviation of 0.084 log units and 0.082 log units, respectively, as shown in Table 4. Statistically, there is no difference between the set of 27 log (*SR* and *P*) values and the total set of 54 log (*SR* or *P*) and log (*GSR* or *K*) values, thus suggesting that $\log C_G = -10.942$ is a feasible value for the 3,4-dimethoxybenzoic acid correlations.

The calculated solute descriptors of 3,4-dimethoxybenzoic acid do account very well for the observed solubilities and partition coefficients; however, the values must reflect chemical properties of the solute, otherwise, the descriptors would be simply “curve-fitting parameters”. Our solute descriptor database does contain benzoic acid (**E** = 0.730, **S** = 900, **A** = 0.590, **B** = 0.400, **V** = 0.9317 and **L** = 4.657) and other methoxy-substituted benzoic acids. Hoover et al.¹¹ previously determined solute descriptors for 2-methoxybenzoic acid (**E** = 0.899, **S** = 1.410, **A** = 0.450, **B** = 0.620, **V** = 1.3133 and **L** = 5.636) and 4-methoxybenzoic acid (**E** = 0.899, **S** = 1.250, **A** = 0.620, **B** = 0.520, **V** = 1.3133 and **L** = 5.741) based largely on experimental solubility data in neat alcohol and ether solvents. For benzoic acid, 4-methoxybenzoic acid and 3,4-dimethoxybenzoic acid, there is a progressive increase in the descriptors **E**, **S**, **B**, **V** and **L** with each added methoxy-functional group. The two lone electron pairs on the oxygen atom of each methoxy-substituent provide additional H-bond donor sites, and increase the electron density of the aromatic ring through resonance and/or inductive effects. The solute descriptors of 2-methoxybenzoic acid do not follow this trend. The lower than expected H-bond acidity for 2-methoxybenzoic acid is likely due to intramolecular hydrogen-bond formation, which has been suggested by both solution IR and proton, ¹³C and ¹⁷O NMR studies.²⁴⁻²⁸ Intramolecular H-bond formation would both reduce the H-bond basicity of the methoxy oxygen atom and increase the basicity of the oxygen atom in the carboxylic –OH group.

Conclusion

The Abraham solvation parameter model has been used to describe mathematically the observed solubility data for 3,4-dimethoxybenzoic acid dissolved in alcohol, alkyl acetate and ether solvents. The computation methodology used to calculate the solute descriptors requires experimental solubility data for the solute in water and in a dozen or so other solvents for Abraham equation coefficients are known. The solute descriptors, once calculated, can be used both to back-calculate the measured solubility data employed in the solute descriptor determination as well as to predict the solute's solubility in additional solvents for which equation coefficients are known.

References

- Acree Jr., W. E., Bertrand, G. L., *J. Pharm. Sci.*, **1981**, *70*, 1033.
- Charlton, A. K., Daniels, C. R., Acree Jr., W. E., Abraham, M. H., *J. Solution Chem.*, **2003**, *32*, 1087.
- Daniels, C. R., Charlton, A. K., Wold, R. M., Moreno, R. J., Acree Jr., W. E., Abraham, M. H., *Phys. Chem. Liq.*, **2004**, *42*, 633.
- Stovall, D. M., Givens, C., Keown, S., Hoover, K. R., Barnes, R., Harris, C., Lozano, J., Nguyen, M., Rodriguez, E., Acree Jr., W. E., Abraham, M. H., *Phys. Chem. Liq.*, **2005**, *43*, 351.
- Hoover, K. R., Pop, K., Acree Jr., W. E., Abraham, M. H., *S. African J. Chem.*, **2005**, *58*, 25.
- Daniels, C. R., Charlton, A. K., Wold, R. M., Acree Jr., W. E., Abraham, M. H., *Can. J. Chem.*, **2003**, *81*, 1492.
- Wilson, A., Tian, A., Chou, V., Quay, A. N., Acree Jr., W. E., Abraham, M. H., *Phys. Chem. Liq.*, **2012**, *50*, 324.
- Hoover, K. R., Cozum, R., Pustejovsky, E., Acree Jr., W. E., Abraham, M. H., *Phys. Chem. Liq.*, **2004**, *42*, 452.
- Ye, S., Saifullah, M., Grubbs, L. M., McMillan-Wiggins, M. C., Acosta, P., Mejorado, D., Flores, I., Acree Jr., W. E., Abraham, M. H., *Phys. Chem. Liq.*, **2011**, *49*, 821.
- De Fina, K. M., Sharp, T. L., Roy, L. E., Acree Jr., W. E., *J. Chem. Eng. Data*, **1999**, *44*, 1265.
- Hoover, K. R., Stovall, D. M., Pustejovsky, E., Cozum, R., Pop, K., Acree Jr., W. E., Abraham, M. H., *Can. J. Chem.* **2004**, *82*, 1353.
- Cozum, R., Hoover, K. R., Pustejovsky, E., Stovall, D. M., Acree Jr., W. E., Abraham, M. H., *Phys. Chem. Liq.*, **2004**, *42*, 313.
- Charlton, A. K., Daniels, C. R., Wold, R. M., Pustejovsky, E., Acree Jr., W. E., Abraham, M. H., *J. Mol. Liq.* **2005**, *116*, 19.
- Hoover, K. R., Cozum, R., Pustejovsky, E., Stovall, D. M., Acree Jr., W. E., Abraham, M. H., *Phys. Chem. Liq.*, **2004**, *42*, 339.
- Fritz, J. S., Lisicki, N. M., *Anal. Chem.*, **1951**, *23*, 589.
- Li, Q., Lu, F., Tian, Y., Feng, S., Shen, Y., Wang, B., *J. Chem. Eng. Data*, **2013**, *58*, 1020.
- Abraham, M. H., *Chem. Soc. Reviews*, **1993**, *22*, 73.
- Abraham, M. H., Ibrahim, A., Zissimos, A. M., *J. Chromatogr. A*, **2004**, *1037*, 29.
- Abraham, M. H., Smith, R. E., Luchtefeld, R., Boorem, A. J., Luo, R., Acree Jr., W. E., *J. Pharm. Sci.*, **2010**, *99*, 1500.
- Platts, J. A., Butina, D., Abraham, M. H., Hersey, A., *J. Chem. Inf. Comp. Sci.*, **1999**, *39*, 835.
- Platts, J. A., Abraham, M. H., Butina, D., Hersey, A., *J. Chem. Inf. Comp. Sci.*, **2000**, *40*, 71.
- BioLoom Database, **2011**, BioByte Corp, 201 W. 4th Street, #204 Claremont, CA 91711-4707.
- Abraham, M. H., McGowan, J. C., *Chromatographia*, **1987**, *23*, 243.
- Etter, M. C., Urbanczyk-Lipkowska, Z., Fish, P. A., Panunto, T. W., Baures, P. W., Frye, J. S., *J. Crystallog. Spectrosc. Res.*, **1988**, *18*, 311.
- Exner, O., Fiedler, P., Budesinsky, M., Kulhanek, J., *J. Org. Chem.*, **1999**, *64*, 3515.
- Lloyd, H. A., Warren, K. S., Fales, H. M., *J. Am. Chem. Soc.*, **1966**, *88*, 3544.
- Schmiedekamp-Schneeweis, L. A., Payne, J. O., *Int. J. Quantum Chem.* **1998**, *70*, 863.
- Kondo, M., *Bull. Chem. Soc. Jpn.*, **1972**, *45*, 2790.

Received: 02.04.2013.
Accepted: 16.04.2013.



SYNTHESIS AND CHARACTERIZATION OF OCTAKIS[(2-PROPYLOXY-2-OXO-1-ETHYL)THIO]-21H, 23H-PORPHYRAZINE FROM 1,2-DICYANO-1,2-THIOETHYLENE

A. Yahyazadeh^{[a]*}, F. Sedigh Zyabari^[b]

Keywords: octakis[(2-propyloxy-2-oxo-1-ethylthio)-21H,23H-porphyrazine, 1,2-dicyano-1,2-thioethylene, sodium cis-1,2-dicyano-1,2-ethylenedithiolate, magnesium propoxide; 1,2-dicyano-1,2-bis(2-ethoxy-2-oxo-1-ethylthio)ethylene

The 1,2-dicyano-1,2-bis(2-ethoxy-2-oxo-1-ethylthio)ethylene has been prepared from sodium cis-1,2-dicyano-1,2-ethylenedithiolate (NaMNT) and ethyl chloroacetate by treatment with sodium iodide in dry acetone. 2,3,7,8,12,13,17,18-octakis[(2-propyloxy-2-oxo-1-ethylthio)-21H,23H-porphyrazine was obtained from 1,2-dicyano-1,2-bis(2-ethoxy-2-oxo-1-ethylthio)ethylene in magnesium propoxide (PrOMg) and dry propanol. All compounds have been fully characterized by spectroscopic data.

Corresponding Authors*

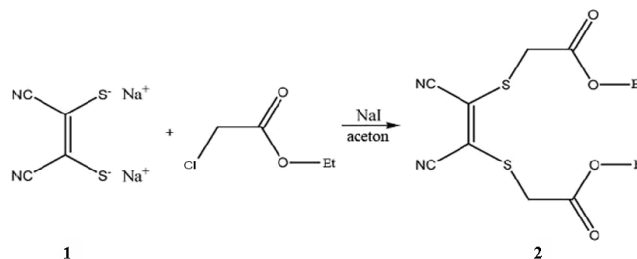
Tel.: +981313233262

Fax: +981313233262

E-Mail: yahyazadehphd@yahoo.com; yahyazadeh@guilan.ac.ir

[a] Department of Chemistry, University of Guilan, P.O. Box 1914, Rasht, Iran

[b] Department of Chemistry, University of Payame Noor Hamedan, Iran



The microanalysis results were satisfactory and the low resolution mass spectrum gave a molecular ion peak at m/z 314[M+1]⁺. In the ¹³C NMR spectrum there were six peaks as expected, with the carbonyl at 169.4 ppm, (-CN) at 122.4 ppm, (C=C) at 111.2 ppm, (O-CH₂) at 59.9 ppm, (S-CH₂) at 40.4 ppm, and (-CH₃) at 26.0 ppm. The presences of (C-H str) were also confirmed by band at 3000 cm⁻¹, (-CN) at 2200 cm⁻¹, (C=O) at 1730 cm⁻¹, (C=C) at 1510 cm⁻¹, (-CH₂ and -CH₃ ben) at 1450 cm⁻¹ and 1375 cm⁻¹ in the infrared spectrum. 1,2-Dicyano-1,2-bis(2-ethoxy-2-oxo-1-ethylthio)ethylene (**2**) was then cyclised to 2,3,7,8,12,13,17,18-octakis[(2-propyloxy-2-oxo-1-ethylthio)-21H, 23H-porphyrazine (**3**) in 24 % yield by treatment with PrOMg in dry propanol.

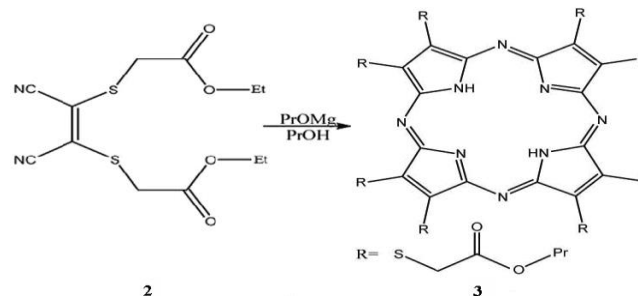
Introduction

Tetrapyrrolic macrocycles are widely used as pigments in textiles, polymers liquid crystal and paints.¹⁻³ The name porphyrazine or in other words meso-tetraaza-substituted porphyrin includes a wide class of macrocyclic porphyrin analogues or heteroanalogues.^{4,5} In the all cases the Linstead method was used.⁶⁻⁹ Various methods such as, the organic dye photosensitization of TiO₂,^{1,6} peripherally bulky annulations of porphyrazine derivatives⁷⁻⁹ and preparation of annulated binuclear phthalocyanines¹⁰ have been developed. The modified porphyrazines possess an intensive absorption in the blue-green region of the solar spectrum; which can practically be applied in diverse areas as, photodynamic therapy (PDT), degradation of pollutants, photosensitizers, and anticancer therapy.¹¹⁻¹⁷ Diphtalocyanine complexes have also gained attention due to their rich redox chemistry and especial π -electron systems. For example, lutetium diphtalocyanine complexes show photochemical behaviors six orders higher than their monomeric counterpart.¹³

Result and Discussion

1,2-dicyano-1,2-bis(2-ethoxy-2-oxo-1-ethylthio)ethylene (**2**) was prepared in high yield by reaction of the sodium cis-1,2-dicyano-1,2-ethylenedithiolate (NaMNT) (**1**) with ethyl chloroacetate with nitrogen atmosphere in presence of a catalytic sodium iodide in dry acetone.¹¹⁻¹⁵

It was fully characterized and the spectroscopic data obtained were in agreement with those previously reported.



Magnesium propoxide (PrOMg) has been prepared from magnesium turnings and iodine were placed in dry propanol and heated under reflux in nitrogen atmosphere overnight.

The elemental analysis and mass spectroscopy results obtained on this compound (**3**) were satisfactory. The ¹H

NMR spectrum showed the presence of 0.97 ppm (t, 24H, CH₃), 1.23 ppm (m, 16H, -CH₂-CH₃), 2.79 ppm (t, 16H, COO-CH₂), 3.21 ppm (s, 16H, S-CH₂). The presences of (N-H) stretching were also confirmed by band at 3400 cm⁻¹, (-CH, str) at 2960 cm⁻¹, (C=O) at 1720 cm⁻¹, (-CH₂ and -CH₃, ben) at 1480cm⁻¹ and 1390 cm⁻¹, (C-N, str) at 1240 cm⁻¹ in the infrared spectrum. The UV-Vis spectrum showed the presence of 630 nm S-Bond and 320 nm Q-Bond.⁸⁻¹⁰

Experimental

All solvents purified and dried using established procedures. The ¹H NMR spectra were recorded on Hitachi-Perkin-Elmer R24B (60 MHz) or Bruker XL 500 (500 MHz) instruments (with *J*-values given in Hz), ¹³C NMR spectra (with DEPT 135) either on a Bruker WP 80 or XL300 instrument, and IR spectra on a Shimadzu IR-470 spectrophotometer. Mass spectra were recorded on a Kratos Concept instrument. The melting points were measured on an electrothermal digital melting point apparatus and are uncorrected.

References

- ¹Zimcik, P., Mrkved, E. H., Andreassen, T., Lenco, J., Novakova, *Polyhedron*, **2008**, *27*, 1368.
- ²Keskin, B., Koseoglu, Y., Avciata, U. and Gul, A., *Polyhedron*, **2008**, *27*, 1155.
- ³Kabay, N., Soyleyici, S. and Gok, Y., *Inorg. Chem. Commun.*, **2009**, *12*, 304.
- ⁴Barret, A. G., Haffman, B. M., Lee, S., Williams, W. D., and White, A. P., *J. Org. Chem.*, **2001**, *66*, 461.
- ⁵Kumashiro, I., Takenishi, T. and Yamada, Y., *Bull. Chem. Soc. Jap.*, **1968**, 1237.
- ⁶Faust, R. and Mitzel, F., *J. Chem. Soc. Perkin Trans. 1*, **2000**, 3767.
- ⁷Karadeniz, H., Gok, H. Y. and Kantekin, H., *Dyes Pigm.*, **2007**, *75*, 498.
- ⁸Kabay, N., Soyleyici, S. and Gok, Y., *Inorg. Chem. Commun.* **2009**, *12*, 304.
- ⁹Donzello, M. P., Ercolani, C. and Stuzhin, P. A., *Coord. Chem. Rev.*, **2006**, *250*, 1530.
- ¹⁰Litwinski, C., Corral, I., Ermilov, E. A., Tannert, S., Fix, D., Makarov, S., Suvorova, O., Gonzalez, L., Wohrle, D. and Roder, B., *J. Phys. Chem.*, **2008**, *112*, 8466.
- ¹¹Alvaro, M., Carbonell, E., Espla, M. and Garcia, H., *Appl. Catal., B: Environmental*, **2005**, *57*, 37.
- ¹²Marais, E., Nyokong, T. and Hazard, J., *Mater.*, **2008**, *152*, 293.
- ¹³Nensala, N. and Nyokong, T., *J. Mol. Catal., A: Chem.* **2000**, *164*, 69.
- ¹⁴Wei, S., Zhou, J., Huang, D., Wang, X., Zhang, B. and Shen, J., *Dyes Pigm.*, **2006**, *71*, 61.
- ¹⁵Atilla, D., Saydan, N., Durmus, M., Gurek, A. G., Khanc, T., Ruck, A., Walt, H., Nyokong, T. and Ahsen, V., *J. Photochem. Photobiol., A: Chem.*, **2007**, *186*, 298.
- ¹⁶Chang, A. T. and Marchon, J. C., *Inorg. Chim. Acta*, **1981**, *53*, 241.
- ¹⁷Nensala, M. and Nyokong, T., *Polyhedron*, **1997**, *16*, 2971.

Received: 09.03.2013.

Accepted: 17.04.2013.



ELECTROCHEMICAL AND SURFACE ANALYSIS STUDIES ON CORROSION INHIBITION OF CARBON STEEL

J. Jeyasundari,^{[a]*} S. Rajendran,^[b] R. Sayee Kannan,^[c] Y. Brightson Arul Jacob^[a]

Keywords: Corrosion inhibition, Carbon steel, Scanning Electron Microscope, Fluorescence spectra, Nano film

The corrosion inhibition of inhibitor tris(hydroxymethyl)amino methane (THAM) and 1-hydroxyethylidenediphosphonic acid (HEDP) in combination with a bivalent cation like Zn^{2+} in controlling corrosion of carbon steel immersed in aqueous solution containing 60 ppm Cl^- was investigated using weight loss method and electrochemical impedance spectroscopy. The combined corrosion inhibition efficiency offered by 50 ppm of THAM, 250 ppm of HEDP, 50 ppm of Zn^{2+} has 86%. The synergistic effect of the inhibiting compound was calculated. The corrosion inhibition was observed due to the formation of more stable and compact protective film on the metal surface. Fluorescence spectral analysis was used in detecting the presence of iron-inhibitor complex and the coordination sites of the metal inhibitor with iron were determined by the FTIR spectra. The surface morphology of the protective film on the metal surface was characterized by using Scanning Electron Microscope (SEM)

Corresponding Authors

*E-Mail: jjsundari16@gmail.com

- [a] Department of chemistry, NMSSVN College, Madurai-625019, Tamilnadu, India. Email: brightson_hai@yahoo.co.in
- [b] Department of Chemistry, RVS School of Engineering & Technology, Dindigul-624005, Tamilnadu, India. Email:susairajendran@yahoo.com
- [c] Department of chemistry, Thiagarajar College, Madurai-625009, Tamilnadu, India. Email: rsamkannan@yahoo.co.in

Infrared Spectroscopy (FTIR) and Scanning Electron Microscopy (SEM).

Materials and Methods

Preparation of mild steel specimens

Carbon steel specimens were chosen from the same sheet of the following composition 0.1 Percent C, 0.026 percent S, 0.06 percent P, 0.4 percent Mn and the balance Fe. Carbon steel specimen of the dimensions $1.0 \times 4.0 \times 0.2$ cm were polished to more finish degreased with trichloroethylene and used for mass loss and surface examination studies. The environment chosen is an aqueous solution containing 60 ppm Cl^- .

Determination of corrosion rate

The weighed specimen, in triplicate were suspended by means of glass hooks in 100 ml beakers containing 100 ml of an aqueous solution containing 60 ppm Cl^- containing various concentration of the inhibitors in the presence and absence of Zn^{2+} for 3 days of immersion. After 3 days of immersion the specimens were taken out, washed in running water, dried and weighed. From the change in weights of the specimen corrosion rates (CR) were calculated using the following relationship.

$$CR = \frac{\Delta m}{S t} \quad (1)$$

where

Δm - loss in weight (mg)

S - surface area of the specimen (dm^2)

t - period of immersion (days)

Corrosion inhibition efficiency (IE) was then calculated using the equation:

Introduction

Corrosion is the gradual destruction of material, usually metal, by chemical reaction with its environment. Phosphonates in combination with zinc ions have been in use as effective corrosion inhibitors for carbon steel in cooling water systems for the past three decades.¹⁻² Several compounds such as nitrite, phosphate,³⁻⁴ silicates,⁵ sodium salicylate,⁶ sodium cinnamate,⁷ molybdate,⁸⁻⁹ phosphonic acids,¹⁰⁻¹² polyacrylamide¹³ and caffeine¹⁴⁻¹⁵ have been used as corrosion inhibitors. Several phosphonic acids have been used as corrosion inhibitor along with metal cation such as Zn^{2+} .¹⁶⁻¹⁸ Phosphonates are derivatives of phosphonic acids that contain direct phosphorous-to carbon bonds (P-C). The P-C bonds are more resistant to hydrolysis than the P-O-C bonds of organic phosphates. Phosphonic acids are used as scale inhibitors in aqueous systems.¹⁹⁻²⁰ Phosphonic acids are extensively used now-a-days due to their complex-forming abilities, high stability under harsh conditions and low toxicity. The inhibition efficiency of phosphonates depends on the number of phosphono groups in a molecule and also on different substituents.

Electrochemical techniques have been used in corrosion inhibition studies of mild steel by phosphonic acid.²¹⁻²² The aim of the present study was to investigate synergistic corrosion inhibition for THAM- Zn^{2+} and HEDP combination to carbon steel immersed in aqueous solution containing 60ppm Cl^- . The corrosion inhibition efficiency was evaluated using mass loss method and the AC impedance spectra. The protective film formed on the metal surface characterized with the help of surface analytical techniques such as Fluorescence Spectra, Fourier Transform

$$IE = 100 \left(1 - \frac{W_2}{W_1} \right) \quad (2)$$

where

W_1 = corrosion rate in the absence of the inhibitor and

W_2 = Corrosion rate in the presence of the inhibitor

AC impedance measurements

EG and G electrochemical impedance analyzer model 6310 was used to record AC impedance measurements. A three electrode cell assembly was used. The working electrode was a rectangular specimen of carbon steel with one face of the electrode of constant 1cm^2 area exposed. A rectangular platinum foil was used as the counter electrode. A time interval of 5 to 10 minutes was given for the system to attain a steady state open circuit potential. Then over this steady state potential, an AC potential of 10 mV was superimposed. The AC frequency was varied from 100 MHZ to 100 KHZ.

The real part (Z') and imaginary part (Z'') of the cell impedance were measured in Ohms for frequencies. The R_t (Charge transfer resistance) and C_{dl} (double layer capacitance) values were calculated. C_{dl} value can be calculated using the following relationship.

$$C_{dl} = \frac{1}{2\pi R_t f_{\max}} \quad (3)$$

Surface characterization studies

The carbon steel specimens were immersed in blank, as well as inhibitor solutions, for a period of three days. After three days, the specimen were taken out and dried. The nature of the film formed on the surface of the metal specimens was analysed by various analysis techniques.

FT-IR spectra

The spectra were recorded in a perkin-Elmer 1600 spectra photometer. The film was carefully removed, mixed thoroughly with KBr and made in to pellets and the FTIR spectra were recorded.

Surface analysis by fluorescence spectroscopy

Fluorescence spectra of solutions and also the films formed on the metal surface were recorded using Jasco-F-6300 spectra fluorometer.

SEM Analysis

SEM provides a pictorial representation in the surface to understand the nature of the surface film in the absence and presence of inhibitors and extent of corrosion of carbon steel. The SEM micrographs of the surface are examined.

Results and Discussion

The corrosion rates (CR) of carbon steel immersed in aqueous solution containing 60 ppm Cl^- and also inhibition efficiencies (IE) in the absence and presence of inhibitor THAM and HEDP obtained by weight loss method are given in Table 2. It is observed from Table 1 that THAM shows some inhibition efficiency. 50 ppm of THAM has 52% inhibition efficiency and 50 ppm of Zn^{2+} has 24% IE . Their combination has 62% IE .

Table 1. Corrosion rates of (CR , mdd) carbon steel immersed in an aqueous solution containing 60 ppm of Cl^- and the inhibition efficiencies (IE %) obtained by weight loss method. Immersion period = 3 days, $\text{pH}=8.84$

Cl^- , ppm	THAM, ppm	Zn^{2+} , ppm	CR , mdd	IE , %
60	0	0	23	-
60	0	50	17.48	24
60	50	50	8.74	62
60	100	50	11.04	52
60	150	50	13.34	42
60	200	50	13.57	41
60	250	50	13.80	40

It is observed that when HEDP is added, the inhibition efficiency of THAM- Zn^{2+} system increases. The increase in IE is more pronounced at 250 ppm of HEDP. Synergistic effect exists between THAM- Zn^{2+} system and HEDP (250 ppm). For example 50ppm of Zn^{2+} and 50ppm THAM has 62% IE . Their combination [THAM (50 ppm) - Zn^{2+} (50 ppm)-HEDP (250 ppm)] has 86% IE .

Table 2. Corrosion rates of (CR mdd) Carbon steel immersed in an aqueous solution containing 60 ppm of Cl^- , and the inhibition efficiencies (IE %) obtained by weight loss method. Immersion period = 3days, $\text{pH} = 8.84$

Cl^- , ppm	THAM, ppm	Zn^{2+} , ppm	CR , mdd	IE , %
60	0	0	23	-
60	0	50	17.48	24
60	50	50	8.74	62
60	100	50	11.04	52
60	150	50	13.34	42
60	200	50	13.57	41
60	250	50	13.80	40

Synergism considerations

According to studies by Gomma²³ the synergism parameter (S_I) can be calculated using the relationship given by Aramaki and Hackmann.²⁴

$$S_I = \frac{1 - \theta_{1+2}}{1 - \theta'_{1+2}} \quad (4)$$

where

$$\theta_{1+2} = (\theta_1 + \theta_2) - (\theta_1\theta_2)$$

θ_1 = surface coverage for substance (HEDP)

θ_2 = surface coverage for substance (THAM- Zn^{2+})

θ'_{1+2} = surface coverage for combined substance (THAM- Zn^{2+} - HEDP), when θ is the surface coverage, $\theta = IE/100$.

The values of synergism parameters are given in Table 3. It is observed that the value of synergism parameter is greater than 1. This suggests that a synergistic effect exists between THAM and Zn^{2+} (50 ppm) system and HEDP (250 ppm) when the value of synergism parameter is less than one. It is an indication that the synergistic effect is not significant.

Table 3 Inhibition efficiencies and synergism parameters for THAM- Zn^{2+} - HEDP systems, when carbon steel immersed in an aqueous solution containing 60 ppm Cl^- ; Immersion period 3 days, pH = 8.84

Cl^- , ppm	THAM, ppm	Zn^{2+} , ppm	CR, mdd	IE, %
60	0	0	23	-
60	0	50	17.48	24
60	50	50	8.74	62
60	100	50	11.04	52
60	150	50	13.34	42
60	200	50	13.57	41
60	250	50	13.80	40

A=HEDP System; B = Zn^{2+} + THAM System; C = THAM- Zn^{2+} -HEDP System

Analysis of AC impedance spectra

AC impedance spectra of carbon steel immersed in aqueous solution containing 60 ppm Cl^- in the absence and presence of inhibitors are shown in Fig. 1 (Nyquist plots) and Fig. 2, Fig. 3 (Bode plots). The corrosion parameters namely charge transfer resistance and double layer capacitance derived from Nyquist plots are given in Table 4. The impedance ($\log Z \text{ ohm}^{-1}$) values derived from Bode plots are also given in Table 4. It is observed that when carbon steel immersed in an aqueous solution containing 60 ppm Cl^- , the R_t value is 428 ohm cm^2 . The C_{dl} value is $1.19 \times 10^{-8} \text{ F cm}^2$. The impedance value [$\log Z \text{ ohm}^{-1}$] is 2.683.

When inhibitors (50 ppm of THAM + 50 ppm of Zn^{2+} + 250 ppm HEDP) are added the R_t value increases from 428 to 1716 ohm cm^2 . The C_{dl} value decreased from 1.19×10^{-8} to $0.297 \times 10^{-8} \text{ F cm}^2$. The shape of the plot suggests that it is a diffusion controlled process. The impedance value increases from 2.683 to 3.90. This observation suggests that a protective film is formed on the metal surface.

Table 4. Corrosion parameters of carbon steel immersed in an aqueous solution containing 60 ppm of Cl^- obtained from AC impedance spectra. Immersion period 3 days, pH = 8.84

Cl^- , ppm	THAM, ppm	Zn^{2+} , ppm	CR, mdd	IE, %
60	0	0	23	-
60	0	50	17.48	24
60	50	50	8.74	62
60	100	50	11.04	52
60	150	50	13.34	42
60	200	50	13.57	41
60	250	50	13.80	40

D = Aqueous solution containing 60 ppm Cl^- ; E = THAM (50 ppm); Zn^{2+} (50 ppm); HEDP (250 ppm)

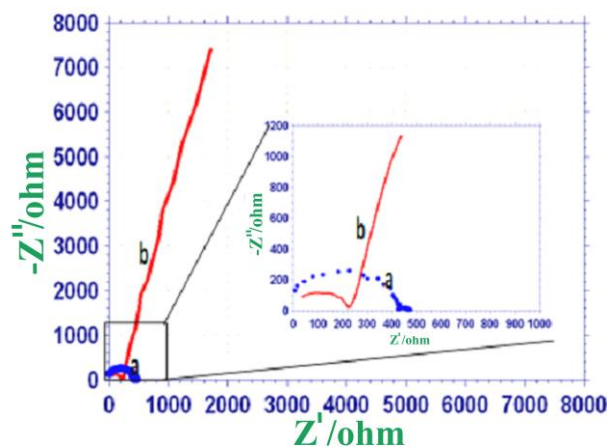


Figure 1. AC impedance spectra of carbon steel immersed in various test solutions (Nyquist Plot); a) 60 ppm Cl^- (blank); b) 60 ppm Cl^- + THAM (50 ppm) + Zn^{2+} (50 ppm) + HEDP (250 ppm)

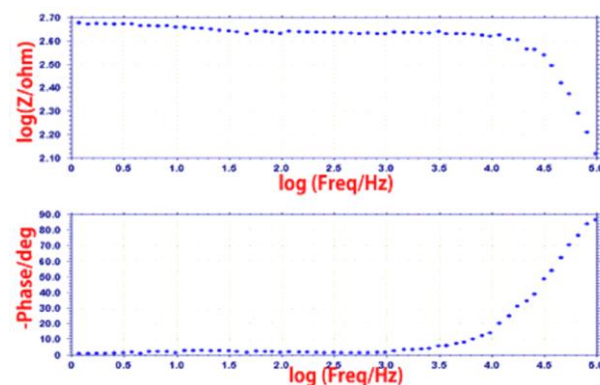


Figure 2. AC impedance spectra of carbon steel immersed in various test solutions (Bode Plot) a) 60 ppm Cl^- (Blank)

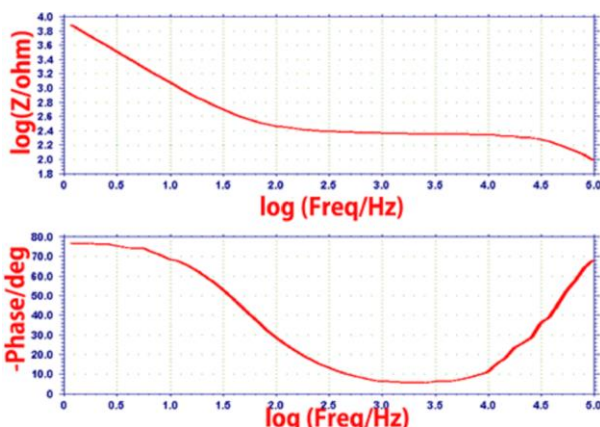


Figure 3. AC impedance spectra of carbon steel immersed in various test solutions (Bode Plot); a) 60 ppm Cl^- + THAM (50 ppm) + Zn^{2+} (50 ppm) + HEDP (250 ppm)

Analysis of the UV-Visible absorption spectra

The UV-Visible absorption spectrum of an aqueous solution containing THAM and Fe^{2+} is shown in Figure 4. A peak appears at 305 nm. This is due to formation of THAM- Fe^{2+} complex in solution. When HEDP solution is added to the above solution, the intensity of the UV-Visible

absorption spectra slightly increases at 314 nm. This peak is due to formation of Fe^{2+} -HEDP complex and THAM- Fe^{2+} complex in solution.²⁵⁻²⁶

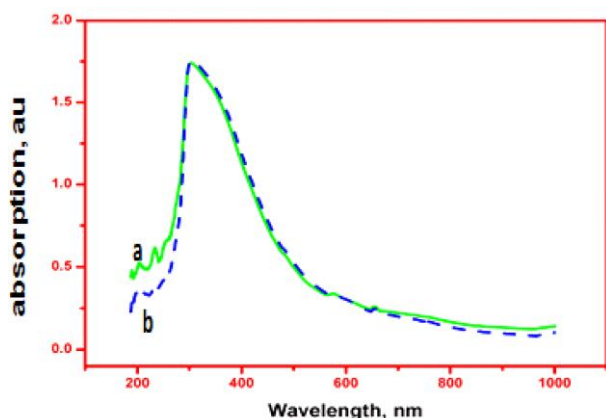


Figure 4. UV-absorption spectra solution containing a) THAM- Fe^{2+} system complex in solution; b) Fe^{2+} -THAM and Fe^{2+} -HEDP complex in solution (Fe^{2+} -THAM+HEDP solution)

Fluorescence spectra

The emission (λ_{ex} 305nm) of solution containing THAM- Fe^{2+} -HEDP complex is shown in Figure 5. A peak appears at 314 nm. The emission spectrum of the film formed on the metal surface after immersion in solution containing 50 ppm of THAM, 50 ppm of Zn^{2+} , 250 ppm of HEDP is shown in Figure 5. A peak appears at 314 nm.

Hence, it is concluded that the protective film consists of Fe^{2+} -THAM complex and Fe^{2+} -HEDP complex, the number of peak obtained is only one. Hence it is informed that the complex of somewhat highly symmetric in solution.²⁷

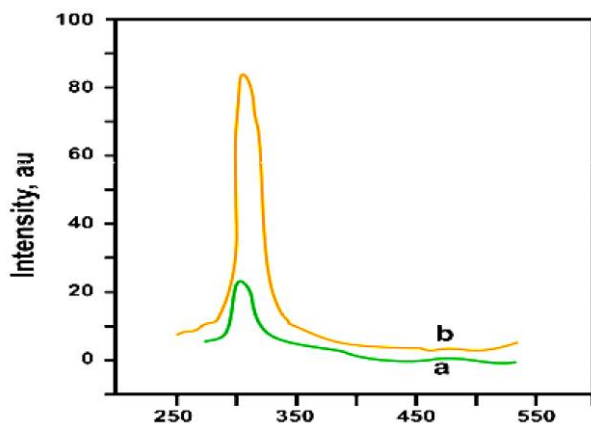


Figure 5. Fluorescence spectra, a) THAM- Fe^{2+} -HEDP complex in solution; b) Film formed on metal surface after immersion in solution containing 50 ppm of THAM and 50 ppm of Zn^{2+} and 250 ppm of HEDP

Analysis of FTIR spectrum

The FTIR spectra have been used to analyze the film formed on the metal surface. The FTIR spectrum of pure THAM is shown in Figure 6. The NH stretching frequency and -OH stretching frequency have overlapped and appears at 3350 cm^{-1} . The CN stretching frequency appears at 1042 cm^{-1} . FTIR spectrum of pure HEDP is shown in Figure 7.

The FTIR spectrum of the film formed on the metal surface after immersion in the solution containing 60 ppm Cl^- , 250 ppm HEDP 50 ppm THAM and 50 ppm of Zn^{2+} is shown in Figure 8. The P-O stretching frequency of HEDP has shifted from 1119 cm^{-1} to 1071 cm^{-1} .²⁸⁻³⁰ This indicates that the formation of Fe^{2+} -HEDP complex on the metal surface. The -OH stretching frequency has shifted from 3350 cm^{-1} to 3403 cm^{-1} . The C-N stretching frequency has shifted from 1042 cm^{-1} to 1021 cm^{-1} . This suggests that HEDP and THAM have coordinated with Fe^{2+} , through their polar groups resulting in the formation of Fe^{2+} -HEDP complex and Fe^{2+} -THAM complex. The peak at 1384 cm^{-1} is due to Zn-O stretching. The -OH stretching frequency appears at 3350 cm^{-1} . These results suggest the formation of $\text{Zn}(\text{OH})_2$ on metal surface.³¹⁻³⁵

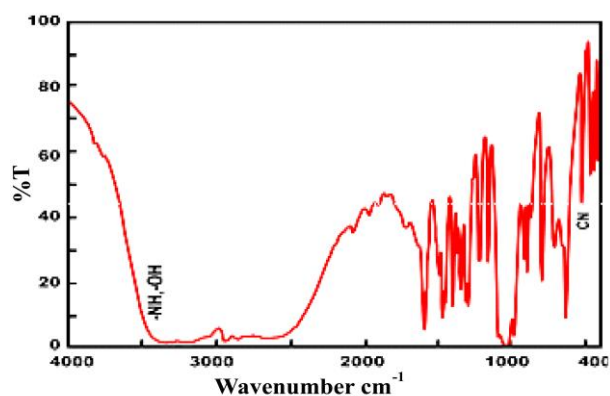


Figure 6. IR spectrum of pure THAM

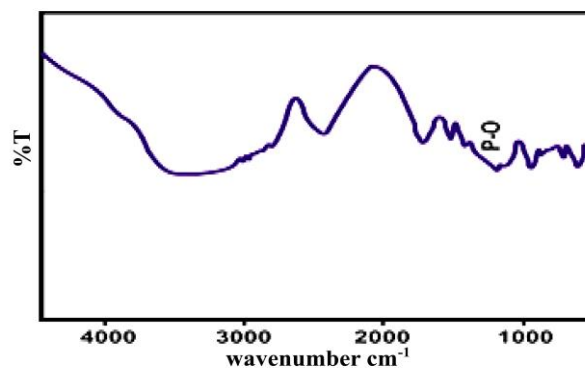


Figure 7. IR spectrum of pure HEDP

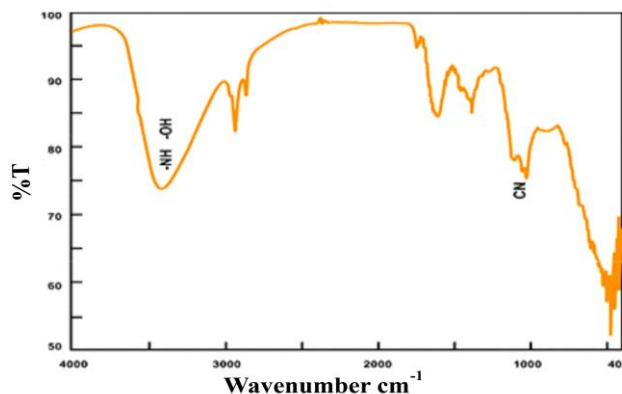


Figure 8. Film formed on carbon steel after immersion in aqueous solution containing Zn^{2+} + 250 ppm of HEDP

SEM analysis of metal surface

The SEM images of different magnification (X500, X1000) of carbon steel specimen immersed in aqueous solution contain 60 ppm of Cl^- for 3 days in the absence and presence on 50 ppm THAM and 50 ppm Zn^{2+} and 250 ppm of HEDP, the surface coverage increases which in turn results in the formation of insoluble complex on the surface of the metal.³⁶ In the presence of THAM and Zn^{2+} and HEDP system the surface is covered by a thin layer of inhibitors which effectively control the dissolution of carbon steel Figure 10.

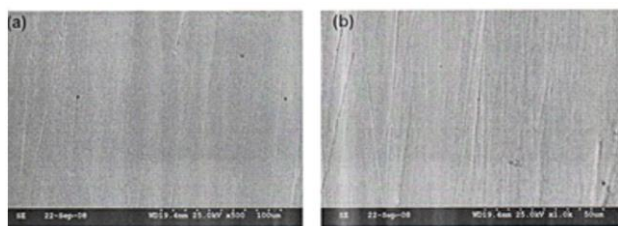


Figure 9. SEM micrographs of a) Carbon steel (control); Magnification-X 500; b) Carbon steel (control); Magnification-X 1000

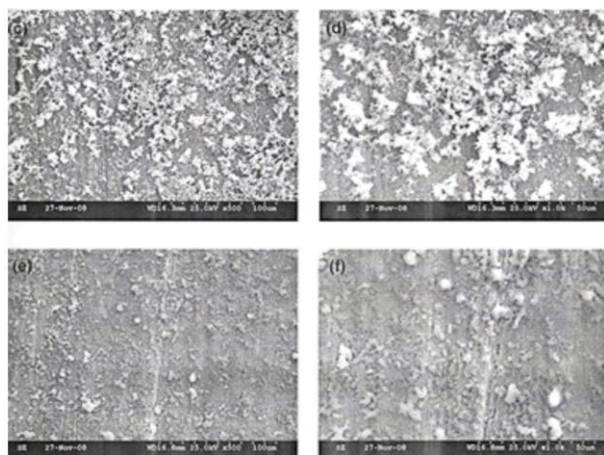


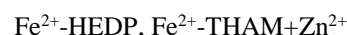
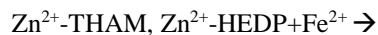
Figure 10. SEM micrographs of a) 60 ppm Cl^- Magnification-X 500; b) 60 ppm Cl^- Magnification-X 1000; c) THAM 50 ppm + Zn^{2+} 50 ppm + 60 ppm Cl^- + HEDP 250 ppm, Magnification - X500; d) THAM 50 ppm + Zn^{2+} 50 ppm + 60 ppm Cl^- + HEDP 250 ppm Magnification -X1000

Conclusion

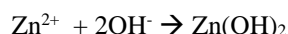
The results of the weight loss study shows that the formulation consisting of 50 ppm THAM and 50 ppm of Zn^{2+} and 250 ppm HEDP has 86% of inhibition efficiency in controlling corrosion of carbon steel. AC impedance spectra reveal that the protective film formed on the metal surface. FTIR spectra reveal that the protective film consists of Fe^{2+} -THAM complex and Fe^{2+} -HEDP complex and $Zn(OH)_2$.

When carbon steel is immersed in solution containing 60 ppm of Cl^- , 50 ppm of THAM, 50 ppm of Zn^{2+} and 250 ppm of HEDP, the Zn^{2+} -THAM, Zn^{2+} -HEDP complex diffuses from the bulk of the solution towards metal surface.

On the metal surface Zn^{2+} -THAM-HEDP complex is converted in to Fe^{2+} -THAM, Fe^{2+} -HEDP complex on the anodic sites. Zn^{2+} is released.



The released Zn^{2+} combines with OH^- to form $Zn(OH)_2$ on the cathodic sites .



References

- Felhosi, I., Keresztes, Z., Karman, F. H., Mohai, M., Bertoti, I. and Kalman, E., *J. Electrochem. Soc.*, **1999**, *146*, 961 – 969.
- Gonzalez, Y., Lafont, M. C., Pebere, N., Moran, F. A., *J. Appl. Electrochem.*, **1996**, *26*, 1259-1265.
- Manasa, J. L. and Szybalski, W., *Corrosion.*, **1952**, *8*, 381.
- Rajagopalan, K. S. and Veni, K., *Indian J. Techn.*, **1968**, *6*, 239.
- Wood, J. W., Beecher, J. S. and Lawrence, P. S., *Corrosion*, **1957**, *13*, 41.
- Bogatyreva, E. V. and Balezin, S. A., *Zh. Prikl. Khim.*, **1962**, *35*, 1071.
- Bogatyreva, E. V. and Nagaev, V. V., *Zh. Prikl. Khim.*, **1962**, *35*, 550.
- Rajendran, S., Aparao, B. V. and Palanisawamy, N. J., *Electrochem. Soc. India.*, **1998**, *47*, 43.
- Rajendran, S., Aparao, B. V. and Palanisawamy, N., *Anti-Corros. Methods Mater.*, **1998**, *45*, 25.
- Kuzentsov, Y. I. and Bardasheva, T., *Zashch. Metall.*, **1998**, *24*, 234.
- Airey, K., Armsmang, R. D. and Handside, T., *Corros. Sci.*, **1998**, *28*, 449.
- Rajendran, S., Apparao, B. V., Mani, A. and Palaniswamy, N., *Anti-Corros. Methods Mater.*, **2000**, *47*, 294.
- Rajendran, S., Apparao, B. V. and Palaniswamy, N., *Anti-Corros. Methods Mater.*, **1997**, *44*, 308.
- Rajendran, S., Vaibhavi, S., Antony, N. and Tirvedi, D. C., *Corrosion.*, **2003**, *59*, 529.
- Rajendran, S., John Amalraj, A., Jasmine Joice, M., Anthony, N., Trivedi, D. C. and Sundaravadivelu, M., *Corros. Rev.*, **2004**, *22*, 233-248.
- Awerd, H. S. and Turgoose, S., *Corros. J.*, **2002**, *37*, 147.
- Braisaz, T. and Tounsi, A., *Corros. Sci.*, **2008**, *50*, 124.
- Tounsi, A., *Corros. Sci.*, **2008**, *50*, 124.
- Gunasekaran, G., Natarajan, R., Muralidharan, V. S., Palaniswamy, N. and Appa Rao, B. V., *Anti-Corros. Methods Mater.*, **1997**, *44*, 248.
- Kinlen, P. J., Ding, Y., Silverman, D. C., *Corrosion.*, **2002**, *6*, 490.
- Shaban, A., Kalman, E. and Biczol, I., *Corros. Sci., Methods Mater.*, **1993**, *35*, 463.

- ²²Muller, B. and Forster, R., *Corros. Sci.*, **1996**, 38, 1103.
- ²³Gomma, G. K., *Mater., Chem. Phys.*, **1998**, 55, 241.
- ²⁴Aramaki, K. and Hackmann, J., *Electrochem. Soc.*, **1969**, 116, 568.
- ²⁵Rajendran, S., Maria Joany, R., Apparao, B. V. and Palani Swamy, N., *Indian J. Chem. Technol.*, **2002**, 9, 197-200.
- ²⁶Rajendran, S., Earnest John Peter, B. R., Peter Pascal Reses, A., John Amalraj, A. and Sundaravadelu, M., *Trans. SABST.*, **2003**, 38(1), 11-15.
- ²⁷Rajendran, S. and John Amalraj, A., *Bull. Electrochem.*, **2005**, 21, 185-191.
- ²⁸Silverstein, R. M., Basler, G. C. and Morrill, T. C., *Spectroscopic Identification of Organic Compounds.*, 4th Ed, John Wiley and Sons, **1981**.
- ²⁹Cross, A. D., *Introduction to Practical Infrared Spectroscopy*, Butterworths Scientific. Publication, **1990**.
- ³⁰Kzaou Nakamoto., *Infrared and Raman Spectra of Inorganic and Coordination Compound.*, Wiley. Interscience, **1986**.
- ³¹Rajendran, S., Apparao, B. V. and Palanisamy, N., *Bull. Electrochem.*, **1996**, 12, 15.
- ³²Sekine, I., Hirakawa, V., *Corrosion.*, 1986, 42, 276.
- ³³Rajendran, S., Apparao, B. V. and Palanisamy, N., *Proc. 2nd Arabian Corros. Conf.*, Kuwait., **1996**, 483.
- ³⁴Rajendran, S., Apparao, B. V. and Palaniswamy, N., *Proc. 8th Eur. Symp. Corros. Inhibitors*, Ferrara, Italy., **1995**, 1, 465.
- ³⁵Ganesha Achary., Sachin, H. P., Shire Kumara, S., Arthoba Naik, Y. and Venkatesha, T. V., *Russ. J. Electrochem.*, **2007**, 43(7), 844-849.
- ³⁶Vera, R., Scherebler, R., Cury, P., Del Rio, R. and Romero, H. J., *Appl. Electrochem.*, **2007**, 37, 519-525.

Received: 06.04.2013.

Accepted: 17.04.2013.



NEW DEVELOPMENTS IN THE RADIOLYSIS AND OZONOLYSIS OF LANDFILL LEACHATE

Franco Cataldo^{[a,b]*}, Giancarlo Angelini^[a]

Keywords: landfill leachate, pollution, COD, radiolysis; ozonolysis

Old and young municipal landfill leachates samples were radiation processed with γ rays at a dose rate of 1 kGy h⁻¹. The fate of the soluble organic matter (humic substance) present in the leachates was followed by the chemical oxygen demand (COD) measurements. The radiolysis of old landfill leachate is a not an effective process in comparison to ozonolysis but can be enhanced significantly by the addition of H₂O₂ to the old leachate prior to radiolysis and by bringing the pH of the leachate to zero. Some radiolyzed sample were further ozonized to reduce to the minimum possible the COD level. Young landfill leachate results instead more prone to radiolysis and less sensitive to ozonolysis than the old landfill leachate.

* Corresponding Authors

E-Mail: franco.cataldo@fastwebnet.it

[a] CNR-Istituto di Metodologie Chimiche, Area della Ricerca di Montelibretti, Via Salaria Km 29,300, 00016, Monterotondo Scalo, Rome, Italy

[b] Lupi Chemical Research srl, Via Casilina, 1626A, 00133 Rome, Italy

Introduction

Landfilling of the municipal wastes is still today one of the major way to get rid of garbages.¹ However, the landfilled wastes release for years a liquor due to the decomposition of the organic garbages and due to the rain waters which pass through the landfill washing away and extracting the soluble or solubilised matter.¹ The black liquor is known as landfill leachate. There is no standard landfill leachate since its properties in terms of type and concentration of soluble organic matter, inorganic components vary with atmospheric conditions and ageing of the landfill site.^{2,3} In general, in the rainy seasons the landfill leachate presents lower concentration of soluble organic matter and inorganic components while in the dry seasons it occurs the opposite. Furthermore, the soluble organic matter present in a leachate is completely different if the leachate is coming out from a recent or an old landfill site.^{2,3} In general, the old landfill leachate is characterized by relatively low content of soluble organic matter as measured by the COD (COD=Chemical Oxygen Demand) in comparison to the very high COD levels of a young leachate.¹⁻³ Additionally, the pH of an old leachate is typically weakly basic in contrast with the COD of a young leachate which is instead acidic.¹⁻³ The relatively low COD level of the old leachate is compensated by the fact that the soluble organic matter present in it under the form of humic substances (HS) is extremely refractory to oxidation even by powerful oxidizing agents like ozone.⁴⁻⁶ It is also not biodegradable by microorganisms because it is already the result of methanogenic fermentation which has transformed the soluble organic matter present in the young leachate into methane and into a refractory HS.¹⁻³ In a previous work we have discussed about chemical structure of the HS of the old leachate.⁷ The reason of its resistance to chemical and biochemical degradation must be attributed to its relatively high molecular weight and high degree of aromatic content.^{2,3,6,7}

The purification of the water containing landfill leachate represents a real challenge. A number of different treatments have been proposed but does not exist “the dedicated treatment” for the landfill leachate.¹⁻⁸ The problem regards not only the degradation of the HS present in the leachate but also the elimination of certain transition metals which occur in the leachates^{1-3,9} as well as the elimination of pathogens¹ which proliferate in a broth rich of nutrients as it is especially the young landfill leachate but also the old leachate. Therefore, the solution to the leachate problem should take into account these three problems all together: mineralization of the HS, elimination or reduction of transition metals and free ammonia (for old leachates) and sterilization of the leachate from the pathogens. In a previous work we have examined the combined action of activated carbon and ozone in the treatment of old leachate with encouraging results.⁸ Indeed, the ozonolysis of old leachate leads to a reasonable, although unsatisfactory, reduction of the COD and to the sterilization of the liquor, while activated carbon is able to adsorb the oxidized HS and even large part of the transition metals.^{6,8} In order to find more radical solutions, we have studied also the action of high energy radiation on old landfill leachate followed by ozonolysis.⁷ Water radiolysis with γ radiation generates essentially •OH radicals which are the powerful oxidizing agents resulting also from advanced oxidation processes.^{5,10-13} With surprise we have found that radiolysis of neat old leachate is completely not effective on the mineralization of HS.⁷ The reason of this failure is certainly to be ascribed to the high concentration of carbonate, bicarbonate ions and free ammonia in the leachate which act as free radical scavengers especially against the •OH radicals hindering the effects. Furthermore, previous studies have recommended the combined action of an oxidizing agent with radiation to treat polluted waters and wastewater.¹⁰⁻¹³

In the present work, the radiolysis of old landfill leachate has been conducted in presence of H₂O₂ as oxidizing agent and also in acidic conditions to decompose the carbonates and bicarbonates and to transform the free ammonia in ammonium ion. The radiolyzed leachate samples were also ozonized wherever possible and in any case the radiolysis effects on COD were compared with the ozonolysis effects. Also a sample of young landfill leachate with high COD was radiolyzed.

Experimental

Landfill leachate sampling

Landfill leachate sample was obtained from a municipal landfill located in the central Italy. Three different samples of landfill leachate were taken from the site. One sample was taken in a site which is 6–7 years old and consists of an old landfill leachate with COD = 5165 mg L⁻¹. The second sample was taken in the oldest area of the landfill site which was about 10 years old and was characterized by a COD = 2376 mg L⁻¹. The third sample was taken in another area which has been recently land-filled and the resulting leachate is defined as young landfill leachate with a COD = 9200 mg L⁻¹.

COD (Chemical Oxygen Demand) measurements

The COD (Chemical Oxygen Demand) was measured with the bichromate methodology according to the ISO 15705 standard test.

Irradiation procedure

The landfill leachate samples in closed vials were irradiated in presence with a ⁶⁰Co γ -ray source at the CNR-IMC facility using a dose rate of 1 kGy h⁻¹.

Old and virgin landfill leachate radiolysis followed by ozonolysis

The virgin old landfill leachate having a starting COD value of 5165 mg L⁻¹ was transferred in 7 different vials which were tightly closed with a screw cap. Each vial was filled with 20 ml of leachate. Only 1 vial was kept as reference and the other vials were irradiated at 12.5, 25, 50, 100, 200 and 400 kGy respectively. After the radiolysis the vials were opened and sampled for the COD analysis and for the pH measurements. Afterwards the radiolyzed sample were ozonized following a standard procedure reported in a previous work.¹⁴ After the ozonolysis the COD of each sample was measured again.

Old landfill leachate radiolysis with H₂O₂ followed by ozonolysis

In this series of experiments the old and virgin leachate had a COD = 2376 mg L⁻¹. The addition of 1 ml of H₂O₂ to the leachate led the COD (after 14 days) at 1872 mg L⁻¹ while the pH remained unchanged at about 8.4. The COD value of 1872 mg L⁻¹ was taken as starting value for all the following experiments. A series of 6 vials were filled with 20 ml each of old landfill leachate and treated with 1 ml each of H₂O₂ 36% solution. Only 1 vial was kept as reference and the other vials were irradiated at 12.5, 25, 50, 100, 200 and 400 kGy respectively. After the radiolysis the vials were opened and sampled for the COD analysis and for the pH

measurements. Afterwards the radiolyzed sample were ozonized following a standard procedure reported in a previous work.¹⁴ After the ozonolysis the COD of each sample was measured again. Also the reference, non-radiolyzed sample having a starting COD = 1872 mg L⁻¹ was ozonized and the COD was measured again after the ozonolysis.

Old landfill leachate radiolysis with H₂O₂ at pH = 0

In this series of experiments the old and virgin leachate had a COD = 2376 mg L⁻¹. The acidification of 20 ml of leachate with 1 ml of HCl 9% brings the pH from 8.4 to nearly zero. After the acidification the COD was found at 1990 mg L⁻¹. The addition of 1 ml of H₂O₂ to the leachate led the COD (after 14 days) at 1858 mg L⁻¹ while the pH=0. The COD value of 1858 mg L⁻¹ was taken as starting value for all the following experiments. A series of 6 vials were filled with 20 ml each of old landfill leachate and treated with 1 ml each of H₂O₂ 36% solution. Only 1 vial was kept as reference and the other vials were irradiated at 12.5, 25, 50, 100, 200 and 400 kGy respectively. After the radiolysis the vials were opened and sampled for the COD analysis and for the pH measurements.

Young and virgin landfill leachate radiolysis

In this series of experiments the young and virgin leachate with a COD = 9200 mg L⁻¹ was irradiated in a series of 3 vials filled with 20 ml each of the young leachate. The vials were irradiated at 100, 200 and 400 kGy respectively. After the radiolysis the vials were opened and sampled for the COD analysis and for the pH measurements. Only the reference sample was ozonized and the resulting COD measured.

Results and Discussion

Radiolysis and ozonolysis of old landfill leachate

As discussed in a previous work⁷ the radiolysis of an old landfill leachate is completely unsuccessful since the COD of the leachate remains practically unaffected by the action of γ radiation at any dose level. Even at the very high dose of 400 kGy (Fig. 1, blue line and circles) the radiolysis of an old landfill leachate does not lead to any evident abatement of the COD level. The ozonolysis of radiolyzed landfill leachate leads to a reduction of the COD but not at the same level reached by direct ozonolysis of pristine and not radiolyzed leachate (Fig. 1).

The COD data can be elaborated as index values according to the following equation:

$$\text{COD}_{\text{Index Value}} = [(\text{COD})_x / (\text{COD})_0] 100 \quad (1)$$

with (COD)₀ the chemical oxygen demand of the pristine, virgin leachate and (COD)_x the chemical oxygen demand measured at any radiation dose level.

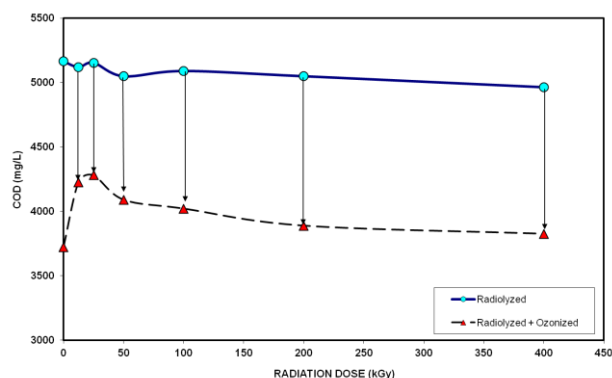


Figure 1. The radiolysis of an old landfill leachate has no effects on its COD and causes a resistance to ozonolysis

Of course, in the condition that $(COD)_x = (COD)_0$ then the $COD_{Index\ Value} = 100$. Then, from Fig. 2 it is possible to observe that after the radiolysis of the landfill leachate up to 400 kGy the COD remained 96% of the starting value, a really negligible reduction. The subsequent ozonolysis reduces the COD to 74% of the original value but the direct ozonolysis of pristine leachate (without radiolysis) leads directly to a COD which is 72% of the starting value.

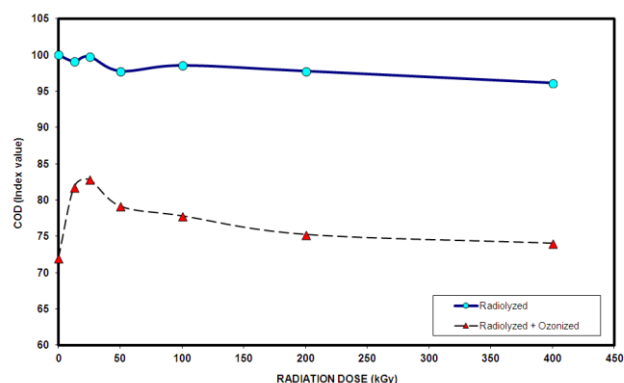


Figure 2. COD index values of radiolyzed (blue circles) and radiolyzed + ozonized (red triangles) landfill leachate

Thus, the conclusion is that high energy radiation is not able to degrade the organic soluble matter present in the leachate which is composed by humic substance and consequently such matter is considered highly refractory to degradation.⁷ As discussed in the introduction, the water radiolysis generates the powerful hydroxyl radicals which are very effective on the degradation of simple aromatic substrates but cannot be as effective with humic acids because these molecules are already highly polyhydroxylated.^{3,7} Another key hindering effect occurring during the radiolysis of a leachate is due to the presence of carbonate ions, ammonium ions and several transition metal ions which certainly scavenge the $\bullet OH$ species inhibiting the degradation reactions expected by the hydroxyl radicals. Only in this way it is explainable the failure of the old leachate radiolysis process.¹⁰⁻¹³

Furthermore, Fig. 2 shows an increased resistance of the landfill leachate to ozonolysis after the radiation processing. Such effect is particularly evident at the low radiation dose of 12,5 and 25 kGy and becomes less evident at higher doses.

For example, at 25 kGy the ozonolysis leads the COD to 83% of the pristine leachate while the direct ozonolysis without radiation processing leads to 72% of the starting value. This fact can be explained in terms of crosslinking reactions occurring in the humic substance especially at low radiation doses making the substrate less prone to react with ozone. After all, it is well known that the radiation processing of macromolecules has a double effect of causing crosslinking reactions and chain scission reactions.¹⁰ For the humic substance present in the landfill leachate it appears that at low radiation dose in weakly alkaline conditions the crosslinking reaction is prevalent reducing the sites where ozone can exert its oxidative degradation action.

Radiolysis and ozonolysis of old landfill leachate after H_2O_2 addition and pH adjustment

Because of the disappointing results from the straight radiolysis of the landfill leachate, it was thought to add an oxidant to the leachate prior to the radiolysis.¹¹ It was expected that the combined action of an oxidant with the radiation will improve the effects of the latter. As described in the experimental section, a new sample of old landfill leachate having lower COD value than that reported in the previous section, was treated with H_2O_2 and then submitted to radiolysis at the usual radiation doses. The starting COD value of the pristine sample was 2376 mg L^{-1} and the addition of H_2O_2 without radiation lowered the COD to 1872 mg L^{-1} which was taken as the real starting value for this series of experiments. The series of experiments on old landfill leachate have shown that the pH of the leachate is not affected by the radiation treatment. In fact, the pH of the leachate was 8.5 in the pristine sample and it was found at the same level also after 400 kGy. Instead, the leachate pre-treated with H_2O_2 and then radiolyzed shows a clear trend toward a reduction in the pH value (Fig.3).

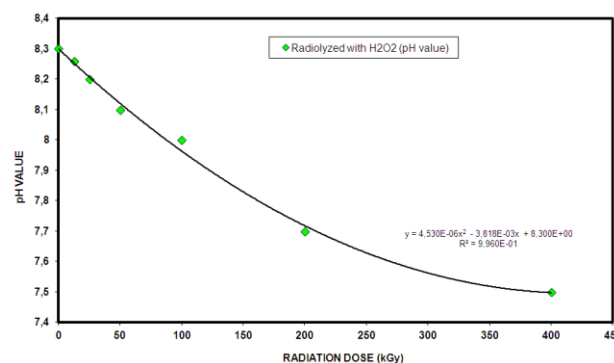


Figure 3. Reduction of the pH as function of the radiation dose: old landfill leachate with H_2O_2

Old landfill leachate is characterized by a weak alkaline pH usually comprised between 8 and 9. Basic pH is due to the presence of free ammonia in the leachate. As shown in Fig. 3, the leachate radiolysis in presence of H_2O_2 leads to a pH reduction from weak basicity toward neutrality. This trend could be explained in terms of reduction of the free ammonia concentration because of its reaction with $\bullet OH$ radicals with formation of hydroxylamine NH_2OH or other oxidation products like nitrite and nitrates.¹⁰

Even more interesting than the pH trend as function of the radiation dose is the COD trend in the leachate radiolyzed with H₂O₂. Fig. 4 shows clearly a trend to lower COD although an induction threshold is also evident till 50 kGy. In other words, the COD level of the H₂O₂ treated leachate remains practically unchanged till a threshold of 50 kGy, showing afterwards, at higher radiation doses, a clear trend to lower COD values never seen in the case of the radiolysis of the virgin leachate as shown in Fig. 1 and 2.

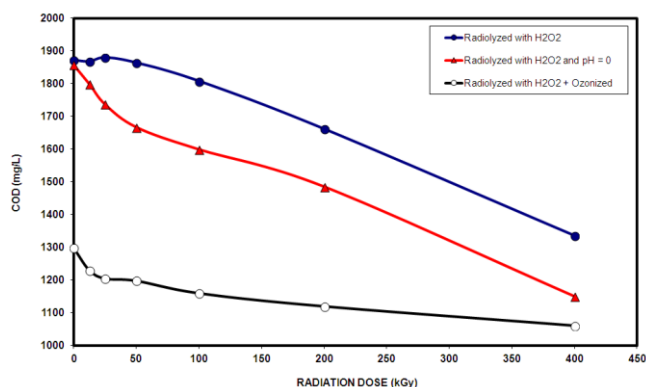


Figure 4. COD values of landfill leachate radiolyzed in presence or without H₂O₂; note the pH=0 effects

Therefore, it can be affirmed that the idea to add H₂O₂ to the leachate prior to the radiolysis was successful in the effectiveness of the partial mineralization of the soluble organic matter. In Fig. 5 the COD reduction occurred in Fig. 4 was indexed according to eq. 1 considering 100 the starting COD level of the leachate treated with H₂O₂.

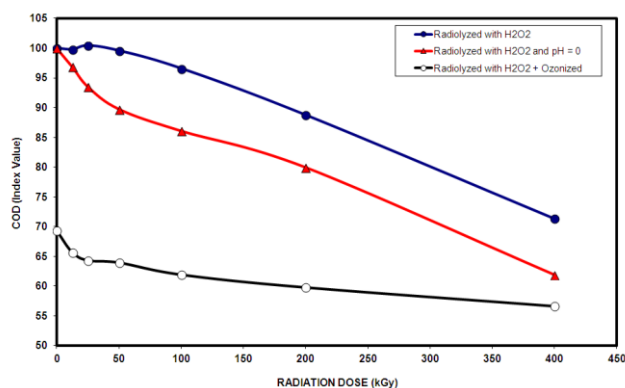


Figure 5. COD data in the ordinate of Fig. 4 are reported as index value by putting 100 the COD of the pristine landfill leachate.

At 200 kGy (Fig. 5) the COD was reduced to 89% of the starting value and at 400 kGy to 71% of the starting value. These results were never reached with the virgin leachate radiolyzed to these dose levels in the absence of H₂O₂ (compare Fig. 2 with Fig.5). The radiolyzed samples treated with H₂O₂ after radiolysis (at any dose used) did not show any residual level of unreacted H₂O₂ suggesting that it was consumed completely in the oxidation process of the soluble humic matter. To assess the complete consumption of H₂O₂, an assay of each radiolyzed sample was treated with a small amount of catalase, the enzyme which specifically decomposes hydrogen peroxide. There were no evidences of O₂ liberation after the addition of catalase, confirming the decomposition of all H₂O₂ originally added. The ozonolysis of the radiolyzed samples brought the COD level between

65% to 58% of the starting value respectively at the lowest and highest radiation dose employed (Fig. 5). These results are significantly better than the results obtained from the direct ozonolysis of the landfill leachate treated with H₂O₂ but not radiolyzed where the COD abatement was stopped to only 69% of the starting value. The ozonolysis results in the COD abatement of the H₂O₂-treated and radiolyzed leachate samples are even better than the ozonolysis results of the radiolyzed virgin leachate samples. In the former case (Fig. 5) the best result is the COD reduction to 58% of the starting value while in the latter case (Fig. 2) the COD reduction due to radiolysis + ozonolysis stopped at 75% of the starting value at 400 kGy for both cases. Furthermore, even at low radiation dose the leachate + H₂O₂ shows a good tendency to undergo the ozonolysis without showing the phenomenon of ozonolysis resistance observed and discussed for the virgin leachate in Fig. 1 and 2 attributable to a prevalent crosslinking reaction at low radiation doses. Thus, the addition of H₂O₂ is beneficial also in this regard.

Fig. 4 and 5 show also the COD reduction occurred to a landfill leachate sample treated with H₂O₂ and also treated with HCl to pH=0 prior to radiolysis. The acidification causes the release of CO₂ by the decomposition of carbonates and bicarbonates and the locking of free ammonia into the ammonium ion. As mentioned previously, the CO₃²⁻ and HCO₃⁻ ions are among the most effective inhibitors and scavengers of the •OH radicals.^{2,4-6} Their elimination with the acidification of the leachate makes the combined effects of the H₂O₂ with the γ radiation more effective in the mineralization of the humic substances. Indeed the COD abatement as function of the radiation dose as shown in Fig. 4 and 5 is immediately measurable even at very low radiation doses, without the dose induction effect observed in the previous case (leachate + H₂O₂ without pH adjustment). At 50 kGy the COD is 90% of the starting value dropping to 80% at 200 kGy and to 62% the starting value at 400 kGy. These results are significantly better than those obtained at the same doses without the pH adjustments (see Fig. 4 and 5). Thus, it is confirmed that the elimination of CO₃²⁻ and HCO₃⁻ ions is a necessary operation to enhance the effect of hydroxyl ions.

Quantitative evaluation of the COD abatement efficiency

In order to quantify the radiolysis efficiency in the COD abatement in the various conditions adopted, we have used the eq.2:

$$\ln \frac{(COD)_x}{(COD)_0} D^{-1} = \eta \quad (2)$$

where the meaning of (COD)_x and (COD)₀ was already defined in the case of eq.1 and *D* is the radiation dose in kGy. Therefore η is expressed in kGy⁻¹ and is a measurement of the efficiency in the COD abatement as function of the radiation dose. By plotting ln[(COD)_x/(COD)₀] against the dose *D* the graphs of Fig. 6 are obtained and the slopes of the experimental data fitted with a line gives η, the efficiency of a given treatment in the COD abatement in the leachate. All the results of such analysis are reported in Table 1.

Table 1. Efficiency η in the COD abatement and residual COD levels

	η [eq.2]	η index	Residual COD at 400 kGy [eq.1]
Old Landfill Leachate Radiolysis	1.08×10^{-4}	100	96.1%
Old Landfill Leachate + H ₂ O ₂ + Radiolysis	9.67×10^{-4}	895	71.4%
Old Landfill Leachate + pH = 0 + H ₂ O ₂ + Radiolysis	1.21×10^{-3}	1120	61.9%
Young Landfill Leachate Radiolysis	4.22×10^{-3}	3910	59.8%
Old Landfill Leachate Ozonolysis only	n.a.	n.a.	72.0% (*)
Old Landfill Leachate Radiolysis followed by ozonolysis	2.70×10^{-4}	350(**)	74.1%
Old Landfill Leachate + H ₂ O ₂ + Ozonolysis only	n.a.	n.a.	69.3% (*)
Old Landfill Leachate + H ₂ O ₂ + Radiolysis followed by ozonolysis	3.64×10^{-4}	1232(**)	56.7%
Young Landfill Leachate Ozonolysis only	n.a.	n.a.	85.1% (*)

n.a. = not applicable; (*) Residual COD after ozonolysis without radiolysis, thus not at 400 kGy; (**) Derived from the sum of η radiolysis with that of ozonolysis

The elaboration of the experimental data to obtain the η is shown in Fig. 6 as example.

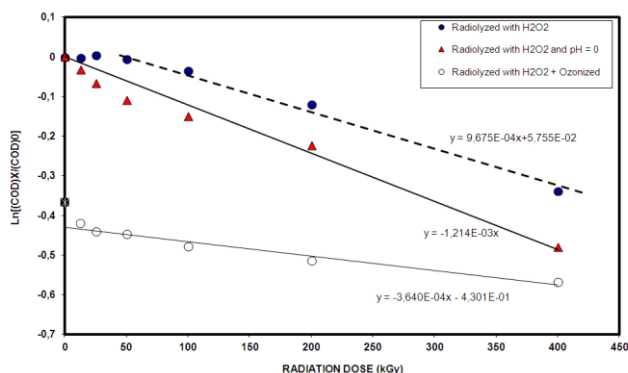


Figure 6. Evaluation of the efficiency η in the COD abatement evaluated according to Eq. 2

As already said, all the data concerning the efficiency of the COD abatement are reported in Table 1.

The radiolysis of old and virgin leachate gives $\eta = 1.08 \times 10^{-4} \text{ kGy}^{-1}$. The addition of H₂O₂ to the old landfill leachate gives $\eta = 9.67 \times 10^{-4} \text{ kGy}^{-1}$. In this case, the first three data points were not considered in the calculation of the slope because of the presence of a threshold effect: only above 50 kGy are evident the effects of radiation on the COD (see also Fig.6). The adjustment of the pH=0 in combination with H₂O₂ yields $\eta = 1.21 \times 10^{-3} \text{ kGy}^{-1}$. As summarized in Table 1, putting as 100 the η value in the COD abatement efficiency in the radiolysis of virgin leachate, the addition of H₂O₂ gives an improvement of a factor 8.95 in η , about one order of magnitude and the results are even above one order of magnitude when the leachate pH is brought to zero together with the addition of H₂O₂, the improvement factor becomes 1.12.

Radiolysis of young leachate

Young landfill leachate is an immature form of landfill leachate with very high COD levels, much higher than those of the old leachate as can be found in Fig. 7.¹⁻³ The young landfill leachate is one or two years old and it is characterized by an acid pH, its COD level although very high is not stabilized and can change with time. Furthermore,

the young leachate is in a phase when the methanogenic fermentation has not yet been started, thus the soluble organic matter has not yet reached the complex polymeric chemical structure typical of the humic substances which are found in the old leachates. In the young leachate the soluble organic matter has lower molecular weight, it is more saturated and less aromatic than the humic substance of the old, mature leachate. Consequently, the young leachate is much less reactive with ozone than the old landfill leachate. In Table 1 it is shown that the COD abatement due to the ozonolysis of a virgin young leachate leads to 85.1% of the starting value while for old and mature leachate the ozonolysis reaches to 72% of the starting COD value. On the other hand the young leachate appears much more sensitive to the radiolysis since, as shown in Fig. 7 the COD undergoes a rapid drop as function of the radiation dose even without the addition of an oxidizing agent.

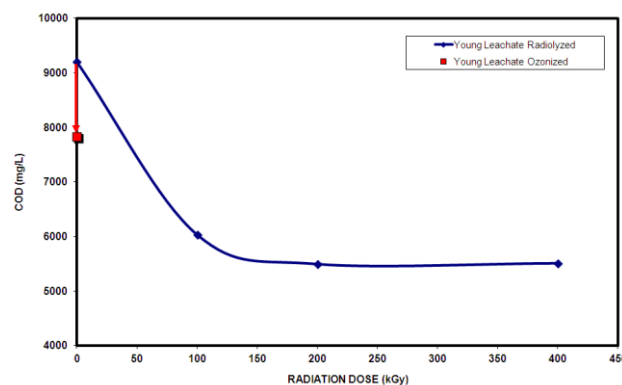


Figure 7. Radiolysis of a young, acidic landfill leachate having an high COD value.

The drop in COD is immediate already at low doses and largely overcomes the COD abatement reachable by simple ozonolysis. In fact, as shown in Table 1, with radiolysis the COD is reduced to 59.8% of the starting value against the 85.1% reachable by using ozonolysis only. Another distinguishable feature of the young landfill leachate regards the fact the maximum of COD abatement is achieved with about 100 kGy. Further radiolysis does not lead to any improvements in the COD even at 400 kGy (see Fig. 7). On the other hand the old landfill leachate with H₂O₂ and even better at pH=0 tends to have a linear response in the COD abatement as function of the radiation dose in the entire dose range explored, i.e. up to 400 kGy.

Using equation 2 and limiting the evaluation in the COD abatement efficiency up to 100 kGy, the young landfill leachate yields $\eta = 4.22 \times 10^{-3} \text{ kGy}^{-1}$ which, as shown in Table 1 corresponds to 3.91 times the η value measured in the radiolysis of virgin and old landfill leachate.

Conclusions

The data in Table 1 clearly show that the radiolysis of virgin old landfill leachate cannot compete with direct ozonolysis since the maximum COD abatement with radiolysis is 96.1% against 72.0% of the original value achieved with ozonolysis.

It was shown that the radiolysis of the landfill leachate in presence of an oxidizing agent like H_2O_2 greatly improves the COD abatement and the response to the radiation dose. With H_2O_2 and radiolysis the COD abatement is reduced to 71.4% of the starting value and hence is comparable to the COD abatement obtained by the combined action of H_2O_2 and ozone without radiolysis: 69.3%. The ozonolysis of the radiolyzed leachate additionated with H_2O_2 leads to a residual COD 56.7% the starting value.

The water radiolysis generates $\bullet\text{OH}$ radicals which are scavenged by a series of ions and chemical species present in the leachate. Old landfill leachate is naturally weakly basic and contains free ammonia, carbonate and hydrogencarbonate anions. All these species are known to be excellent scavengers of the $\bullet\text{OH}$ radicals. This is the reason why the radiolysis of old and pristine landfill leachate is an unsuccessful process and becomes satisfactory only when an oxidant like H_2O_2 is added as a further source of $\bullet\text{OH}$ radicals. The present work as demonstrated that the acidification to $\text{pH}=0$ of an old landfill leachate combined with the H_2O_2 addition and with radiolysis leads to further improvements in the mineralization of the soluble organic matter as suggested by a residual COD at 400 kGy of 61.9% in comparison to 71.4% when the radiolysis of the leachate is conducted with H_2O_2 but in weakly alkaline medium and against 96.1% reached in weakly alkaline medium and in the absence of H_2O_2 .

Young landfill leachate is naturally acidic and the soluble organic matter present in it has not reached the degree of complexity and aromaticity of that present in the old, mature landfill leachate. Thanks to the acidic ambient and to a less "refractory" soluble organic matter, the young landfill leachate is radiolyzed more easily than the old type yielding satisfactory results in the COD reduction already at relatively low dose.

For example, the COD level is reduced to 59.8% with only 100 kGy whereas for the old landfill leachate we have reported previously the results achieved at 400 kGy. Radiolysis is more effective than ozonolysis in the case of virgin young landfill leachate since the radiolysis leads to a residual COD 59.8% of the starting value while the ozonolysis stops at 85.1%. This result is opposite to that with virgin and old landfill leachate which instead is more responsive to ozonolysis (72% residual COD vs starting value) than radiolysis (96.1% residual COD vs starting value).

References

- ¹Christensen, Th. H., Kjeldsen, P., Bjerg, P. L., Jensen, D. L., Christensen, J. B., Baun, A., Albrechtsen, A. J., Heron, G. *Appl. Geochem.*, **2001**, *16*, 659.
- ²Renou, S., Givaudan, J. G., Poulain, S., Dirassouyan, F., Moulin, P. *J. Hazard. Mater.*, **2008**, *150*, 468.
- ³Kang, K. H., Sang Shin, H., Park, H. *Water Res.*, **2002**, *36*, 4023.
- ⁴Kurniawan, T. A., Lo, W., Chan, G. Y. S., *Chem. Eng. J.*, **2006**, *125*, 35.
- ⁵Wu, J. J., Wu, C. C., Ma, H. W., Chang, C. C. *Chemosphere*, **2004**, *54*, 997.
- ⁶Van Aken, P., Lambert, N., Degreve, J., Liers, S., Luyten, J. *Ozone: Sci. Eng.*, **2011**, *33*, 294
- ⁷Cataldo, F., Angelini, G. *J. Radioanal. Nucl. Chem.*, **2012**, *293*, 141
- ⁸Cataldo, F., Angelini, G. *Ozone: Sci. Eng.*, **2013**, *35*, 55
- ⁹Cataldo, F., *J. Radioanal. Nucl. Chem.*, **2012**, *293*, 119
- ¹⁰Woods, R.J., Pikaev, A.K. "Applied Radiation Chemistry", Wiley-Interscience, New York, **1994**
- ¹¹Getoff, N. *Radiat. Phys. Chem.*, **1996**, *47*, 581
- ¹²Emmi, S. S., Takacs, E. "Water remediation by electron beam treatment" In: Spothem-Maurizot, M., Mostafavi, M., Douki, T., Belloni, J. (eds) "Radiation chemistry from basics to applications in material and life science". EDP Sciences, Les Ulis, **2008**.
- ¹³Von Sonntag, C., Schuchmann, H.P., "The chemistry behind the application of ionizing radiation in water pollution abatement". In: Jonah, C., Madhava Rao, B.S. (eds) "Radiation Chemistry Present Status and Future Trends". Elsevier, Amsterdam, **2001**.
- ¹⁴Cataldo, F., Ursini, O., Lilla, E., Angelini, G. *Ozone: Sci. Eng.*, **2010**, *32*, 274

Received: 27.03.2013.

Accepted: 16.04.2013.



ECO-FRIENDLY SYNTHESIS AND SPECTRAL CORRELATIONS IN SOME 1-PHENYL-3-(5-BROMOTHIOPHEN-2-YL)-5-(SUBSTITUTED PHENYL)-2-PYRAZOLINES

G. Thirunarayanan^{[a]*}, P. Mayavel^[a], K. Thirumurthy^[a], S. Dinesh Kumar^[a],
R. Sasikala^[a], P. Nisha^[b] and A. Nithyaranjani^[b]

Keywords: 1-phenyl-3(5-bromothiophen-2-yl)-5-(substituted phenyl)-2-pyrazolines; Green synthesis; IR and NMR spectra; Hammett correlations

A series containing eight 1-phenyl-3(5-bromothiophen-2-yl)-5-(substituted phenyl)-2-pyrazoline derivatives have been synthesized by microwave assisted, solid acidic green catalyst $\text{SiO}_2\text{-H}_3\text{PO}_4$ catalyzed cyclization of 5-bromo-2-thienyl chalcones and phenyl hydrazine hydrochloride under solvent free conditions. The yields of the pyrazolines were more than 85%. The purities of these pyrazolines were checked by their physical constant, micro analysis, Infrared, Nuclear magnetic resonance and Mass spectroscopic data published earlier in literature. From the spectral frequencies, infrared $\nu(\text{cm}^{-1})$ of C=N, C-S, C-Br, ^1H and ^{13}C NMR chemical shifts (δ , ppm) of pyrazoline ring proton, carbon and C=N carbons were assigned and correlated with Hammett substituent constants, F and R parameters. From the results of statistical analysis the effects of substituent on the spectral frequencies have been discussed.

* Corresponding Author

Tel.: +914144238282,

E-Mail: drgtnarayanan@gmail.com

[a] Department of Chemistry, Annamalai University, Annamalainagar-608 002, India.

[b] Department of Chemistry, Dhanalakshmi Srinivasan College of Arts and Science for Women, Perambalur-621 212, India.

INTRODUCTION

The ^1H pyrazolines are well-known important di-nitrogen containing five membered heterocyclic stereo-bioorganic molecules. Hydrazine hydrate or phenylhydrazine hydrate or phenylhydrazine hydrochloride were used for synthesis of pyrazoles derivatives by cyclization of enones. The pyrazoline ring protons were bonded with carbon atoms spatially different environment. The α,β -unsaturated ketones can play the role of versatile precursors in the synthesis of the corresponding pyrazolines.¹⁻⁶ Numerous solvent assisted and solvent-free methods have been reported for the preparation of pyrazoline derivatives. Cyclization of chalcones with phenyl hydrazine hydrochloride using ultrasonic sound assisted synthesis of pyrazolines was reported by, Li *et al.*,⁷ The K_2CO_3 -mediated microwave irradiation has been shown to be an efficient method for the synthesis of pyrazolines.⁸ The regioselective formation of pyrazolines have been synthesized by the reaction of substituted hydrazine with α,β -unsaturated ketones.^{9,10} Many solvent free catalysts and methods such as solution phase MWI,¹¹ K_2CO_3 /Basic alumina,¹² Surfactant THAC,¹³ $\text{KF}/\text{Al}_2\text{O}_3$,¹⁴ HSBM,¹⁵ fly-ash: H_2SO_4 ,¹⁶ Thermal solvent-free¹⁷ heating were available for synthesis of pyrazoline derivatives. These pyrazolines used widely in the current decades due to various biological and pharmacological activities such as analgesic,¹⁸ anti-inflammatory,^{19, 20} anti-microbial,²¹ anti-amoebic,^{22, 23} anti-tubercular,^{24,25} hypoglycemic,²⁶ anti-coagulant,²⁷ anti-depressant,²⁸⁻³⁰ pesticides,³¹ fungicides,³² anti-bacterial³³ and anti-con-vulsant activities.³⁴ Recent report shows some new pyrazoline substituted thiazolone based compounds exhibit anti-cancer activity.³⁵ Apart from biological

activities, pyrazolines are also extensively used as synthons in organic synthesis,³⁶⁻³⁸ optical brightening agent for textiles, paper, fabrics, and as a hole-conveying medium in photoconductive materials.³⁹⁻⁴³

Spectroscopic data is useful for predicting the ground state equilibrium of organic compounds.⁴⁴⁻⁴⁷ The ultraviolet spectroscopic data of absorption maxima (λ_{max} , nm) is also applied for prediction of effects of substituent.⁴⁸ In pyrazoline molecules (^1H pyrazoles), the infrared spectra is used for predicting the effects of substituents on the vibrations of C=N, C-H, N-H. From NMR spectroscopy, the spatial arrangements of the protons Ha, Hb and Hc or Ha, Hb, Hc and Hd of the types shown in Fig. 1 were predictable by their frequencies with multiplicities viz., doublet or triplet or doublet of doublets. Based on the geometry, the chemical shift of the protons of respective pyrazoles has been predicted and the effects of substituents will be studied. The effects of substituents on the pyrazoline ring protons were studied first by Sakthinathan *et. al.*⁴⁴ In their study, they synthesized some 2-naphthyl based pyrazolines and characterized by infrared and NMR spectroscopic data.

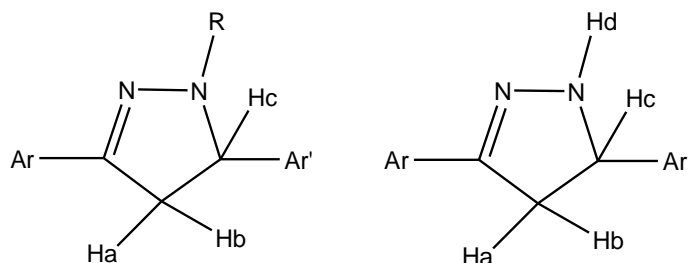


Figure 1. General structure of pyrazoles

From infrared spectra, the C=N stretches(cm^{-1}) have been assigned and these vibrations were correlated with Hammett substituent constants. In this correlations they observed satisfactory r values. From ^1H NMR chemical

shifts of these pyrazolines the H_a , H_b and H_c values were assigned and studied the effects of substituents by correlation with these frequencies and Hammett substituent constants, F and R values. Similarly the ^{13}C chemical shifts (δ , ppm) of these pyrazolines also correlated. In this present study the authors have taken efforts to synthesis some 1-aryl-3(5-substituted aryl-2-yl)-5-(substituted phenyl)-2-pyrazolines from various chalcones and phenyl hydrazine hydrochloride in presence of $\text{SiO}_2\text{-H}_3\text{PO}_4$. The purities of these pyrazolines were checked by their physical constants and spectral data published earlier in literature. The infrared and nuclear magnetic resonance spectral group frequencies of 5-bromo-2-thienyl based pyrazolines have been assigned and correlated with Hammett substituent constants, F and R parameters.

EXPERIMENTAL

Materials and methods

All chemicals used were procured from Sigma-Aldrich and E-Merck companies. Melting points of all pyrazolones have been determined in open glass capillaries on Mettler FP51 melting point apparatus and are uncorrected. Infrared spectra (KBr , $4000\text{-}400\text{ cm}^{-1}$) have been recorded on BRUKER (Thermo Nicolet) Fourier transform spectrophotometer. The NMR spectra of all pyrazolines have been recorded on Bruker AV400 spectrometer operating at 400 MHz for recording ^1H and 100 MHz for ^{13}C spectra in CDCl_3 solvent using TMS as internal standard. Mass spectra have been recorded on SHIMADZU spectrometer using chemical ionization technique.

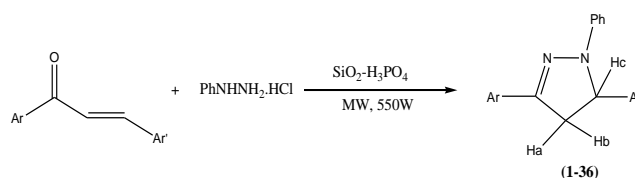
Preparation of solid $\text{SiO}_2\text{-H}_3\text{PO}_4$ catalyst

In a 50mL Borosil beaker, 2g of silica (10-20 μ) 2mL of ortho phosphoric acid were taken and mixed thoroughly with glass rod. This mixture was heated on a hot air oven at 85°C for 1h, cooled to room temperature, stored in a borosil bottle and tightly capped. This was characterized by infrared spectra and SEM analysis.⁴⁹

Infrared spectral data of $\text{SiO}_2\text{-H}_3\text{PO}_4$ were $\nu(\text{cm}^{-1})$: 3437(P-OH); 2932, 2849 (P-O-H); 1747, (O=P-OH); 1091(P=O), 800(P-O).

Synthesis of pyrazoline derivatives

An appropriate equi-molar quantities of chalcones (2 mmol), phenyl hydrazine hydrochloride (2 mmol) and $\text{SiO}_2\text{-H}_3\text{PO}_4$ (0.5 g) have been taken in borosil tube and tightly capped. The mixture has been subjected to microwave irradiation for 6-8 minutes in a microwave oven at 550 watts, 2540 MHz frequency (Scheme 1) (Samsung Grill, GW73BD Microwave oven, 230V A/c, 50Hz, 2450Hz, 100-750W (IEC-705), and then cooled to room temperature. After separating the organic layer with dichloromethane the solid product has been obtained on evaporation. The solid, on recrystallization from benzene-hexane mixture afforded glittering product. The insoluble catalyst has been recycled by washing with ethyl acetate (8 mL) followed by drying in an oven at 100°C for 1h and reused for further reactions.



Scheme 1. Synthesis of pyrazolines

RESULTS AND DISCUSSION

In our organic chemistry research laboratory, we attempts to synthesize pyrazoline derivatives by cyclization of electron withdrawing as well as electron donating group substituted chalcones and phenylhydrazine hydrochloride in the presence of acidic catalyst $\text{SiO}_2\text{-H}_3\text{PO}_4$ in microwave irradiation. Hence the authors have synthesized the pyrazoline derivatives by the cyclization of 2 mmole of chalcone, 2 mmole of phenylhydrazine hydrochloride in microwave irradiation with 0.5g of $\text{SiO}_2\text{-H}_3\text{PO}_4$ catalyst at 550W, 6-8 minutes (Samsung Grill, GW73BD Microwave oven, 230V A/c, 50Hz, 2450Hz, 100-750W (IEC-705), (Scheme 1). During the course of this reaction $\text{SiO}_2\text{-H}_3\text{PO}_4$ catalyzes cyclization between aryl enones and phenylhydrazine hydrochloride to elimination of water followed by proton transfer gave the pyrazoline derivatives. The yields of the pyrazolines in this reaction are more than 85%. The proposed general mechanism of this reaction is given in Scheme 2. Further we have investigated this cyclization reaction with equimolar quantities of the styryl-5-bromo-2-thienyl ketones (entry 21) and phenylhydrazine hydrochloride.

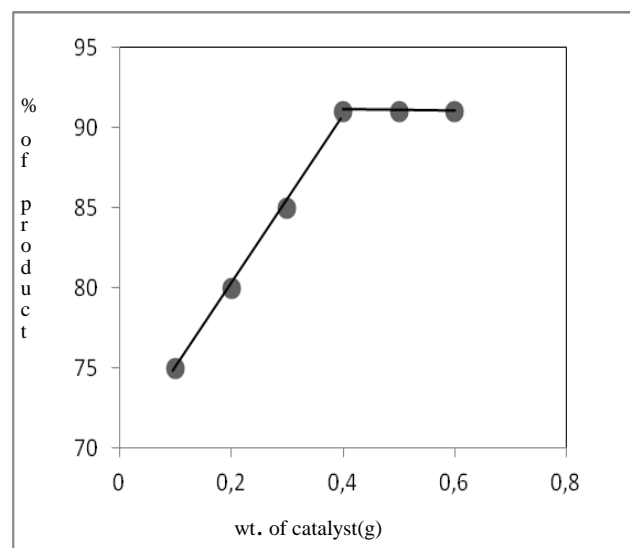
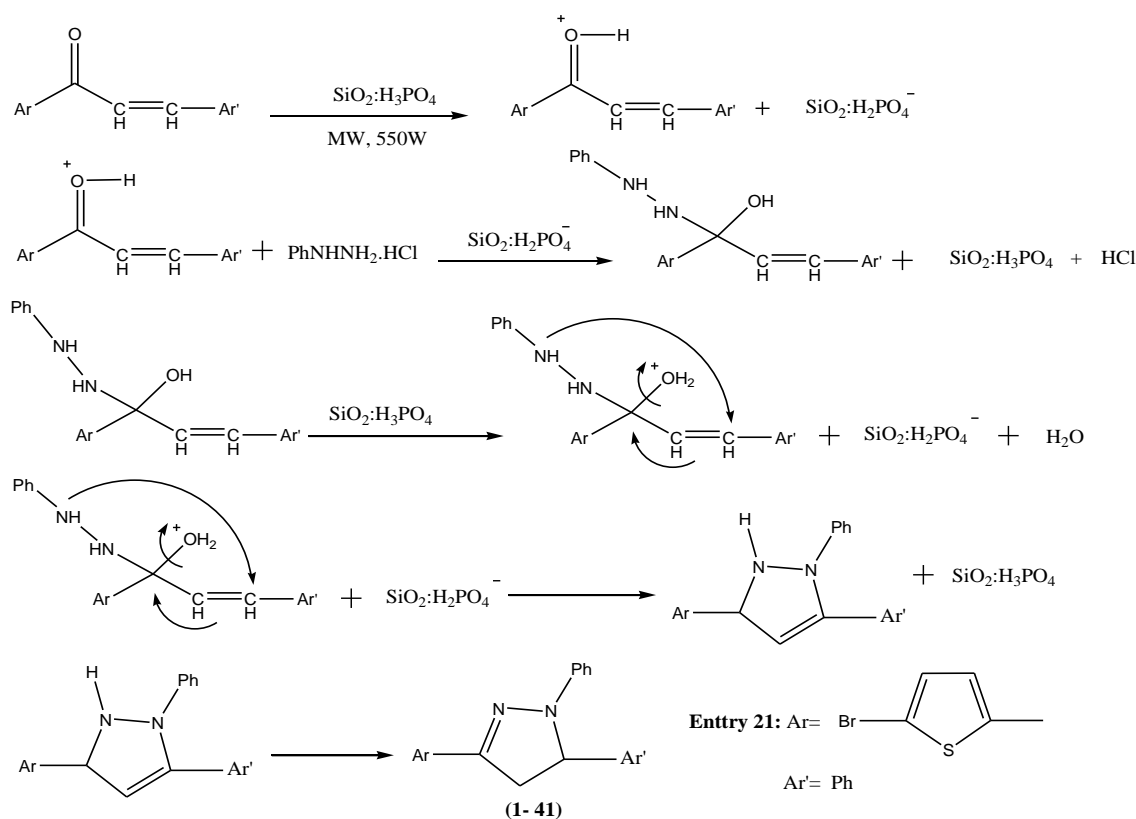


Figure 2. Effect of catalyst loading

In this reaction the obtained yield was 91%. The effect of catalyst on this reaction was studied by varying the catalyst quantity from 0.1 to 1g. As the catalyst quantity is increased from 0.1 to 1g, the percentage of yield of product is increased from 75 to 91%. Further increase the catalyst amount, there is no significant increasing of the percentage of product.



Scheme 2. Proposed mechanism for synthesis of pyrazolines by cyclization of chalcones and phenylhydrazine hydrochloride in presence of $\text{SiO}_2:\text{H}_3\text{PO}_4$ under microwave irradiation

This catalytic effect is shown in (Fig. 2). The optimum quantity of catalyst loading was found to be 0.4g. We have carried out this reaction with various aryl chalcones and phenyl hydrazine hydrochloride. There is no significant effect of substituents on the cyclization reaction. The results, analytical and mass spectral data are summarized in Table 1. The reusability of this catalyst was studied the cyclization of 5-bromo-2-thienyl chalcone and phenyl hydrazine hydrochloride (entry 21) and is presented in Table 2.

From the Table 2, first two runs gave 91% product. The third, fourth and fifth runs of reactions gave the yields 90.5%, 90.5% and 90% of pyrazolines. There was no appreciable loss in its effect of catalytic activity were observed up to fifth run. The effect of solvents on the yield also studied with methanol, ethanol, dichloromethane and tetrahydrofuran from each component of the catalyst (entry 21). Similarly the effect of microwave irradiation was studied on the each component of the catalysts. The effect of solvents on the yields of pyrazolines were presented in Table 3. From the table highest yield of the pyrazolines obtained from the condensation of chalcone and phenylhydrazine hydrochloride with catalyst $\text{SiO}_2:\text{H}_3\text{PO}_4$ in microwave irradiation.

IR SPECTRAL STUDY

The synthesis of pyrazoline derivative is shown in Scheme 1. In the present study, the authors have chosen a series of pyrazoline derivatives namely 1-phenyl-3-(5-bromothiophen-2-yl)-5-(substituted phenyl)-2-pyrazolines (entries 21-27) for studying the effects of substituent on the spectral group frequencies.

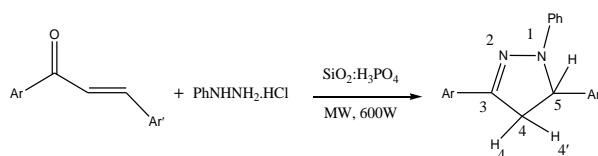
The infrared $\nu\text{C}=\text{N}$ stretching frequencies (cm^{-1}) of these pyrazolines have been recorded and are presented in Table 4. These data are correlated with Hammett substituent constants⁴⁴⁻⁴⁹ and Swain-Lupton's⁵¹ parameters. In this correlation the structure parameter Hammett equation employed is as shown in equation (1).

$$\nu = \rho\sigma + \nu_0 \quad (1)$$

where ν_0 is the frequency for the parent member of the series.

The observed $\nu\text{C}=\text{N}$ stretching frequencies (cm^{-1}) are correlated with various Hammett substituent constants and F and R parameters through single and multi-regression analyses including Swain-Lupton's⁵¹ parameters. The results of statistical analysis of single parameter correlation are shown in Table 5.

The correlation of $\nu\text{C}=\text{N}$ (cm^{-1}) frequencies of pyrazolines with R parameter was satisfactorily ($r=0.907$). The remaining Hammett substituent constants and F parameter were found to be poor in correlation. A satisfactory correlation was obtained for $\nu\text{C}-\text{S}$ (cm^{-1}) frequencies of pyrazolines with Hammett substituents and F parameter. The R parameter was fail in correlation. All correlations produce positive ρ values. This implies that there is a normal substituent effect operates in all systems. The correlation of $\nu\text{C}-\text{Br}$ (cm^{-1}) frequencies of pyrazolines with Hammett substituent constants, F and R parameters were gave poor correlation. This failure in correlation was due to the absence of inductive and polar effects of the substituent and is associated with the conjugated structure shown in Fig.3.

Table 1. Analytical and mass spectral data of pyrazolines synthesized by solvent-free cyclization of chalcones and phenylhydrazine hydrochloride reaction of the type

Entry	Ar	Ar'	M.W.	Yield (%)	M.p. (°C)	Mass (m/z)
1	C ₆ H ₅	C ₆ H ₅	298	90	134-135; (134-135)[7]	298[M ⁺]
2	C ₆ H ₅	3-BrC ₆ H ₄	376	89	142-143; (141-143)[7]	376[M ⁺], 378[M ⁺²]
3	C ₆ H ₅	2-ClC ₆ H ₄	333	87	135-136; (134-135)[7]	333[M ⁺], 335[M ⁺²]
4	C ₆ H ₅	3-ClC ₆ H ₄	333	87	133-134; (134-136)[7]	333[M ⁺], 335[M ⁺²]
5	C ₆ H ₅	4-ClC ₆ H ₄	333	87	134-135; (135-136)[7]	333[M ⁺], 335[M ⁺²]
6	C ₆ H ₅	4-N(CH ₃) ₂ C ₆ H ₄	341	85	219-220; (220)[11]	341[M ⁺]
7	C ₆ H ₅	2-OHC ₆ H ₄	314	87	192-193; (192)[11]	314[M ⁺]
8	C ₆ H ₅	4-OCH ₃ C ₆ H ₄	328	87	112-113; (110-112)[7]	328[M ⁺]
9	C ₆ H ₅	4-NO ₂ C ₆ H ₄	343	66	157-158 (trace)[7] (225)[11]	343[M ⁺]
10	4-ClC ₆ H ₄	C ₆ H ₅	333	87	144-145; (143-145)[11]	333[M ⁺]
11	4-OHC ₆ H ₄	C ₆ H ₅	314	88	279-280; (281) [11]	314[M ⁺]
12	4-OHC ₆ H ₄	4-ClC ₆ H ₄	348	86	234-235; (234) [11]	348[M ⁺], 350[M ⁺²]
13	4-OHC ₆ H ₄	4-N(CH ₃) ₂ C ₆ H ₄	357	87	265-266; (265) [11]	357[M ⁺]
14	4-OHC ₆ H ₄	2-OHC ₆ H ₄	330	86	195-196; (194) [11]	330[M ⁺]
15	4-OHC ₆ H ₄	4-NO ₂ C ₆ H ₄	359	89	196-197; (198) [11]	359[M ⁺]
16	3-NO ₂ C ₆ H ₄	C ₆ H ₅	343	90	132-133(trace) [7]	343[M ⁺]
17	C ₄ H ₃ S	C ₆ H ₅	349	92	164-165; (161-165) [6d]	349[M ⁺]
18	C ₄ H ₃ S	4-BrC ₆ H ₄	382	91	249-250; (241-252) [6d]	382[M ⁺], 384[M ⁺²]
19	C ₄ H ₃ S	4-N(CH ₃) ₂ C ₆ H ₄	347	89	212-213; (212-215) [6d]	347[M ⁺]
20	C ₄ H ₃ S	2,4,5-(OCH ₃) ₃ C ₆ H ₂	394	88	170-171; (170-174) [6d]	394[M ⁺]
21	C ₄ H ₂ BrS	C ₆ H ₅	383	91	152-153; (152-153)[16]	383[M ⁺]
22	C ₄ H ₂ BrS	4-BrC ₆ H ₄	462	92	148-149; (148-149)[16]	462[M ⁺], 466[M ⁺²], 468[M ⁺³]
23	C ₄ H ₂ BrS	2-ClC ₆ H ₄	417	90	142-144; (142-144)[16]	417[M ⁺], 419[M ⁺²], 421[M ⁺³]
24	C ₄ H ₂ BrS	4-ClC ₆ H ₄	417	93	147-149; (147-149)[16]	417[M ⁺], 419[M ⁺²], 421[M ⁺³]
25	C ₄ H ₂ BrS	4-IC ₆ H ₄	509	91	146-148; (146-148)[16]	509[M ⁺], 511[M ⁺²], 513[M ⁺³]
26	C ₄ H ₂ BrS	4-OCH ₃ C ₆ H ₄	413	90	128-130; (128-130)[16]	413[M ⁺], 415[M ⁺²]
27	C ₄ H ₂ BrS	4-CH ₃ C ₆ H ₄	397	93	148-149; (148-149)[16]	397[M ⁺], 379[M ⁺²]
28	C ₄ H ₂ BrS	3,4-(OCH ₃) ₂ C ₆ H ₃	443	92	140-142; (140-142)[16]	443[M ⁺], 445[M ⁺²]
29	C ₁₀ H ₇	C ₆ H ₅	348	92	116-117; (116-117)[44]	348[M ⁺]
30	C ₁₀ H ₇	3-BrC ₆ H ₄	426	89	64-65; (64-65)[44]	426[M ⁺], 428[M ⁺²]
31	C ₁₀ H ₇	4-ClC ₆ H ₄	383	91	62-68; (62-68)[44]	383[M ⁺], 385[M ⁺²]
32	C ₁₀ H ₇	2-OCH ₃ C ₆ H ₄	378	87	104-105; (104-105)[44]	378[M ⁺]
33	3-CH ₃ C ₆ H ₄	C ₆ H ₅	326	93	110-111; (110-111)[50]	326[M ⁺]
34	3-CH ₃ C ₆ H ₄	3-BrC ₆ H ₄	391	92	60-61; (60-61)[50]	391[M ⁺], 393[M ⁺²]
35	3-CH ₃ C ₆ H ₄	3-ClC ₆ H ₄	346	90	54-55; (54-55)[50]	346[M ⁺], 348[M ⁺²]
36	3-CH ₃ C ₆ H ₄	4-NO ₂ C ₆ H ₄	326	91	58-59; (58-59)[50]	326[M ⁺], 328[M ⁺²]

Table 2. Reusability of catalyst on cyclization of styryl 5-bromo-2-thienyl ketone (2 mmol) and phenylhydrazine hydrochloride (2 mmol) under microwave irradiation (entry 21).

Run	1	2	3	4	5
Yield, %	91	91	90.5	90.5	90

Table 3. The effect of solvents in conventional heating and without solvent in microwave irradiation on yield of pyrazoline (entry 21)

Solvents											Microwave irradiation			
MeOH			EtOH			DCM			THF					
SiO ₂	PA	SiO ₂ :PA	SiO ₂	PA	SiO ₂ :PA	SiO ₂	PA	SiO ₂ :PA	SiO ₂	PA	SiO ₂ :PA	SiO ₂	PA	SiO ₂ :PA
73	77	78	74	75	80	73	80	80	75	81	81	82	80	91

MeOH=Methanol; EtOH=Ethanol; DCM= Dichloromethane; THF=Tetrahydrofuran; PA=Phosphoric acid

Table 4. The infrared $\nu(\text{cm}^{-1})$ of C=N, C-S, C-Br, ^1H and ^{13}C NMR chemical shifts (δ , ppm) of pyrazoline ring proton, carbons of 1-phenyl-3(5-bromothiophen-2-yl)-5-(substituted phenyl)-2-pyrazolines(entries 21-28)

Entry	Substituent	$\nu\text{C}=\text{N}$	$\nu\text{C}-\text{S}$	$\nu\text{C}-\text{Br}$	$\delta\ \text{H}_4$	$\delta\ \text{H}_4'$	$\delta\ \text{H}_5$	$\delta\ \text{C}_3$	$\delta\ \text{C}_4$	C_5	$\delta\ \text{C}=\text{N}$
21	H	1593	679	562	3.06	3.77	5.25	155.60	43.66	64.68	154.56
22	4-Br	1596	685	562	3.07	3.82	5.26	155.56	43.53	64.10	155.56
23	2-Cl	1595	690	566	3.01	3.93	5.66	157.50	42.08	61.50	157.50
24	4-Cl	1594	688	531	3.10	3.80	5.28	155.82	43.70	64.75	155.82
25	4-I	1595	680	531	3.04	3.78	5.21	156.11	43.52	64.21	156.11
26	4-OCH ₃	1596	670	553	3.07	3.77	5.24	155.81	43.75	64.29	159.13
27	4-CH ₃	1594	680	546	3.07	3.77	5.24	156.10	43.72	64.47	156.10

The single parameter correlations of $\nu\text{C}=\text{N}$, C-S and C-Br (cm^{-1}) frequencies with Hammett substituent constants of resonance and inductive effects fail. So, the authors think that it is worthwhile to seek the multi regression analysis and which produce a satisfactory correlation with Resonance, Field and Swain-Lupton's⁵¹ constants. The corresponding equations are given in (2-7).

$$\nu_{\text{CN}}(\text{cm}^{-1}) = 1593.76(\pm 0.553) + 3.805\sigma_{\text{I}}(\pm 1.627) + 2.584\sigma_{\text{R}}(\pm 1.611) \quad (2)$$

($R=0.978$, $P > 95\%$, $n=7$)

$$\nu_{\text{CN}}(\text{cm}^{-1}) = 1593.06(\pm 0.512) + 2.388\text{F}(\pm 1.429) - 4.173\text{R}(\pm 1.714) \quad (3)$$

($R=0.998$, $P > 95\%$, $n=7$)

$$\nu_{\text{CS}}(\text{cm}^{-1}) = 677.98(\pm 1.947) + 7.680\sigma_{\text{I}}(\pm 1.535) + 24.399\sigma_{\text{R}}(\pm 5.668) \quad (4)$$

($R=0.931$, $P > 90\%$, $n=7$)

$$\nu_{\text{CS}}(\text{cm}^{-1}) = 682.05(\pm 3.402) + 24.577\text{F}(\pm 9.496) + 31.947\text{R}(\pm 11.386) \quad (5)$$

($R=0.985$, $P > 95\%$, $n=7$)

$$\nu_{\text{CBr}}(\text{cm}^{-1}) = 552.39(\pm 11.595) - 6.515\sigma_{\text{I}}(\pm 3.407) + 5.965\sigma_{\text{R}}(\pm 3.337) \quad (6)$$

($R=0.915$, $P > 90\%$, $n=7$)

$$\nu_{\text{CBr}}(\text{cm}^{-1}) = 554.19(\pm 13.979) + 13.627\text{F}(\pm 3.972) + 0.576\text{R}(\pm 0.041) \quad (7)$$

($R=0.918$, $P > 95\%$, $n=7$)

^1H NMR SPECTRAL STUDY

The ^1H NMR spectra of seven pyrazoline derivatives under investigation have been recorded in deuteriochloroform solution employing tetramethylsilane (TMS) as internal standard. The signals of the pyrazoline ring protons have been assigned. They have been calculated as AB or AA' systems respectively. The chemical shifts (δ , ppm) of H_4 are at higher fields than those of H_4' and H_5 in this series of pyrazolines. This is due to the deshielding of H_4' and H_5 which are in different chemical as well as magnetic environment. These H_4 protons gave an AB pattern and the H_4' proton doublet of doublet in most cases was well separated from the signals H_5 and the aromatic protons. The assigned chemical shifts (δ , ppm) of the pyrazoline ring H_4 , H_4' and H_5 protons are presented in Table 4.

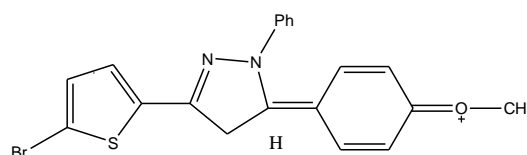
In nuclear magnetic resonance spectra, the ^1H or the ^{13}C chemical shifts (δ , ppm) depend on the electronic environment of the nuclei concerned. These chemical shifts have been correlated with reactivity parameters. Thus the Hammett equation may be used in the form as shown in (8).

$$\log \delta = \log \delta_0 + \rho\sigma \quad (8)$$

where δ_0 is the chemical shift of the corresponding parent compound.

The assigned H_{44} , H_4' and H_5 proton chemical shifts (ppm) of pyrazoline ring have been correlated with various Hammett sigma constants.⁴⁴⁻⁴⁹ The results of statistical analysis are presented in Table 5.

The H_4 proton chemical shifts (ppm) with Hammett σ^+ and R parameters gave satisfactory correlation. The remaining substituent constants and F parameters were fail in correlation. The failure in correlation is associated with the conjugative structure shown in Fig. 3.

**Figure 3.** Resonance-conjugative structure

The results of statistical analysis of H_4' proton chemical shifts (δ , ppm) with Hammett substituents are shown in Table 5. The H_4' proton chemical shifts (δ , ppm) with Hammett substituent constants and F parameters gave satisfactory correlation excluding 2-Cl and 3-OCH₃ substituents. The R parameter was fail in correlation. This is due to the absence of resonance effect of substituents on the H_4' proton chemical shifts and it is associated with the conjugative structure shown in Fig. 3.

The results of statistical analysis of H_5 proton chemical shifts (ppm) with Hammett substituents are presented in Table 5. The H_5 proton chemical shifts with Hammett σ , σ^+ , σ_{I} constants and F parameters gave satisfactory correlation excluding 2-Cl substituent. All correlations produce positive ρ values. This means that the normal substituent effect operates in all systems. This failure in correlation is associated with conjugative structure shown in Fig. 3.

Table 5. Results of statistical analysis of $\nu(\text{cm}^{-1})$ of C=N, C-S, C-Br bands, ^1H and ^{13}C NMR chemical shifts (δ , ppm) of pyrazoline ring protons, carbons of 1-Ph-3(5-bromothiophen-2-yl)-5-(aryl)-2-pyrazolines, Hammett σ , σ^+ , σ_{I} , σ_{R} constants and F and R parameters (entries **21-28**).

Functionality	Constants	r	I	ρ	s	n	Correlated derivatives
vC=N	σ	0.806	1594.71	0.032	1.21	7	H, 4-CH ₃ , 2-Cl, 4-Cl, 4-Br, 4-I, 4-OCH ₃
	σ^+	0.805	1594.71	0.153	1.21	7	H, 4-CH ₃ , 2-Cl, 4-Cl, 4-Br, 4-I, 4-OCH ₃
	σ_{I}	0.806	1593.84	3.000	0.97	7	H, 4-CH ₃ , 2-Cl, 4-Cl, 4-Br, 4-I, 4-OCH ₃
	σ_{R}	0.802	1594.80	1.432	1.16	7	H, 4-CH ₃ , 2-Cl, 4-Cl, 4-Br, 4-I, 4-OCH ₃
	F	0.866	1593.65	3.703	0.91	7	H, 4-CH ₃ , 2-Cl, 4-Cl, 4-Br, 4-I, 4-OCH ₃
	R	0.907	1593.49	5.255	0.75	6	H, 4-CH ₃ , 2-Cl, 4-Cl, 4-I, 4-OCH ₃
vC-S	σ	0.908	680.24	27.109	3.95	7	H, 4-CH ₃ , 2-Cl, 4-Cl, 4-Br, 4-I, 4-OCH ₃
	σ^+	0.981	681.82	13.765	3.47	7	H, 4-CH ₃ , 2-Cl, 4-Cl, 4-Br, 4-I, 4-OCH ₃
	σ_{I}	0.905	677.30	15.206	3.32	5	2-Cl, 4-Cl, 4-Br, 4-I, 4-OCH ₃
	σ_{R}	0.989	680.07	26.720	3.01	5	2-Cl, 4-Cl, 4-Br, 4-I, 4-OCH ₃
	F	0.904	697.57	14.510	3.06	7	H, 4-CH ₃ , 2-Cl, 4-Cl, 4-Br, 4-I, 4-OCH ₃
	R	0.705	686.53	20.815	6.28	7	H, 4-CH ₃ , 2-Cl, 4-Cl, 4-Br, 4-I, 4-OCH ₃
vC-Br	σ	0.701	550.52	-7.121	15.98	7	H, 4-CH ₃ , 2-Cl, 4-Cl, 4-Br, 4-I, 4-OCH ₃
	σ^+	0.701	550.13	5623	15.84	7	H, 4-CH ₃ , 2-Cl, 4-Cl, 4-Br, 4-I, 4-OCH ₃
	σ_{I}	0.782	552.56	-8.355	15.93	7	H, 4-CH ₃ , 2-Cl, 4-Cl, 4-Br, 4-I, 4-OCH ₃
	σ_{R}	0.821	550.63	7.931	15.94	7	H, 4-CH ₃ , 2-Cl, 4-Cl, 4-Br, 4-I, 4-OCH ₃
	F	0.789	554.10	-13.810	15.78	7	H, 4-CH ₃ , 2-Cl, 4-Cl, 4-Br, 4-I, 4-OCH ₃
	R	0.707	551.70	6.752	16.02	7	H, 4-CH ₃ , 2-Cl, 4-Cl, 4-Br, 4-I, 4-OCH ₃
δH_4	σ	0.802	3.061	-0.026	0.03	7	H, 4-CH ₃ , 2-Cl, 4-Cl, 4-Br, 4-I, 4-OCH ₃
	σ^+	0.903	3.068	-0.025	0.02	5	H, 4-CH ₃ , 2-Cl, 4-Cl, 4-I
	σ_{I}	0.781	3.065	-0.020	0.03	7	H, 4-CH ₃ , 2-Cl, 4-Cl, 4-Br, 4-I, 4-OCH ₃
	σ_{R}	0.812	3.062	0.033	0.02	7	H, 4-CH ₃ , 2-Cl, 4-Cl, 4-Br, 4-I, 4-OCH ₃
	F	0.715	3.066	-0.021	0.03	7	H, 4-CH ₃ , 2-Cl, 4-Cl, 4-Br, 4-I, 4-OCH ₃
	R	0.902	3.058	-0.005	0.02	5	4-CH ₃ , 2-Cl, 4-Cl, 4-Br, 4-I
$\delta\text{H}_4'$	σ	0.905	3.797	0.147	0.05	6	H, 4-CH ₃ , 4-Cl, 4-Br, 4-I, 4-OCH ₃
	σ^+	0.906	3.805	0.087	0.04	6	H, 4-CH ₃ , 2-Cl, 4-Cl, 4-I, 4-OCH ₃
	σ_{I}	0.906	3.763	0.147	0.05	6	H, 4-CH ₃ , 4-Cl, 4-Br, 4-I, 4-OCH ₃
	σ_{R}	0.904	3.797	0.178	0.05	6	H, 4-CH ₃ , 2-Cl, 4-Cl, 4-Br, 4-I
	F	0.901	3.763	0.145	0.05	6	H, 4-CH ₃ , 2-Cl, 4-Cl, 4-Br, 4-I
	R	0.803	3.808	0.171	0.06	7	H, 4-CH ₃ , 2-Cl, 4-Cl, 4-Br, 4-I, 4-OCH ₃
δH_5	σ	0.903	5.297	1.257	0.16	6	H, 4-CH ₃ , 4-Cl, 4-Br, 4-I, 4-OCH ₃
	σ^+	0.904	5.308	1.025	0.15	6	H, 4-CH ₃ , 2-Cl, 4-Cl, 4-I, 4-OCH ₃
	σ_{I}	0.903	5.228	1.266	0.15	6	H, 4-CH ₃ , 4-Cl, 4-Br, 4-I, 4-OCH ₃
	σ_{R}	0.801	5.289	1.271	0.15	7	H, 4-CH ₃ , 2-Cl, 4-Cl, 4-Br, 4-I, 4-OCH ₃
	F	0.903	5.236	0.246	0.16	6	H, 4-CH ₃ , 4-Cl, 4-Br, 4-I, 4-OCH ₃
	R	0.803	5.312	0.036	0.17	7	H, 4-CH ₃ , 2-Cl, 4-Cl, 4-Br, 4-I, 4-OCH ₃
δCN	σ	0.822	156.03	0.722	0.712	7	H, 4-CH ₃ , 2-Cl, 4-Cl, 4-Br, 4-I, 4-OCH ₃
	σ^+	0.823	156.07	0.511	0.681	7	H, 4-CH ₃ , 2-Cl, 4-Cl, 4-Br, 4-I, 4-OCH ₃
	σ_{I}	0.729	155.82	0.861	0.697	7	H, 4-CH ₃ , 2-Cl, 4-Cl, 4-Br, 4-I, 4-OCH ₃
	σ_{R}	0.703	156.00	1.166	0.674	7	H, 4-CH ₃ , 2-Cl, 4-Cl, 4-Br, 4-I, 4-OCH ₃
	F	0.825	155.82	0.858	0.704	7	H, 4-CH ₃ , 2-Cl, 4-Cl, 4-Br, 4-I, 4-OCH ₃
	R	0.805	156.02	0.245	0.728	7	H, 4-CH ₃ , 2-Cl, 4-Cl, 4-Br, 4-I, 4-OCH ₃
δC_4	σ	0.841	43.48	-1.181	0.59	7	H, 4-CH ₃ , 2-Cl, 4-Cl, 4-Br, 4-I, 4-OCH ₃
	σ^+	0.751	43.42	-0.783	0.54	7	H, 4-CH ₃ , 2-Cl, 4-Cl, 4-Br, 4-I, 4-OCH ₃
	σ_{I}	0.742	43.75	-1.129	0.59	7	H, 4-CH ₃ , 2-Cl, 4-Cl, 4-Br, 4-I, 4-OCH ₃
	σ_{R}	0.900	43.49	1.761	0.58	6	H, 4-CH ₃ , 2-Cl, 4-Cl, 4-Br, 4-I
	F	0.903	43.73	1.095	0.61	6	H, 4-CH ₃ , 4-Cl, 4-Br, 4-I, 4-OCH ₃
	R	0.900	43.35	0.145	0.65	6	H, 4-CH ₃ , 4-Cl, 4-Br, 4-I, 4-OCH ₃
δC_5	σ	0.735	64.09	1.671	1.17	7	H, 4-CH ₃ , 2-Cl, 4-Cl, 4-Br, 4-I, 4-OCH ₃
	σ^+	0.704	64.00	1.121	1.09	7	H, 4-CH ₃ , 2-Cl, 4-Cl, 4-Br, 4-I, 4-OCH ₃
	σ_{I}	0.904	64.61	2.137	1.11	6	H, 4-CH ₃ , 4-Cl, 4-Br, 4-I, 4-OCH ₃
	σ_{R}	0.803	64.10	1.974	1.16	7	H, 4-CH ₃ , 2-Cl, 4-Cl, 4-Br, 4-I, 4-OCH ₃
	F	0.937	64.61	2.145	1.14	6	H, 4-CH ₃ , 4-Cl, 4-Br, 4-I, 4-OCH ₃
	R	0.904	64.15	0.685	1.22	6	H, 4-CH ₃ , 4-Cl, 4-Br, 4-I, 4-OCH ₃

r = correlation coefficient; ρ = slope; I = intercept; s = standard deviation; n = number of substituents

In view of the inability of the Hammett σ constants to produce individually satisfactory correlation, the authors think that it is worthwhile to seek multiple correlations involving either σ_I and σ_R constants or Swain-Lupton's⁵¹ F and R parameters. The correlation equations for H₄–H₅ protons are given in (9-14).

$$\delta_{H4}(\text{ppm}) = 3.065 (\pm 0.021) - 0.119 (\pm 0.006)\sigma_I + 0.290 (\pm 0.005)\sigma_R \quad (9)$$

(R=0.927, P> 90%, n=7)

$$\delta_{H4}(\text{ppm}) = 3.063 (\pm 0.260) - 0.247 (\pm 0.007)F + 0.158 (\pm 0.002)R \quad (10)$$

(R=0.917, P > 90%, n=7)

$$\delta_{H4}(\text{ppm}) = 3.765 (\pm 0.341) - 0.119 (\pm 0.007)\sigma_I + 0.929 (\pm 0.004)\sigma_R \quad (11)$$

(R=0.966, P> 95%, n=7)

$$\delta_{H4}(\text{ppm}) = 3.777 (\pm 0.046) + 0.173 (\pm 0.001)F + 0.960 (\pm 0.015)R \quad (12)$$

(R=0.955, P > 95%, n=7)

$$\delta_{H5}(\text{ppm}) = 5.234 (\pm 0.111) + 0.202 (\pm 0.0326)\sigma_I - 0.207 (\pm 0.002)\sigma_R \quad (13)$$

(R=0.947, P> 90%, n=7)

$$\delta_{H5}(\text{ppm}) = 5.297 (\pm 0.143) + 0.292 (\pm 0.004)F + 0.162 (\pm 0.002)R \quad (14)$$

(R=0.934, P > 90%, n=7)

¹³C NMR SPECTRA

Spectroscopic chemists and organic chemistry researchers⁴⁴⁻⁴⁹ have made extensive study of ¹³C NMR spectra for a large number of different ketones, styrenes and keto-epoxides. They have studied linear correlation of the chemical shifts (δ , ppm) of C _{α} , C _{β} and CO carbons with Hammett σ constants in alkenes, alkynes, acid chlorides and styrenes. In the present study, the chemical shifts (δ , ppm) of pyrazoline ring C₃ (C=N), C₄, and C₅ carbon, have been assigned and are presented in Table 4. Attempts have been made to correlate the above said carbon chemical shifts (δ , ppm) with Hammett substituent constants, field and resonance parameters, with the help of single and multi-regression analyses to study the reactivity through the effect of substituents.

The chemical shifts (δ , ppm) observed for the δC_3 (C=N), C₄, and C₅ have been correlated with Hammett substituent constants and the results of statistical analysis are presented in Table 5. The $\delta C=N$ chemical shifts (δ , ppm) gave poor correlation with Hammett substituent constants and F and R parameters. Here the polar, inductive and resonance effects were incapable for predicting their effects on the C=N carbon chemical shifts (δ , ppm). The chemical shifts (δ , ppm) observed for the δC_4 carbon have been correlated satisfactorily with Hammett σ_R constant, F and R parameters. Here the polar and inductive effects were incapable for predicting their effects on the C₄ carbon chemical shifts (δ , ppm). The chemical shifts (δ , ppm) observed for the δC_5 carbon have been correlated satisfactorily with Hammett σ_I constant, F and R parameters. Here the polar and resonance effects were incapable for predicting their

effects on the C₅ carbon chemical shifts (δ , ppm). This is due to the reason stated earlier and it is associated with the resonance - conjugative structure shown in Fig. 3.

In view of inability of some of the σ constants to produce individually satisfactory correlation, the authors think that it is worthwhile to seek multiple correlation involving all σ_I , σ_R , F and R parameters. The correlation equations are given in (15 and 20).

$$\delta_{CN}(\text{ppm}) = 155.848 (\pm 0.480) + 0.560 (\pm 1.411)\sigma_I - 0.991 (\pm 0.137)\sigma_R \quad (15)$$

(R=0.943, P> 90%, n=7)

$$\delta_{CN}(\text{ppm}) = 155.852 (\pm 0.623) + 9.235 (\pm 0.173)F + 0.198 (\pm 0.002)R \quad (16)$$

(R=0.926, P> 90%, n=7)

$$\delta_{C4}(\text{ppm}) = 43.724 (\pm 0.480) - 0.845 (\pm 0.111)F + 0.920 (\pm 0.010)R \quad (17)$$

(R=0.953, P> 95%, n=7)

$$\delta_{C4}(\text{ppm}) = 43.281 (\pm 1.024) + 0.525 (\pm 1.424)\sigma_I - 0.981 (\pm 0.125)\sigma_R \quad (18)$$

(R=0.916, P> 90%, n=7)

CONCLUSION

A series of some aryl pyrazolines including 1-phenyl-3-(5-bromothiophen-2-yl)-5-(substituted phenyl)-2-pyrazoline derivatives have been synthesized by microwave assisted, solid acidic green catalyst SiO₂-H₃PO₄ catalyzed cyclization of 5-bromo-2-thienyl chalcones and phenyl hydrazine hydrochloride under solvent free conditions. The yields of the pyrazolines were more than 85%. The spectral frequencies, infrared $\nu(\text{cm}^{-1})$ of C=N, C-S, C-Br, ¹H and ¹³C NMR chemical shifts (δ , ppm) of pyrazoline ring proton, carbon and C=N carbons were assigned and correlated with Hammett substituent constants, F and R parameters. From the results of statistical analysis the effects of substituents on the spectral frequencies have been discussed.

REFERENCES

- Elguero, J., Bultou, In., Mckillop (editors). *Comprehensive Heterocyclic Chemistry*, Pergamon Press., **1984**, 5, 293.
- Dambal, D. B., Pattanashetti, P. P., Tikare, R. K., Badami, B. V., Puranik, G. S., *Indian J. Chem.* **1984**, 23B, 186.
- Sachchar, S. P., Singh, A. K., *J. Indian Chem. Soc.* **1985**, 62, 142.
- Kulkarni, S. E., Mane, R. A., Ingle, D. B., *Indian J. Chem.* **1986**, 25B, 452.
- Cremlyn, R. J., Swinbourne, F. J., Mookerjee, E., *Indian J. Chem.* **1986**, 25B, 562.
- (a) Sid, A., Lamara, K., Mokhtari, M., Ziani, N., Mosset, P., *Eur. J. Chem.* **2011**, 2, 311; (b) Patel, M., Desai, K. R., *Arkivoc.* **2004**, 1, 123; (c) Gothwal, P., Srivastava, Y. K., *Der Chem. Sincica.* **2012**, 3, 318; (d) Patil, V. S., Wadher, S. J., Karande, N. A., Yeole, P. G., *Int. J. Univ. Pharm. Life Sci.* **2011**, 1, 16; (e) Kumar, B., Pathak, V., Rani, S., Kant, R., Tewari, I. C., *Int. J. Microbiol. Res.* **2009**, 1, 20.
- Li, J. T., Zhang, X. H., Lin, Z. P., *Beil. J. Org. Chem.* **2007**, 3, 13.

- ⁸Kidwai, M., Kukreja, S., Thakur, R., *Lett. Org. Chem.* **2006**, *3*, 135.
- ⁹Katritzky, A. R., Wang, M. Y., Zhang, S. M., Vonkov, A. V., Steel, P. J., *J. Org. Chem.* **2001**, *66*, 6787.
- ¹⁰Kuz'menok, N. M., Koval'chuk, T. K., Zvonok, A. M., *Synth. Lett.* **2005**, *3*, 485.
- ¹¹Malhotra, P., Pattan, S., Nikale, A. P., *Int. J. Pharm. Pharm. Sci.* **2010**, *2(2)*, 21.
- ¹²Kidwai, M., Mothra, P., *Indian J. Chem.* **2006**, *45B*, 2330.
- ¹³Dadiboyena, S., Hamme, A. T., *4th Int. Symp. Recent Adv. Environ. Health Res.*, September 16-19, **2007**, PA 76, College of Science, Engineering and Technology, Jackson State University, Jackson, MS 39217, USA.
- ¹⁴Bougrin, K., Loupy, A., Soufiaoui, M., *J. Photochem. Photobiol C: Photochem. Rev.* **2005**, *6*, 139.
- ¹⁵Zhu, X., Li, Z., Jin, C., Xu, L., Wu, Q., Su, W., *Green Chem.* **2009**, *11*, 163.
- ¹⁶Sasikala, R., Thirumurthy, K., Mayavel, P., Thirunarayanan, G., *Org. Med. Chem. Lett.* **2012**. doi:10.1186/2191-2858-2-20
- ¹⁷Siddiqui, Z. N., Musthafa, T. N. M., Ahmad, A., Khan, A. U., *Bioorg. Med. Chem. Lett.* **2011**, *21*, 2860.
- ¹⁸Sahu, S. K., Banerjee, M., Samantray, A., Behera, C., Azam, M. A., *Trop. J. Pharm. Res.* **2008**, *7(2)*, 961.
- ¹⁹Karabasanagouda, T., Adhikari, A. V., Girisha, M., *Ind. J. Chem.* **2009**, *48B*, 430.
- ²⁰Farghaly, M., Chaaban, L., Khali, M. A., Behkit, A. A., *Arch. Pharm (Weinheim)*. **1990**, 311.
- ²¹Ramalingam, K., Thyvekikakath, G. X., Berlin, K. D., Chesnut, R. W., Brown, R. A., Durham, N. N., Ealick, A. E., Vender, H. D., *J. Med. Chem.* **1997**, *20*, 847.
- ²²Abid, M., Azam, A., *Bioorg. Med. Chem.* **2005**, *15*, 2213.
- ²³Abid, M., Azam, A., *Bioorg. Med. Chem. Lett.* **2006**, *16*, 2812.
- ²⁴Shahar Yar, M., Ahmad Siddiqui, A., Ali, M. A., *J. Serb. Chem. Soc.* **2007**, *72(1)*, 5.
- ²⁵Hatri, H. Z., Vunii, S. A., *J. Ind. Chem. Soc.* **1981**, *58*, 168.
- ²⁶Das, N., Verma, A., Shrivastava, P. K., Shrivastava, S. K., *Ind. J. Chem.* **2008**, *47B*, 1555.
- ²⁷Jia, Z., Wu, Y., Huang, W., Zhang, P., Song, Y., Scarborough, R. M., Zhu, B. Y., *Bioorg. Med. Chem. Lett.* **2004**, *14*, 1229.
- ²⁸Can, O. D., Ozkay, U. D., Kaplanclkl, Z. A., Ozturk, Y., *Arch. Pharm. Res.* **2009**, *32*, 1293.
- ²⁹Palaska, E., Eroid, D., Demirdamar, R., *Eur. J. Med. Chem.* **1996**, *31*, 43.
- ³⁰Prasad, Y. R., Rao, A. L., Prasoona, K., Murali, K., Ravikumar, P., *Bioorg. Med. Chem. Lett.* **2005**, *15*, 5030.
- ³¹Berghot, M. A., Moawad, E. B., *Eur. J. Pharm. Sci.* **2003**, *20*, 173.
- ³²Nauduri, D., Reddy, G. B., *Chem. Pharm. Bull.* **1998**, *46*, 1254.
- ³³Korgaokar, S. S., Patil, P. H., Shah, M. T., Prekh, H. H., *Indian J. Pharm. Sci.* **1996**, *58*, 222.
- ³⁴Guniz, K. S., Rollas, S., Erdeniz, H., Kiraz, M., Cevdet, E. A., Vidin, A., *Eur. J. Med. Chem.* **2000**, *35*, 761.
- ³⁵Havrylyuk, D., Zimenkovsky, B., Vasylenko, O., Zaprutko, L., Gzella, A., Lesyk, R., *Eur. J. Med. Chem.* **2009**, *44*, 1396.
- ³⁶Klimova, E. I., Marcos, M., Klimova, T. B., Cecilio, A. T., Ruben, A. T., Lena, R. R., *J. Organomet. Chem.* **1999**, *585*, 106.
- ³⁷Padmavathi, V., Sumathi, R. P., Chandrasekhar, B. N., Bhaskar Reddy, D., *J. Chem. Res.* **1999**, 610.
- ³⁸Bhaskar Redy, D., Chandrasekhar, B. N., Padmavathi, V., Sumathi, R. P., *Synthesis*, **1998**, 491.
- ³⁹Soni, N., Pande, K., Kalsi, R., Gupta, T. K., Parmar, S. S., Barthwal, J. P., *Res. Commun. Chem. Pathol. Pharm.* **1987**, *56*, 129.
- ⁴⁰Frigolo, M., Barros, H. M., Marquardt, A. R., Tanhauser, M., *Pharmacol. Biochem. Behav.* **1998**, *60*, 431.
- ⁴¹Erhan, P., Mutlu, A., Tayfun, U., Dilek, E., *J. Med. Chem.* **2001**, *36*, 539.
- ⁴²Shader, R. I., Greenblatt, D. J., *J. Clin. Psychopharm.* **1999**, *19*, 105.
- ⁴³Urichuk, L. J., Allison, K., Holt, A., Greenshaw, A. J., Baker, G. B., *J. Affec. Disord.* **2000**, *58*, 135.
- ⁴⁴Sakthnathan, S. P., Vanangamudi, G., Thirunarayanan, G., *Spectrochim. Acta.* **2012**, *95A*, 693.
- ⁴⁵Thirunarayanan, G., Gopalakrishnan, M., Vanangamudi, G., *Spectrochim. Acta.* **2007**, *67A*, 1106.
- ⁴⁶Thirunarayanan, G., Vanangamudi, G., Subramanian, M., *Org. Chem: An Indian J.* **2013**, *9*, 1.
- ⁴⁷Vanangamudi, G., Ranganathan, K., Thirunarayanan, G., *World J. Chem.* **2012**, *7*, 22.
- ⁴⁸Sakthnathan, S. P., Suresh, R., Mala, V., Sathiyamoorthi, K., Kamalakkannan, D., Ranganathan, K., Arulkumar, R., Vijayakumar, S., Sundararajan, R., Vanangamudi, G., Thirunarayanan, G., *Int. Lett. Chem. Phys. Astron.* **2013**, *6*, 77.
- ⁴⁹Janaki, P., Sekar, K. G., Thirunarayanan, G., *Org. Chem: An Indian J.* **2013**, *9*, 68.
- ⁵⁰Nithyanjani, A., Nisha, P., Thirunarayanan, G., *Natl. Conf. Exploring Excellence in Chemistry (NCEEC-12)*, December 21, 2012, P21, Dhanalakshmi Srinivasan College of Arts and Science for Women, Perambalur-621 212, Tamilnadu, India.
- ⁵¹Swain, C. G., Lupton, Jr. E. C., *J. Am. Chem. Soc.* **1968**, *90*, 4328.

Received: 17.03.2013.

Accepted: 18.04.2013.



PHASE BEHAVIOR AND PHYSICOCHEMICAL PROPERTIES OF WATER/CETYLTRIMETHYLAMMONIUM BROMIDE/*N*- PROPANOL/ALLYLBENZENE MICELLAR SYSTEMS

Monzer Fanun,^{[a]*} Ahmad Shakarnah,^[a] Oday Mustafa,^[a] Michael Schwarze,^[b] Reinhard Schomäcker^[b] and Jochanan Blum^[c]

Keywords: phase behavior, ultrasonic velocity, density, isentropic compressibility, hydrodynamic diameter; cetyltrimethylammonium bromide, allylbenzene, *n*-propanol, water

Water/*n*-propanol/cetyltrimethylammonium bromide/allylbenzene micellar systems were formulated. The ratio (w/w) of *n*-propanol/cetyltrimethylammonium bromide equals 2/1. The extent of the micellar region as function of temperature was determined. The micellar systems were characterized by the volumetric parameters, density, excess volume, ultrasonic velocity and isentropic compressibility. The micellar densities increase with the increase in the water volume fraction. Excess volumes increase with the water volume fraction and temperature. Ultrasonic velocities increase with water volume fraction up to 0.8 then decrease. Ultrasonic velocities increase with temperature for water volume fractions below 0.8 and increase for water volume fractions above 0.8. Isentropic compressibilities decrease with the water volume fraction up to 0.8 then increase. Isentropic compressibilities increase with temperature for water volume fractions below 0.8 and decrease for water volume fractions above 0.8. Structural transitions from water-in-oil to bicontinuous to oil-in-water occur along the micellar phase. The particle hydrodynamic diameter of the oil-in-water micellar systems decrease with temperature. In the diluted region nanoemulsions systems were observed.

Corresponding Authors

Tel: + 972 5 22 40 60 61;

Fax: + 972 22 79 69 60

E-Mail: Fanunm@gmail.com, ormfanun@science.alquds.edu

- [a] Colloids and Surfaces Research Center, Al-Quds University, East Jerusalem 51000, Palestine
[b] Institut für Chemie, Technische Universität Berlin, Strasse des 17. Juni 124, D-10623 Berlin, Germany
[c] Institute of Chemistry, The Hebrew University of Jerusalem, Jerusalem 91904, Israel

Introduction

Nanoemulsions have homogeneous and very tiny droplet sizes, usually in the range of 20–500 nm.^{1,2} Use of nanoemulsions in industrial applications is very attractive since they do not require a high concentration of surfactants. These systems can be prepared using moderate surfactant concentrations (in the range of 4–8 wt%). The properties of these systems that are kinetically stable, with low viscosity and optical transparency make them very attractive systems for many industrial applications.^{3–9} Nanoemulsions are used as drug delivery systems,^{3,4} in personal care and cosmetics^{5,6} and also as reaction media.^{7–10} In this study, we report on the use of the ultrasonic velocity measurement and dynamic light scattering techniques for analysis of a pseudoternary system consisting of allylbenzene as the oil phase, the cationic surfactant, cetyltrimethylammonium bromide, a cosurfactant (*n*-propanol), and water. Changes in the ultrasonic velocity and in the density were measured as a function of water volume fraction and temperature. The particle sizes of the diluted systems (i.e., at water volume fractions above 0.90) were determined.

Experimental

Materials

Allylbenzene (ALB), *n*-propanol (*n*-PrOH), and cetyltrimethylammonium bromide (CTAB), were purchased from Sigma-Aldrich Chemical Company. All of the components were used as supplied without further purification. Triply distilled water was used for all experiments.

Methods

Sample preparation for pseudoternary phase diagram at constant temperature

The behavior of a four-component system is described in pseudoternary phase diagrams in which the weight ratio of surfactant/co-surfactant is fixed. The determination of the phase diagram was performed in a thermostated bath ($T \pm 0.1$ K). Ten weighted samples composed of mixtures of (surfactant + co-surfactant) and oil were prepared in culture tubes sealed with viton-lined screw caps at predetermined weight ratios of surfactant/co-surfactant/oil. The mixtures were titrated with water along dilution lines drawn to the aqueous phase apex from the opposite side of the triangle. In all of the samples tested, evaporative losses were negligible. Nearly all samples were equilibrated during a time interval of up to 24 h. The different phases were determined visually and by optical (crossed polarizers) methods. Appearance of turbidity was considered as an indication for phase separation. The phase behavior of such samples was determined only after sharp interfaces had become visible.

The completion of this process was accelerated by centrifuging the samples. Every sample that remained transparent and homogeneous after vigorous vortexing was considered as a one phase region in the phase diagram.^{11,12}

The solubilization capacity was determined for the one phase region of the relevant pseudoternary phase diagrams. Li et al.¹³ proposed the total one phase area in the phase diagram as a solubilization parameter. We call this area A_T . The relative error in determining the A_T was estimated to be $\pm 2\%$ for all systems studied.

Ultrasonic velocity and density

The ultrasonic velocity and density of the various one phase transparent samples were measured using a density and sound velocity analyzer (DSA 500M- Anton Paar, Austria) with a sound velocity resolution of 0.5 ms^{-1} and density resolution of $(5 \times 10^{-6} \text{ g cm}^{-3})$. A 3 ml degassed sample is introduced using Hamilton glass syringe into a U-shaped borosilicate glass tube that is being excited electronically to vibrate at its characteristic frequency. The characteristic frequency (high frequency (above 100 kHz) acoustic waves) changes depending on the density of the sample. Through precise determination of the characteristic frequency and a mathematical conversion, the density of the sample can be calculated. The measuring cell is closed by an ultrasonic transmitter on the one side and by a receiver on the other side. The transmitter sends sound waves of a known frequency through the sample. The velocity of sound was calculated by determining of the period of received sound waves and by considering the distance between transmitter and receiver. Due to the high dependency of the density and velocity of sound values on the temperature, the measuring cells have to be thermostated precisely with two integrated Pt 100 platinum thermometers together with Peltier elements provide an precise thermostating of the sample that equals $\pm 0.01^\circ\text{C}$. Viscosity-related errors were automatically corrected over the full viscosity range by measuring the damping effect of the viscous sample followed by a mathematical correction of the density value. The instrument automatically detects gas bubbles in the density measuring cell by an advanced analysis of its oscillation pattern and generates a warning message. Each sample was degassed before placing it in the analyzer. Measurements were made at 298, 310, 318 K.

Dynamic light scattering

Zetasizer Nano S (ZEN 1600) by Malvern Instruments Ltd. (Worcestershire, United Kingdom) for the measurements of the size of diluted micellar particles. The equipment includes a 4mW, 633nm He-Ne laser. Size measurement range between 0.6nm to $6 \mu\text{m}$, size measurement angle equals 173° . 1.5 ml micellar sample was introduced in a disposable polystyrene cuvettes and measured at temperatures range between 303 and 323 K by steps of 5 K. The particle hydrodynamic diameter was calculated from the translational diffusion coefficient (D) using the Stokes-Einstein relationship:

$$d_H = \frac{k_B T}{6\pi\eta D} \quad (1)$$

where

d_H is the hydrodynamic diameter,

k_B is Boltzmann's constant,

T is the absolute temperature and

η is the solvent viscosity.

The results are averages of 3 experiments.

Results and Discussion

Phase behavior

Figure 1 presents the phase behavior of water/cetyltrimethylammonium bromide/*n*-propanol/allylbenzene systems at 298 K. The ratio (w/w) of *n*-propanol/surfactant equals 2/1. As shown in the Figure 1, the phase behavior of the cationic surfactant cetyltrimethylammonium bromide is similar to that of the anionic sodium dodecyl sulfate and is different from that observed with the nonionic surfactants sucrose monolaurate presented elsewhere.^{12,14,15}

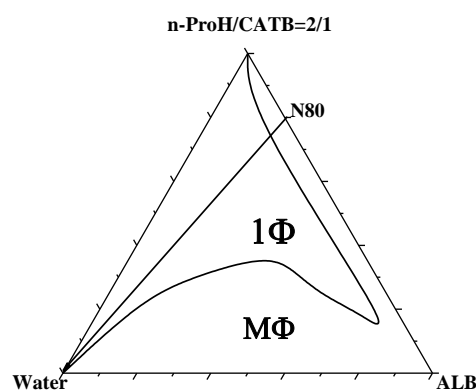


Figure 1. Pseudoternary phase diagram of the water/*n*-propanol/cetyltrimethylammonium bromide/allylbenzene system at 298 K. The mixing ratio (w/w) of *n*-propanol/surfactant equals 2/1. The isotropic one phase region is designated by 1Φ , and the multiple phase regions are designated by $(M\Phi)$. N80 is the dilution line where the weight ratio of (surfactant + propanol)/allylbenzene equals 4/1.

In the case of the cetyltrimethylammonium bromide, the transparent micellar region appears after the addition of about 10 wt. % of water. Similar findings on the behavior of cetyltrimethylammonium bromide in the presence of other aromatic oils were reported.^{12,14-17} The area of the one phase region varies very slightly with temperature.

Volumetric properties

The ultrasonic wave propagates through materials and as it transverses a sample, compressions and decompressions in the ultrasonic wave change the distance between molecules within the material, which, in turn, respond by intermolecular repulsions and attractions and probes the elastic properties of samples.¹⁸⁻²⁰ Figure 2 represent the variation in the density as function of the water volume fraction for the water/*n*-propanol/ cetyl trimethylammonium

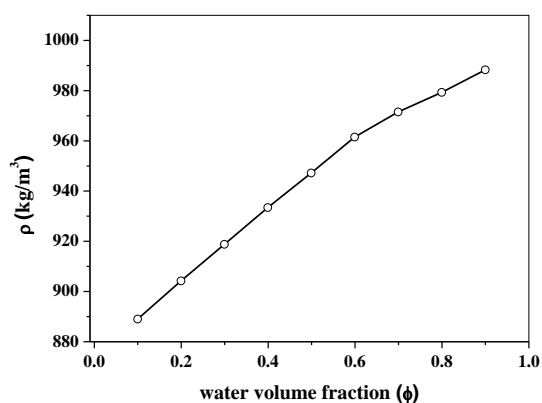


Figure 2. Variation of the density as function of water volume fraction along N80 for the micellar system presented in Figure 1.

bromide /allylbenzene systems. The relation (2) can evaluate the excess volume of micelle formation, keeping in view the additivity of volumes of micellar, aqueous and oil phase,

$$V^E = V_{mic} - \sum_i \phi_i V_i \quad (2)$$

where

V^E is the excess volume,

V_{mic} is the measured micellar specific volume,

ϕ_i is the volume fraction of component i in the micellar system and

V_i is the specific volume of component i .

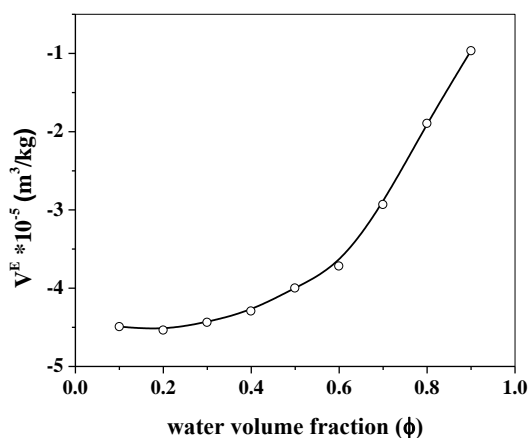


Figure 3. Variation of the excess volume as function of water volume fraction along N80 for the micellar system presented in Figure 1.

Figure 3 presents the variation in the excess volume as function of water volume fraction. In the case of the cationic surfactant cetyltrimethyl ammonium bromide the excess volume increases with the water volume fraction. The excess volume values are negative indicating that the system contracts upon addition of water. Similar behaviors of excess volume with ionic and nonionic surfactants were presented elsewhere.^{12,14,15} The values of excess volume were also determined as function of temperature and it was found that excess volume increases with temperature indicating expansion of the micellar systems with

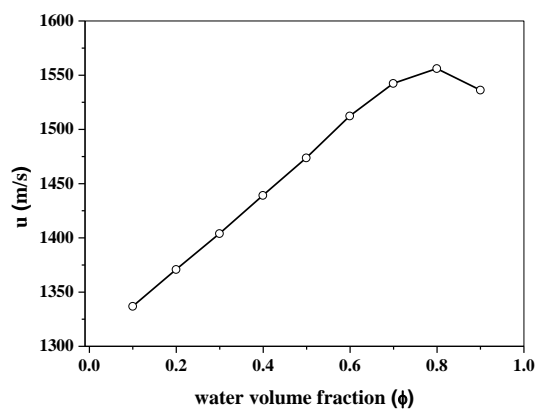


Figure 4. Variation of the ultrasonic velocity as function of water volume fraction along N80 for the micellar system presented in Figure 1.

temperature. This behavior could be related to breakage of hydrogen bonds or to dissociation of ionic head groups. Figure 4 represents the variation of the ultrasonic velocity as function of the water volume fraction for the water/n-propanol/cetyltrimethyl ammonium bromide/allylbenzene systems. The ultrasonic velocity increases with the water volume fraction upto 0.8 thereafter decreases. The variation in the values of ultrasonic velocity as function of water volume fraction provides information on the state of water. At low water volume fraction the properties of water are very different from those of bulk water indicating the entrapment of water in the micellar core suggesting the presence of water-in-oil microstructure. The increase in the values of ultrasonic velocity upon addition of water indicates structural transitions along the water dilution line. For water volume fraction above 0.8 the ultrasonic velocity approaches that of pure water indicating that water is the continuous phase and oil-in-water microstructure is present. Since ultrasonic velocity is determined by the change of physical properties at the interface between the particle core and the continuous medium, the ultrasonic velocity variation shall also be correlated to the variation of the size of the particle core. In order to better understand these results, we analyzed the ultrasonic velocity in terms of isentropic compressibility k_s , which represents a relative change of volume per unit of pressure applied at constant entropy. k_s is much more sensitive to structural changes than the velocity and can provide qualitative information about the physical nature of the aggregates. The isentropic compressibility k_s values have been evaluated with the help of the Laplace equation:²¹⁻²³

$$K_S = \frac{1}{u^2 \rho} \quad (3)$$

Figure 5 presents the variation of the isentropic compressibility k_s as function of the water volume fraction. The isentropic compressibility decreases with the water volume fraction below 0.8 and increases thereafter. The variation in the values of isentropic compressibility as function of increasing water volume fraction indicates structural transitions from water-in-oil to bicontinuous to oil-in-water microstructure. The values of the isentropic compressibility were determined as function of temperature (see Figure 6) and found to increase with temperature for water volume fractions below 0.8 while for water volume

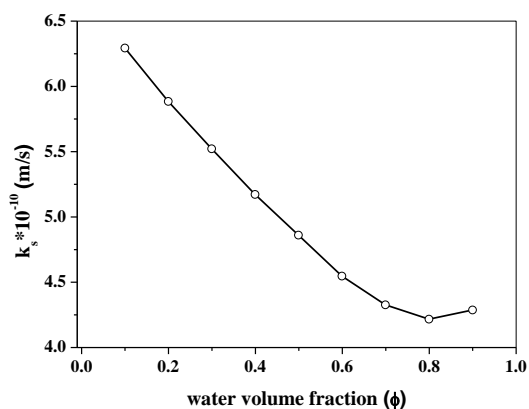


Figure 5. Variation of the isentropic compressibility as function of water volume fraction along N80 for the micellar system presented in Figure 1.

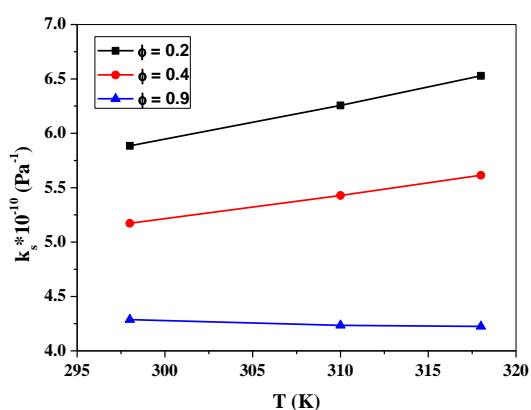


Figure 6. Variation of the isentropic compressibility as function of temperature along N80 for the micellar system presented in Figure 1.

fraction above 0.8 the isentropic compressibility values decrease. Possible microstructure transitions in the studied micellar system are presented schematically in Figure 7.

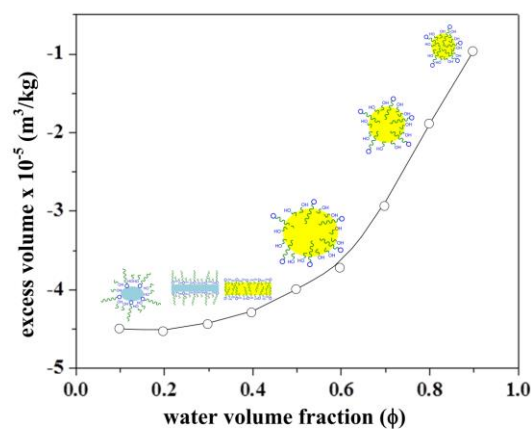


Figure 7. Schematic presentation (not for scale) of the structural transitions along N80 for the micellar system presented in Figure 1.

Diffusion properties

For diluted micellar systems consisting of closed aggregates the diffusion of the aggregated components is given solely by the aggregate diffusion. At water volume fraction of 0.90 and on the assumption that exchange processes are negligible for the surfactant, we can estimate the hydrodynamic diameter (d_H) of the micelles in the water-rich region at water volume fraction about 0.90 using equation 1. The variation in the values of the hydrodynamic diameter (d_H) at water volume fraction of 0.90 for the different systems used in this study as function of temperature are shown in Figure 8. As shown in Figure 8 the hydrodynamic diameter decreases with temperature from 299 nm at 303K to 256 nm at 318K. The value of the hydrodynamic diameter indicates that the micellar systems formed with cetyltrimethyl ammonium bromide are nanoemulsions.

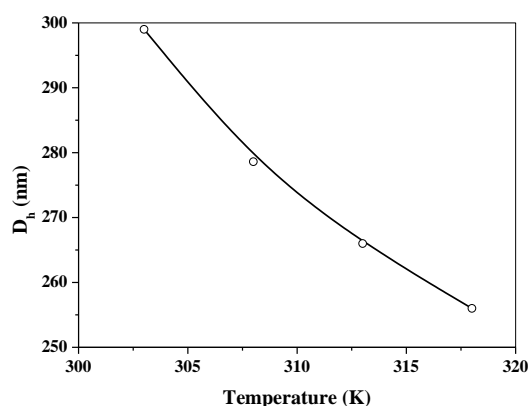


Figure 8. Variation of the particle hydrodynamic diameter as function of temperature along N80 for the diluted micellar system presented in Figure 1.

Conclusion

Temperature insensitive micellar systems were formulated for performing reactions with hydrophobic reagents that will lead to a significant reduction in the vast amount of organic solvents used currently in organic syntheses, and consequently increase the safety and diminish the cost of chemical processes. Quantitative analysis of the studied properties enabled the characterization of structural transition along the micellar phase. Nanoemulsion system were revealed by the determination of the particle size diameters of the diluted systems. Since the particle size of the micellar system is an important parameter in determining the yield of isomerization reaction of allylbenzene, the results presented in this study recommend performing these reactions at water volume fractions above 0.85 or at surfactant contents slightly above the critical micelle concentration and at high temperatures.

Acknowledgment

We gratefully acknowledge the financial support of this trilateral study by the Deutsche Forschungsgemeinschaft (DFG) through grant SCHO 687/8-2.

References

- ¹Forgiarini, A., Esquena, J., Gonzalez, C., Solans, C., *Langmuir* **2001**, *17*, 2076.
- ²Wang, L., Li, X., Zhang, G., Dong, J., Eastoe, J., *J. Colloid Interfac. Sci.*, **2007**, *314*, 230.
- ³Ravi Theaj Prakash, U., Thiagarajan, P., *Res. Biotechnol.*, **2011**, *2*, 1.
- ⁴Sarker, D. K., *Curr Drug Deliv.*, **2005**, *2*, 297.
- ⁵Yilmaz, Y., Borchert, H. H., *Int. J. Pharm.*, **2006**, *307*, 232.
- ⁶Simonnet, J. T., Sonnevile, O., Legret, S., US Patent US 6689371, **2004**.
- ⁷Antonietti, M., Landfester, K., *Org. Polym. Sci.*, **2002**, *27*, 689
- ⁸Tiarks, F., Landfester, K., Antonietti, M., *Langmuir*, **2001**, *17*, 908.
- ⁹Porras, M., Martinez, A., Solans, C., Gonzalez, C., Gutierrez, J. M., *Colloids Surfaces A: Physicochem. Eng. Aspects*, **2005**, *270–271*, 189.
- ¹⁰Meltzer, D., Avnir, D., Fanun, M., Gutkin, V., Popov, I., Schomacker, R., Schwarze, M., Blum, J., *J. Mol. Catal. A: Chem.*, **2011**, *335*, 8.
- ¹¹Fanun, M., *J. Colloid Interface Sci.*, **2010**, *343*, 496.
- ¹²Fanun, M., Shakarnah, A., Meltzer, D., Schwarze, M., Schomaecker, R., Blum, J., *Tenside Surfact. Deterg.*, **2011**, *48*, 400.
- ¹³Li, G., Kong, X., Guo, R., Wang X., *J. Disp. Sci. Technol.*, **1989**, *5*, 29.
- ¹⁴Fanun, M., Ayad, Z., Mudalal, S., Dahoah, S., Meltzer, D., Schwarze, M., Schomaecker, R., Blum, J., *J. Surfact. Deterg.* **2012**, *15*, 505.
- ¹⁵Fanun, M., Shakarnah, A., Mustafa, O., Schwarze, M., Schomaecker, R., Blum, J., *Eur. Chem. Bull.*, **2012**, *1*, 141.
- ¹⁶Rushforth, D.S., Sanchez-Rubio, M., Santo-Vidals, L. M., Wormuth, K. R., Kaler, E. W., Cuevas, R., Puig, J. E., *J. Phys. Chem.*, **1986**, *90*, 6668.
- ¹⁷Belloq, A. M., Biais, J., Clin, B., Gelot, A., Lalanne, P., Lemanceau, B., *J. Colloid Interface Sci.*, **1980**, *74*, 311.
- ¹⁸Hickey, S., Lawrence, M. J., Hagan, S. A. and Buckin, V., *Langmuir*, **2006**, *22*, 5575.
- ¹⁹Mehta, S.K., Bala, K., *Fluid Phase Equilibria*, **2000**, *172*, 197.
- ²⁰Alberola, C., Dederichs, T., Emeis, D., Moller, M., Sokolowski, T., Witten, K.P., *J. Colloid Interface Sci.*, **2007**, *307*, 500.
- ²¹Ye, L., Weitz, D. A., Sheng, P., Bhattacharya, S., Huang, J. S., Higgins, H. J., *J. Phys. Rev. Lett.* **1989**, *63*, 263.
- ²²Wood, A. B., *A Textbook of Sound*, G. Bell, London, **1941**.
- ²³Barret-Gultepe M. A., Yeager, E. B., *J. Phys. Chem.* **1983**, *87*, 1039.

Received: 19.02.2013.

Accepted: 18.04.2013.



SYNTHESIS OF AZETIDINONE DERIVATIVES OF 2-AMINO-5-NITROTHIAZOLE AND THEIR MEDICINAL IMPORTANCE

Pushkal Samadhiya*, Ritu Sharma, Santosh K. Srivastava

Keywords: Synthesis, 2-amino-5-nitrothiazole, azetidinone, antimicrobial, antitubercular, antiinflammatory.

New series of *N*-[3-(2-amino-5-nitrothiazolyl)-propyl]-4-(substitutedphenyl)-3-chloro-2-oxo-1-azetidine-carboxamide, compounds **4a-4j** have been synthesized and characterized by chemical and spectral analyses such as IR, ¹H NMR, ¹³C NMR and FAB-Mass. All the synthesized compounds **4a-4j** were screened for their antibacterial and antifungal activities against some selected bacteria and fungi with their MIC values and antitubercular activity screened against *M. tuberculosis*. Anti-inflammatory activity was *in vivo* screened against albino rats. Some compounds of the series showed good activities.

* Corresponding Authors

E-Mail: pushkalsamadhiya@rediffmail.com

[a] Department of Chemistry, Dr. H.S. Gour University (A Central University), Sagar, M.P. India 470003.

INTRODUCTION

Bacterial and fungal infection is most common problem of the world. Some serious and life threatening diseases also caused by bacterial or fungal infection. Tuberculosis is one of the most common infectious diseases. According to World Health Organization (WHO), 196 countries reported 2.6 million new smear positive TB cases in 2008, of which 1.78 million people died from it. Another hand inflammation is also major problem of all over the world because many people die every year cause of inflammation. In case of accident and organ transplantation or surgery microbial infection is also common problem. From the last decade, researchers made a continuous effort to fight these diseases.

Several new classes of chemotherapeutic agents have been introduced in the last decade. Several azole or azetidine constitute containing drugs displayed promising results. Benzotriazole derivatives are also member of significant class of chemistry because of their wide use in organic synthesis and pharmaceutical chemistry. Thiazole is one of the most intensively investigated class of aromatic five membered heterocyclic system has been employed as a anticonvulsant¹, fungicidal². Some of the thiazole analogues are also used as antibiological³, antibacterial^{4,5}. All these facts were driving force to develop novel thiazole derivatives with wide structure variations.

2-Azetidinone derivatives play a vital role owing to their wide range biological activity and industrial importance⁶. Recently found application in drug development for the treatment of antimicrobial⁷, anticonvulsant⁸, antiinflammatory⁹, antibacterial^{10,11}. As part of interest in heterocycles that have been explored for developing pharmaceutically important molecules.

The biological activities of both 2-oxo-azetidine and thiazole aroused our interest in the synthesis of 2-oxo-azetidine derivatives of 2-amino-5-nitrothiazole (scheme **1**).

All synthesized compounds were screened against some selected bacteria and fungi for their antimicrobial activity and antitubercular activity screened against *M. tuberculosis* using H37Rv strain. Anti-inflammatory activity was *in vivo* screened against albino rats. The structures of all the newly synthesized compounds were confirmed by elemental analysis, IR, ¹H NMR, ¹³C NMR, and FAB-Mass.

EXPERIMENTAL

Melting points were taken in open capillaries and are uncorrected. Progress of reaction was monitored by silica gel-G coated TLC plates using MeOH: CHCl₃ system (2:8). The spot was visualized by exposing dry plate at iodine vapours chamber. IR spectra were recorded in KBr disc on a Shimadzu 8201 PC, FTIR spectrophotometer (ν_{\max} in cm⁻¹) and ¹H NMR and ¹³C NMR spectra were measured on a Bruker DRX-300 spectrometer in CDCl₃ at 300 and 75 MHz using TMS as an internal standard respectively. All chemical shifts were reported on δ scales. The FAB-Mass spectra were recorded on a Jeol SX-102 mass spectrometer. Elemental analyses were performed on a Carlo Erba-1108 analyzer. The analytical data of all the compounds were highly satisfactory. For column chromatographic purification of the products, Merck silica Gel 60 (230-400 Mesh) was used. The reagent grade chemicals were purchased from the commercial sources and further purified before use.

Biological importance

Antimicrobial activity

The MIC values of compounds **4a-4j** have been determined using the filter paper disc diffusion method and the concentrations have been used in $\mu\text{g/mL}$. All the final synthesized compounds **4a-4j** have been screened for their antibacterial activity against *B. subtilis*, *E. coli*, *S. aureus* and *K. pneumoniae* and screened for their antifungal activity against *A. niger*, *A. flavus*, *F. oxisporium* and *C. albicans*. The MIC values of standard Streptomycin and Griseofulvin for all bacteria and fungi were in the range of 1.25-3.25 and 6.25-12.5 $\mu\text{g/mL}$ respectively. The MIC values of the compounds **4a-4j** were presented in Table 1.

Antitubercular activity

The synthesized compounds **4a-4j** were screened against *M. tuberculosis* (H37Rv strain) using L. J. medium (Conventional) method at 50 µg/mL and lower concentrations. The standard antitubercular drugs Isoniazid and Rifampicin (MIC range 2-4 µg/mL) were taken as standards. The results were showing in Table 2.

Antiinflammatory activity

Carageenan induced rat paw oedema method was employed for evaluating the antiinflammatory activity of compounds at a dose 50 mg/ kg bw in albino rats (weighing 80-110 gm, each group contain 5 animal) using phenylbutazone as a standard drug for comparison at a dose 30 mg/ kg bw. The percentage inhibition of inflammation was calculated by applying Newbould formula. Results of some active compounds were given in Table 3.

Synthesis of 1-(3-chloropropyl)-2-amino-5-nitrothiazole, (1)

2-Amino-5-nitrothiazole (0.345 mole) and 1-bromo-3-chloropropane (0.345 mole) in methanol (100 ml) were stirred on a magnetic stirrer for about 6.30 hours at room temperature. The completion of the reaction was monitored by silica gel-G coated TLC plates. After the completion of the reaction the product was filtered and purified over a silica gel packed column chromatography using CHCl₃ : CH₃OH (8 : 2 v/v) system as eluant (120 ml). The purified product was dried under vacuo and recrystallized from ethanol at room temperature to yield compound **1** (Figure 1).

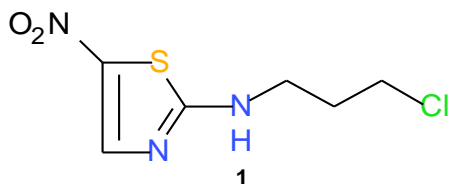


Figure 1. Structure of compound **1**.

1-(3-Chloropropyl)-2-amino-5-nitrothiazole (1): Yield: 62%; m.p. 173-175 °C; IR (cm⁻¹): 727 (C-Cl), 881 (C-S), 968 (C-NO), 1313 (N-CH₂), 1362, 1532 (NO₂), 1559 (C=C), 1436, 2832, 2897 (CH₂), 3009 (CH-Ar), 3388 (NH); ¹H NMR (300 MHz, CDCl₃, TMS) δ: 1.91-1.95 (m, 2H H-8), 3.27 (t, 2H, J = 7.35 Hz, H-9), 3.85-3.89 (m, 2H, H-7), 7.71 (s, 1H, H-4), 7.83 (br, s, 1H, H-6); ¹³C NMR (75 MHz, CDCl₃, TMS) δ: 34.4 (C-8), 41.7 (C-9), 45.9 (C-7), 134.2 (C-4), 137.8 (C-5), 166.5 (C-2); FAB-Mass (m/z): 221 [M⁺]; Anal. Calcd. for C₆H₈N₃O₂SCl: C; 32.51, H; 3.63, N; 18.95; Found: C; 32.49, H; 3.59, N; 18.87.

Synthesis of N-[3-(2-amino-5-nitrothiazolyl)-propyl]-urea, (2)

Compound **1** (0.2256 mol) and urea (0.2256 mol) in methanol (100 ml) were stirred on a magnetic stirrer for about 6.30 hours at room temperature. The completion of the reaction was monitored by silica gel-G coated TLC

plates. After the completion of the reaction the product was filtered and purified over a silica gel packed column chromatography using CHCl₃ : CH₃OH (8 : 2 v/v) system as eluant (120 ml). The purified product was dried under vacuo and recrystallized from ethanol at room temperature to yield compound **2** (Figure 2).

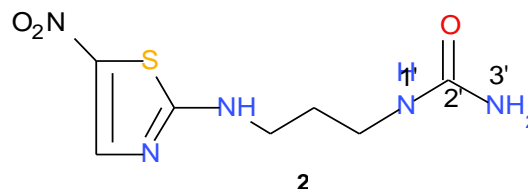


Figure 2. Structure of compound **2**.

N-[3-(2-Amino-5-nitrothiazolyl)propyl]urea (2): Yield: 70%; m.p. 153-155 °C; IR (cm⁻¹): 879 (C-S), 966 (C-NO), 1324 (N-CH₂), 1360, 1533 (NO₂), 1559 (C=C), 1662 (C=O), 1432, 2885, 2918 (CH₂), 3021 (CH-Ar), 3387 (NH), 3452 (NH₂); ¹H NMR (300 MHz, CDCl₃, TMS) δ: 2.08-2.12 (m, 2H, H-8), 3.19-3.24 (m, 2H, H-9), 3.82-3.90 (m, 2H, H-7), 5.67 (s, 1H, H-1'), 5.97 (br s, 2H, H-3'), 7.65 (s, 1H, H-4), 7.80 (br, s, 1H, H-6); ¹³C NMR (75 MHz, CDCl₃, TMS) δ: 33.4 (C-8), 38.6 (C-9), 44.1 (C-7), 133.8 (C-4), 138.5 (C-5), 163.4 (C-2'), 165.3 (C-2); FAB-Mass (m/z): 245 [M⁺]; Anal. Calcd. for C₇H₁₁N₅O₃S: C; 34.28, H; 4.52, N; 28.55; Found: C; 34.25, H; 4.48, N; 28.51.

Synthesis of N-[3-(1H-2-amino-5-nitrothiazolyl)propyl]-N'-[phenylmethylidene]urea, compound 3a:

The compound **2** (0.0330 mole) and benzaldehyde (0.0330 mole) in methanol (100 ml) in the presence of 2-4 drops of glacial acetic acid were first stirred on a magnetic stirrer for about 2.00 hours followed by reflux on a steam bath for about 3.30 hours. The completion of the reaction was monitored by silica gel-G coated TLC plates. The product was filtered and cooled at room temperature. The filtered product was purified over a silica gel packed column chromatography using CH₃OH : CHCl₃ (7 : 3 v/v) as eluant (75 ml). The purified product was dried under vacuo and recrystallized from ethanol at room temperature to furnish compound **3a** (Figure 3).

Compounds **3b-3j** have also been synthesized by using similar method as above.

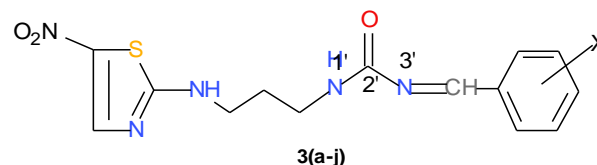


Figure 3. Structure of compound **3a-3j**.

N-[3-(2-Amino-5-nitrothiazolyl)-propyl]-N'-(phenylmethylidene)urea (3a): Yield: 62%; m.p. 148-149 °C; IR (cm⁻¹): 856 (C-S), 961 (C-NO), 1329 (N-CH₂), 1356, 1531 (NO₂), 1547 (C=C), 1565 (N=CH), 1661 (C=O), 1427, 2878, 2912 (CH₂), 3016 (CH-Ar), 3382 (NH); ¹H NMR (300 MHz, CDCl₃, TMS) δ: 2.02-2.07 (m, 2H, H-8), 3.20-3.25 (m, 2H, H-9), 3.80-3.85 (m, 2H, H-7), 5.60 (s, 1H, H-1'), 7.24 (s, 1H, H-4),

7.89 (s, 1H, H-6), 8.02 (s, 1H, H-10), 6.75-7.84 (m, 5H, Ar-H); ^{13}C NMR (75 MHz, CDCl_3 , TMS) δ : 28.2 (C-8), 36.5 (C-9), 42.4 (C-7), 126.7 (C-12 and C-16), 128.4 (C-14), 129.3 (C-13 and C-15), 130.7 (C-4), 136.6 (C-5), 137.2 (C-11), 147.4 (C-10), 160.5 (C-2'), 168.8 (C-2); Anal. Calcd. for $\text{C}_{14}\text{H}_{15}\text{N}_5\text{O}_3\text{S}$: C; 50.44, H; 4.53, N; 21.00; Found: C; 50.35, H; 4.55, N; 20.95; FAB-Mass (m/z): 333 [M^+].

N-[3-(2-Amino-5-nitrothiazolyl)propyl]-*N'*-[(4-chlorophenyl)methylidene]urea (**3b**): Yield: 62%; m.p 178-179°C; IR (cm^{-1}): IR: 744 (C-Cl), 870 (C-S), 968 (C-NO), 1342 (N-CH₂), 1365, 1541 (NO₂), 1556 (C=C), 1568 (N=CH), 1670 (C=O), 1430, 2884, 2917 (CH₂), 3022 (CH-Ar), 3390 (NH); ^1H NMR (300 MHz, CDCl_3 , TMS) δ : 2.11-2.15 (m, 2H, H-8), 3.22-3.27 (m, 2H, H-9), 3.83-3.88 (m, 2H, H-7), 5.64 (s, 1H, H-1'), 7.89 (s, 1H, H-4), 7.98 (s, 1H, H-6), 8.13 (s, 1H, H-10), 6.94-7.65 (m, 4H, Ar-H); ^{13}C NMR (75 MHz, CDCl_3 , TMS) δ : 28.6 (C-8), 40.1 (C-9), 43.2 (C-7), 126.6 (C-12 and C-16), 128.9 (C-14), 129.6 (C-13 and C-15), 130.9 (C-4), 135.2 (C-5), 141.4 (C-11), 147.7 (C-10), 160.2 (C-2'), 168.4 (C-2); FAB-Mass (m/z): 367 [M^+]; Anal. Calcd. for $\text{C}_{14}\text{H}_{14}\text{N}_5\text{O}_3\text{SCl}$: C; 45.71, H; 3.83, N; 19.04; Found: C; 45.60, H; 3.81, N; 19.01.

N-[3-(2-Amino-5-nitrothiazolyl)propyl]-*N'*-[(3-chlorophenyl)methylidene]urea (**3c**): Yield: 62%; m.p 174-175°C; IR (cm^{-1}): IR: 745 (C-Cl), 866 (C-S), 977 (C-NO), 1336 (N-CH₂), 1360, 1536 (NO₂), 1550 (C=C), 1558 (N=CH), 1667 (C=O), 1434, 2892, 2930 (CH₂), 3026 (CH-Ar), 3386 (NH); ^1H NMR (300 MHz, CDCl_3 , TMS) δ : 2.11-2.15 (m, 2H, H-8), 3.28-3.32 (m, 2H, H-9), 3.84-3.89 (m, 2H, H-7), 5.72 (s, 1H, H-1'), 7.30 (s, 1H, H-4), 7.95 (s, 1H, H-6), 8.14 (s, 1H, H-10), 6.82-7.93 (m, 4H, Ar-H); ^{13}C NMR (75 MHz, CDCl_3 , TMS) δ : 30.3 (C-8), 39.6 (C-9), 43.5 (C-7), 127.7 (C-12), 128.4 (C-16), 129.4 (C-14), 130.3 (C-13), 131.7 (C-15), 133.4 (C-4), 137.1 (C-5), 141.9 (C-11), 151.2 (C-10), 161.3 (C-2'), 169.8 (C-2); FAB-Mass (m/z): 367 [M^+]; Anal. Calcd. for $\text{C}_{14}\text{H}_{14}\text{N}_5\text{O}_3\text{SCl}$: C; 45.71, H; 3.83, N; 19.04; Found: C; 45.67, H; 3.77, N; 18.98.

N-[3-(2-Amino-5-nitrothiazolyl)propyl]-*N'*-[(2-chlorophenyl)methylidene]urea (**3d**): Yield: 62%; m.p 172-173°C; IR (cm^{-1}): IR: 747 (C-Cl), 860 (C-S), 962 (C-NO), 1330 (N-CH₂), 1358, 1534 (NO₂), 1549 (C=C), 1566 (N=CH), 1663 (C=O), 1428, 2880, 2913 (CH₂), 3017 (CH-Ar), 3384 (NH); ^1H NMR (300 MHz, CDCl_3 , TMS) δ : 2.08-2.12 (m, 2H, H-8), 3.30-3.35 (m, 2H, H-9), 3.82-3.86 (m, 2H, H-7), 5.70 (s, 1H, H-1'), 7.31 (s, 1H, H-4), 7.91 (s, 1H, H-6), 8.18 (s, 1H, H-10), 6.86-7.84 (m, 4H, Ar-H); ^{13}C NMR (75 MHz, CDCl_3 , TMS) δ : 31.2 (C-8), 38.8 (C-9), 44.7 (C-7), 127.3 (C-12), 128.6 (C-16), 129.7 (C-14), 130.4 (C-13), 132.5 (C-15), 134.5 (C-4), 138.2 (C-11), 138.9 (C-5), 151.6 (C-10), 162.4 (C-2'), 169.3 (C-2), (Ar); FAB-Mass (m/z): 367 [M^+]; Anal. Calcd. for $\text{C}_{14}\text{H}_{14}\text{N}_5\text{O}_3\text{SCl}$: C; 45.71, H; 3.83, N; 19.04; Found: C; 45.65, H; 3.75, N; 19.02.

N-[3-(2-Amino-5-nitrothiazolyl)propyl]-*N'*-[(4-bromophenyl)methylidene]urea (**3e**): Yield: 62%; m.p 170-171°C; IR (cm^{-1}): IR: 638 (C-Br), 858 (C-S), 970 (C-NO), 1335 (N-CH₂), 1370, 1537 (NO₂), 1551 (C=C), 1575 (N=CH), 1674 (C=O), 1440, 2886, 2921 (CH₂), 3019 (CH-Ar), 3387 (NH); ^1H NMR (300 MHz, CDCl_3 , TMS) δ : 2.07-2.12 (m, 2H, H-8), 3.29-3.34 (m, 2H, H-9), 3.81-3.85 (m, 2H, H-7), 5.73 (s, 1H, H-1'), 7.28 (s, 1H, H-4), 7.91 (s, 1H, H-6), 8.20 (s, 1H, H-10), 6.70-7.85 (m, 4H, Ar-H); ^{13}C NMR (75 MHz, CDCl_3 , TMS) δ : 29.3 (C-8), 36.8 (C-9), 42.6 (C-7), 128.6 (C-12 and

C-16), 130.5 (C-14), 131.2 (C-13 and C-15), 132.2 (C-4), 136.3 (C-5), 138.8 (C-11), 150.7 (C-10), 162.1 (C-2'), 170.4 (C-2); FAB-Mass (m/z): 412 [M^+]; Anal. Calcd. for $\text{C}_{14}\text{H}_{14}\text{N}_5\text{O}_3\text{SBr}$: C; 40.78, H; 3.42, N; 16.98; Found: C; 45.75, H; 3.39, N; 6.92.

N-[3-(2-Amino-5-nitrothiazolyl)propyl]-*N'*-[(3-bromophenyl)methylidene]urea (**3f**): Yield: 62%; m.p 169-170°C; IR (cm^{-1}): IR: 643 (C-Br), 860 (C-S), 963 (C-NO), 1337 (N-CH₂), 1374, 1540 (NO₂), 1554 (C=C), 1571 (N=CH), 1671 (C=O), 1432, 2888, 2922 (CH₂), 3025 (CH-Ar), 3388 (NH); ^1H NMR (300 MHz, CDCl_3 , TMS) δ : 2.10-2.17 (m, 2H, H-8), 3.30-3.36 (m, 2H, H-9), 3.87-3.92 (m, 2H, H-7), 5.67 (s, 1H, H-1'), 7.39 (s, 1H, H-4), 7.99 (s, 1H, H-6), 8.16 (s, 1H, H-10), 6.69-7.81 (m, 4H, Ar-H); ^{13}C NMR (75 MHz, CDCl_3 , TMS) δ : 31.8 (C-8), 37.2 (C-9), 45.4 (C-7), 128.3 (C-12), 128.7 (C-16), 130.8 (C-14), 131.6 (C-13), 132.7 (C-4), 133.8 (C-15), 136.4 (C-5), 139.4 (C-11), 148.6 (C-10), 161.9 (C-2'), 170.7 (C-2); FAB-Mass (m/z): 412 [M^+]; Anal. Calcd. for $\text{C}_{14}\text{H}_{14}\text{N}_5\text{O}_3\text{SBr}$: C; 40.78, H; 3.42, N; 16.98; Found: C; 40.73, H; 3.37, N; 16.94.

N-[3-(2-Amino-5-nitrothiazolyl)propyl]-*N'*-[(2-bromophenyl)methylidene]urea (**3g**): Yield: 62%; m.p 165-167°C; IR (cm^{-1}): IR: 645 (C-Br), 871 (C-S), 965 (C-NO), 1332 (N-CH₂), 1359, 1533 (NO₂), 1552 (C=C), 1560 (N=CH), 1664 (C=O), 1437, 2883, 2914 (CH₂), 3024 (CH-Ar), 3385 (NH); ^1H NMR (300 MHz, CDCl_3 , TMS) δ : 2.11-2.16 (m, 2H, H-8), 3.25-3.29 (m, 2H, H-9), 3.88-3.93 (m, 2H, H-7), 5.71 (s, 1H, H-1'), 7.40 (s, 1H, H-4), 7.94 (s, 1H, H-6), 8.14 (s, 1H, H-10), 6.71-7.89 (m, 4H, Ar-H); ^{13}C NMR (75 MHz, CDCl_3 , TMS) δ : 31.5 (C-8), 37.6 (C-9), 45.8 (C-7), 129.4 (C-12), 130.6 (C-16), 131.3 (C-14), 132.1 (C-13), 133.7 (C-15), 133.9 (C-4), 137.5 (C-5), 140.6 (C-11), 148.9 (C-10), 163.6 (C-2'), 171.4 (C-2); FAB-Mass (m/z): 412 [M^+]; Anal. Calcd. for $\text{C}_{14}\text{H}_{14}\text{N}_5\text{O}_3\text{SBr}$: C; 40.78, H; 3.42, N; 16.98; Found: C; 40.70, H; 3.36, N; 16.93.

N-[3-(2-amino-5-nitrothiazolyl)propyl]-*N'*-[(4-nitrophenyl)methylidene]urea (**3h**): Yield: 62%; m.p 167-168°C; IR (cm^{-1}): IR: 865 (C-S), 974 (C-NO), 1340 (N-CH₂), 1367, 1532 (NO₂), 1560 (C=C), 1573 (N=CH), 1673 (C=O), 1435, 2891, 2925 (CH₂), 3021 (CH-Ar), 3393 (NH); ^1H NMR (300 MHz, CDCl_3 , TMS) δ : 2.12-2.15 (m, 2H, H-8), 3.24-3.30 (m, 2H, H-9), 3.91-3.96 (m, 2H, H-7), 5.65 (s, 1H, H-1'), 7.32 (s, 1H, H-4), 7.99 (s, 1H, H-6), 8.17 (s, 1H, H-10), 6.74-7.95 (m, 4H, Ar-H); ^{13}C NMR (75 MHz, CDCl_3 , TMS) δ : 29.8 (C-8), 40.4 (C-9), 44.5 (C-7), 129.8 (C-12 and C-16), 131.2 (C-14), 132.7 (C-13 and C-15), 134.8 (C-4), 138.6 (C-5), 140.3 (C-11), 150.7 (C-10), 160.4 (C-2'), 171.3 (C-2); FAB-Mass (m/z): 378 [M^+]; Anal. Calcd. for $\text{C}_{14}\text{H}_{14}\text{N}_6\text{O}_5\text{S}$: C; 44.44, H; 3.72, N; 22.21; Found: C; 44.40, H; 3.69, N; 22.19.

N-[3-(2-Amino-5-nitrothiazolyl)propyl]-*N'*-[(3-nitrophenyl)methylidene]urea (**3i**): Yield: 62%; m.p 165-166°C; IR (cm^{-1}): IR: 859 (C-S), 972 (C-NO), 1338 (N-CH₂), 1371, 1545 (NO₂), 1557 (C=C), 1563 (N=CH), 1665 (C=O), 1431, 2894, 2927 (CH₂), 3030 (CH-Ar), 3394 (NH); ^1H NMR (300 MHz, CDCl_3 , TMS) δ : 2.11-2.15 (m, 2H, H-8), 3.29-3.33 (m, 2H, H-9), 3.85-3.89 (m, 2H, H-7), 5.66 (s, 1H, H-1'), 7.33 (s, 1H, H-4), 7.92 (s, 1H, H-6), 8.15 (s, 1H, H-10), 6.78-7.86 (m, 4H, Ar-H); ^{13}C NMR (75 MHz, CDCl_3 , TMS) δ : 30.7 (C-8), 38.3 (C-9), 45.8 (C-7), 131.4 (C-4), 130.1 (C-12), 130.9 (C-16), 132.6 (C-14), 133.4 (C-13), 134.1 (C-15), 136.9 (C-5), 137.5 (C-11), 149.2 (C-10), 163.6 (C-2'), 172.7

(C-2); FAB-Mass (m/z): 378 [M^+]; Anal. Calcd. for $C_{14}H_{14}N_6O_5S$: C; 44.44, H; 3.72, N; 22.21; Found: C; 44.38, H; 3.66, N; 22.17.

N-[3-(2-Amino-5-nitrothiazolyl)-propyl]-*N'*-[(2-nitrophenyl)methylidene]urea (**3j**): Yield: 62%; m.p 162-163°C; IR (cm^{-1}): 864 (C-S), 976 (C-NO), 1341 (N-CH₂), 1369, 1541 (NO₂), 1553 (C=C), 1561 (N=CH), 1669 (C=O), 1438, 2890, 2924 (CH₂), 3028 (CH-Ar), 3397 (NH); ¹H NMR (300 MHz, CDCl₃, TMS) δ : 2.15-2.19 (m, 2H, H-8), 3.20-3.26 (m, 2H, H-9), 3.87-3.93 (m, 2H, H-7), 5.68 (s, 1H, H-1'), 7.36 (s, 1H, H-4), 7.96 (s, 1H, H-6), 8.10 (s, 1H, H-10), 6.80-7.90 (m, 4H, Ar-H); ¹³C NMR (75 MHz, CDCl₃, TMS) δ : 30.7 (C-8), 39.7 (C-9), 44.5 (C-7), 131.8 (C-4), 130.5 (C-12), 131.6 (C-16), 132.4 (C-14), 133.6 (C-13), 134.5 (C-15), 137.3 (C-5), 139.7 (C-11), 149.9 (C-10), 163.2 (C-2'), 172.1 (C-2); FAB-Mass (m/z): 378 [M^+]; Anal. Calcd. for $C_{14}H_{14}N_6O_5S$: C; 44.44, H; 3.72, N; 22.21; Found: C; 44.35, H; 3.70, N; 22.18.

Synthesis of *N*-[3-(2-amino-5-nitrothiazolyl)-propyl]-4-phenyl-3-chloro-2-oxo-1-azetidine-carboxamide (**4a**):

The compound **3a** (0.009 mole) and chloroacetyl chloride (0.009 mole) in methanol (100 ml) in the presence of Et₃N (0.009 mole) were allowed to react at room temperature. The reaction mixture was first stirred on a magnetic stirrer for about 2.00 hours followed by reflux on a steam bath for about 3.30 hours. The completion of the reaction was monitored by silica gel-G coated TLC plates. The product was filtered and cooled at room temperature. The filtered product was purified over a silica gel packed column chromatography using CH₃OH : CHCl₃ (7 : 3 v/v) as eluant (90 ml). The purified product was dried under vacuo and recrystallized from acetone at room temperature to furnish compound **4a** (Figure 4).

Compounds **4b-4j** have also been synthesized by using similar method as above.

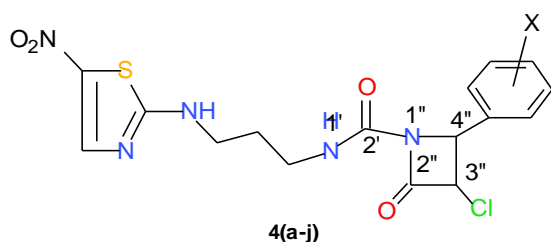


Figure 4. Structure of compound **4a-4j**.

N-[3-(2-Amino-5-nitrothiazolyl)-propyl]-4-(phenyl)-3-chloro-2-oxo-1-azetidinecarboxamide (**4a**): Yield: 61%; m.p. 169-170 °C; IR (cm^{-1}): 860 (C-S), 964 (C-NO), 1335 (N-CH₂), 1360, 1536 (NO₂), 1551 (C=C), 1666 (C=O), 1736 (CO cyclic), 1432, 2884, 2917 (CH₂), 2957 (CH-Cl), 3021 (CH-Ar), 3385 (NH); ¹H NMR (300 MHz, CDCl₃, TMS) δ : 2.07-2.11 (m, 2H, H-8), 3.22-3.29 (m, 2H, H-9), 3.88-3.94 (m, 2H, H-7), 4.36 (d, 1H, $J = 4.80$ Hz, H-3''), 5.12 (d, 1H, $J = 4.80$ Hz, H-4''), 5.65 (s, 1H, H-1'), 7.81 (s, 1H, H-4), 7.94 (s, 1H, H-6), 6.72-7.96 (m, 5H, Ar-H); ¹³C NMR (75 MHz, CDCl₃, TMS) δ : 29.1 (C-8), 37.5 (C-9), 44.9 (C-7), 50.2 (C-3''), 59.4 (C-4''), 128.1 (C-11 and C-16), 128.5 (C-15), 129.7 (C-12 and C-14), 132.7 (C-4), 136.6 (C-5), 138.5

(C-10), 161.5 (C-2'), 169.2 (C-2), 170.2 (C-2''); Mass (FAB): 409M⁺; Anal. Calcd. for $C_{16}H_{16}N_5O_4S$: C; 46.88, H; 3.93, N; 17.08%; Found: C; 46.82, H; 3.91, N; 17.02%;

N-[3-(2-Amino-5-nitrothiazolyl)-propyl]-4-(4-chlorophenyl)-3-chloro-2-oxo-1-azetidinecarboxamide (**4b**): Yield: 64%; m.p 178-179 °C; IR (cm^{-1}): 758 (C-Cl), 863 (C-S), 966 (C-NO), 1345 (N-CH₂), 1362, 1540 (NO₂), 1560 (C=C), 1667 (C=O), 1742 (CO cyclic), 1436, 2887, 2921 (CH₂), 2960 (CH-Cl), 3026 (CH-Ar), 3391 (NH); ¹H NMR (300 MHz, CDCl₃, TMS) δ : 2.12-2.16 (m, 2H, H-8), 3.25-3.31 (m, 2H, H-9), 3.88-3.90 (m, 2H, H-7), 4.38 (d, 1H, $J = 4.80$ Hz, H-3''), 5.15 (d, 1H, $J = 4.80$ Hz, H-4''), 5.66 (s, 1H, H-1'), 7.92 (s, 1H, H-4), 7.95 (s, 1H, H-6), 6.83-7.97 (m, 4H, Ar-H); ¹³C NMR (CDCl₃, 75 MHz) δ : 29.6 (C-8), 38.3 (C-9), 45.1 (C-7), 52.6 (C-3''), 60.2 (C-4''), 128.6 (C-11 and C-16), 129.1 (C-15), 129.9 (C-12 and C-14), 135.2 (C-4), 138.8 (C-10), 139.5 (C-5), 163.5 (C-2'), 179.2 (C-2), 170.6 (C-2''); Mass (FAB): 444M⁺. Anal. Calcd. for $C_{16}H_{15}N_5O_4S$: C; 43.25, H; 3.40, N; 15.76%; Found: C; 43.23, H; 3.34, N; 15.68%.

N-[3-(2-Amino-5-nitrothiazolyl)-propyl]-4-(3-chlorophenyl)-3-chloro-2-oxo-1-azetidinecarboxamide (**4c**): Yield: 65%; m.p 182-183 °C; IR (cm^{-1}): 763 (C-Cl), 866 (C-S), 973 (C-NO), 1336 (N-CH₂), 1363, 1541 (NO₂), 1557 (C=C), 1674 (C=O), 1740 (CO cyclic), 1434, 2890, 2919 (CH₂), 2968 (CH-Cl), 3025 (CH-Ar), 3395 (NH); ¹H NMR (300 MHz, CDCl₃, TMS) δ : 2.15-2.18 (m, 2H, H-8), 3.31-3.36 (m, 2H, H-9), 3.89-3.92 (m, 2H, H-7), 4.40 (d, 1H, $J = 4.80$ Hz, H-3''), 5.16 (d, 1H, $J = 4.80$ Hz, H-4''), 5.68 (s, 1H, H-1'), 7.95 (s, 1H, H-4), 7.97 (s, 1H, H-6), 6.74-7.80 (m, 4H, Ar-H); ¹³C NMR (CDCl₃, 75 MHz) δ : 30.4 (C-8), 38.7 (C-9), 46.2 (C-7), 54.2 (C-3''), 61.3 (C-4''), 127.9 (C-11), 128.5 (C-16), 129.4 (C-15), 130.8 (C-12), 131.3 (C-14), 133.6 (C-4), 138.4 (C-5), 142.2 (C-10), 163.7 (C-2'), 171.4 (C-2), 172.5 (C-2''); Mass (FAB): 444M⁺. Anal. Calcd. for $C_{16}H_{15}N_5O_4S$: C; 43.25, H; 3.40, N; 15.76%; Found: C; 43.19, H; 3.35, N; 15.71%.

N-[3-(2-Amino-5-nitrothiazolyl)-propyl]-4-(2-chlorophenyl)-3-chloro-2-oxo-1-azetidinecarboxamide (**4d**): Yield: 67%; m.p 188-189 °C; IR (cm^{-1}): 765 (C-Cl), 867 (C-S), 974 (C-NO), 1337 (N-CH₂), 1368, 1537 (NO₂), 1554 (C=C), 1668 (C=O), 1743 (CO cyclic), 1441, 2893, 2927 (CH₂), 2966 (CH-Cl), 3022 (CH-Ar), 3389 (NH); ¹H NMR (300 MHz, CDCl₃, TMS) δ : 2.19-2.20 (m, 2H, H-8), 3.30-3.34 (m, 2H, H-9), 3.92-3.97 (m, 2H, H-7), 4.45 (d, 1H, $J = 4.75$ Hz, H-3''), 5.19 (d, 1H, $J = 4.75$ Hz, H-4''), 5.72 (s, 1H, H-1'), 7.86 (s, 1H, H-4), 7.98 (s, 1H, H-6), 6.65-7.98 (m, 4H, Ar-H); ¹³C NMR (CDCl₃, 75 MHz) δ : 30.8 (C-8), 39.3 (C-9), 46.8 (C-7), 51.3 (C-3''), 61.8 (C-4''), 128.6 (C-11), 129.8 (C-16), 130.2 (C-15), 130.8 (C-12), 131.7 (C-14), 134.0 (C-4), 137.6 (C-5), 139.1 (C-10), 164.2 (C-2'), 171.9 (C-2), 172.8 (C-2''); Mass (FAB): 444M⁺. Anal. Calcd. for $C_{16}H_{15}N_5O_4S$: C; 43.25, H; 3.40, N; 15.76%; Found: C; 43.21, H; 3.38, N; 15.73%.

N-[3-(2-Amino-5-nitrothiazolyl)-propyl]-4-(4-bromophenyl)-3-chloro-2-oxo-1-azetidinecarboxamide (**4e**): Yield: 66%; m.p 186-187 °C; IR (cm^{-1}): 567 (C-Br), 871 (C-S), 965 (C-NO), 1342 (N-CH₂), 1364, 1546 (NO₂), 1563 (C=C), 1672 (C=O), 1737 (CO cyclic), 1439, 2894, 2926 (CH₂), 2963 (CH-Cl), 3024 (CH-Ar), 3396 (NH); ¹H NMR (300 MHz, CDCl₃, TMS) δ : 2.15-2.20 (m, 2H, H-8), 3.32-3.38 (m, 2H, H-9), 3.94-3.98 (m, 2H, H-7), 4.42 (d, 1H, $J =$

4.80Hz, H-3"), 5.30 (d, 1H, $J = 4.80\text{Hz}$, H-4"), 5.69 (s, 1H, H-1'), 7.88 (s, 1H, H-4), 8.01 (s, 1H, H-6), 6.6-7.73 (m, 4H, Ar-H); ^{13}C NMR (CDCl_3 , 75 MHz) δ : 31.5 (C-8), 37.9 (C-9), 44.8 (C-7), 54.7 (C-3"), 62.1 (C-4"), 129.3 (C-11 and C-16), 130.6 (C-15), 131.2 (C-12 and C-14), 134.4 (C-4), 139.5 (C-10), 140.7 (C-5), 164.8 (C-2'), 170.5 (C-2), 171.1 (C-2"); Mass (FAB): 489M^+ . Anal. Calcd. for $\text{C}_{16}\text{H}_{15}\text{N}_5\text{O}_4\text{SBrCl}$: C; 39.31, H; 3.09, N; 14.32%; Found: C; 39.26, H; 3.06, N; 14.24%.

N-[3-(2-Amino-5-nitrothiazolyl)-propyl]-4-(3-bromophenyl)-3-chloro-2-oxo-1-azetidincarboxamide (**4f**): Yield: 68%; m.p 184-185 °C; IR (cm^{-1}): 565 (C-Br), 871 (C-S), 967 (C-NO), 1340 (N-CH₂), 1366, 1539 (NO₂), 1553 (C=C), 1650 (C=O), 1736 (CO cyclic), 1441, 2829 (NH), 2910 (CH₂), 2964 (CH-Cl), 3043 (CH-Ar), 3352 (NH); ^1H NMR (300 MHz, CDCl_3 , TMS) δ : 2.12-2.16 (m, 2H, H-8), 3.34-3.39 (m, 2H, H-9), 3.96-3.99 (m, 2H, H-7), 4.43 (d, 1H, $J = 4.75\text{Hz}$, H-3"), 5.22 (d, 1H, $J = 4.75\text{Hz}$, H-4"), 5.70 (s, 1H, H-1'), 7.95 (s, 1H, H-4), 8.04 (s, 1H, H-6), 6.72-7.01 (m, 4H, Ar-H); ^{13}C NMR (CDCl_3 , 75 MHz) δ : 31.7 (C-8), 41.8 (C-9), 48.2 (C-7), 52.4 (C-3"), 62.5 (C-4"), 130.7 (C-11), 131.5 (C-16), 132.1 (C-4), 132.7 (C-15), 133.4 (C-12), 134.9 (C-14), 137.5 (C-5), 142.0 (C-10), 162.6 (C-2'), 169.8 (C-2), 170.9 (C-2") (6C, Ar); Mass (FAB): 444M^+ . Anal. Calcd. for $\text{C}_{16}\text{H}_{15}\text{N}_5\text{O}_4\text{SBrCl}$: C; 39.31, H; 3.09, N; 14.32%; Found: C; 39.27, H; 3.01, N; 14.29%.

N-[3-(2-Amino-5-nitrothiazolyl)-propyl]-4-(2-bromophenyl)-3-chloro-2-oxo-1-azetidincarboxamide (**4g**): Yield: 67%; m.p 179-180 °C; IR (cm^{-1}): 572 (C-Br), 864 (C-S), 980 (C-NO), 1346 (N-CH₂), 1369, 1542 (NO₂), 1553 (C=C), 1663 (C=O), 1741 (CO cyclic), 1438, 2892 (CH₂), 2924, 2965 (CH-Cl), 3029 (CH-Ar), 3394 (NH); ^1H NMR (300 MHz, CDCl_3 , TMS) δ : 2.07-2.10 (m, 2H, H-8), 3.31-3.35 (m, 2H, H-9), 3.89-3.93 (m, 2H, H-7), 4.39 (d, 1H, $J = 4.70\text{Hz}$, H-3"), 5.23 (d, 1H, $J = 4.70\text{Hz}$, H-4"), 5.72 (s, 1H, H-1'), 7.89 (s, 1H, H-4), 8.05 (s, 1H, H-6), 6.75-7.76 (m, 4H, Ar-H); ^{13}C NMR (CDCl_3 , 75 MHz) δ : 32.3 (C-8), 41.4 (C-9), 45.7 (C-7), 50.6 (C-3"), 63.8 (C-4"), 129.7 (C-11), 130.5 (C-16), 131.4 (C-15), 131.7 (C-4), 132.4 (C-12), 133.7 (C-14), 138.6 (C-5), 140.2 (C-10), 162.9 (C-2'), 171.7 (C-2), 172.3 (C-2") (6C, Ar); Mass (FAB): 444M^+ . Anal. Calcd. for $\text{C}_{16}\text{H}_{15}\text{N}_5\text{O}_4\text{SBrCl}$: C; 39.31, H; 3.09, N; 14.32%; Found: C; 39.28, H; 3.05, N; 14.28%.

N-[3-(2-Amino-5-nitrothiazolyl)-propyl]-4-(4-nitrophenyl)-3-chloro-2-oxo-1-azetidincarboxamide (**4h**): Yield: 65%; m.p 178-179 °C; IR (cm^{-1}): 870 (C-S), 975 (C-NO), 1339 (N-CH₂), 1367, 1543 (NO₂), 1554 (C=C), 1665 (C=O), 1746 (CO cyclic), 1440, 2891, 2918 (CH₂), 2961 (CH-Cl), 3021 (CH-Ar), 3399 (NH); ^1H NMR (300 MHz, CDCl_3 , TMS) δ : 2.16-2.18 (m, 2H, H-8), 3.32-3.36 (m, 2H, H-9), 3.90-3.94 (m, 2H, H-7), 4.47 (d, 1H, $J = 4.70\text{Hz}$, H-3"), 5.25 (d, 1H, $J = 4.70\text{Hz}$, H-4"), 5.76 (s, 1H, H-1'), 7.90 (s, 1H, H-4), 8.07 (s, 1H, H-6), 6.78-7.80 (m, 4H, Ar-H); ^{13}C NMR (CDCl_3 , 75 MHz) δ : 33.4 (C-8), 41.9 (C-9), 46.8 (C-7), 52.3 (C-3"), 63.7 (C-4"), 126.9 (C-11 and C-16), 128.2 (C-15), 130.5 (C-12 and C-14), 137.9 (C-4), 139.6 (C-5), 143.7 (C-10), 161.8 (C-2'), 170.9 (C-2), 171.2 (C-2"); Mass (FAB): 454M^+ . Anal. Calcd. for $\text{C}_{16}\text{H}_{15}\text{N}_6\text{O}_6\text{SCl}$: C; 42.25, H; 3.32, N; 18.47%; Found: C; 42.14, H; 3.22, N; 18.41%.

N-[3-(2-Amino-5-nitrothiazolyl)-propyl]-4-(3-nitrophenyl)-3-chloro-2-oxo-1-azetidincarboxamide (**4i**): Yield: 69%; m.p 177-178 °C; IR (cm^{-1}): 865 (C-S), 969 (C-NO), 1343 (N-CH₂), 1365, 1544 (NO₂), 1561 (C=C), 1670 (C=O), 1739 (CO cyclic), 1442, 2888, 2925 (CH₂), 2958 (CH-Cl), 3028 (CH-Ar), 3392 (NH); ^1H NMR (300 MHz, CDCl_3 , TMS) δ : 2.09-2.12 (m, 2H, H-8), 3.31-3.37 (m, 2H, H-9), 3.90-3.97 (m, 2H, H-7), 4.48 (d, 1H, $J = 4.80\text{Hz}$, H-3"), 5.26 (d, 1H, $J = 4.80\text{Hz}$, H-4"), 5.76 (s, 1H, H-1'), 7.92 (s, 1H, H-4), 8.10 (s, 1H, H-6), 6.77-7.83 (m, 4H, Ar-H); ^{13}C NMR (CDCl_3 , 75 MHz) δ : 33.2 (C-8), 39.8 (C-9), 47.7 (C-7), 53.4 (C-3"), 64.7 (C-4"), 130.4 (C-11), 131.7 (C-16), 132.5 (C-15), 132.9 (C-12), 133.6 (C-14), 136.8 (C-4), 139.4 (C-5), 140.8 (C-10), 162.2 (C-2'), 172.8 (C-2), 173.6 (C-2"); Mass (FAB): 454M^+ . Anal. Calcd. for $\text{C}_{16}\text{H}_{15}\text{N}_6\text{O}_6\text{SCl}$: C; 42.25, H; 3.32, N; 18.47%; Found: C; 42.15, H; 3.26, N; 18.43%.

N-[3-(2-Amino-5-nitrothiazolyl)-propyl]-4-(2-nitrophenyl)-3-chloro-2-oxo-1-azetidincarboxamide (**4j**): Yield: 62%; m.p 180-181 °C; IR (cm^{-1}): 869 (C-S), 971 (C-NO), 1350 (N-CH₂), 1370, 1538 (NO₂), 1556 (C=C), 1671 (C=O), 1741 (CO cyclic), 1437, 2889, 2920 (CH₂), 2959 (CH-Cl), 3023 (CH-Ar), 3387 (NH); ^1H NMR (300 MHz, CDCl_3 , TMS) δ : 2.11-2.15 (m, 2H, H-8), 3.30-3.34 (m, 2H, H-9), 3.94-3.98 (m, 2H, H-7), 4.49 (d, 1H, $J = 4.75\text{Hz}$, H-3"), 5.28 (d, 1H, $J = 4.75\text{Hz}$, H-4"), 5.78 (s, 1H, H-1'), 7.94 (s, 1H, H-4), 8.12 (s, 1H, H-6), 6.90-7.84 (m, 4H, Ar-H); ^{13}C NMR (CDCl_3 , 75 MHz) δ : 33.5 (C-8), 40.7 (C-9), 48.6 (C-7), 51.5 (C-3"), 64.1 (C-4"), 131.1 (C-11), 132.2 (C-16), 132.7 (C-15), 133.4 (C-12), 133.9 (C-4), 134.3 (C-14), 136.3 (C-5), 141.4 (C-10), 163.2 (C-2'), 170.7 (C-2), 171.5 (C-2"); Mass (FAB): 454M^+ . Anal. Calcd. for $\text{C}_{16}\text{H}_{15}\text{N}_6\text{O}_6\text{SCl}$: C; 42.25, H; 3.32, N; 18.47%; Found: C; 42.18, H; 3.29, N; 18.44%.

RESULTS AND DISCUSSION

N-[3-(2-amino-5-nitrothiazolyl)-propyl]-4-(substituted phenyl)-3-chloro-2-oxo-1-azetidine-carboxamide, compounds **4a-4j** were synthesized in four different steps: 2-amino-5-nitrothiazole on reaction with $\text{Cl}(\text{CH}_2)_3\text{Br}$ at room temperature to afford 1-(3-chloropropyl)-2-amino-5-nitrothiazole, compound **1**. IR spectrum of compound **1** displayed absorption at 1313 and 727 cm^{-1} for (N-CH₂) and (C-Cl) respectively. In the FAB-Mass spectrum of compound **1** parent ion peak found at 221 M^+ . The compound **1** on reaction with urea at room temperature yielded *N*-[3-(2-amino-5-nitrothiazolyl)-propyl]-urea, compound **2**. IR spectrum of compound **2** showed absorption for NH at 3387 and for CO at 1662 cm^{-1} while absorption of (C-Cl) has been disappeared.

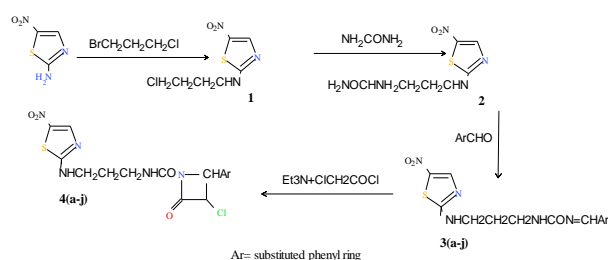


Table 1. Antibacterial and antifungal activities of compounds **4(a-j)**.

Compd.	<i>B. subtilis</i>	<i>E. coli</i>	<i>S. aureus</i>	<i>K. pneumoniae</i>	<i>A. niger</i>	<i>A. flavus</i>	<i>F. oxisporium</i>	<i>C. albicans</i>
4a	10.25	13.5	7.25	13.5	>25	>25	13.5	>25
4b	15.5	7.25	7.25	9.25	13.5	>25	13.5	>25
4c	5.25	6.25	4.25	7.25	7.5	7.5	10.5	13.5
4d	6.25	7.50	7.25	7.25	8.25	10.5	10.25	12.75
4e	8.25	4.25	7.25	7.25	10.5	9.5	8.5	12.5
4f	4.25	7.25	6.25	6.25	9.5	8.75	10.25	13.25
4g	7.25	13.5	7.25	7.25	13.5	12.5	13.5	13.5
4h	4.25	4.25	7.25	4.25	7.50	8.5	8.5	12.75
4i	4.25	4.25	4.25	6.25	8.25	6.75	8.75	12.5
4j	4.25	6.25	4.25	4.25	7.50	7.25	8.5	12.5
Streptomycin	1.25	2.25	3.25	2.75	-	-	-	-
Griseofulvin	-	-	-	-	7.25	6.25	8.50	12.5

The ¹H NMR spectrum of compound **2** displayed signal of (CH₂-N) appear at δ 3.19-3.24 ppm and its ¹³C NMR value of CO group appeared at δ 163.4 ppm. In the FAB-MS spectrum of compound **2** parent ion peaks found at (m/z) 245. The compound **2** on further reaction with selected several substituted aromatic aldehydes produced *N*-[3-(1*H*-2-amino-5-nitrothiazolyl)-propyl]-*N'*-[(substituted phenyl)-methylidene]urea, compounds **3a-3j**. For the compounds **3a-3j** characteristic absorption for Schiff base (N=CH) in IR spectra appeared in the range of 1558-1575cm⁻¹ and in the ¹H NMR chemical shift at δ 8.02-8.20 ppm while in its ¹³C NMR signal found at δ 147.4-151.6 ppm. In the ¹H NMR a broad signal of NH₂ has been disappeared at δ 5.96 ppm. In the FAB-Mass spectrum of **3a** parent ion peak found at (m/z) 333.

The compounds **3a-j** on treatment with ClCH₂COCl in the presence of Et₃N furnished final products compounds **4a-4j**. In the spectra of compounds **4a-4j** carbonyl group of β-lactam ring showed characteristic absorptions in the range of 1736-1746 cm⁻¹ and ¹H NMR spectrum two doublet appeared for (N-CH) and (CH-Cl) in the range of δ 5.12-5.30 and 4.36-4.49 ppm respectively with coupling constant J 5.00 Hz but in the ¹³C NMR spectra three signals appeared for (N-CH), (CH-Cl) and (CO cyclic) at (δ) 59.4-64.7, 50.2-54.7 and 170.2-173.6 ppm respectively. The IR absorption ¹H and ¹³C NMR signal of (N=CH) have been disappeared. The results of the all described activities (antibacterial, antifungal, antitubercular and antiinflammatory) were summarized in Tables 1, 2 and 3.

Table 2. Antitubercular activity of compounds **4a-j**.

Compound	Concentration	Compound	Concentration
4a	6.50	4f	2.75
4b	2.25	4g	3.50
4c	2.75	4h	2.25
4d	3.25	4i	2.25
4e	3.25	4j	2.50

The results of the antimicrobial screening data revealed that all the compounds **4a-4j** showed considerable and varied activity against the selected microorganism. A new series of *N*-[3-(2-amino-5-nitrothiazolyl)-propyl]-4-(substituted phenyl)-3-chloro-2-oxo-1-azetidine-carboxamide, compounds **4a-4j** were prepared and screened for their antimicrobial, antitubercular and anti-inflammatory activities data (as shown in Table 1 and 2) revealed that all the

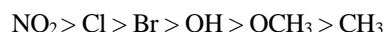
synthesized compounds **4a-4j** have a structure activity relationship (SAR) because activities of compounds varies with substitution. Nitro group containing compounds (**4h**, **4i** and **4j**) showed higher activity than chloro (**4c**, **4d**), or bromo group containing compounds (**4e**, **4f**).

Table 3. Anti-inflammatory activity of compounds **4(a-j)**.

Compound	Paw volume (cm ³) ^a	Paw volume (cm ³) ^b	Inhibition, %
4a	0.66 ± 0.02	0.15 ± 0.02	50.00
4b	0.68 ± 0.02	0.14 ± 0.02	53.33
4c	0.65 ± 0.02	0.13 ± 0.01	56.67
4d	0.66 ± 0.02	0.13 ± 0.02	56.67
4e	0.68 ± 0.02	0.12 ± 0.01	60.00
4f	0.69 ± 0.03	0.13 ± 0.02	56.67
4g	0.65 ± 0.02	0.13 ± 0.01	56.67
4h	0.67 ± 0.03	0.12 ± 0.02	60.00
4i	0.68 ± 0.02	0.11 ± 0.03	63.33
4j	0.6 ± 0.03	0.11 ± 0.01	63.33
Control	0.69 ± 0.02	0.30 ± 0.01	-
Standard ^c	0.70 ± 0.03	0.10 ± 0.02	66.67

a) Before carageenan administration; (mean ± SEM) b) Total increase in paw volume after 5 hours (mean ± SEM); c) phenylbutazone standard

Chloro and bromo derivatives also have higher activity than other rested compounds. On the basis of SAR, concluded that the activity of compounds depends on electron withdrawing nature of the substituted groups. The sequence of the activity is following



The investigation of antimicrobial (antibacterial, antifungal and antitubercular) data revealed that the compounds **4c**, **4d**, **4e**, **4f**, **4h**, **4i** and **4j** displayed high activity in the series, the compounds **4b** and **4g** showed moderate activity and rest compounds showed less activity against all the strains compared with standard drugs. In the anti-inflammatory activity (Table 3) compounds **4c**, **4d**, **4e**, **4f**, **4h**, **4i** and **4j** showed high activity while rested compounds displayed moderate to less activity.

CONCLUSION

Concluded that all compounds have been synthesized successfully and screened for antimicrobial, antitubercular and anti-inflammatory activities data of compounds (shown in Table 1, 2 and 3) revealed that the compounds shows moderate to good activities against all the strains compared with standard drugs.

ACKNOWLEDGEMENT

The authors are thankful to SAIF, Central Drugs Research Institute Lucknow (India) for providing spectral and analytical data of the compounds. We are also thankful to Head, Department of Chemistry Dr. H. S. Gour, University, Sagar (India) for giving the facilities to carryout the work.

REFERENCES

- ¹Soliman, R., Gabr, M., Abouzeit-Har, M. S., Sharabi, F. M. *J. Pharm. Sci.* **1981**, 70, 94.
- ²Pattan, S. R., Dighe, N. S., Nirmal, S. A., Merekar, A. N., Laware, R. B., Shinde, H. V., Musmade, D. S. *Asian J. Res. Chem.*, **2009**, 2, 196.

- ³Popov-Pergal, K., Rancic, M., Pergal, M., Bogdanovic, G., Kojic, V., Djokovic, D. *J. Serb. Chem. Soc.*, **2006**, 71, 861.
- ⁴Kaplancikli, Z., Turan-Zitouni, A., Gulhan, R., Gven K. G., *Arch. Pharm. Res.*, **2004**, 27, 1081.
- ⁵Sonwane, S. K., Srivastava, S. D. *Proc. Natl. Acad. Sci. India*, **2008**, 78, 129.
- ⁶Desai, K. G., Desai, K. R. *Indian J. Chem.*, **2005**, 44, 2093.
- ⁷Sharma, M. C., Kohli, D. V., Sahu, N. K., Sharma, S., Chaturvedi, S. C. *Digest J. Nanomater. Biostruct.*, **2009**, 4, 339.
- ⁸Srivastava, S. K., Srivastava, S., Srivastava, S. D. *Indian J. Chem.*, **1999**, 38, 183.
- ⁹Srivastava, S. K., Srivastava, S. L., Srivastava, S. D. *Indian J. Chem.*, **2000**, 39, 464.
- ¹⁰Raval, J. P., Patel, H. V., Patel, P. S., Patel, N. H., Desai, K. R. *Asian J. Res. Chem.*, **2009**, 2, 171.
- ¹¹Patel, K. H., Mehta, A. G. *E-J. Chem.*, **2006**, 3, 103.

Received: 01.03.2013.

Accepted: 18.04.2013.



SYNTHESIS AND ANTIMICROBIAL EVALUATIONS OF NEW BIOACTIVE DYES AND THEIR CYCLIZED DERIVATIVES SYNTHESIZED FROM 4,5,6,7-TETRAHYDROBENZO[b]-THIOPHENE

Rafat M. Mohareb^[a], Amira E. M. Abdallah^[b], Maher H. E. Helal^[b], Heba Allah N. A. Mohammed^[b]

Keywords: Tetrahydrobenzo[b]thiophene, pyridazines, pyrazoles, antimicrobial activity

The reaction of 3-cyano-2-diazo-4,5,6,7-tetrahydrobenzo[b]thiophene (**1**) with active methylene reagents **2a-e** gave the respective hydrazono derivatives **3a-e**. The reactivity of the latter derivatives towards different chemical reagents was studied. The antimicrobial activity of the newly obtained products was studied and evaluated in terms of minimal inhibitory concentration (MIC) in $\mu\text{g mL}^{-1}$. The results showed that compounds **3b**, **7a** and **15a** are the most active compounds towards *E. coli* ECT 101; compounds **5f**, **13b**, **17a** and **23** are active towards *B. Cereus* CECT 148; while **10**, **19a** and **19b** towards *B. subtilis* CECT 498 and **3c**, **5c** and **13b** towards *C. albicans* CECT 1394.

Corresponding Authors

E-Mail: raafat_mohareb@yahoo.com

[a] Department of Chemistry, Faculty of Science, Cairo University, Giza, A. R. Egypt

[b] Department of Chemistry, Faculty of Science, Helwan University, Ain Helwan, Cairo A. R. Egypt

Introduction

2-Aminothiophene derivatives are an important class of heterocycles found in several biologically active and natural compounds. This class of compounds has demonstrated a broad spectrum of activities and applications as pharmaceuticals and agrochemicals, dyes, biodiagnostics, and electronic and optoelectronic devices.¹ They have been reported to exert antitubercular,² anti-inflammatory,³ antimicrobial⁴ and antianxiety⁵ properties. A survey of the literature also reveals that substituted 2-aminothiophenes are potent and selective inhibitors of human leukocyte elastase,⁶ kinesin spindle protein (KSP),⁷ tubulin⁸ and tyrosine kinases of the fibroblast growth factor receptors (FGFR),⁹ as well as adenosine A1 receptor allosteric enhancers.¹⁰ Antifungal¹¹ and antitumor¹² properties have also been extensively described, resulting in marketed antifungal agents such as sertaconazol.

The synthetic strategy of the investigated dyes and their cyclized products depended on the competition of the reaction pathways which followed nucleophilic displacement,^{13,14} β -attack, Gewald type reaction,^{15, 16} dinucleophilic bielectrophilic attack, dipolar cyclization and condensation reactions. This led to the diversity of the reaction products.

Within the scope of these diverse synthetic methods and the utility of thiophene-based systems and in continuation to our interest in the design of bioactive heterocycles,¹⁷⁻²¹ we focused our efforts to synthesized a series of hydrazono dyes **3a-e** based on the key precursor 3-cyano-4,5,6,7-tetrahydrobenzo[b]thiophene-2-diazonium chloride (**1**)

which coupled with some active methylene reagents. The antimicrobial activity of the new systems was studied and evaluated.

Experimental

All melting points were determined on an Electrothermal digital melting point apparatus and are uncorrected. IR spectra (KBr discs) were recorded on a FTIR plus 460 or Pye Unicam SP-1000 spectro-photometer. ¹H-NMR spectra were recorded with Varian Gemini-200 (200 MHz) (Cairo University) instrument in DMSO-d₆ as solvent using TMS as internal standard and chemical shifts are expressed as δ ppm. The mass spectra were recorded with Hewlett Packard 5988 A GC/MS system and GCMS-QP 1000 Ex Shimadzu instruments. Analytical data were obtained from the Micro-analytical Data Unit at Cairo University and were performed on Vario EL III Elemental CHNS analyzer.

Synthesis of 3-cyano-4,5,6,7-tetrahydrobenzo[b]thiophen-2-yl-hydrazono derivatives (3a-e)

General procedure: To a cold solution (0–5 °C) of 2-cyano-*N*-phenyl-acetamide **2a** (1.60 g, 0.01 mol), malonic acid diethyl ester **2b** (1.60 g, 0.01 mol), *N*-(4-chlorophenyl)-2-cyano-acetamide **2c** (1.94 g, 0.01 mol), 2-cyano-*N*-(4-methoxy-phenyl)-acetamide **2d** (1.90 g, 0.01 mol) and 2-cyano-*N*-*p*-tolyl-acetamide **2e** (1.74 g, 0.01 mol) in ethanol (20 mL) containing sodium hydroxide (1.00 g) an equimolar amount of diazotized 2-amino-4,5,6,7-tetrahydrobenzo[b]thiophene-3-carbonitrile **1** [which was prepared by adding NaNO₂ (0.7 g, 0.01 mol) solution to a cold solution of 2-amino-4,5,6,7-tetrahydrobenzo[b]thiophene-3-carbonitrile²² (1.78 g, 0.01 mol) in acetic acid (20 mL), HCl (6.0 mL)] was gradually added while stirring. The solid product formed upon cooling in an ice-bath was collected by filtration, washed with water and crystallized from acetic acid.

2-Cyano-2-[3-cyano-4,5,6,7-tetrahydrobenzo[*b*]thiophen-2-yl]-hydrazono]-*N*-phenyl-acetamide (3a)

Reddish brown crystals, m.p. 138–140 °C, yield: 3.04 g (87%); Anal. for C₁₈H₁₅N₅OS (349.41), (% Calcd./Found): 61.87/61.50 (C), 4.33/3.99 (H), 20.04/19.70 (N), 9.18/8.80 (S); IR (ν , cm⁻¹): 3431 (2NH), 3050 (CH aromatic), 2935 (CH₂), 2219, 2200 (2CN), 1687 (C=O), 1596, 1496 (C=C), 1531(=N-NH); ¹H-NMR (δ , ppm): 1.76-1.98 (m, 4H, cyclohexene 2CH₂), 2.20-2.89 (m, 4H, cyclohexene 2CH₂), 6.80-7.80 (m, 5H, C₆H₅), 8.40 (s, 1H, NH), 9.40 (s, 1H, NH); MS m/z (%): 349 [M⁺] (63.41), 348 [M⁺¹] (67.07), 328 (100.00), 76 (75.61).

2-[3-Cyano-4,5,6,7-tetrahydrobenzo[*b*]thiophen-2-yl]-hydrazono]-malonic acid diethyl ester (3b)

Pale brown crystals, m.p. 98–100 °C, yield: 2.51 g (72%); Anal. for C₁₆H₁₉N₃O₄S (349.40), (% Calcd./Found): 55.00/55.38 (C), 5.48/5.10 (H), 12.03/12.40 (N), 9.18/9.50 (S); IR (ν , cm⁻¹): 3434 (2NH), 3100 (CH aromatic), 2935 (CH₂, CH₃), 2215 (CN), 1682, 1680 (2C=O), 1540, 1441 (C=C), 1530 (=N-NH); ¹H-NMR (δ , ppm): 1.14-1.21 (2t, 6H, 2CH₃); 1.71-1.92 (m, 4H, cyclohexene 2CH₂), 1.99-2.92 (m, 4H, cyclohexene 2CH₂), 4.10-4.20 (2q, 4H, 4CH₂), 6.91 (s, 1H, NH); MS m/z (%): 350 [M⁺¹] (3.54), 349 [M⁺] (3.73), 178 (68.13), 177 (47.73).

***N*-(4-Chloro-penta-2,4-dienyl)-2-cyano-2-[3-cyano-4,5,6,7-tetrahydrobenzo[*b*]thiophen-2-yl]-hydrazono]-acetamide (3c)**

Pale brown crystals, m.p. 108–110 °C, yield: 3.45 g (90%); Anal. for C₁₈H₁₄N₅OSCl (383.85), (% Calcd./Found): 56.32/55.92 (C), 3.68/3.99 (H), 18.24/17.84 (N), 8.35/8.70 (S); IR (ν , cm⁻¹): 3433 (2NH), 3100 (CH aromatic), 2935 (CH₂), 2215, 2190 (2CN), 1687 (C=O), 1589, 1494 (C=C), 1533 (=N-NH); ¹H-NMR (δ , ppm): 1.76-1.98 (m, 4H, cyclohexene 2CH₂), 2.40-2.90 (m, 4H, cyclohexene 2CH₂), 7.45-7.83 (m, 4H, C₆H₄), 8.40 (s, 1H, NH), 10.50 (s, 1H, NH); MS m/z (%): 382 [M⁺¹] (1.72), 381 [M⁺²] (3.00), 127 (100.00), 176 (2.30).

2-Cyano-2-[3-cyano-4,5,6,7-tetrahydrobenzo[*b*]thiophen-2-yl]-hydrazono]-*N*-(4-methoxy-phenyl)-acetamide (3d)

Brown crystals, m.p. 101–103 °C, yield: 3.42 g (90%); Anal. for C₁₉H₁₇N₅O₂S (379.44), (% Calcd./Found): 60.14/59.75 (C), 4.52/4.58 (H), 18.46/18.06 (N), 8.45/8.84 (S); IR (ν , cm⁻¹): 3420 (2NH), 3100 (CH aromatic), 2934 (CH₂), 2213-2191 (2CN), 1682 (C=O), 1601, 1445 (C=C), 1510 (=N-NH); ¹H-NMR (δ , ppm): 1.23 (s, 3H, CH₃), 1.71-1.98 (m, 4H, cyclohexene 2CH₂), 2.13-2.82 (m, 4H, cyclohexene 2CH₂), 6.89-7.64 (m, 4H, C₆H₄), 8.30 (s, 1H, NH), 10.10 (s, 1H, NH); MS m/z (%): 381 [M⁺²] (0.37), 380 [M⁺¹] (0.15), 379 [M⁺] (0.14), 77 [C₆H₅]⁺, 64 (100.00).

2-Cyano-2-[3-cyano-4,5,6,7-tetrahydrobenzo[*b*]thiophen-2-yl]-hydrazono]-*N*-*p*-tolyl-acetamide (3e)

Pale brown crystals, m.p. 103–105 °C, yield: 3.38 g (93%); Anal. for C₁₉H₁₇N₅OS (363.44), (% Calcd./Found): 62.79/62.44 (C), 4.71/5.10 (H), 19.27/18.88 (N), 8.82/9.20

(S); IR (ν , cm⁻¹): 3433 (2NH), 3090 (CH aromatic), 2934 (CH₂), 2214, 2192 (2CN), 1685 (C=O), 1591, 1410 (C=C), 1520 (=N-NH); ¹H-NMR (δ , ppm): 1.23 (s, 3H, CH₃), 1.77-1.98 (m, 4H, cyclohexene 2CH₂), 2.19-2.89 (m, 4H, cyclohexene 2CH₂), 6.98-7.48 (m, 4H, C₆H₄), 8.30 (s, 1H, NH), 10.30 (s, 1H, NH); MS m/z (%): 365 [M⁺²] (0.18), 364 [M⁺¹] (0.11), 363 [M⁺] (0.26), 107 (100.00), 77 [C₆H₅]⁺ (47.77).

Synthesis of 3-cyano-4,5,6,7-tetrahydrobenzo[*b*]thiophen-2-yl-functionalized pyridazine carboxylic acid derivatives (5a-f)

General procedure: To a solution of either compound **3a** (3.49 g, 0.01 mol), **3c** (3.83 g, 0.01 mol) or **3d** (3.79 g, 0.01 mol) in 1,4-dioxane (35 mL) containing triethylamine (1.00 mL), either malononitrile **4a** (0.66 g, 0.01 mol) or ethyl cyanoacetate **4b** (1.13 g, 0.01 mol) was added. The reaction mixture was heated under reflux for 5 h, then cooled and neutralized by pouring onto ice/water mixture containing few drops of hydrochloric acid. The solid product formed in each case was collected by filtration and crystallized from 1,4-dioxane.

4-Amino-5-cyano-1-(3-cyano-4,5,6,7-tetrahydrobenzo[*b*]thiophen-2-yl)-6-imino-1,6-dihydro-pyridazine-3-carboxylic acid phenylamide (5a)

Dark brown crystals, m.p. 198–200 °C, yield: 3.49 g (84%); Anal. for C₂₁H₁₇N₇OS (415.47), (% Calcd./Found): 60.71/60.35 (C), 4.12/3.89 (H), 23.60/23.22 (N), 7.72/8.10 (S); IR (ν , cm⁻¹): 3429-3300 (2NH, NH₂), 3100 (CH aromatic), 2932 (CH₂), 2298, 2201 (2CN), 1685 (C=O), 1588, 1435 (C=C); ¹H-NMR (δ , ppm): 1.81-2.27 (m, 4H, cyclohexene 2CH₂), 2.57-2.94 (m, 4H, cyclohexene 2CH₂), 4.44 (s, 2H, NH₂), 6.91-7.40 (m, 5H, C₆H₅), 8.30 (s, 1H, NH), 8.40 (s, 1H, NH); MS m/z (%): 415 [M⁺] (3.01), 77 [C₆H₅]⁺ (22.35), 64 (100.00), 50 (6.40).

5-Amino-2-(3-cyano-4,5,6,7-tetrahydrobenzo[*b*]thiophen-2-yl)-3-imino-6-phenylcarbamoyl-2,3-dihydro-pyridazine-4-carboxylic acid ethyl ester (5b)

Dark brown crystals, m.p. 143–145 °C, yield: 4.21 g (91%); Anal. for C₂₃H₂₂N₆O₃S (462.52), (% Calcd./Found): 59.73/59.68 (C), 4.79/4.96 (H), 18.17/17.80 (N), 6.93/7.30 (S); IR (ν , cm⁻¹): 3431-3200 (2NH, NH₂), 3100 (CH aromatic), 2931 (CH₂, CH₃), 2203 (CN), 1734, 1689 (2C=O), 1523, 1440 (C=C); ¹H-NMR (δ , ppm): 1.06 (t, 3H, CH₃), 1.15-1.78 (m, 4H, cyclohexene 2CH₂), 2.61-2.73 (m, 4H, cyclohexene 2CH₂), 4.00 (s, 2H, NH₂), 4.20 (q, 2H, CH₂), 6.80-7.90 (m, 5H, C₆H₅), 8.29 (s, 1H, NH), 9.90 (s, 1H, NH); MS m/z (%): 463 [M⁺¹] (0.03), 462 [M⁺] (0.03), 135 (100.00), 77 [C₆H₅]⁺ (20.94).

4-Amino-5-cyano-1-(3-cyano-4,5,6,7-tetrahydrobenzo[*b*]thiophen-2-yl)-6-imino-1,6-dihydro-pyridazine-3-carboxylic acid (4-chloro-phenyl)-amide (5c)

Pale brown crystals, m.p. 178–180 °C, yield: 3.82 g (85%); Anal. for C₂₁H₁₆N₇OSCl (449.92), (% Calcd./Found): 56.06/56.19 (C), 3.58/3.63 (H), 21.79/21.40

(N), 7.13/6.78 (S); IR (ν , cm^{-1}): 3329-3209 (2NH, NH_2), 3090 (CH aromatic), 2922-2850 (CH_2), 2260, 2199 (2CN), 1685 (C=O), 1520, 1435 (C=C); $^1\text{H-NMR}$ (δ , ppm): 1.16-2.40 (m, 4H, cyclohexene 2CH_2), 2.56-2.89 (m, 4H, cyclohexene 2CH_2), 3.57 (s, 2H, NH_2), 7.15-7.76 (m, 4H, C_6H_4), 8.29 (s, 1H, NH), 9.40 (s, 1H, NH); MS m/z (%): 451 [$\text{M}^+ + 1$] (12.50), 450 [M^+] (10.96), 76 [C_6H_4] $^+$ (35.77), 57 (100.00).

5-Amino-6-(4-chloro-phenylcarbamoyl)-2-(3-cyano-4,5,6,7-tetrahydrobenzo[b]thiophen-2-yl)-3-imino-2,3-dihydro-pyridazine-4-carboxylic acid ethyl ester (5d)

Pale brown crystals, m.p. 248–250 °C, yield: 4.62 g (93%); Anal. for $\text{C}_{23}\text{H}_{21}\text{N}_6\text{O}_3\text{SCl}$ (496.97), (% Calcd./Found): 55.59/55.16 (C), 4.26/3.88 (H), 16.91/16.55 (N), 6.45/6.14 (S); IR (ν , cm^{-1}): 3433 (2NH, NH_2), 3100 (CH aromatic), 2927 (CH_2 , CH_3), 2207 (CN), 1684, 1682 (2C=O), 1610, 1438 (C=C); $^1\text{H-NMR}$ (δ , ppm): 1.05 (t, 3H, CH_3), 1.21-2.33 (m, 4H, cyclohexene 2CH_2), 2.63-2.95 (m, 4H, cyclohexene 2CH_2), 3.57 (s, 2H, NH_2), 3.99 (q, 2H, CH_2), 6.00 (s, 1H, NH), 6.60 (s, 1H, NH), 6.90-7.60 (m, 4H, C_6H_4); MS m/z (%): 496 [$\text{M}^+ - 1$] (0.72), 495 [$\text{M}^+ - 2$] (0.96), 105 (100.00), 76 [C_6H_4] $^+$ (5.36).

4-Amino-5-cyano-1-(3-cyano-4,5,6,7-tetrahydrobenzo[b]thiophen-2-yl)-6-imino-1,6-dihydro-pyridazine-3-carboxylic acid (4-methoxy-phenyl)-amide (5e)

Brown crystals, m.p. over 300 °C, yield: 3.43 g (77%); Anal. for $\text{C}_{22}\text{H}_{19}\text{N}_7\text{O}_2\text{S}$ (445.50), (% Calcd./Found): 59.31/58.99 (C), 4.30/3.90 (H), 22.01/21.70 (N), 7.20/6.80 (S); IR (ν , cm^{-1}): 3431 (2NH, NH_2), 3100 (CH aromatic), 2930 (CH_2), 2200, 2190 (2CN), 1687 (C=O), 1590, 1431 (C=C); $^1\text{H-NMR}$ (δ , ppm): 1.22 (s, 3H, CH_3), 1.82-2.40 (m, 4H, cyclohexene 2CH_2), 2.56-2.90 (m, 4H, cyclohexene 2CH_2), 3.99 (s, 2H, NH_2), 6.00 (s, 1H, NH), 6.89-7.23 (m, 4H, C_6H_4), 8.10 (s, 1H, NH); MS m/z (%): 445 [M^+] (10.75), 444 [$\text{M}^+ - 1$] (2.04), 76 [C_6H_4] $^+$ (12.24), 55 (100.00).

5-Amino-2-(3-cyano-4,5,6,7-tetrahydrobenzo[b]thiophen-2-yl)-3-imino-6-(4-methoxy-phenylcarbamoyl)-2,3-di-hydro-pyridazine-4-carboxylic acid ethyl ester (5f)

Brown crystals, m.p. 248–250 °C, yield: 3.69 g (75%); Anal. for $\text{C}_{24}\text{H}_{24}\text{N}_6\text{O}_4\text{S}$ (492.55), (% Calcd./Found): 58.52/58.20 (C), 4.91/4.55 (H), 17.06/16.70 (N), 6.51/6.16 (S); IR (ν , cm^{-1}): 3434 (2NH, NH_2), 3090 (CH aromatic), 2930 (CH_2 , CH_3), 2208 (CN), 1686, 1680 (2C=O), 1509, 1450 (C=C); $^1\text{H-NMR}$ (δ , ppm): 1.19 (t, 3H, CH_3), 1.77-2.44 (m, 4H, cyclohexene 2CH_2), 2.55-2.97 (m, 4H, cyclohexene 2CH_2), 4.00 (s, 2H, NH_2), 4.10 (q, 2H, CH_2), 6.91-7.70 (m, 4H, C_6H_4), 7.90 (s, 1H, NH), 8.30 (s, 1H, NH); MS m/z (%): 492 [M^+] (23.47), 491 [$\text{M}^+ - 1$] (20.58), 64 (100.00).

Synthesis of 3-cyano-4,5,6,7-tetrahydrobenzo[b]thiophen-2-yl- functionalized 3-thioxo-2,3,4,5-tetrahydro-[1,2,4]triazine-6-carboxylic acid derivatives, 7a-c

General procedure: Equimolar amounts of **3a** (3.49 g, 0.01 mol), **3b** (3.49 g, 0.01 mol), **3d** (3.79 g, 0.01 mol) and phenylisothiocyanate **6** (1.35 g, 0.01 mol) in 1,4-dioxane (35 mL) containing triethylamine (1.0 mL) were heated under reflux for 5h. After cooling, the reaction mixture in each

case was acidified by hydrochloric acid and the crude product was precipitated, collected by filtration and crystallized from 1,4-dioxane.

2-(3-Cyano-4,5,6,7-tetrahydrobenzo[b]thiophen-2-yl)-5-imino-4-phenyl-3-thioxo-2,3,4,5-tetrahydro-[1,2,4]triazine-6-carboxylic acid phenylamide (7a)

Reddish brown crystals, m.p. 203–205 °C, yield: 3.49 g (72%); Anal. for $\text{C}_{25}\text{H}_{20}\text{N}_6\text{O}_3\text{S}$ (484.60), (% Calcd./Found): 61.96/61.72 (C), 4.16/4.47 (H), 17.34/17.00 (N), 13.23/13.39 (S); IR (ν , cm^{-1}): 3355 (2NH), 3100 (CH aromatic), 2930 (CH_2 , CH_3), 2206 (CN), 1680 (C=O), 1592, 1499 (C=C), 1317, 1239 (C=S); $^1\text{H-NMR}$ (δ , ppm): 1.18-2.43 (m, 4H, cyclohexene 2CH_2), 2.56-2.89 (m, 4H, cyclohexene 2CH_2), 7.12-7.50 (m, 10H, $2\text{C}_6\text{H}_5$), 8.29 (s, 1H, NH), 9.80 (s, 1H, NH); MS m/z (%): 486 [$\text{M}^+ + 2$] (26.80), 485 [$\text{M}^+ + 1$] (53.09), 484 [M^+] (44.85), 483 [$\text{M}^+ - 1$] (31.96), 82 (100.00).

2-(3-Cyano-4,5,6,7-tetrahydrobenzo[b]thiophen-2-yl)-5-oxo-4-phenyl-3-thioxo-2,3,4,5-tetrahydro-[1,2,4]triazine-6-carboxylic acid ethyl ester (7b)

Reddish brown crystals, m.p. 233–235 °C, yield: 3.46 g (79%); Anal. for $\text{C}_{21}\text{H}_{18}\text{N}_4\text{O}_3\text{S}_2$ (438.52), (% Calcd./Found): 57.52/57.15 (C), 4.14/4.13 (H), 12.78/13.18 (N), 14.62/14.65 (S); IR (ν , cm^{-1}): 3429 (NH), 3090 (CH aromatic), 2930 (CH_2), 2207 (CN), 1686, 1682 (2C=O), 1593, 1439 (C=C), 1320, 1257 (C=S); $^1\text{H-NMR}$ (δ , ppm): 1.03 (t, 3H, CH_3), 1.14-1.98 (m, 4H, cyclohexene 2CH_2), 2.03-2.89 (m, 4H, cyclohexene 2CH_2), 4.30 (q, 2H, CH_2), 6.61-7.80 (m, 10H, $2\text{C}_6\text{H}_5$), 8.29 (s, 1H, NH); MS m/z (%): 440 [$\text{M}^+ + 2$] (18.07), 439 [$\text{M}^+ + 1$] (18.99), 438 [M^+] (16.85), 437 [$\text{M}^+ - 1$] (25.88), 77 [C_6H_5] $^+$ (32.01), 78 (100.00).

2-(3-Cyano-4,5,6,7-tetrahydrobenzo[b]thiophen-2-yl)-5-imino-4-phenyl-3-thioxo-2,3,4,5-tetrahydro-[1,2,4]triazine-6-carboxylic acid (4-methoxy-phenyl)-amide (7c)

Reddish brown crystals, m.p. 188–190 °C, yield: 3.76 g (73%); Anal. for $\text{C}_{26}\text{H}_{22}\text{N}_6\text{O}_2\text{S}_2$ (514.62), (% Calcd./Found): 60.68/60.33 (C), 4.31/4.00 (H), 16.33/15.99 (N), 12.46/12.15 (S); IR (ν , cm^{-1}): 3430 (2NH), 3100 (CH aromatic), 2929 (CH_2 , CH_3), 2204 (CN), 1686 (C=O), 1595, 1436 (C=C), 1320, 1242 (C=S); $^1\text{H-NMR}$ (δ , ppm): 1.14 (s, 3H, CH_3), 1.16-1.98 (m, 4H, cyclohexene 2CH_2), 2.04-2.73 (m, 4H, cyclohexene 2CH_2), 6.53-7.50 (m, 9H, C_6H_4 , C_6H_5), 8.29 (s, 1H, NH), 9.80 (s, 1H, NH); MS m/z (%): 516 [$\text{M}^+ + 2$] (32.45), 515 [$\text{M}^+ + 1$] (23.51), 514 [M^+] (0.99), 70 (100.00).

Synthesis of 4-amino-1-(3-cyano-4,5,6,7-tetrahydrobenzo[b]thiophen-2-yl)-6-oxo-1,6-dihydropyridazine-3-carboxylic acid phenylamide (9)

To a solution of **3a** (3.49 g, 0.01 mol) in acetic acid/acetic anhydride (10: 3 mL) was added. The reaction mixture was heated under reflux for 1 h. The solid product formed upon pouring onto ice/water mixture was collected by filtration, washed with water and crystallized from 1,4-dioxane.

Brown crystals, m.p. 104–106 °C, yield: 3.56 g (91%); Anal. For $C_{20}H_{17}N_5O_2S$ (391.45), (% Calcd./Found): 61.37/60.99 (C), 4.38/4.00 (H), 17.89/17.55 (N), 8.19/7.80 (S); IR (ν , cm^{-1}): 3431 (NH, NH₂), 3050 (CH aromatic), 2931 (CH₂), 2213 (CN), 1685, 1682 (C=O), 1545, 1437 (C=C); ¹H-NMR (δ , ppm): 1.74-2.43 (m, 4H, cyclohexene 2CH₂), 2.57-2.96 (m, 4H, cyclohexene 2CH₂), 3.42 (s, 2H, NH₂), 3.90 (s, 1H, pyridazine CH-5), 7.12-7.82 (m, 5H, C₆H₅), 8.29 (s, 1H, NH); MS m/z (%): 393 [M^{+2}] (0.39), 392 [M^{+1}] (4.92), 391 [M^{+}] (3.60), 381 (100.00).

Synthesis of 2-[(3-cyano-4,5,6,7-tetrahydrobenzo[b]thiophen-2-yl)hydrazono]-N-(4-methoxy-phenyl)-malonamide (10)

Equimolar amounts of **3d** (3.79 g, 0.01 mol) in ethanolic hydrochloric acid (30: 10 mL) were heated under reflux for 10h. The solid product formed upon pouring onto ice/water mixture was collected by filtration, washed with water and crystallized from ethanol.

Brown crystals, m.p. 168–170 °C, yield: 3.10 g (78%); Anal. for $C_{19}H_{19}N_5O_3S$ (397.45), (% Calcd./Found): 57.42/57.47 (C), 4.82/4.55 (H), 17.62/17.22 (N), 8.07/8.40 (S); IR (ν , cm^{-1}): 3412 (2NH, NH₂), 3110 (CH aromatic), 2930-2850 (CH₂, CH₃), 2211 (CN), 1689, 1680 (C=O), 1513, 1440 (C=C); ¹H-NMR (δ , ppm): 1.20 (s, 3H, CH₃), 1.75-2.50 (m, 4H, cyclohexene 2CH₂), 2.51-2.86 (m, 4H, cyclohexene 2CH₂), 3.60 (s, 2H, NH₂), 6.86-7.34 (m, 4H, C₆H₄), 8.29 (s, 1H, NH), 9.30 (s, 1H, NH); MS m/z (%): 397 [M^{+}] (14.52), 369 [M^{+1}] (15.26), 395 [M^{+2}] (5.88), 80 (100.00).

Synthesis of 4,5,6,7-tetrahydrobenzo[b]thiophene-3-carbonitrile derivatives 12a-d

General procedure: To a solution of compound **3a** (3.49 g, 0.01 mol) or **3b** (3.49 g, 0.01 mol) in 1,4-dioxane (25 mL), either hydrazine hydrate **11a** (0.50 g, 0.01 mol), or phenyl hydrazine **11b** (1.08 g, 0.01 mol) was added. The reaction mixture, in each case, was heated under reflux for 5 h. The solid products formed, in each case, upon pouring onto ice/water mixture containing few drops of hydrochloric acid were collected by filtration, and crystallized from 1,4-dioxane.

2-[N'-(3-Amino-5-phenylimino-1,5-dihydro-pyrazol-4-ylidene)hydrazino]-4,5,6,7-tetrahydrobenzo[b]thiophene-3-carbonitrile (12a)

Brown crystals, m.p. 153–155 °C, yield: 3.13 g (86%); Anal. for $C_{18}H_{17}N_7S$ (363.44), (% Calcd./Found): 59.49/59.22 (C), 4.71/4.70 (H), 26.98/26.58 (N), 8.82/9.20 (S); IR (ν , cm^{-1}): 3400-3328 (2NH, NH₂), 3100 (CH aromatic), 2932-2854 (CH₂), 2208 (CN), 1597, 1441 (C=C), 1520 (=N-NH); ¹H-NMR (δ , ppm): 1.71-2.40 (m, 4H, cyclohexene 2CH₂), 2.61-2.91 (m, 4H, cyclohexene 2CH₂), 6.91 (s, 1H, pyrazole NH), 7.09-7.36 (m, 5H, C₆H₅), 8.29 (s, 1H, NH); MS m/z (%): 365 [M^{+2}] (0.25), 364 [M^{+1}] (0.33), 361 [M^{+2}] (0.31), 77 [C₆H₅]⁺ (8.70), 80 (100.00).

2-[N'-(3-Amino-1-phenyl-5-phenylimino-1,5-dihydro-pyrazol-4-ylidene)hydrazino]-4,5,6,7-tetrahydrobenzo[b]thiophene-3-carbonitrile (12b)

Brown crystals, m.p. 178–180 °C, yield: 2.77 g (63%); Anal. for $C_{24}H_{21}N_7S$ (439.54), (% Calcd./Found): 65.58/65.20 (C), 4.82/4.77 (H), 22.31/21.98 (N), 7.30/7.70 (S); IR (ν , cm^{-1}): 3426 (NH, NH₂), 3050 (CH aromatic), 2928 (CH₂), 2205 (CN), 1590, 1431 (C=C), 1513 (=N-NH); ¹H-NMR (δ , ppm): 1.81-2.49 (m, 4H, cyclohexene 2CH₂), 2.79-2.94 (m, 4H, cyclohexene 2CH₂), 3.57 (s, 2H, NH₂), 6.00-7.80 (m, 10H, 2C₆H₅), 8.20 (s, 1H, NH), 8.90 (s, 1H, NH); MS m/z (%): 441 [M^{+2}] (0.20), 440 [M^{+1}] (0.15), 438 [M^{+1}] (0.26), 77 [C₆H₅]⁺ (5.10), 57 (100.00).

2-[N'-(3-Hydroxy-5-oxo-1,5-dihydro-pyrazol-4-ylidene)hydrazino]-4,5,6,7-tetrahydrobenzo[b]thiophene-3-carbonitrile (12c)

Dark brown crystals, m.p. 158–160 °C, yield: 2.02 g (72%); Anal. for $C_{12}H_{11}N_5O_2S$ (289.31), (% Calcd./Found): 49.82/50.20 (C), 3.83/4.20 (H), 24.21/23.83 (N), 11.08/11.44 (S); IR (ν , cm^{-1}): 3432-3196 (2NH, OH), 2933 (CH₂), 2210 (CN), 1685 (C=O), 1600, 1402 (C=C); ¹H-NMR (δ , ppm): 1.71-2.49 (m, 4H, cyclohexene 2CH₂), 2.57-2.89 (m, 4H, cyclohexene 2CH₂), 7.10 (s, 1H, pyrazole NH), 7.30 (s, 1H, NH), 8.29 (s, 1H, OH); MS m/z (%): 291 [M^{+2}] (0.82), 290 [M^{+1}] (0.32), 289 [M^{+}] (0.33), 288 [M^{+1}] (0.10), 150 (100.00).

2-[N'-(3-Hydroxy-5-oxo-1-phenyl-1,5-dihydro-pyrazol-4-ylidene)hydrazino]-4,5,6,7-tetrahydrobenzo[b]thiophene-3-carbonitrile (12d)

Brown crystals, m.p. 213–215 °C, yield: 2.37 g (65%); Anal. for $C_{18}H_{15}N_5O_2S$ (365.41), (% Calcd./Found): 59.16/58.77 (C), 4.14/4.30 (H), 19.17/18.80 (N), 8.78/9.10 (S); IR (ν , cm^{-1}): 3426 (NH, OH), 3050 (CH aromatic), 2931-2859 (CH₂), 2206 (CN), 1687 (C=O), 1592, 1438 (C=C), 1530 (=N-NH); ¹H-NMR (δ , ppm): 1.51-2.32 (m, 4H, cyclohexene 2CH₂), 2.61-2.89 (m, 4H, cyclohexene 2CH₂), 6.93 (s, 1H, NH), 7.10-7.55 (m, 5H, C₆H₅), 8.00 (s, 1H, OH); MS m/z (%): 366 [M^{+1}] (2.94), 365 [M^{+}] (0.58), 364 [M^{+1}] (1.00), 51 (100.00).

Synthesis of the 2,3,4,5-tetrahydro-[1,2,4]triazine-6-carboxylic acid hydrazide and phenylhydrazide derivatives 13a,b

General procedure: Equimolar amounts of **7b** (4.38 g, 0.01 mol) and either hydrazine hydrate **11a** (0.50 g, 0.01 mol), or phenyl hydrazine **11b** (1.08g, 0.01 mol) in 1,4-dioxane (25 mL) were heated under reflux for 5 h. The reaction mixture, in each case, pouring onto ice/water mixture containing few drops of hydrochloric acid was collected by filtration, and crystallized from 1,4-dioxane.

2-(3-Cyano-4,5,6,7-tetrahydrobenzo[b]thiophen-2-yl)-3-hydrazono-5-oxo-4-phenyl-2,3,4,5-tetrahydro-[1,2,4]triazine-6-carboxylic acid hydrazide (13a)

Brown crystals, m.p. 243–245 °C, yield: 3.69 g (87%); Anal. for $C_{19}H_{18}N_8O_2S$ (422.46), (% Calcd./Found):

54.02/54.40 (C), 4.29/4.14 (H), 26.52/26.14 (N), 7.59/7.90 (S); IR (ν , cm^{-1}): 3424 (NH, 2NH₂), 3100 (CH aromatic), 2930 (CH₂), 2206 (CN), 1684, 1682 (2C=O), 1557, 1436 (C=C); ¹H-NMR (δ , ppm): 1.17-2.32 (m, 4H, cyclohexene 2CH₂), 2.62-2.89 (m, 4H, cyclohexene 2CH₂), 3.60 (s, 2H, NH₂), 4.00 (s, 2H, NH₂), 6.91-7.62 (m, 5H, C₆H₅), 8.30 (s, 1H, NH); MS m/z (%): 424 [M⁺+2] (5.58), 423 [M⁺+1] (2.66), 422 [M⁺] (7.81), 77 [C₆H₅]⁺ (45.42), 174 (100.00).

2-(3-Cyano-4,5,6,7-tetrahydrobenzo[b]thiophen-2-yl)-5-oxo-4-phenyl-3-(phenyl-hydrazono)-2,3,4,5-tetrahydro-[1,2,4]triazine-6-carboxylic acid N'-phenyl-hydrazide (13b)

Reddish brown crystals, m.p. 183–185 °C, yield: 4.40 g (88%); Anal. for C₃₁H₂₆N₈O₂S (574.66), (% Calcd./Found): 64.79/64.40 (C), 4.56/4.20 (H), 19.50/19.88 (N), 5.58/5.98 (S); IR (ν , cm^{-1}): 3427 (3NH), 3100 (CH aromatic), 2930-2850 (CH₂), 2207 (CN), 1688, 16820 (2C=O), 1563, 1440 (C=C); ¹H-NMR (δ , ppm): 1.17-1.91 (m, 4H, cyclohexene 2CH₂), 2.08-2.89 (m, 4H, cyclohexene 2CH₂), 6.92-7.44 (m, 10H, 2C₆H₅), 7.95 (s, 1H, NH), 8.10 (s, 1H, NH), 8.30 (s, 1H, NH); MS m/z (%): 573 [M⁺-1] (21.83), 572 [M⁺+2] (24.65), 188 (100.00).

Synthesis of 2-(4-oxo-4,5-dihydro-thiazol-2-yl)-acetamide and N-phenyl-acetamide derivatives (15a, b)

General procedure: To a solution of **3a** (3.49 g, 0.01 mol) or **3c** (3.83 g, 0.01 mol) in acetic acid (30 mL), thioglycolic acid **14** (0.92 g, 0.01 mol) was added. The reaction mixture was heated under reflux for 5 h. The solid product formed upon pouring onto ice/water mixture was collected by filtration, washed with water and crystallized from acetic acid.

2-[(3-Cyano-4,5,6,7-tetrahydrobenzo[b]thiophen-2-yl)-hydrazono]2-(4-oxo-4,5-dihydro-thiazol-2-yl)-N-phenyl-acetamide (15a)

Brown crystals, m.p. 218–220 °C, yield: 2.79 g (66%); Anal. for C₂₀H₁₇N₅O₂S₂ (423.51), (% Calcd./Found): 56.72/56.37 (C), 4.05/4.27 (H), 16.54/16.22 (N), 15.14/15.06 (S); IR (ν , cm^{-1}): 3406 (2NH), 3050 (CH aromatic), 2932 (CH₂), 2211 (CN), 1688, 1681 (2C=O), 1530, 1435 (C=C); ¹H-NMR (δ , ppm): 1.80-2.43 (m, 4H, cyclohexene 2CH₂), 2.57-2.99 (m, 4H, cyclohexene 2CH₂), 3.65 (s, 2H, thiazole C5-H), 7.39-7.70 (m, 5H, C₆H₅), 8.30 (s, 1H, NH), 10.50 (s, 1H, NH); MS m/z (%): 423 [M⁺] (0.51), 422 [M⁺-1] (0.49), 421 [M⁺-2] (0.75), 77 [C₆H₅]⁺ (3.31), 69 (100.00).

N-(4-Chloro-phenyl)-2-[(3-cyano-4,5,6,7-tetrahydrobenzo[b]thiophen-2-yl)-hydrazono]2-(4-oxo-4,5-dihydro-thiazol-2-yl)-acetamide (15b)

Dark brown crystals, m.p. 228-230 °C, yield: 2.98 g (65%); Anal. for C₂₀H₁₆N₅O₂S₂Cl (457.96), (% Calcd./Found): 52.45/52.85 (C), 3.52/3.82 (H), 15.29/14.90 (N), 14.00/13.66 (S); IR (ν , cm^{-1}): 3428 (2NH), 3050 (CH

aromatic), 2929 (CH₂), 2205 (CN), 1690, 1683 (2C=O), 1588, 1490 (C=C); ¹H-NMR (δ , ppm): 1.51-2.32 (m, 4H, cyclohexene 2CH₂), 2.73-2.99 (m, 4H, cyclohexene 2CH₂), 3.99 (s, 2H, thiazole C5-H), 6.00 (s, 1H, NH), 6.92 (s, 1H, NH), 7.03-7.80 (m, 4H, C₆H₄); MS m/z (%): 460 [M⁺+2] (3.50), 459 [M⁺+1] (3.08), 458 [M⁺] (5.41), 135 (100.00), 76 [C₆H₄]⁺ (4.98).

Synthesis of the pyridazine carboxylic acid amide and the ethyl ester derivatives 17a,b

General procedure: To a solution of **3c** (3.83 g, 0.01 mol) in 1,4-dioxane (30 mL) containing triethylamine (1.00 mL), either α -cyanocinnamitrile **16a** (1.54 g, 0.01 mol) or ethyl cyanocinnamate **16b** (2.01 g, 0.01 mol) was added. The reaction mixture, in each case, was heated under reflux for 5 h, then cooled and neutralized by pouring onto ice/water mixture containing few drops of hydrochloric acid. The solid product formed, in each case, was filtered off and crystallized from 1,4-dioxane.

5-Cyano-1-(3-cyano-5-propyl-thiophen-2-yl)-4-imino-6-phenyl-1,4-dihydro-pyridazine-3-carboxylic acid (4-chloro-phenyl)-amide (17a)

Brown crystals, m.p. 223–225 °C, yield: 3.58 g (70%); Anal. for C₂₇H₁₉N₆O₃Cl (511.00), (% Calcd./Found): 63.46/63.47 (C), 3.75/4.03 (H), 16.45/16.40 (N), 6.27/6.60 (S); IR (ν , cm^{-1}): 3434(2NH), 3040 (CH aromatic), 2930 (CH₃), 2255, 2202 (2CN), 1688 (C=O), 1593, 1435 (C=C); ¹H-NMR (δ , ppm): 1.71-2.40 (m, 4H, cyclohexene 2CH₂), 2.49-2.89 (m, 4H, cyclohexene 2CH₂), 7.08-7.98 (m, 9H, C₆H₄, C₆H₅), 8.29 (s, 1H, NH), 8.70 (s, 1H, NH); MS m/z (%): 511 [M⁺] (0.17), 510 [M⁺-1] (0.35), 77 [C₆H₅]⁺ (7.15), 69 (100.00).

6-(4-Chloro-phenylcarbamoyl)-2-(3-cyano-4,5,6,7-tetrahydrobenzo[b]thiophen-2-yl)-5-imino-3-phenyl-2,5-dihydro-pyridazine-4-carboxylic acid ethyl ester (17b)

Dark brown crystals, m.p. 228-230 °C, yield: 3.96 g (71%); Anal. for C₂₉H₂₄N₅O₃S₂Cl (558.05), (% Calcd./Found): 62.42/62.11 (C), 4.33/3.96 (H), 12.55/12.58 (N), 5.75/6.10 (S); IR (ν , cm^{-1}): 3430 (2NH), 3100 (CH aromatic), 2931 (CH₂, CH₃), 2205 (CN), 1690, 1683 (2C=O), 1555, 1438 (C=C); ¹H-NMR (δ , ppm): 1.03 (t, 3H, CH₃); 1.18-1.91 (m, 4H, cyclohexene 2CH₂), 2.06-2.91 (m, 4H, cyclohexene 2CH₂), 4.36 (q, 2H, CH₂), 6.00-8.19 (m, 9H, C₆H₄, C₆H₅), 8.29 (s, 1H, NH), 8.40 (s, 1H, NH); MS m/z (%): 558 [M⁺] (19.35), 557 [M⁺-1] (15.87), 77 [C₆H₅]⁺ (63.09), 55 (100.00).

Synthesis of the 4,5,6,7-tetrahydrobenzo[b]thiophene-3-carbonitrile derivatives 19a,b

General procedure: Equimolar amounts of **3b** (3.49 g, 0.01 mol) and either urea **18a** (0.60 g, 0.01 mol), or thiourea **18b** (0.76 g, 0.01 mol) in sodium ethoxide solution [prepared by adding metallic sodium (0.23 g, 0.01 mol) in absolute ethanol (30 mL)] were heated under reflux for 5 h. The reaction mixture, in each case, pouring onto ice/water mixture containing few drops of hydrochloric acid and the

formed solid product was collected by filtration and crystallized from 1,4-dioxane.

2-[N'-(2,4,6-Trioxo-tetrahydro-pyrimidin-5-ylidene)hydrazino]-4,5,6,7-tetrahydrobenzo[b]thiophene-3-carbonitrile (19a)

Brown crystals, m.p. 243-245 °C, yield: 2.44 g (77%); Anal. for C₁₃H₁₁N₅O₃S (317.32), (% Calcd./Found): 49.21/49.60 (C), 3.49/3.89 (H), 22.07/21.70 (N), 10.10/10.46 (S); IR (ν , cm⁻¹): 3430 (3NH), 2927 (CH₃), 2210 (CN), 1685, 1683-1680 (3C=O), 1510, 1434 (C=C); ¹H-NMR (δ , ppm): 1.76-1.78 (m, 4H, cyclohexene 2CH₂), 2.60-2.72 (m, 4H, cyclohexene 2CH₂), 6.99 (s, 1H, NH), 7.16 (s, 1H, NH), 7.33 (s, 1H, NH); MS m/z (%): 319 [M⁺+2] (0.13), 318 [M⁺+1] (0.15), 317 [M⁺] (0.13), 64 (100.00).

2-[N'-(4,6-Dioxo-2-thioxo-tetrahydro-pyrimidin-5-ylidene)-hydrazino]-4,5,6,7-tetrahydrobenzo[b]thiophene-3-carbonitrile (19b)

Brown crystals, m.p. 203-205 °C, yield: 3.00 g (90%); Anal. for C₁₃H₁₁N₅O₂S₂ (333.39), (Calcd./Found): 46.83/47.22 (C), 3.33/3.70 (H), 21.01/20.70 (N), 19.24/18.88 (S); IR (ν , cm⁻¹): 3423 (3NH), 2930 (CH₃), 2205 (CN), 1690, 1683 (2C=O), 1564, 1435 (C=C), 1320, 1278 (C=S); ¹H-NMR (δ , ppm): 1.43-2.50 (m, 4H, cyclohexene 2CH₂), 2.60-2.72 (m, 4H, cyclohexene 2CH₂), 7.34 (s, 1H, NH), 7.77 (s, 1H, NH), 8.29 (s, 1H, NH); MS m/z (%): 335 [M⁺+2] (0.12), 334 [M⁺+1] (0.12), 333 [M⁺] (0.10), 78 (100.00).

Synthesis of the malonic acid diethyl ester derivatives, 21a, b

General procedure: To a solution of compound **3b** (3.49 g, 0.01 mol) in 1,4-dioxane (30 mL), either ethyl chloroacetate **20a** (1.22 g, 0.01 mol), or chloroacetone **20b** (0.92 g, 0.01 mol) was added in the presence of a catalytic amount of potassium carbonate. The reaction mixture, in each case, was heated under reflux for 5 h. The solid products formed, in each case, upon pouring onto ice/water mixture containing few drops of hydrochloric acid were collected by filtration, and crystallized from 1,4-dioxane.

1-(3-Cyano-4,5,6,7-tetrahydrobenzo[b]thiophen-2-yl)-4-hydroxy-1H-pyrazole-3,5-dicarboxylic acid diethyl ester (21a)

Brown crystals, m.p. 220-222 °C, yield: 3.46 g (89%); Anal. for C₁₈H₁₉N₃O₅S (389.43), (% Calcd./Found): 55.52/55.23 (C), 4.92/5.30 (H), 10.79/11.10 (N), 8.23/8.60 (S); IR (ν , cm⁻¹): 3433 (OH), 2929 (CH₂, CH₃), 2210 (CN), 1723, 1684 (2C=O), 1600, 1436 (C=C); ¹H-NMR (δ , ppm): 1.03 (t, 3H, CH₃), 1.19 (t, 3H, CH₃) 1.51-2.27 (m, 4H, cyclohexene 2CH₂), 2.58-2.95 (m, 4H, cyclohexene 2CH₂), 3.85 (q, 2H, CH₂), 4.15 (q, 2H, CH₂), 8.29 (s, 1H, OH); MS m/z (%): 391 [M⁺+2] (25.39), 387 [M⁺+2] (17.02), 78 (100.00).

5-Acetyl-1-(3-cyano-4,5,6,7-tetrahydrobenzo[b]thiophen-2-yl)-4-hydroxy-1H-pyrazole-3-carboxylic acid ethyl ester (21b)

Dark brown crystals, m.p. 148-150 °C, yield: 3.13 g (87%); Anal. for C₁₇H₁₇N₃O₄S (359.40), (% Calcd./Found): 56.81/57.20 (C), 4.77/4.88 (H), 11.69/11.99 (N), 8.92/9.32 (S); IR (ν , cm⁻¹): 3429 (OH), 2929 (CH₂, CH₃), 2208 (CN), 1724, 1684 (2C=O), 1591, 1438 (C=C); ¹H-NMR (δ , ppm): 1.03 (t, 3H, CH₃), 1.20 (s, 3H, CH₃) 1.71-2.40 (m, 4H, cyclohexene 2CH₂), 2.60-2.79 (m, 4H, cyclohexene 2CH₂), 4.10 (q, 2H, CH₂), 8.28 (s, 1H, OH); MS m/z (%): 360 [M⁺+1] (11.53), 201 (93.30), 57 (100.00).

Synthesis of 2-[(3-cyano-4,5,6,7-tetrahydrobenzo[b]thiophen-2-yl)-hydrazono]-N-phenyl-malonamic acid ethyl ester (23)

To a solution of **3b** (3.49 g, 0.01 mol) in 1,4-dioxane (30 mL), aniline **22** (0.93 g, 0.01 mol) was added. The reaction mixture was heated under reflux for 5 h. The solid product formed upon pouring onto ice/water mixture was collected by filtration, washed with water and crystallized from 1,4-dioxane.

Brown crystals, m.p. 223-225 °C, yield: 3.49 g (88%); Anal. for C₂₀H₂₀N₄O₃S (396.46), (% Calcd./Found): 60.59/60.22 (C), 5.08/4.69 (H), 14.13/14.53 (N), 8.09/8.44 (S); IR (ν , cm⁻¹): 3698-3426 (2NH), 2932 (CH₂, CH₃), 2209 (CN), 1688, 1683 (2C=O), 1588, 1496 (C=C); ¹H-NMR (δ , ppm): 1.24 (t, 3H, CH₃); 1.76-2.43 (m, 4H, cyclohexene 2CH₂), 2.57-2.89 (m, 4H, cyclohexene 2CH₂), 3.57 (q, 2H, CH₂), 6.00 (s, 1H, NH), 6.90 (s, 1H, NH), 7.10-8.30 (m, 5H, C₆H₅); MS m/z (%): 397 [M⁺+1] (0.75), 396 [M⁺] (0.72), 77 [C₆H₅]⁺ (14.38), 367 (100.00).

Antimicrobial activity of the newly synthesized compounds

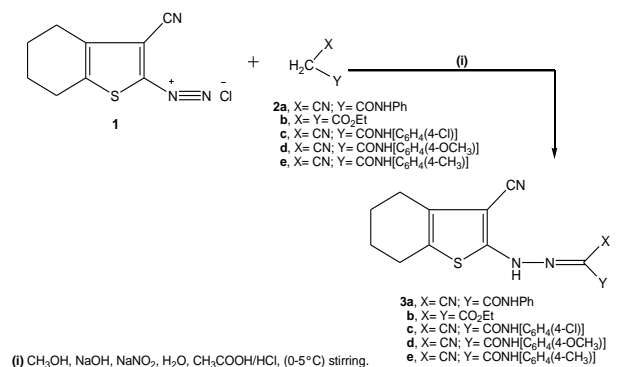
Microorganisms used were obtained from Microbial Chemistry Department, National Research Center, Cairo, Egypt. For the *in vitro* antimicrobial activity evaluation, microorganism suspensions were prepared to contain approximately 10⁸ cfu/mL and the plates were inoculated. A stock solution of each of the synthesized compounds (1000 μ g mL⁻¹) in DMSO was prepared and graded dilutions of the tested compounds were incorporated in a cavity (depth 3 mm, diameter 4 mm) made in the center of the Petri dish (nutrient agar for bacteria and Sabouraud vs. dextrose agar medium for fungi).

The plates were incubated in duplicates for 24 h at 37 °C (for bacteria) and at 30 °C (for fungi). A positive control using only inoculation and a negative control using only DMSO in the cavity were carried out. The results of antimicrobial screening of the synthesized and standard antibiotics are given in Table I.

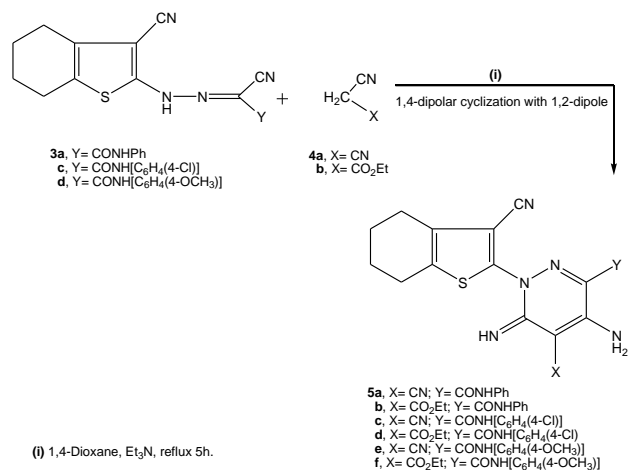
Results and discussion

3-Cyano-4,5,6,7-tetrahydrobenzo[b]thiophene-2-diazonium chloride (**1**) reacted with the active methylene reagents (XCH₂Y, X=CN, Y=CONHPh; X=Y=CO₂Et; X=CN, Y=CONH[C₆H₄(4-Cl)]; X=CN, Y=CONH[C₆H₄(4-OCH₃)];

X=CN, Y=CONH[C₆H₄(4-CH₃)] (**2a-e**) to give the hydrazone derivatives **3a-e** (Scheme 1). The analytical and spectral data of the products were in analogous with their respective structures. Thus, the mass spectral data for compounds **3a-e** revealed a molecular formula C₁₈H₁₅N₅O₂ (*m/z* 349 [M⁺]), C₁₆H₁₉N₃O₄S (*m/z* 349 [M⁺]), C₁₈H₁₄N₅O₂Cl (*m/z* 382 [M⁺-1]), C₁₉H₁₇N₅O₂S (*m/z* 379 [M⁺]) and C₁₉H₁₇N₅O₂S (*m/z* 363 [M⁺]), respectively which confirmed their structures. Compounds **3a**, **3c** and **3d** reacted with the cyanomethylene reagents (XCH₂Y, X=Y=CN; X=CN, Y=CO₂Et) (**4a, b**) to give the iminopyridazine derivatives **5a-f** (Scheme 2).



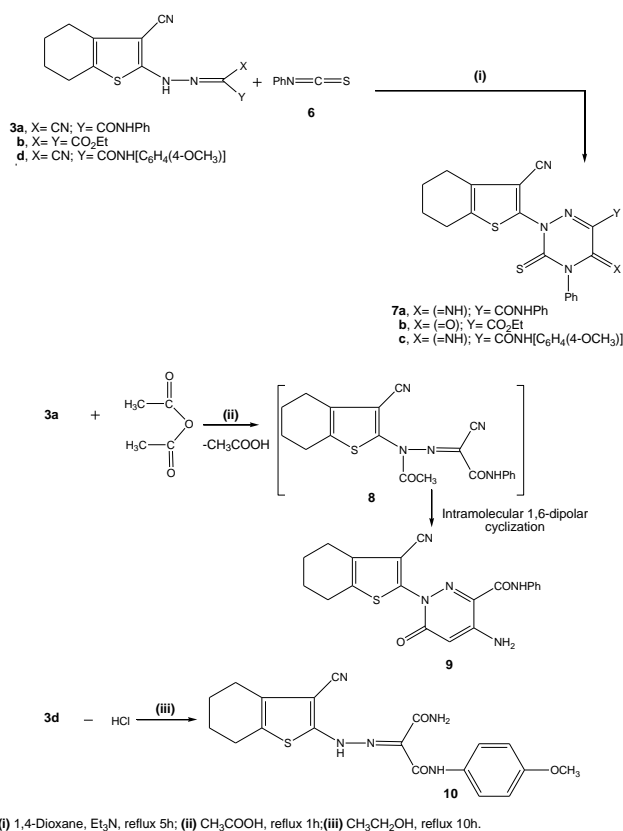
Scheme 1. Synthesis of the hydrazone derivatives **3a-e**



Scheme 2. Synthesis of the pyridazine derivatives **5a-f**

The reaction involved 1,4-dipolar cyclization of compounds **3a**, **3c** and **3d** with 1,2-dipoles (**4a, b**). The structures of the latter products were based on their respective analytical and spectral data. Thus, ¹H-NMR spectrum of **5a** showed two multiplets about δ 1.81-2.27 ppm and δ 2.57-2.94 ppm that integrated for four cyclohexene CH₂ protons, δ 4.44 ppm for NH₂ protons, multiplets at δ 6.91-7.40 ppm for phenyl moiety and at δ 8.30 and 8.40 for 2NH protons. Mass spectra of **5a, 5b, 5c, 5d, 5e** and **5f** exhibited a molecular ions *m/z* 415 [M⁺], *m/z* 462 [M⁺], *m/z* 450 [M⁺], 496 [M⁺-1], *m/z* 445 [M⁺] and *m/z* 492 [M⁺] corresponding to their molecular formulae, respectively.

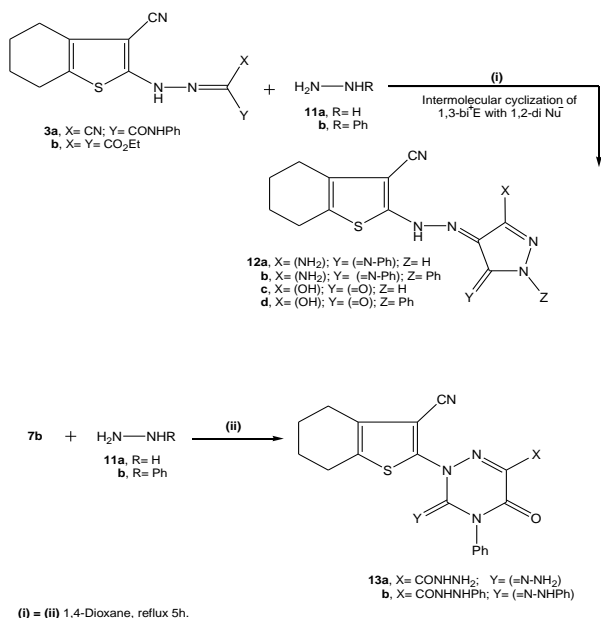
On the other hand the reaction of either compounds **3a, 3b** or **3d** with phenylisothiocyanate (**6**) gave the triazine derivatives **7a-c** (Scheme 3). The reaction took place via nucleophilic attack of NH moiety of compounds **3a, 3b** or **3d** on isocyanate C=S terminal followed by 1,6-dipolar cyclization. The analytical and spectral data of **7a-c** are consistent with their corresponding structures (see experimental section). As an example, the appearance of two C=O stretching modes about 1600 and 1620 cm⁻¹ region cited for triazene oxo function and ethoxy carbonyl in the IR spectrum of **7b**. Also, the mass spectrum of **7b** showed molecular ion *m/z* 438 corresponding to molecular formula C₂₁H₁₈N₄O₃S₂. Treatment of **3a** with acetic anhydride/AcOH mixture under refluxing conditions gave pyridazine-3-one derivative **9**.



Scheme 3. Synthesis of the triazine **7a-c**, pyridazinone **9** and diamido **10** derivatives

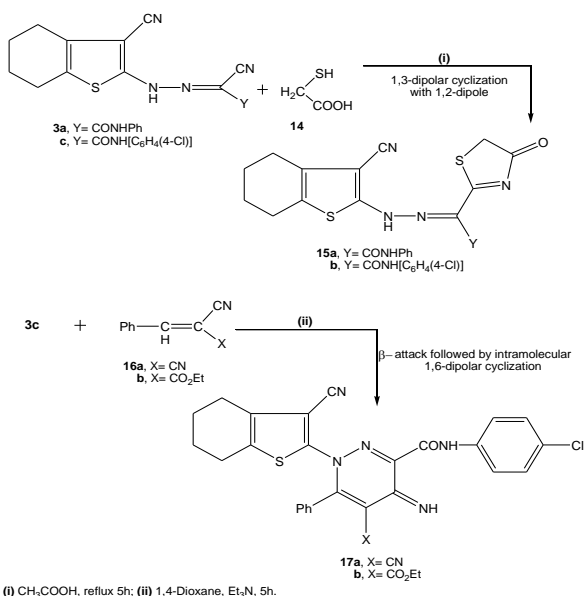
The reaction took place through formation of the intermediate **8** followed by 1,6-dipolar intramolecular cyclization to give **9**. ¹H-NMR spectrum of compound **9** showed two multiplets about δ 1.74-2.43 ppm and δ 2.57-2.96 ppm for four cyclohexene CH₂ protons, δ 3.42 ppm for NH₂ protons, pyridazine C5-H protons at δ 3.90 ppm, multiplets at δ 7.12-7.82 ppm for phenyl moiety and a singlet at δ 8.29 integrated for NH proton. The mass spectrum of **9** exhibited a molecular ion *m/z* 391 [M⁺] corresponding to molecular formula C₂₀H₁₇N₅O₂S. Compound **3d** underwent ready hydrolysis in HCl/EtOH to give the diamido derivative **10**. Microanalysis, IR and ¹H-NMR of **10** are fully consistent with the proposed structure.

Next, we moved towards studying the reactivity of the hydrazone derivatives **3a** and **3b** towards hydrazines ($\text{H}_2\text{N-NHR}$, $\text{R}=\text{H}$; $\text{R}=\text{Ph}$) namely hydrazine hydrate (**11a**) and phenylhydrazine (**11b**) to afford the respective pyrazole derivatives **12a-d** (Scheme 4). The reaction involved intermolecular cyclization of 1,3-bielectrophilic compounds **3a, b** with 1,2-dinucleophiles (**11a**) and (**11b**). The analytical and spectral data of the latter products were the basis of their structural elucidation.



Scheme 4. Synthesis of pyrazole **12a-d** and triazine **13a, b** derivatives

Thus, $^1\text{H-NMR}$ spectrum of **12a** (as an example) showed two multiplets about δ 1.71-2.40 ppm and δ 2.61-2.91 ppm for four cyclohexene CH_2 protons, δ 3.39 ppm for singlet NH_2 protons, a singlet pyrazole NH proton at δ 6.92 ppm, multiplets at δ 7.09-7.36 ppm for phenyl moiety and a singlet NH proton at δ 8.29 ppm.

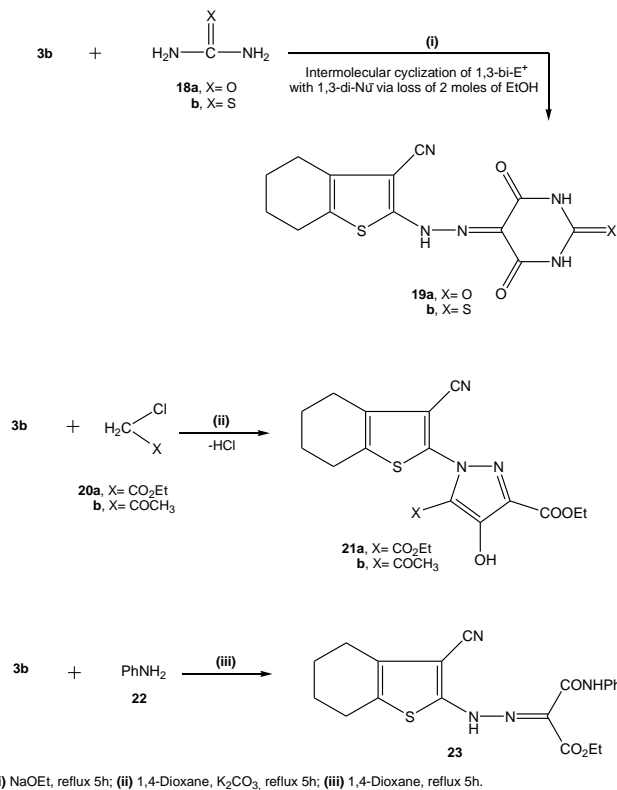


Scheme 5. Synthesis of the thiazolone **15a, b** and pyridazine **17a, b** derivatives.

In the mass spectra of **12a-d** the existing $[\text{M}^+ + 1]$ ions ($m/z=364$, $m/z=440$) and $[\text{M}^+]$ ions ($m/z=289$, $m/z=365$), confirmed their respective molecular weights. The absence of $\text{C}=\text{O}$ absorption in the 1600-1800 cm^{-1} region confirmed the assignment for pyrazole structures **12a** and **12b**. The appearance of $\text{C}=\text{O}$ and a broad OH bands in the regions 1625, 1620 and 3432, 3426 cm^{-1} , respectively confirmed the structures of **12c** and **12d**.

The reaction of the pyridazine derivative **7b** with either hydrazine hydrate (**11a**) or phenylhydrazine (**11b**) gave the hydrazide derivatives **13a** and **13b**, respectively (Scheme 4). The reaction involved the loss of H_2S and two moles of EtOH . The mass spectra of **13a** and **13b** showed molecular ion peaks $[\text{M}^+]=424$ and $[\text{M}^+ - 1]=499$ corresponding to their respective molecular formulae $\text{C}_{19}\text{H}_{16}\text{N}_6\text{O}_2\text{S}_2$ and $\text{C}_{25}\text{H}_{20}\text{N}_6\text{O}_2\text{S}_2$.

Interestingly, the reaction of either of compounds **3a** or **3c** with thioglycolic acid (**14**) gave the thiazole derivatives **15a** and **15b**, respectively (Scheme 5). The reactions took place through 1,3-dipolar cyclization with 1,2-dipole via nucleophilic attack by SH group on the cyano moiety in **3a** or **3c** followed by water elimination.



Scheme 6. Synthesis of the pyrimidine **19a, b**, 4-hydroxy-pyrazole **21a, b** and hydrazone-malonamic acid ethyl ester **23** derivatives

Next, we studied the reaction of **3c** with cinnamitrile derivatives (**16a, b**) ($\text{PhCH}=\text{C}(\text{CN})\text{X}$, $\text{X}=\text{CN}$; $\text{X}=\text{CO}_2\text{Et}$) with the aim of formation of biologically active pyridazine derivatives.²³⁻²⁶ Thus, the reaction of **3c** with either α -cyanocinnamitrile (**16a**) or ethyl cyanocinnamate (**16b**) in refluxing 1,4-dioxane containing a catalytic amount of triethylamine afforded the pyridazine derivatives **17a** and **17b**, respectively (Scheme 5). The reaction occurs via β -attack followed by 1,6-dipolar intramolecular cyclization.

Table 1. Antimicrobial activity data of the synthesized compounds in terms of MIC in $\mu\text{g mL}^{-1}$.

Compound No.	<i>E. coli</i> ECT 101	<i>B. Cereus</i> CECT 148	<i>B. subtilis</i> CECT 498	<i>C. albicans</i> CECT 1394
3a	Not active	4.62	8.39	12.62
3b	0.46	8.66	25.33	12.22
3c	Not active	12.34	6.13	0.40
3d	Not active	6.05	12.42	4.55
3e	Not active	6.22	12.89	18.42
5a	Not active	8.42	10.29	16.02
5b	2.66	4.73	12.8	11.32
5c	Not active	18.32	6.22	0.40
5d	Not active	20.15	23.16	100
5e	10.46	8.66	25.33	12.22
5f	Not active	0.08	5.23	8.44
7a	0.81	6.46	20.63	10.22
7b	Not active	7.39	4.33	12.77
7c	Not active	10.23	2.56	28.60
9	6.82	4.92	2.11	10.39
10	Not active	7.03	0.68	20.50
12a	2.77	4.66	12.33	8.41
12b	2.46	8.55	18.33	12.42
12c	12.46	10.66	2.33	10.22
12d	10.12	6.13	2.22	10.25
13a	Not active	25	23	26
13b	Not active	0.05	3.13	0.61
15a	0.86	2.44	15.92	10.11
15b	Not active	12.32	16.32	14.40
17a	16.64	0.06	6.33	50
17b	Not active	12.30	4.22	12.55
19a	8.22	5.23	0.22	16.22
19b	Not active	22.01	0.48	25.60
21a	Not active	6.25	20	30
21b	12.50	20	6.25	8.65
23	Not active	0.08	2.22	6.44
Ampicillin	6.25	3.13	12.50	-
cycloheximide	-	-	-	12.50

Thus, $^1\text{H-NMR}$ of **17a** and **17b** revealed signals due to two NH protons at about δ 8.29-8.70 ppm. Signals integrated for ester protons in compound **17b** were also observed in their respective fields. The mass spectra of **17a** and **17b** exhibited molecular ion peaks $[\text{M}^+]$ at m/z 511 and m/z 558 respectively corresponding to their molecular formulae.

The high yield of **3b** encouraged us to synthesize biologically active systems via reaction with some chemical reagents. Thus, compound **3b** reacted with either urea (**18a**) or thiourea (**18b**) in sodium ethoxide solution to give pyrimidine derivatives **19a** and **19b**, respectively (Scheme 6). The reaction took place via 1,3-intermolecular cyclization of compound **3b** with 1,3-dinucleophiles **18a** and **18b** via loss of two moles of ethanol. The analytical and spectral data of the latter products were based on analytical and spectral data. Thus, $^1\text{H-NMR}$ spectrum of **19a** showed two multiplets about δ 1.76-1.78 ppm and δ 2.60-2.72 ppm for four cyclohexene CH_2 protons and three singlets at δ 6.99, 7.16 and 7.33 for 3NH protons. The appearance of three $\text{C}=\text{O}$ stretching about 1600, 1634 and 1660 cm^{-1} cited for pyrimidine oxo functions and the presence of $\text{C}=\text{S}$ stretching bands at 1320 and 1278 cm^{-1} in

the IR spectra of **19a** and **19b** proved the proposed structures.

Moreover, the reaction of **3b** with α -halocarbonyl reagents (XCH_2Cl , $\text{X}=\text{CO}_2\text{Et}$; $\text{X}=\text{COCH}_3$) namely ethyl chloroacetate (**20a**) and α -chloroacetone (**20b**) gave the pyrazole derivatives **21a** and **21b**, respectively (Scheme 6). The reaction took place through 1,5-dipolar intramolecular cyclization via loss of ethanol. The mass spectra of **21a** and **21b** displayed molecular ions $[\text{M}^+2]$ at m/z 391 and $[\text{M}^+-1]$ at m/z 360 corresponding to their respective molecular formulae.

Finally the reaction of **3b** with aniline (**22**) gave the anilide derivative **23** (Scheme 6). The analytical and spectral data of compound **23** were in agreement with its respective structure (see experimental section).

In vitro evaluation of antibacterial and antifungal activities.

The synthesized compounds were screened in vitro for their antimicrobial activity against a variety of bacterial and

fungus isolates. Evaluation of the antibacterial activity against Gram-negative (*Escherichia coli* ECT 101 and *Pseudomonas aeruginosa*) and Gram-positive bacteria (*Bacillus subtilis* CECT 498 and *Bacillus cereus* CECT 148) and the antifungal activity against *Candida albicans* CECT 1394 as a representative species of fungi were assessed for the synthesized compounds. The minimal inhibitory concentration (MIC in $\mu\text{g mL}^{-1}$) was determined using an adaptation of agar streak dilution method based on radial diffusion.^{27, 28} Different concentrated solutions of ampicillin (antibacterial) and cycloheximide (antifungal) were used as standards. The MIC was considered to be the lowest concentration of the tested compounds which inhibits growth of bacteria or fungi on the plate.

The results indicated that most of the synthesized compounds exhibited noticeable antimicrobial activity, and that the bacterial isolates were less active to the synthesized compounds than the fungal species.

Gram-negative bacteria (*Escherichia coli* ECT 101 and *Pseudomonas aeruginosa*) showed low activity than Gram-positive bacteria (*Bacillus subtilis* CECT 498 and *Bacillus cereus* CECT 148), where all the compounds tested were not active against *Pseudomonas aeruginosa* starting from DMSO solutions of 1000 $\mu\text{g mL}^{-1}$ of each compound.

Compounds **3b**, **7a** and **15a** exhibited the highest inhibitory activity against *Escherichia coli* ECT 101, compounds **5f**, **13b**, **17a** and **23** are highly active against *Bacillus cereus* CECT 148, compounds **10**, **19a** and **19b** showed the highest inhibitory activity towards *Bacillus subtilis* CECT 498, while compounds **3c**, **5c** and **13b** demonstrated the highest inhibitory activity against the fungal species *C. albicans* CECT 1394. It is noteworthy that all the aforementioned compounds showed higher inhibitory activity than the selected standards (ampicillin and cycloheximide).

On the other hand, compounds **5e**, **12c**, **12d**, **17a** and **21b** showed the lowest inhibitory activity against *Escherichia coli* ECT 101, compounds **3c**, **5c**, **5d**, **13a**, **15b**, **17b**, **19b** and **21b** are less active towards *Bacillus cereus* CECT 148, compounds **3b**, **5d**, **5e**, **7a**, **12b**, **13a**, **15a**, **15b** and **21a** exhibited the lowest inhibitory activity towards *Bacillus subtilis* CECT 498. Compounds **5d**, **7c**, **10**, **13a**, **17a**, **19b** and **21a** showed lower inhibitory activity against *C. albicans* CECT 1394 compared with the standard itself. The rest of compounds showed moderate inhibitory activity.

It was also observed that while compound **13b** is totally active against tested Gram-positive bacteria and fungi, it is inactive against Gram-negative bacteria used. Compound **5d** is totally inactive towards all tested bacteria and fungi isolates.

Comparing compounds **13a** and **13b** indicated that **13b** (X=CONHNHPh) showed higher inhibitory effect against Gram-positive bacteria and fungi used than **13a** (X=CONHNH₂). Similarly for compounds **15a** and **15b** it is obvious that compound **15a** (Y=CONHPh) showed higher inhibitory activity than **15b** (Y=CONH[C₆H₄(4-Cl)]).

On the other hand, compound **17a** (X=CN) showed high inhibitory effect towards all tested bacteria than **17b**

(X=CO₂Et). Also, compound **19a** (X=O) indicated higher inhibitory activity than **19b** (X=S).

Conclusion

We have reported a convenient synthesis of a variety of bioactive dyes (**3a-e**) from 3-cyano-2-diazo-4,5,6,7-tetrahydrobenzo[b]thiophene (**1**) which coupled with active methylene reagents (**2a-e**). The reactivity of bioactive dyes (**3a-e**) towards different chemical reagents were studied. Most of the synthesized systems were found to be promising antibacterial agents and hence deserve further pharmacological investigation. Currently, we are investigating the potential antitumor activity of the synthesized systems and related derivatives. The results of these investigation will be published in due time.

References

- Puterová, Z., Krutoíková, A. and Végh, D., *Arkivoc*, **2010** (i), 209.
- Balamurugan, K., Perumal, S., Reddy, A. S. K., Yogeewari, P., Sriram, D., *Tetrahedron Lett.*, **2009**, *50*, 6191.
- Fakhr, I. M. I., Radwan, M. A. A., El-Batran, S., Omar, M. E., El-Salam, A. and El-Shenawy, S. M., *Eur. J. Med. Chem.*, **2009**, *44*, 1718.
- Isloor, A. M., Kalluraya, B. and Pai, K. S., *Eur. J. Med. Chem.*, **2010**, *45*, 825.
- Amr, A. E. G. E., Sherif, M. H., Assy, M. G., Al-Omar, M. A. and Raga, I., *Eur. J. Med. Chem.*, **2010**, *45*, 5935.
- Gütschow, M., Kuerschner, L., Neumann, U., Pietsch, M., Löser, R., Koglin, N. and Eger, K., *J. Med. Chem.*, **1999**, *42*, 5437.
- Pinkerton, A. B., Lee, T. T., Hoffman, T. Z., Wang, Y., Kahraman, M., Cook, T. G., Severance, D., Gahman, T. C., Noble, S. A., Shiau, A. K. and Davis, R. I., *Bioorg. Med. Chem. Lett.*, **2007**, *17*, 3562.
- Romagnoli, R., Baraldi, P. G., Pavani, M. G., Tabrizi, M. A., Preti, D., Fruttarolo, F., Piccagli, L., Jung, M. K., Hamel, E., Borgatti, M. and Gambari, R., *J. Med. Chem.*, **2006**, *49* (13), 3906.
- Ravindranathan, K. P., Mandiyan, V., Ekkati, A. R., Bae, J. H., Schlessinger, J. and Jorgensen, W. L., *J. Med. Chem.*, **2010**, *53*, 1662.
- Aurelio, L., Valant, C., Figler, H., Flynn, B. L., Linden, J., Sexton, P. M., Christopoulos, A. and Scammells, P. J., *Bioorg. Med. Chem.*, **2009**, *17* (20), 7353.
- Mendonça, F. J. B. Jr., Lima-Neto, R. G., Oliveira, T. B., Lima, M. C. A., Pitta, I. R., Galdino, S. L., Cruz, R. M. D., Araújo, R. S. A. and Neves, R. P., *Lat. Am. J. Pharm.*, **2011**, *30*, 1492.
- Abu-Hashem, A. A., El-Shehry, M. F. and Badria, F. A., *Acta Pharm.*, **2010**, *60*, 311.
- Starčević, K., Karminski-Zamola, G., Piantanida, I.; Zinić, M., Šuman, L. and Kralj, M., *J. Am. Chem. Soc.*, **2005**, *127*, 1074.
- Pillai, A. D., Rathod, P. D., Xavier, F.P., Vasu, K.K., Padh, H. and Sudarsanam, V., *Bioorg. Med. Chem.*, **2004**, *12*, 4667.
- Pinto, I.L., Jarvest, R.L. and serafinowska, H.T., *Tetrahedron Lett.*, **2000**, *41*, 1597.
- Baraldi, P. G., Pavani, M. G., Shryock, J. C., Moorman, A. R., Iannotta, V., Borea, P. A. and Romagnoli, R., *Eur. J. Med. Chem.*, **2004**, *39*, 855.
- Shams, H. Z., Elkholy, Y. M., Azzam, R. A. and Mohareb, R. M., *Phosph. Sulf. Silicon.*, **1999**, *155*, 215.

- ¹⁸Shams, H. Z., Mohareb, R. M., Helal, M. H. and Mahmoud, A. E., *Phosph. Sulf. Silicon.*, **2007**, *182*, 237.
- ¹⁹Sherif, S. M., Mohareb, R. M., Shams, H. Z. and Gaber, H. M., *J. Chem. Res.*, **1995**, (S), 434; (M) 2658.
- ²⁰Hoda Z. S., Rafat M. M., Maher H. H. and Amira E. M., *Molecules*, **2011**, *16*, 52.
- ²¹Hoda Z. S., Rafat M. M., Maher H. H. and Amira E. M., *Molecules*, **2011**, *16*, 6271.
- ²²Gewald, K. and Schindler, R., *J. Prakt. Chem.*, **1990**, *332*, 223.
- ²³Deeb, A. El-Mariah, F. and Hosny, M., *Bioorg. Med. Chem.*, **2004**, *14* (19), 5013.
- ²⁴Butnariu, R. M. and Mangalagiu, I. I., *Bioorg. Med. Chem.*, **2009**, *17* (7), 2823.
- ²⁵Bahashwan, S. A., Al-Harbi, N. O., Fayed, A. A., Amr, A. E., Shadid, K. A., Alalawi, A. M. and Bassati, I. M. S., *Int. J. Biol. Macromol.*, **2012**, *51*, 7.
- ²⁶Kakanejadifard, A., Azarbani, F., Zabardasti, A. Kakanejadifard, S., Ghasemian, M., Esna-ashari, F., Omid, S., Shirali, S. and Rafieefar, M., *Dyes Pigment.*, **2013**, *97*, 215.
- ²⁷Hawkey, P. M., Lewis, D. A., *medical bacteriology—a practical approach*, Oxford University Press: UK, **1994**, pp 181–194.
- ²⁸Rameshkumar, N., Ashokkumar, M., Subramanian, E. H., Ilavarasan, R. and Sridhar, S. K., *Eur. J. Med. Chem.*, **2003**, *38*, 1001.

Received: 26.03.2013.

Accepted: 16.04.2013.



MAGNETIC FIELD INDUCED ENHANCED ADSORPTION EFFICIENCY OF IRON OXIDE NANOPARTICLES BASED MAGNETIC FERROFLUID: A PRELIMINARY INVESTIGATION

Uzma Nadeem^[a]

Keywords: Magnetic field; Ferrofluid; Maghemite; Nanoparticle; Adsorption; Wastewater; Zinc removal

Solid state synthesis approach was used to prepare magnetic ferrofluid loaded with maghemite nanoparticles. This magnetic material was then used to study adsorptive removal of zinc ions in presence of applied magnetic field. Studies revealed that application of magnetic field results in remarkably increased adsorption efficiency of these ferrofluids.

Corresponding Authors

Tel.: (+91).(011).(9711870215)

E-Mail: uzmanadeem3@gmail.com

[a] Chemistry Department, University of Delhi, Delhi, 110007, India.

Introduction

Magnetic nanoparticles with a proper surface coating acts as a glue to keep the magnetic core together. These magnetic nanoparticles can be dispersed into suitable solvents, forming homogeneous suspensions called ferrofluids.¹ Although a variety of examples exist for the use of bare magnetic particles for species extraction in effluent processing and metal ion removal, other recent studies have demonstrated that nanomaterials usually enhance removal of toxic metals from wastewater.^{2,3}

In present work, monocrystalline iron oxide nanoparticles based ferrofluid (maghemite, synthesized by the method described elsewhere⁴) was used as possible adsorbent for the removal of zinc metal. In order to study the influence of magnetic field environment, the work has been done in absence and presence of magnetic field. Contact time and adsorption isotherms in presence of magnetic field have also been discussed.

Experimental

Following reagents were used in appropriate proportions: FeCl₃(Anhydrous, Loba), FeSO₄.7H₂O (Extrapure AR, Merck), KCl, KOH (both Merck) etc.

Synthesis of maghemite nanoparticles was done by mixing powders of 0.81 g FeCl₃ (0.005 M), 0.70 g of FeSO₄.7H₂O (0.0025 M) and 3.9 g of KCl in a mortar at room temperature for 30 minutes followed by addition of 1.12 g (0.02 M) KOH powder and further grinding for another 30 minutes at room temperature. Finally, a dark brown transparent colloid was obtained with a loading of γ -Fe₂O₃ nanoparticles. The pH value of the colloid was between 4 and 5. To obtain a powder sample the colloid was centrifuged, dried at 50 °C for 6 h, and then cooled down to room temperature.

Wastewater containing zinc ions was collected from IFFCO, Phulpur, Allahabad. Batch adsorption studies were carried out taking a certain amount of maghemite and 50 mL solution of zinc ion and observations were recorded in the presence (vertical field of ~1.0 tesla applied with the help of 1"×1"×3" bar magnets) and absence of magnetic field. A mechanical shaker operating at 120 rpm was used for agitation. Metal concentration was determined by Atomic Absorption Spectrophotometer (AAS, ECIL - 4141) using the standard method.

The removal efficiency ϕ was calculated by the following equation:

$$\phi = \frac{(A - B)}{A} 100 \quad (1)$$

where, A and B are the initial and final metal ion concentrations (mg L⁻¹) respectively.

Results and discussion

Adsorption of heavy metals from aqueous solutions depends on the properties of adsorbent and transfer of molecules, ions of adsorbate from the solution to the solid phase. Adsorption efficiency of heavy metals is strongly sensitive to pH of the solution. It has also been reported that as the solution pH increases, sorption also increases.⁵ The adsorption efficiency of maghemite nanoparticles for zinc ions at different pH (pH=2-7) in the presence of magnetic field and without magnetic field is shown in Figure 1, which suggests that the maghemite possessed maximum sorption efficiency for the zinc ions at pH value 3 in both the cases. In contrast to this, it has been found that the adsorption efficiency of maghemite for zinc ions was 97.10 % in the presence of magnetic field but it was 85.34 %, without applying magnetic field.

Kinetic study revealed that maximum adsorption efficiency/metal removal efficiency for zinc was achieved generally in the first 60 minutes of contact. Metal removal was rapid during this period, after that, it reaches equilibrium.

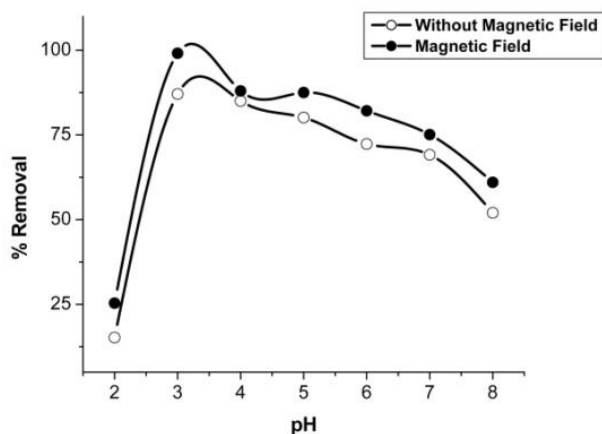


Figure 1. Effect of pH on Zn(II) removal using maghemite ferrofluid in presence and absence of magnetic field.

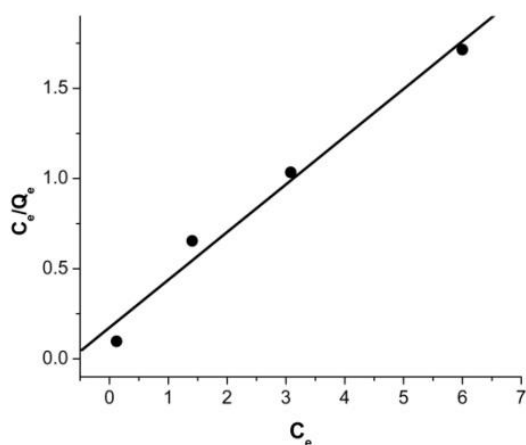


Figure 2. The linearized Langmuir adsorption plot for Zn(II) on maghemite nanoparticles in presence of magnetic field at 25 °C

Data in presence of magnetic field was also fitted to the classical Freundlich and Langmuir isotherm equations. The linearized forms of isotherm equations used are (see supporting information for more detail):

$$\log Q_e = \log K + \frac{1}{n} \log C_e \quad (2)$$

(Freundlich equation)

Plot of $\log Q_e$ versus $\log C_e$ gives a straight line of slope $1/n$ and intercept $\log K$. The correlation coefficient (R^2) was found to be 0.9872.

$$\frac{C_e}{Q_e} = \frac{1}{Q_{\max} b} + \frac{C_e}{Q_{\max}} \quad (3)$$

(Langmuir Equation)

Plot of the specific sorption C_e/Q_e against equilibrium concentration C_e , as shown in Figure 2, gave the linear isotherm parameters Q_{\max} and b . The correlation coefficient (R^2) in this case was found to be 0.9799.

An essential characteristic of the Langmuir isotherm can be expressed in terms of a dimensionless constant, separation factor or equilibrium parameter, R_L . The R_L values between 0 and 1 indicate favourable adsorption.⁶ In the present study the R_L were 0.1159, 0.0615, 0.0419, 0.0317 and 0.0255, for the initial concentrations of zinc ions from 5-25 mg L⁻¹ indicating that the adsorption of zinc ions on maghemite nanoparticles was favourable.

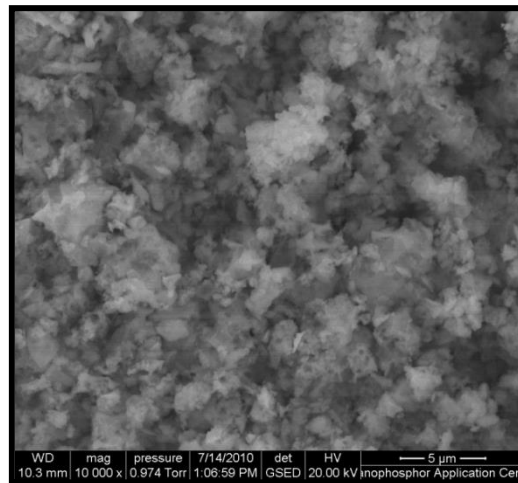


Figure 3. SEM image of maghemite nanoparticles

Scanning electron microscopy (SEM) was used for analysis of the samples morphology. SEM image of maghemite nanoparticles (Fig. 3) indicates the presence of granular structure of various sizes for these nanoparticles.

Conclusion

In present work, the adsorption of zinc from industrial wastewater by magnetic nanoparticles, i.e., maghemite loaded ferrofluid, was carried out in the presence of magnetic field. Equilibrium was attained within 60 minutes of contact time between maghemite and zinc sample. It was observed that maximum removal of zinc from wastewater occurred at pH 3. The experimental results were examined using Freundlich and Langmuir isotherms over the studied concentration range.

Acknowledgements

The authors are thankful for the financial assistance received from the University Grants Commission (UGC).

References

- ¹Gupta, A. K. ; Gupta, M.; *Biomaterials*, **2005**, 26, 3995-4021.
- ²Hristovski, K. D. ; Westerhoff, P. K. ; Crittenden, J. C.; Olson, L. W.; *Environ. Sci. Technol.*, **2008**, 42, 3786-3790.
- ³Filip, J.; Zboril, R.; Schneeweiss, O.; Zeman, Z.; Cernik, M.; Kvapil, P.; Otyepka, M.; *Environ. Sci. Technol.*, **2007**, 41, 4367-4374.
- ⁴Lu, J. ; Yang, S. ; Ng, K. M. ; Su, C.H. ; Yen, C.S. ; Wu Y.N. ; Sheih, D.B. ; *Nanotechnology*, **2006**, 17, 5812-20.
- ⁵Yin P. H. ; Yu, Q. M. ; Ling, Z.; *Water Res.*, **1999**, 33, 1960-1963.
- ⁶Ahalya, N.; Kanamadi, R. D.; Ramachandra, T. V. ; *Indian J. Chem. Technol.*, **2006**, 13, 122-127.

Received: 31.03.2013.

Accepted: 18.04.2013.



SYNTHESIS AND CHARACTERIZATION OF POLYIMIDES BASED ON A FLEXIBLE DIAMINE

M. Saeed Butt^{[a]*}, Zareen Akhter^[a] and M. Zafar-uz-Zaman^[b]

Keywords: Polyimides, ether diamines, 1,4-phenylenedi(oxy-4,4'-aniline), solubility, thermal stability

The diamine 1,4-phenylenedi(oxy-4,4'-aniline) was prepared via the nucleophilic substitution reaction and polymerized with different dianhydrides either by a one step solution polymerization reaction or a two steps procedure. These polymers had inherent viscosities ranging from 0.64-0.83 dL g⁻¹. Few of the polymers were soluble in most of the organic solvents such as DMSO, DMF, DMAc, NMP and m-cresol even at room temperature and some were soluble on heating. The degradation temperature of the resultant polymers falls in the ranges from 300-450 °C in nitrogen (with only 10% weight loss). The specific heat capacity at 200 °C ranges -4.0322-2.4059 J g⁻¹ K⁻¹. The maximum degradation temperature ranges from 550-600 °C. T_g values of the polyimides were found from 207 to 228 °C. The activation energy and enthalpy of the polyimides were found in the range of 36.6-94.5 and 34.8-92.5 kJ mole⁻¹ and the moisture absorption from 0.24-0.75%.

Corresponding Authors*

Fax: 00925190133154

Tel: 00925190133271

E-Mail: Saeed2_butt@yahoo.com

[a] Department of Chemistry, Quaid-i-Azam University, Islamabad-45320, Pakistan

[b] National Engineering and Scientific Commission P.O.Box 2801 Islamabad Pakistan

Introduction

Aromatic polyimides have excellent reputation as high performance materials based on their excellent thermal stability, chemical resistance and mechanical properties. Because of above mentioned properties polyimides can be used in a wide variety of applications such as polymer matrices for high temperature advanced composites, membranes for the low temperature energy separation of industrial gases, interlayer dielectrics, high temperature adhesive and coatings.¹⁻⁴ Despite their widespread use, most of them have high melting or softening temperatures and limited solubility in most of the organic solvents because of their rigid backbones and strong intermolecular interactions which may restrict their use in some fields. For such difficulties to be overcome, polymer structure modifications become necessary. Considerable research efforts have been done in designing and synthesizing new dianhydrides⁵ and diamines⁶⁻¹¹ thus producing a great variety of soluble and processable polyimides for various purposes. Since 1960, essentially the beginning of the search for high temperature polymers, more attention was focused on the polyimides than any other high performance/high temperature polymers. This is primarily due to the availability of the polyimide monomers (particularly aromatic diamines and dianhydrides), the ease of polymer synthesis, and their unique combination of physical and mechanical properties. However, most fully aromatic polyimides are insoluble in any organic solvent, and they have very high glass transition temperatures, often higher than their decomposition temperatures, which greatly limits their usefulness for many applications. Therefore, much work has been done to

improve the processability of aromatic polyimides while maintaining their excellent level of thermal and mechanical properties.^{12,13} To meet these aims, by balancing processability and performance, a number of approaches for structural modifications have been pursued such as incorporation of additional ether, ester, urethane, or amide linkages onto the polymer backbone.¹⁴⁻¹⁷ Incorporation of aryl ether unit is particularly successful method for improving solubility with slight reduction in thermal properties.^{18,19} In the present study the diamine 1,4-phenylenedi(oxy-4,4'-aniline) was synthesized and used to prepare a series of polyimides using various dianhydrides. Due to the presence of flexible moiety in the polyimide backbone, a decrease in the rigidity of the polymer chain would be expected which could improve the solubility of the polymers.

Experimental

Materials

Hydroquinone, p-fluoronitrobenzene, potassium carbonate, 3,3',4,4'-benzophenonetetracarboxylic acid dianhydride (BP), 4,4'-(hexafluoroisopropylidene)diphthalic anhydride (HF), 3,4,9,10-perylenetetracarboxylic acid dianhydride (PD) and pyromellitic dianhydrides (PMDA) of analytical grade from Aldrich were used as received. All the other reagents and solvents were of analytical grade and used without further purification.

Measurements

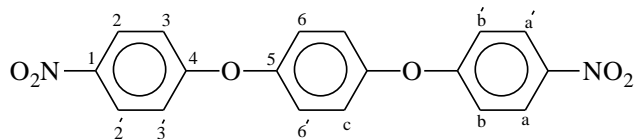
¹H and ¹³C NMR spectra were obtained on instrument Jeol 270 spectrophotometer in DMSO using tetramethylsilane as an internal reference. Infrared measurements (KBr pellets) were recorded in the range of 400-4000 cm⁻¹ on Bio-Rad Excalibur FTIR Model FTS 3000 MX. Melting points were recorded on Electrothermal IA 9000 series digital melting

point apparatus. Inherent viscosities were obtained using Gilmount falling ball viscometer at 0.2 g dL^{-1} in DMSO and H_2SO_4 . Thermal and DSC analysis were carried out using Perkin Elmer TGA-7 and DSC 404C Netzsch under nitrogen atmosphere. Elemental analysis was carried out using Perkin Elmer CHNS/O 2400. Wide-angle diffractograms were obtained using 3040/60 X'Pert PRO diffractometer. Moisture absorption was determined by weighing the changes of the dried pellets before and after immersion in distilled water at $25 \text{ }^\circ\text{C}$ for 24 hours. Activation energy, entropy and enthalpy were calculated using Horowitz and Metzger method.²⁰

Monomer Synthesis

1,4-Phenylenedi(oxy-4,4'-nitrobenzene) PONB (1)

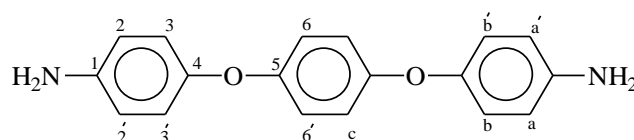
A mixture of 2.0g (0.018 mol) of hydroquinone, 5.0g (0.036 mol) of anhydrous K_2CO_3 and 3.81 ml (0.036 mol) of 4-fluoronitrobenzene in a two neck round bottom flask having 70 ml of DMAc was heated at $100 \text{ }^\circ\text{C}$ for 20 h under nitrogen atmosphere. The colour of the solution changes from yellow to dark brown as the reaction proceeded. After cooling to room temperature, the reaction mixture was poured in 800 ml of water to form yellow solid which was washed thoroughly with water and then separated by filtration. The crude product was recrystallized from ethanol. Yield 87 %, m.p. $238 \text{ }^\circ\text{C}$. Elemental analysis calculated for $\text{C}_{18}\text{H}_{12}\text{N}_2\text{O}_6$ (352): C = 61.36%, H = 3.409%, N = 7.95% and found C = 61.02%, H = 3.69%, N = 7.45%. FTIR (KBr pellet) in cm^{-1} : 1589 (aromatic C=C), 1506 and 1340 (NO_2), 1235 (C–O–C). $^1\text{H-NMR}$ (DMSO- d_6) in δ (ppm) and $J(\text{Hz})$: 7.22 (4H, d, $J_{ab}=J_{a'b'}=9.30$), 7.3(4H, s), 8.31 (4H, d, $J_{ba}=J_{b'a'}=9.30$). $^{13}\text{C-NMR}$ (DMSO- d_6) in δ (ppm): 116.093 (2C, C5), 125.82 (4C, C3, 3'), 127.31 (4C, C6, 6'), 145.469 (4C, C2, 2'), 149.625 (2C, C4), 163.24 (2C, C1). Yield 87 %, m.p. $238 \text{ }^\circ\text{C}$. Crystal data: almost colorless crystal grown during slow crystallization in ethanol/water (4:1) v/v, $0.38 \text{ mm} \times 0.11 \text{ mm} \times 0.10 \text{ mm}$, triclinic, P1 with $a=7.2861(6)$, $b=10.1381(9)$, $c=12.0838(11) \text{ \AA}$, $\alpha=91.973(7)$, $\beta=106.497(7)$, $\gamma=110.152(6)^\circ$ where $D_x=1.472 \text{ Mg m}^3$ for $Z=2$ and volume (V) = $794.74 (12) \text{ \AA}^3$.²²



1,4-Phenylenedi(oxy-4,4'-aniline) POA (2)

A 250 ml two neck flask was charged with 1.0g (2.84 mmol) of (1), 10 ml of hydrazine monohydrate, 80 ml of ethanol and 0.06g of 5% palladium on carbon (Pd–C). The mixture was refluxed for 16 hours and then filtered to remove Pd–C and the solvent was evaporated and the crude solid was recrystallized from ethanol to yield 85% of the theoretically calculated yield, m.p. $182 \text{ }^\circ\text{C}$. Elemental analysis calculated for $\text{C}_{18}\text{H}_{16}\text{N}_2\text{O}_6$ (MW=292): C = 73.97%, H = 5.47%, N = 9.58 and found C = 73.75%, H = 5.12%, N = 9.79%. FTIR (KBr pellet) in cm^{-1} : 3400 and 3312 (NH_2), 1639 (N–H bending), 1213 (C–O–C), 1495 (NH

deformation). $^1\text{H NMR}$ (DMSO- d_6) in δ (ppm) and J (Hz): 5.08 (4H, s), 6.51 (4H, d, $J_{ab}=J_{a'b'}=8.27$), 6.82 (4H, d, $J_{ba}=J_{b'a'}=8.28$), 6.91 (4H, s). $^{13}\text{C NMR}$ (DMSO- d_6) in δ (ppm): 115.885 (4C, C3, 3'), 118.856 (4C, C6, 6'), 126.328 (4C, C2, 2'), 145.49 (2C, C1) 147.55 (2C, C5), 156.58 (2C, C4). Yield 85%, m.p. 182°C . Crystal data: almost colorless crystal grown during slow crystallization in ethanol/water (4:1) v/v, $0.42\text{mm} \times 0.40\text{mm} \times 0.20 \text{ mm}$, monoclinic, $\text{P2}_1/\text{c}$ with $a=6.9579(9)$, $b=22.664(3)$, $c=5.1202(7) \text{ \AA}$, $\beta=111.287 (2)^\circ$ where $D_x=1.290 \text{ Mg/m}^3$ for $Z=2$ and volume (V) = $752.34 (7) \text{ \AA}^3$.²³



Polymer Synthesis

To a stirred solution of POA (0.36 g, 1.238 mmol) in 8 ml of DMAc was added 3,3',4,4'-benzophenonetetracarboxylic acid dianhydride (BP) (0.4 g, 1.238 mmol). The mixture was stirred at room temperature for 2 hours under argon atmosphere to form a polyamic acid (precursor). The film was casted onto a glass plate by heating polyamic acid solution for 18 hours at $80 \text{ }^\circ\text{C}$, 2 hours at $150 \text{ }^\circ\text{C}$, 2 hours at $200 \text{ }^\circ\text{C}$, 2 hours at $250 \text{ }^\circ\text{C}$ and 2 hours at $280 \text{ }^\circ\text{C}$ which converted polyamic acid into polyimide films. The same procedure was adopted for the polymerization of POA with 4,4'-hexafluoroisopropylidene diphthalic anhydride (HF) and pyromellitic dianhydride (PMDA) however, the polymerization with perylene dianhydride (PD) was carried out by following procedure. In a 250 ml two neck round bottom flask fitted with nitrogen inlet and outlet the diamine POA [(0.37g, 1.27 mmol), dianhydride (0.5g, 1.27 mmol)], m-cresol (20 ml) and isoquinoline (1 ml) were added. The mixture was heated to $180\text{--}200 \text{ }^\circ\text{C}$ under nitrogen for 6 hours and then cooled to room temperature. The resulting dark red solution was poured into 300 ml of acetone and the resulting solid was washed with (1 N) sodium hydroxide followed by water. After drying at $150 \text{ }^\circ\text{C}$ overnight, polyimide was obtained as dark red solid. The inherent viscosities of the polymers were subsequently determined at concentration 0.2 g dL^{-1} at $25 \text{ }^\circ\text{C}$ in DMSO and H_2SO_4 .

Results and Discussion

Monomer Synthesis

The diamine POA was synthesized according to the well developed method (Scheme-1) The first step is Williamsons etherification²¹ reaction of 1,4-dihydroxybenzene and p-fluoronitrobenzene in the presence of potassium carbonate in DMAc, followed by stirring of the mixture at $100 \text{ }^\circ\text{C}$ for 20 h. The diamine POA was readily obtained in good yield by the catalytic reduction of the intermediate dinitro compound with hydrazine hydrate and Pd–C catalyst in refluxing ethanol. The schematic diagram of diamine

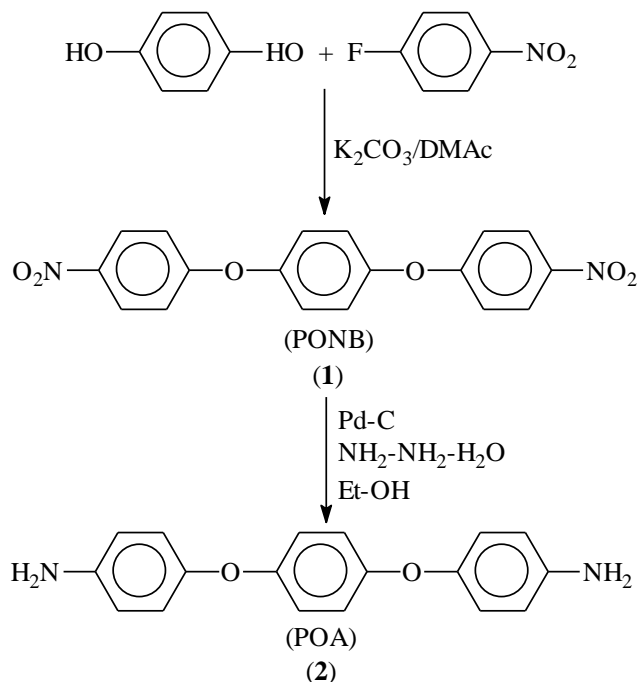


Figure 1. Schematic diagram for the synthesis of 1,4-phenylenedi(oxy-4,4'-aniline)

synthesis is shown in the Fig. 1. Elemental, FTIR and NMR analysis were carried out to confirm the structures of intermediate and diamine. The nitro group of intermediate compound gave two absorption band at 1506 and 1340 cm^{-1} (NO_2 a symmetric and symmetric stretching). The PONB crystallizes with two half-molecules in the asymmetric unit. All molecules lie on a centre of inversion. The dihedral angles between the central and terminal benzene rings are $74.75(4)$ and $85.25(5)^\circ$ for the two molecules in the asymmetric unit.²² After reduction the characteristic absorption of the nitro compound disappeared, and the amino group showed a pair of N–H stretching bands in the region of $3300\text{--}3500\text{ cm}^{-1}$. The diamine POA is located on a crystallographic inversion center and the terminal aminophenoxy rings are almost perpendicular to the central benzene ring with a dihedral angle of $85.40(4)^\circ$. The molecular conformation is stabilized by N–H...O and N–H...N intermolecular hydrogen-bonding interactions.²³ All the spectroscopic data obtained was in good agreement with the expected structure.

Polymer Synthesis

The diamine monomers were polymerized with four different aromatic dianhydrides namely 3,3',4,4'-benzophenone tetracarboxylic acid dianhydride (BP), 4,4'-hexafluoroisopropylene)diphthalic anhydride (HF), 3,4,9,10-perylene tetracarboxylic acid dianhydride (PD) and pyromellitic dianhydride (PMDA) as shown in Fig. 2. The polyimides of BP, HF and PMDA were prepared by following a conventional two step procedure which includes the ring-opening polyaddition at room temperature to poly(amic acid), followed by sequential heating to $280\text{ }^\circ\text{C}$. The polyimide of perylene dianhydride was prepared by a different method. The polyamic acid precursors were prepared by the addition of dianhydride to the diamine solution gradually. The molecular weights were high enough

to cast tough and transparent polyimide films. A rapid temperature elevation resulted in cracked or brittle films. The inherent viscosities determined for some polymer films give values in the range of $0.64\text{--}0.83\text{ dL g}^{-1}$ at concentration of 0.2 g dL^{-1} at $25\text{ }^\circ\text{C}$ which indicates high molecular weights of the polymers as shown in Table-2. The polyimides obtained were subjected to solubility and thermal studies. Some of the thermally cured polyimides exhibited excellent solubility in polar solvents such as DMSO, DMF and DMAc. The formation of polyimides was confirmed by IR and elemental analysis (Table-1). All the polyimides exhibited the characteristic imide group absorption around 1780 and 1725 cm^{-1} (typical of imide carbonyl (symmetric and asymmetric stretching), 1380 cm^{-1} (C–N stretch) and 1100 and 730 cm^{-1} (imide ring deformation). The disappearance of the amide and carboxyl bands indicated a virtually complete conversion of the poly(amic acid) precursor into polyimides. The results of the elemental analysis of all the synthesized polyimides are listed in Table 1. The values found were in good agreement with the calculated one.

	BP=3,3',4,4'-Benzophenone-tetracarboxylic acid dianhydride
	HF=4,4'-(Hexafluoroisopropylidene)diphthalic anhydride
	PD= 3,4,9,10-Perylenetetracarboxylic acid dianhydride
	PMDA=Pyromellitic dianhydride

Figure 2. Four different acid dianhydrides used for polymerization.

Organo Solubility and Moisture Absorption.

The inherent viscosities determined for polymer films except POA-BP gave values in the range of $0.64\text{--}0.83\text{ dLg}^{-1}$, reflecting high molecular weight of the polymers. The solubility of the polyimides was determined qualitatively and the results are listed in Table 2. The solvents like DMSO, DMF, DMAc, m-cresol and THF were tested. Some polymers are found soluble on heating while others are slightly soluble and some are insoluble. The organo solubility behaviour of the polymers is generally depended on their chain packing ability and intermolecular interactions that was affected by the rigidity, symmetry and the regularity of the backbone. From the Table 2 it was noticed that the introduction of fluorinated dianhydride component (HF) is especially effective for the high solubility, irrespective of the diamine component. This increase in solubility might be attributed to the molecular asymmetry and the presence of bulky trifluoromethyl groups,

Table 1. Elemental Analysis of the polymers

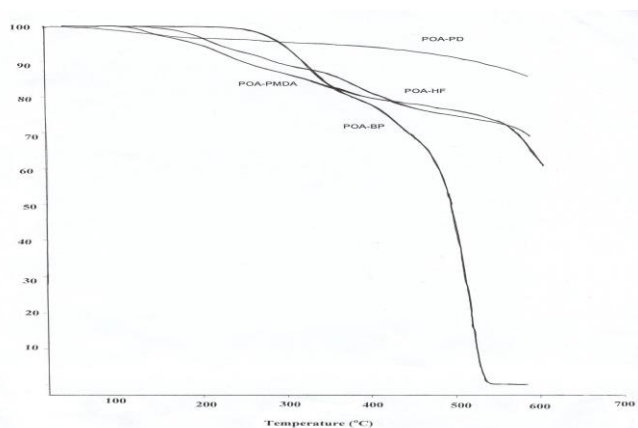
Polyimide	Formula of the Repeat Unit (Formula Wt.)	C%		H%		N%	
		Calc.(Found)	Calc.(Found)	Calc. (Found)	Calc. (Found)		
POA-BP	C ₃₅ H ₁₈ N ₂ O ₇ (578)	72.66 (71.95)	3.11 (3.20)	4.84 (4.48)			
POA-HF	C ₃₇ H ₁₈ N ₂ O ₆ F ₆ (700)	63.42 (63.14)	2.57 (2.61)	4.00 (3.79)			
POA-PD	C ₄₂ H ₂₀ N ₂ O ₆ (648)	77.77 (77.01)	3.08 (3.29)	4.32 (4.10)			
POA-PMDA	C ₂₈ H ₁₄ N ₂ O ₆ (474)	70.88 (71.83)	2.95 (3.10)	5.90 (6.58)			

Table 2. Inherent Viscosity, solubility and moisture absorption of polymers

Polymer	DMSO	DMF	DMAc	m-cresol	THF	H ₂ SO ₄	η_{inn} , dL g ⁻¹	Moisture absorption ^c , %
POA-BP	–	–	–	–	–	+	–	0.61
POA-HF	+++	+++	+++	+++	–	+++	0.83 ^a	0.24
POA-PD	+	+	+	+	–	++	0.64 ^b	0.75
POA-PMDA	–	–	–	–	–	++	0.71 ^b	0.51

+++ = soluble at room temperature, ++ = soluble on heating, + = slightly soluble on heating, – = insoluble; a) measured from 0.2 g dL⁻¹ at 25°C in DMSO; b) measured from 0.2 g dL⁻¹ at 25 °C in H₂SO₄; c) moisture absorption was measured at 25±1 °C for 24 hours

which increase the disorder in the chains and hinders the dense chain stacking, thereby reducing the interchain interactions and so enhancing solubility. The poor solubility of the remaining polyimides might be attributed to crosslinking within polymer chain or the tight chain packing and aggregation during imidization at elevated temperature. The moisture absorption of the synthesized polyimides was found in the range of 0.24-0.61 %. The fluorinated polyimide was found to absorb lowest absorption as compared to other polyimides because the trifluoromethyl group possesses the amphiprotic feature, which inhibits the absorption of moisture molecules on the surface of the fluorinated polyimides.²⁴

**Figure 3.** TGA curves of the synthesized polyimides

X-ray Diffraction Data

All the polyimides were characterized with WAXD studies. The WAXD pattern is shown in Figure 4. All polyimides except POA-HF, displayed a semicrystalline pattern where as POA-HF displayed nearly completely amorphous pattern because of the bulky CF₃ group which disrupted the symmetry or dense chain packing leading to highly ordered regions. The bulky CF₃ also induces looser chain packing and reveals a large decrease in crystallinity leading to highly ordered regions.²⁴

Thermal Properties

Thermal properties of the polyimides were investigated by the thermogravimetric analysis (TGA) and differential scanning calorimetry (DSC) at heating rate of 10 °C min⁻¹. Table 3 presents the thermal properties of the polyimides. The results of the TGA analysis showed no significant weight loss below 300 °C in nitrogen. The maximum degradation temperature (T_{max}) for most of the polymers lies between 550-600 °C.

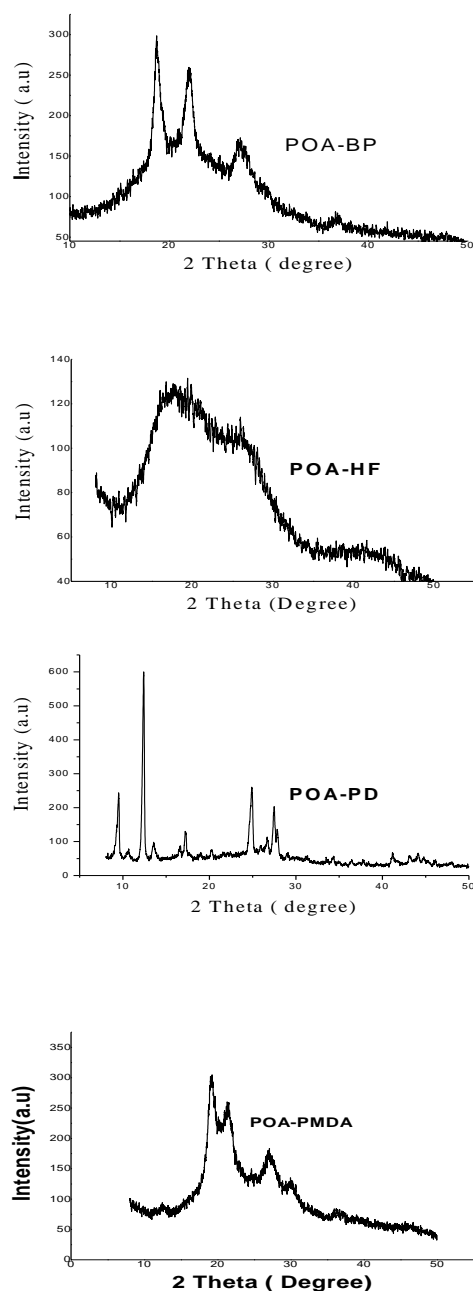
The thermal stability of the polymers was also evaluated in term of 10 % weight loss (T_{10}), maximum degradation temperature (T_{max}) and residual weight at 600 °C as listed in Table 3. It has been seen by comparing T_{10} of the polymers that the introduction of the diacid PD is especially effective to improve the thermal stability of the polyimides regardless of the diamine component. This increase in thermal stability is attributed to rigid and bulky PD unit which inhibit the rotation of bonds, resulting in an increase in chain stiffness while the polyimides having HF unit are less thermally stable than PD unit which is probably due to the different packing density of the polymer aggregation and the interaction of the polymer chain. The presence of bulky CF₃ group reduces the chain interactions and causes the poor packing of the polymer chain and lowers the thermal stability. This thermal behaviour is in agreement with the literature.²⁵

The thermal degradation kinetics for the polymers was calculated from TGA curves and the activation energy of the pyrolysis was obtained using the Horowitz and Metzger method which is an integral method for the determination of kinetic parameters. In this method, double logarithm of the reciprocal of the weight fraction of the reactant was plotted against the temperature difference and the kinetic parameters were calculated by some mathematical calculations using battery programme based on Horowitz and Metzger method. The thermal degradation of the polyimides in the absence of the oxygen was believed to involve the direct cleavage of the C-N bond. The specific heat capacity ranges from -4.0322 to 2.4059 J g⁻¹ K⁻¹ at

Table 3. Thermal behaviour of pPolymers in nitrogen flow.

Polymer	Specific heat capacity ^a at 200 °C, J g ⁻¹ K ⁻¹	Thermal Stability ^b		R ₆₀₀ (%) ^e	T _g (°C) ^f	Activation energy, kJ mol ⁻¹	Entropy, kJ mol ⁻¹ .K	Enthalpy kJ mol ⁻¹
		T ₁₀ (°C) ^c	T _{max} (°C) ^d					
POA-BP	2.4059	350	550	80.5	228	53.8	0.265	52.0
POA-HF	0.5162	300	580	66.0	225	48.8	0.213	40
POA-PD	-4.0322	450	600	85.6	-	94.5	0.672	92.5
POA-PMDA	2.3949	300	600	62.8	207	36.6	0.093	34.8

a) Measured from DSC under nitrogen at heating rate of 10 °C min⁻¹; b) Measured from TGA under nitrogen at heating rate of 10 °C min⁻¹; c) Temperature at 10% weight loss; d) Maximum degradation temperature obtained from differential curves; e) Residual weight at 600°C; f) T_g (glass transition temperature)

**Figure 4.** Wide-angle X-ray diffractograms of the prepared polymers

200 °C. T_g values of the polyimides ranged from 207 to 228 °C. The activation energy and enthalpy of the polyimides are in the range of 36.6-94.5²⁶ and 34.8-92.5 kJ mol⁻¹, respectively, and are comparable with the literature.

Conclusions

The diamine POA was successfully prepared in high purity and high yield and was polymerized with four different aromatic dianhydrides to obtain moderate to high molecular weight polyimides. Polyimides with 3,3',4,4'-benzophenone tetracarboxylic acid dianhydride, 4,4'-(hexafluoroisopropylidene) diphthalic anhydride and pyromellitic dianhydrides could be thermally converted into tough and flexible polyimide films. Few polyimides synthesized were soluble in most of the organic solvents such as DMSO, DMF, DMAc and m-cresol. The degradation for 10% weight loss ranges from 300-450°C. The maximum degradation temperature ranges from 550-600 °C and specific heat capacity -4.0322 to 2.2.4059 J g⁻¹ K⁻¹ at 200 °C. T_g values of the polyimides ranged from 207 to 257 °C. All polyimides show semicrystalline pattern except POA-HF which shows completely amorphous pattern. The moisture absorption of the polyimides is in the range of 0.24-0.75%. Activation energy and enthalpy of the polyimides is in the range of 36.6-94.5 kJ mol⁻¹ and 34.8-92.5 kJ mol⁻¹, respectively. These polyimides could be considered as processable high performance polymeric materials.

Acknowledgments

The authors are grateful to Department of Chemistry Quaid-I-Azam University Islamabad Pakistan and Institut für Anorganische Chemie, J.W.Goethe-Universität Frankfurt, Germany for providing laboratory and analytical facilities.

References

- ¹Kyung, H. C., Kyung, H. L., Jung, J. C., *J. Polym. Sci., Part A: Polym. Chem.*, **2001**, 39, 3818.
- ²Mittal, K.L., Ed: *Polyimides Synthesis, Characterization and Applications*, Plenum: New York, **1985**.
- ³Bessonov, M. I., Koton, M. M., Kudryatsev, V. V., Laisus, L. A., *Polyimides Thermally Stable Polymers, Consultants Bureau: New York*, **1987**.
- ⁴Abadie, M. J. M., Sillion, B., Eds., *Polyimides and Other High Temperature Polymers*, Elsevier, Amsterdam, **1991**.

- ⁵Li, W. M., Li, S. H., Zhang, S. B., *Macromolecules*, **2007**, *40*, 8205-8211.
- ⁶Jeong, K. U., Jo, Y. J., Yoon, T. H., *J. Polym. Sci. Part A. Polym. Chem.*, **2001**, *39*, 3335-47.
- ⁷Liu, J. G., Li, Z. X., Wu, J. T., Zhou, H.W., Wang, F. S., Yang, S. H., *J. Polym. Sci. Part A. Polym. Chem.*, **2002**, *40*, 1583-93.
- ⁸Reddy, D. S., Choy, C-H., Shu, C-F., Lee, G-H., *Polymer*, **2003**, *44*, 557-63.
- ⁹Hsiao, S-H., Huang, T-L., *J. Polym. Res.*, **2004**, *1*, 9.
- ¹⁰Hsiao, H-S., Lin, K-H., *J. Polym. Sci. Part A. Polym. Chem.*, **2005**, *43*, 331-41.
- ¹¹Liaw, D-J., Chang, F-C., Leung, M., Chou, M-H., Mullen, K., *Macromolecules*, **2005**, *38*, 4024-29.
- ¹²Jung, J. C., Park, S-B., *J. Polym. Sci. Part A. Polym. Chem.*, **1996**, *34*, 357-65.
- ¹³Sat, M., *Polyimides*, In *Handbook of Thermoplastics*; Olabisi O, Ed; Dekker: New York, **1997**.
- ¹⁴Kricheldorf, H. R., Ed. *Advances in Polymer Science: Progress in Polyimide Chemistry, Vols. I and II*; Springer-Verlag: Berlin/New York, **1998**.
- ¹⁵Ayala, A., Lozano, A. E., Abajo, J. D., De La Campa, J. G., *J. Polym. Sci., Part A: Polym. Chem.*, **1999**, *37*, 805-14.
- ¹⁶Yang, C. P., Hsiao, S. H., Yang, H. W., *Macromol. Chem. Phys.*, **2000**, *201*, 409-18.
- ¹⁷Ghosh, M. K., Mittal, K. L., *Polyimides: Fundamentals and Applications*; Marcel Dekker: New York, **1996**.
- ¹⁸Harris, F. W., Lanier, L. H., In: Harris, F. W., Seymour, R. B., Editors. *Structure-solubility-relationships in polyimides*. New York: Academic Press, **1977**, p. 183
- ¹⁹Eastmond, G. G., Paprotny, J., *Macromolecules*, **1996**, *29*, 1382-88.
- ²⁰Horowitz, H. H., Metzger, G., *Anal. Chem.*, **1963**, *35*, 1464-68.
- ²¹Hsiao, H. S., Yang, C. P., Chung, C. L., *J. Polym. Sci. Part A. Polym. Chem.*, **2003**, *41*, 2001-18.
- ²²Butt, M. S., Akhter, Z., Bolte, M., Humaira, M. S. *Acta Cryst. Sect. E.*, **2006**, *E62*, o3992-o3993.
- ²³Shemsi, M. A., Butt, M. S., Fettouhi, M., Humaira, M. S., Akhter, Z., *Acta Cryst. Sect. E.* **2008**, *E64*, o581
- ²⁴Hsiao, S. H., Yang, C. P., Yang, C. Y., *J. Polym. Sci., Part A: Polym. Chem.*, **1997**, *35*, 1487-97.
- ²⁵Butt, M. S., Akhter, Z., Zaman, M. Z., Munir, A., *Eur. Polym. J.*, **2005**, *41*, 1638-46.
- ²⁶Brekner, M-J., Feger, C., *J. Polym. Sci. Part A: Polym. Chem.* **1987**, *25*, 2479-2491.

Received: 14.03.2013.

Accepted: 19.04.2013.



SYNTHESIS OF NOVEL ANTIBACTERIAL AND ANTIFUNGAL α -AMINO ACIDS AND HETEROCYCLIC COMPOUNDS

Maher A. El-Hashash^[a], Sameh A. Rizk^{[a]*}

Keywords: (E)-4-aryl-4-oxo-2-butenic acid, furanones, thiadiazoles, pyridazinones, imidazolo[2,3-b]1,3,4-thiadiazoles, thiadiazolopyrimidines, bezoxazinones, fused quinoxalinyquinazolinones

Utility of (E)-4-(acetylamino)phenyl-4-oxo-2-butenic acid with new sulfur reagents e.g. 2-amino-5-aryl-thiadiazoles **2** to afford the corresponding adducts (**3**, **4**, **5**, **6**). Reaction of the latter compounds with different electrophilic and nucleophilic reagents affords some important heterocycle such as various furanones, thiadiazoles, pyridazinones, imidazolo[2,3-b]1,3,4-thiadiazoles, thiadiazolopyrimidines, bezoxazinones, fused quinoxalinyquinazolinones

*Corresponding Authors

*E-mail: Samehrizk2006@gmail.com

[a] Chemistry department, Science Faculty, Ain-Shams University

INTRODUCTION

Amino acids are the smallest units of proteins and are useful components in a variety of metabolic activities. There are numerous advantages of taking amino acids as dietary supplements, also provide many useful biological activities. In vitro data [1] about amino acids include muscle protein maintenance, potentiation of immune function, affecting neuronal activities in the brain, tissue repair acceleration, protecting liver from toxic agents, pain relief effect, lowering blood pressure, modulating cholesterol metabolism, stimulating insulin of growth hormone secretion and so on. It is important to be note that they are part of complex pathway and biological systems. Amino acids have proven to play a significant role in the synthesis of novel drug candidate with the use of non-proteinogenic and unnatural amino acids²⁻⁷. Over the last decade the synthesis of non-proteinogenic unnatural amino acids has received significant attention of organic chemists, who have tried to find out cost effective and less time consuming synthetic pathways. From this point of view the authors have made an attempt to investigate the reaction of 4-aryl-4-oxo-but-2-enoic acids with 2-amino-1,3,4-thiadiazole under aza-michael reaction conditions which produced adducts **3-6** as α -amino acid types with acetic anhydride at different condition and N_2H_4 to give the corresponding furanone, imidazolo[2,3-b]1,3,4-thiadiazole, 1,3,4-thiadiazolopyrimidine and pyridazinone derivatives, respectively with an aim to obtain some interesting heterocyclic compounds with non-mixing and mixing system. Hence, keeping these reports in view and continuation of our earlier search work⁸ for aza-Michael adducts.

EXPERIMENTS

All melting points are uncorrected. Elemental analyses were carried out in the Microanalytical Center, the center

publication for research, Cairo, Egypt. By Elementar Viro El Microanalysis IR spectra (KBr) were recorded on IR spectrometer ST-IR DOMEM Hartman Braun, Model: MBB 157, Canada and ¹H-NMR spectra recorded on a varian 300 MHz (Germany 1999) using TMS as internal standard. The mass spectra were recorded on Shimadzu GCMS-QP-1000 EX mass spectrometer at 70e.v. homogeneity of all compounds synthesized was checked by TLC.

Compounds 3-6

A solution of 4-(4-Acetylamino)phenyl-4-oxo-2-butenic acid (0.01 mol) and 5-aryl-2-amino-1,3,4-thiadiazole (0.016 mol) in 30 ml ethanol was refluxed for 3 h. The crude product was washed by petroleum ether (b.p 40- 60°C), and then crystallized from ethanol to give the following compounds.

4-(4-Acetylamino)phenyl-4-oxo-2-(5-phenyl-2-thiadiazolylamino)butanoic acid (**3**)

Yield 80%, Mp 160-162 °C. IR for CO for acid and ketone groups (1695 – 1665) cm^{-1} , ¹H NMR (DMSO-*d*₆) 2.5 (s, 3H, CH₃CO), 3.4 (2 dd, CH₂-C=O, J=15.2, J=7.7) (diastereotopic protons), 4.2 (dd, CH-COOH, methine proton), 6.7 (s, NH), 7.6-8.1 (m, 9H, ArH), 8.2 (s, 1H, COOH), 8.6 (s, 1H, C=O-NH). EIMS *m/z* 410 (M⁺). Anal. Calc. for (C₂₀H₁₈N₄SO₄): C 58.53, H 4.39; Found: C 58.50, H 4.40.

4-(4-Acetylamino)phenyl-4-oxo-2-(5-(4-chlorophenyl)-2-thiadiazolyl amino)butanoic acid (**4**)

Yield 75%. Mp. 174-174 °C. IR for CO for acid and ketone groups are at 1695–1630 cm^{-1} . ¹H NMR (DMSO-*d*₆) exhibits signals at 2.5 (s, 3H, CH₃CO), 3.4 (2 dd, CH₂-C=O, J=15.2, J=7.7) (diastereotopic protons), 4.2 (dd, CH-COOH, methine proton), 6.7 (s, NH), 7.6-8.1 (m, 8H, ArH), 8.2 (s, 1H, COOH), 8.6 (s, 1H, C=O-NH). *m/z* 358 (M⁺-(CO₂+CH₂=CO)). Anal. Calc. for (C₂₀H₁₇N₄SO₄ Cl): C 54.05, H 3.83; Found: C 54.00, H 3.80.

4-(4-Acetylamino-phenyl)-4-oxo-2-(5-styryl-2-thiadiazolyl amino)butanoic acid (5)

Yield 70%. Mp. 180-182 °C. IR: CO for acid and ketone groups are at 1694–1660 cm^{-1} . $^1\text{H-NMR}$ spectrum in DMSO- d_6 exhibits signals at 2.5 (s, 3H, CH_3CO), 3.4 (2 dd, $\text{CH}_2\text{C}=\text{O}$, $J=15.2$, $J=7.7$) (diastereotopic protons), 4.2 (dd, CH-COOH, methine proton), 6.7 (s, NH), 7.6-8.1 (m, 11H, ArH and olefinic protons), 9.5 (s, 1H, COOH), 10.2 (s, 1H, C=O-NH). m/z : 392 (M^+-CO_2). Anal.Calc. for ($\text{C}_{22}\text{H}_{20}\text{N}_4\text{SO}_4$): C 60.55, H 4.58; Found: C 60.50, H 4.60.

4-(4-Acetylamino-phenyl)-4-oxo-2-(5-phthalimido methyl-2-thiadiazolyl amino)butanoic acid(6)

Yield 35%. Mp. 150-152 °C. IR: CO for imide, acid and ketone groups are at 1770, 1690 and 1660 cm^{-1} . $^1\text{H-NMR}$ spectrum (DMSO- d_6) exhibits signals at 2.5 (s, 3H, CH_3CO), 3.4 (2 dd, $\text{CH}_2\text{-C}=\text{O}$, $J=15.2$, $J=7.7$) (diastereotopic protons), 4.2 (dd, CH-COOH, methine proton), 6.7 (s, NH), 7.6-8.1 (m, 8H, ArH), 8.2 (s, 1H, COOH), 8.6 (s, 1H, C=O-NH). m/z : 475 ($\text{M}^+-\text{H}_2\text{O}$). Anal.Calc. for ($\text{C}_{23}\text{H}_{19}\text{N}_5\text{SO}_6$): C 55.98, H 3.81; Found: C 55.90, H 3.80.

Compounds 7, 8

A mixture of **7** (3 g; 0.005 mol) and acetic anhydride (9.4 mL) was heated under reflux for 1 h upon water bath. The solid that separated on cooling was crystallized from pet.ether (80-100) to afford **7** and from ethanol to afford **8**.

2-(5-Acetylamino-phenyl-2-oxo-furan-3-yl)amino-5-phenyl-1,3,4-thiadiazole (7)

Yield 50%, m.p. 200-202 °C, M.wt= 391 ($\text{C}_{20}\text{H}_{17}\text{N}_4\text{O}_3\text{S}$). IR: ν_{NH} 3297-3100, ν_{CH} 3055-2890, the band at 1767 and 1693 cm^{-1} can be attributable to ν_{CO} lactonic and acetamido groups, respectively, and $^1\text{H-NMR}$ spectrum(DMSO- d_6) exhibits signals at δ 2,1 (s 3H, CH_3CO), 4 (dd, 1H, $-\text{CH}-\text{NH}$, $J=8.5$), 6.7 (bs, NH), 7.5-7.9 (m, 9H of Ar), 6.9 (d, 1H, CH furanone moiety, $J=8.5$), 12.7 (s, 1H, $-\text{C}=\text{O}-\text{NH}$) acidic protons are exchangeable in D_2O . Elem. Anal.: Calcd: C 61.5, H 4.3, N 14, S 8.3; Found C 61.4, H 4.2, N 13.8, S 8.2.

5-(4-Acetylamino-phenylmethyl)-2-Phthalimidomethyl-4-oxo-imidazo[2,1-b]-1,3,4-thiadiazole (8)

M.wt = 497 ($\text{C}_{21}\text{H}_{13}\text{N}_4\text{O}_4\text{SBr}$), Mp. 230-232 °C, yield 35%. calcd/found: C 50.89/51.00, H 2.64/2.22, N 11.30/11.62, Br 16.12/16.08, S 6.74/6.38. IR: $\nu_{\text{C}=\text{O}}$ are at 1772, 1720, 1691 and 1668 cm^{-1} . $^1\text{H-NMR}$ (DMSO- d_6) exhibits signals at 3.2 (2dd, $\text{CH}_2\text{-C}=\text{O}$, $J=7.7$) (diastereotopic protons), 3.9 (dd, CH-COOH, methine proton), 5.2 (s, 2H, $\text{CH}_2\text{-N}$), 6.7 (s, 1H, bridgeCH, 1,3-double bond shift), 7.2-7.7 (m, 8H, ArH). The EI-MS shows the molecular ion peak at m/e 498, 496 corresponding to ($\text{M}+2$) $^+$ and (M^+), respectively.

1-(4-Acetylamino-phenyl-6-(N-phthalimido)methyl-1,3,4-thiadiazolo [3,2-a] pyrimidine (9)

Boiling of **3** (3 g; 0.005 mol) with acetic anhydride (9.4 mL) on a hot plate was heated under reflux for 4 h. The reaction mixture was poured on to H_2O and the solid

compound was separated and crystallized from ethanol. M.wt=453 ($\text{C}_{20}\text{H}_{13}\text{N}_4\text{O}_2\text{SBr}$), M. 230 °C, yield 65%, calcd/found: C 52.98/52.80, H 2.86/2.62, N 12.63/12.52, Br 17.66/17.45, S 7.06/6.88. IR: $\nu_{\text{C}=\text{O}}$ are at 1772, 1668 cm^{-1} . $^1\text{H-NMR}$ (DMSO- d_6) exhibits signals at 5.2 (s, 2H, $\text{CH}_2\text{-N}$), 6.7 (s, 1H, bridgeCH, 1,3-double bond shift), 7.2-7.7 (m, 10H, ArH).

Pyridazinones 10 -12

An equimolar mixture of compound **7** (2.75 g; 5mmol) and hydrazine hydrate (1.7mL, 0.015 mol) was refluxed in boiling ethanol for 3 h and the solid that separated out was filtered off, dried and then crystallized from ethanol.

6-(Acetylamino-phenyl)-4-(5-phenyl-2-amino-1,3,4 thiadiazole)-2,3,4,5-tetrahydro 3(2H)-pyridazinones (10)

Yield 70-75 %. IR(KBr) 1674, 1708 (CO), 3177 (NH). ^1H NMR (DMSO- d_6): δ 2.2(s, 3H, CH_3), 3.7 (2dd, 2H, $\text{CH}_2\text{-C}=\text{N}$), 4.2 (2 dd, CH, methine proton) 6.7 (s, NH, NH of thiadiazole moiety), 7.43-7.81 (m, 9H, Ar-H), 11.59 (brs, 2H, NH of acetamido and pyridazinone moieties). EIMS: m/z : 406 (M^+). Anal.: Calcd. $\text{C}_{20}\text{H}_{18}\text{N}_6\text{SO}_2$: C 59.11, H 4.43; Found: C 59.20, H 4.43.

6-(Acetylamino-phenyl)-4-(5-(4-chlorophenyl)-2-amino-1,3,4-thiadiazole)-2,3,4,5-tetrahydro-3(2H)-pyridazinones (11)

Yield 70-75 %. IR(KBr) 1674, 1708 (CO), 3177 (NH). ^1H NMR (DMSO- d_6): δ 2.2(s, 3H, CH_3), 3.7(2 dd, 2H, $\text{CH}_2\text{-C}=\text{N}$), 4.2 (2 dd, CH, methine proton), singlet broad band at 6.5 ppm assigned for NH of thiadiazole moiety.) 7.6-8.1 (m, 8H, ArH), singlet at 10.2 was assigned for the two acidic protons of acetamido and pyridazinone moieties. EIMS m/z : 405 (M^+-Cl). Anal.: Calcd. for **11** $\text{C}_{20}\text{H}_{17}\text{N}_6\text{SO}_2\text{Cl}$: C 54.54, H 3.86; Found: C 54.50, H 3.86.

6-(Acetylamino-phenyl)-4-(5-styryl-2-amino 1,3,4 thiadiazole)-2,3,4,5-tetrahydro-3(2H)-pyridazinones (12)

Yield 70-75%. IR (KBr) 1674, 1708 (CO), 3177 (NH). ^1H NMR (DMSO- d_6): δ 2.2 (s, 3H, CH_3), 3.7 (2 dd, 2H, $\text{CH}_2\text{-C}=\text{N}$), 4.2 (2 dd, CH, methine proton), singlet broad band at 6.5 ppm assigned for NH of thiadiazole moiety.) 7.6-8.1(m, 11H, ArH and olefinic protons), singlet at 10.2 assigned for two acidic protons of acetamido and pyridazinone moieties. EIMS: m/z : 432 (M^+). Anal. Calc. $\text{C}_{22}\text{H}_{20}\text{N}_6\text{SO}_2$: C 61.11, H 4.62; Found: C 61.18, H 4.60.

Ethyl N-[6-(4-acetylamino-phenyl)-3-oxo-pyridazin-4-yl]-N-[(5-phenyl-1,3,4-thiadiazol-2-yl)] glycinate (13)

An equimolar mixture of compound **10** (2.0 g; 5 mmol) and ethylchloroacetate (1.4 mL, 0.015 mol) in 50 mL dry pyridine was refluxed for 3 h. The reaction mixture was poured on to ice/HCl and the solid that separated out was filtered off, dried and then, crystallized from ethanol. Yield 35 %. Mp. 190-192. IR (KBr) 1630 (C=N), 1650, 1743 (CO), 3320, 3188 (NH). ^1H NMR (DMSO- d_6): δ 1.12 (t, 3H, CH_3), 2.08 (s, 3H, CH_3), 3.72-3.86 (m, 3H, CH_2CH), 4.13 (s, 2H, $\text{CH}_2\text{-N}$), 4.80 (q, 2H, $\text{CH}_2\text{-O}$), 7.46-7.92 (m, 9H, Ar-H),

11.36 (brs, 2H, NH of acetamido and pyridazinone moieties). Anal.: Calcd. for $C_{24}H_{24}N_6SO_4$: C 58.53, H 4.87, N 17.07; Found: C 52.40, H 4.76, N 17.00.

3-Oxo-4-(5-phenyl-1,3,4-thiadiazol-2-yl)-6-(4-acetylaminophenyl)-1,2,3,4-tetrahydro1,4-oxazino[2,3-c]pyridazine (14)

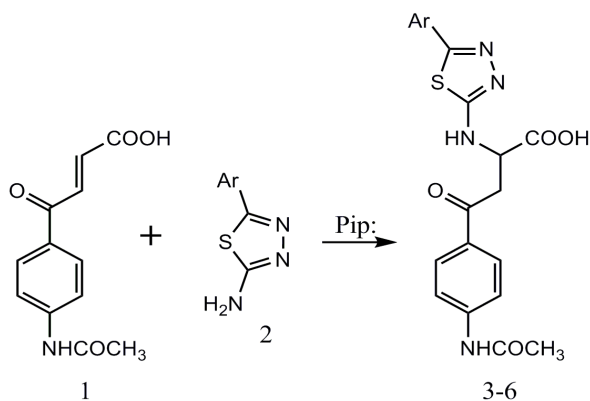
An equimolar mixture of compound **10** (2.0 g; 5 mmol), ethylchloroacetate (1.4 mL, 0.015 mol) and anhydrous K_2CO_3 (4 g) in 50 mL dry acetone was refluxed for 24 h. The reaction mixture was then poured on to H_2O/ice . The solid that separated out was filtered off, dried and then, crystallized from benzene. Yield 65 %. Mp. 162-164 °C. IR (KBr) 1630 (C=N), 1650, 1685 (CO), 3320, 3188 (NH). 1H NMR (DMSO- d_6): δ 2.08(s, 3H, CH_3), 3.72-3.76(m, 3H, CH_2CH), 5.933 (s, 2H, OCH_2CO), 7.46-7.92 (m, 9H, Ar-H), 11.36 (brs, 1H, NH of acetamido moiety). Anal.: Calcd. for $C_{22}H_{18}N_6SO_3$: C 59.19, H 4.03, N 18.83; Found: C 59.30, H 4.00, N 18.70.

1-((2-(4-Acetylamino-phenyl))-2-oxoethyl-7-oxo-quinoxalino-[1,2-b]-quinazoline (16)

A mixture of benzoxazinone **15** (0.01 mol) and o-phenylene diamine (0.01 mol) in ethanol (50 mL) was heated and refluxed for 5h. The reaction mixture was allowed to cool and the product was filtered, dried and recrystallized from ethanol. Yield 70 %. Mp. 126-128 °C. IR (KBr) 1709, 1735 (CO), 3423 (NH). 1H -NMR (DMSO- d_6): δ 2.5 (s, 3H, CH_3), 3.4 (m, 3H, CH_2-CH), 6.2 (s, 1H, pyrazine moiety), 7.46-8.11 (m, 12H, Ar-H), 12.40 (brs, 1H, NH of acetamido moiety). Anal.: Calcd. for $C_{25}H_{20}N_4O_3$: C 70.75, H 4.71, N 13.20; Found: C 70.70, H 4.64, N 13.15.

RESULTS AND DISCUSSION

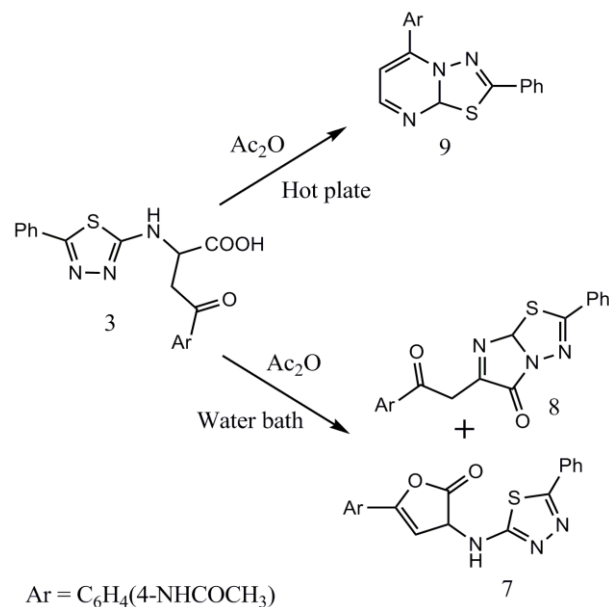
When 4-(4-acetylaminophenyl)-4-oxo-but-2-enoic acid (**1**) was allowed to react with 2-amino 5-aryl thiadiazole derivatives (**2**), it produced 3-(4-acetamidobenzoyl)-2-(5-aryl 2-thiadiazolylamino)propanoic acids (**3-6**) as α -amino acid types that differ in biological activity by differing the aryl groups. Outline in Table 1 the presence of halogen atom enhances the antibacterial activity rather than chromophore moiety $-CH=CH-$ (Scheme 1).



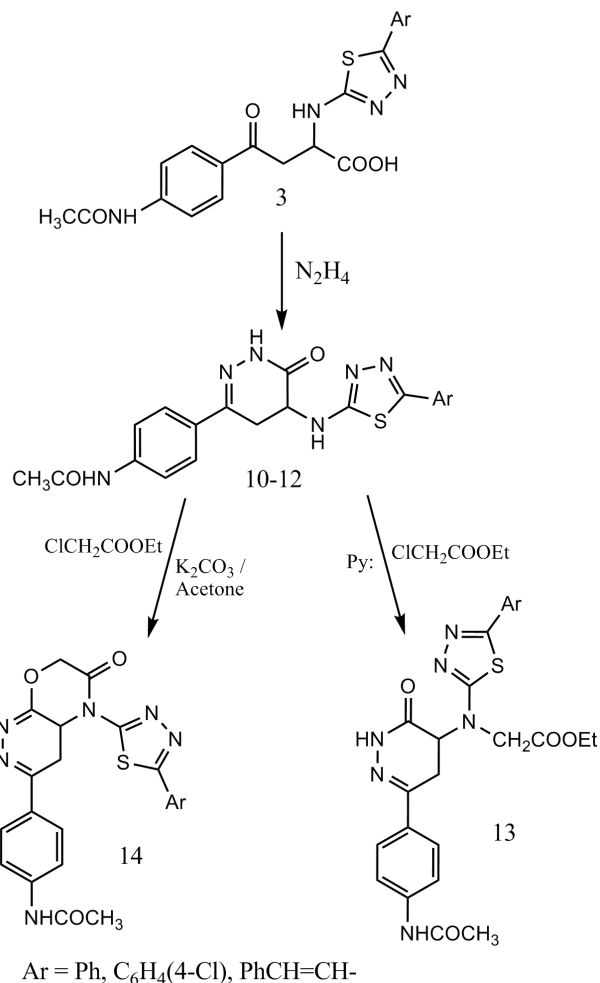
Scheme 1.

The recent efforts made for the development of new ascorbic acid analogues in obtaining anti-oxidant⁹⁻¹³, anti-tumour¹⁴ agents have resulted 2(3H)-furanones as a new

antioxidant and anti-inflammatory agents. In the synthesis of lactone derivatives related to ascorbic acid, the NH group in the position **3** is acting as OH group in ascorbic acid, we also have found out that some 3,5-diaryl-2(3H) furanone possess significant anti-inflammatory and anti-oxidant activities¹⁵.



Scheme 2.



Scheme 3.

Table 1. Antibacterial and Antifungal activities for some important synthesized compounds

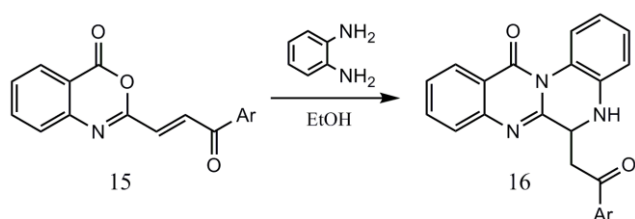
Compound / Ar	<i>Escherichia coli</i> G ⁻	<i>Staphylococcus aureus</i> G ⁺	<i>Aspergillus flavus</i> (Fungus)	<i>Candida albicans</i> (Fungus)
3/C ₆ H ₅ -	14	14	12	10
4/4-ClC ₆ H ₄	16	16	13	12
5/Phthalimidoylmethyl	14	14	14	12
6/ β -styryl	14	13	0	0
10	16	16	13	12
11	18	16	15	14
13	12	14	10	12
14	14	13	12	13

The antimicrobial screening of all the synthesized compounds can be done using the agar diffusion assay. Tetracycline (Antibacterial agent): 32-30, Amphotericin (Antifungal agent): 18-16

These results prompted us that lactones can be obtained by the lactonization of hydroxyl acids. Thus, the adduct **3** (new α -amino acid) with design and synthesized new furanones. The synthesis of freshly distilled acetic anhydride afforded 2-(5-acetylaminophenyl-2-oxo-furan-3-yl)amino-5-phenyl 1,3,4-thiadiazole (**7**) and 2-phenyl-4-oxo-5-(4-acetylaminobenzoylmethyl)imidazo[2,1-b]-1,3,4-thiadiazole derivatives (**8**). The ¹H-NMR spectrum of compounds **8** and **9** showed singlet peak at 6.7 corresponding to bridged CH, 1,3-double bond shift that explained the proton spend apart of life time as methine proton. Fused thiadiazolo pyrimidine **9** can be synthesized by the treatment of aza-adducts **3** with boiling acetic anhydride, through decarboxylation followed by ring closure (Scheme 2).

It was reported¹⁶ that the pyridazinone substituted 1,3,4-thiadiazolene were fungicidally active and their activity was influenced by the nature of the substituents. Thus, when the acid **1a** was allowed to react with hydrazine hydrate in boiling ethanol, it produced **13**. Reaction of the pyridazinone derivative **13** with ethylchloroacetate in boiling pyridine produced glycinate ester derivative **14**. But, when the above reaction of pyridazinone **10** with ethylchloroacetate is carried out in the presence of anhydrous carbonate and dry acetone^{8f} it produced 1,4-oxazino[2,3-c]pyridazine derivatives **14** (Scheme 3).

In one pot reaction, 4-(4-acetylaminophenyl)-4-oxo-but-2-enoic acid (**1**) was allowed to react with phosphorous pentachloride and then refluxed with anthranilic in the presence of acetic anhydride produced benzoxazinone **15**^{8g}. The preparation of quinoxaline and its derivatives plays an important role in organic synthesis¹⁷, displaying a broad spectrum of biological activities¹⁸, as a building blocks in the synthesis of organic semiconductors¹⁹, rigid subunits in macro cyclic receptors or molecular recognition²⁰ and chemically controlled switches²¹.



Ar = C₆H₄(4-NHCOCH₃)

Scheme 4.

Treatment of the benzoxazinone **15** with o-phenylene diamine in boiling ethanol can be produced with new derivative of quinoxaline **16** (Scheme 4).

REFERENCES

- Toshikazu, K., *Food Ingred. J. Japan*, **2002**, 206.
- Barrett, D., Tanaka, A.; Harada, K.; Ohki, H., Watabe, E., Maki, K., Ikeda, F. *Bioorg. Med. Chem. Lett.*, **2001**, *11*, 479-482.
- Kovalainen, J. T.; Christains, J. A. M.; Kotisaati, S.; Laitinen, J. T.; Mannisto, P. T., *J. Med. Chem.*, **1999**, *42*, 1193.
- El-Faham, A., Elmassry, A. M., Amer, A., Gohar, Y. M.; *Lett. Pept. Sci.*, **2002**, *9*, 49
- a) Polyak, F.; Lubell, W. D. *J. Org. Chem.*, **1998**, *63*, 5937. b) Roy, S., Lombart, H. G., Lubell, W. D., Hancock, R. E. W., Farmer, S. W. *J. Peptide Res.*, **2002**, *60*, 198.
- Marsham, P. R., Wardleworth, J. M., Boyle, F. T., Hennequin, L. F., Brown, K. M., Jackman, A. L. *Med. Chem.*, **1999**, *42*, 380.
- Xia, Y., Yang, Z-V.; Xia, P., Bastow, K. F., Nakanishi, Y., Lee, K.-H. *Bioorg. Med. Chem. Lett.*, **2000**, *10*, 699.
- a) EL-Hashash, M. A., Rizk, A. A., Shaker, S. A., Mostafa, K.K., *Egypt. J. Chem.*, **2012**, *55*(1), b) Rizk, S. A., El-Hashash, M. A., Mostafa, K. K., *Egypt. J. Chem.* **2008**, *51*(5), 116-121; c) Elhashash, M., Soliman A., Madkour, M., Rev. Roum. Chim., **1993**, *38*(8), 955; d) El-Hashash, M., Amine, M., Soliman, F., Morsi, M., *J. Serb. Chem. Soc.*, **1992**, *57*(9), 563; e) Youssef, A., Madkour, H., Marzouk, M., El-Hashash, M., El-Soll, A., *Can. J. Chem.*, **2005**, *83*, 251 f) Rizk, S. A., *Am. J. Chem.*, **2011**, *1*(1), 66-72, DOI: 10.5923/j.chemistry.20110101.01.; g) El-Hashash, M. A., Rizk, S.A., *Eur. Chem. Bull.*, **2013**, *2*(7), 456-460.
- Cotelle, P., Cotelle, N., Teissier, E., Vezin, H. *Bioorg. Med. Chem.* **2003**, *11*, 1087-1093.
- Weber, V., Coudert, P., Rubat, C., Duroux, E., Vallee-Gramain, J.-C., Couquelet, J., Madesclaire, M., *Bioorg. Med. Chem.* **2002**, *10*, 1647.
- Weber, V., Coudert, P., Rubat, C., Duroux, E., Leal, F., Couquelet, J., *J. Pharm. Pharmacol.*, **2000**, *52*, 523
- Manfredini, S., Vertuani, S., Manfredi, B., Rossini, G., Calviello, G., Palozza, P., *Bioorg. Med. Chem.* **2000**, *8*, 2791.
- Mashino, T., Takigawa, Y., Saito, N., Wong, L. Q., Mochizuki, M., *Bioorg. Med. Chem. Lett.*, **2000**, *10*, 2783.
- Raic-Malic, S., Svedruzic, D., Gazivoda, T., Marunovic, A., Hergold-Brundic, A., Nagl, A., Balzarini, J., DeClercq, E., Mintas, M., *J. Med. Chem.*, **2000**, *43*, 4806.
- Weber, V., Rubat, C., Duroux, E., Lartigue, C., Madesclaire, M., Couderta, P., **2005**, *13*, 4552-4564.

- ¹⁶Xia-Juan., Z., Lu-Hua, L., Gui-Yu J., and Zu-Xing Zhang, *J. Agric. Food. Chem.*, **2002**, 50(13), 3757-3760.
- ¹⁷a) Shivaji, V. M., Sastry, M. N., Wang, C. C., Ching-Fa, Y. *Tetrahedron Lett.*, **2005**, 46, 6354; b) Sato, N. in A. R. Katritzky, C. W. Rees Scriven (Eds), *Comprehensive Heterocyclic Chemistry II*, vol. 6 Pergamon, Oxford, **1996**, p.233.
- ¹⁸a) Sakata, G., Makino, K., Kurasama, Y., *Heterocycles* **1988**, 27, 2481; b) Seitz, L. E., Suling, W. J., Reynolds, R. C., *J. Med. Chem.*, **2002**, 45, 5604; c) Uxey, T., Tempest, P., Hulme, C. *Tetrahedron Lett.*, **2002**, 43, 1637.
- ¹⁹Dailey, S., Feast, J. W., Peace, R. J., Sage, I. C. I., Till, S., Wood, E. L., *J. Mater. Chem.*, **2001**, 11, 2238.
- ²⁰a) Mizuno, T., Wei, W. H., Eller, L. R., Sessler, J. L. *J. Am. Chem. Soc.*, **2002**, 124, 1134; b) Elwahy, A. H. M. *Tetrahedron* **2000**, 56, 897.
- ²¹Crossley, J. C., Johnston, L. A., *Chem. Commun.*, **2002**, 1122

Received: 11.03.2013.

Accepted: 20.04.2013.



VOLUMETRIC, VISCOSITY AND ULTRASONIC BEHAVIOUR OF n-BUTYL PROPIONATE + ETHER (THF, 1,4-DIOXANE, ANISOLE AND BUTYL VINYL ETHER) MIXTURES AT 303.15, 308.15 AND 313.15 K

M. V. Rathnam,^{[a]*} D. R. Ambavadekar,^[a] M. Nandini^[b]

Keywords: density, viscosity, speed of sound, binary mixture, n-butyl propionate

Density, viscosity and speed of sound of binary liquid mixtures of butyl propionate with tetrahydrofuran, 1,4-dioxane, anisole and butyl vinyl ether were measured at (303.15, 308.15 and 313.15) K and over the entire composition range. From the experimental data values of excess volume V^E , viscosity deviations $\Delta\eta$, deviation in speeds of sound Δu , isentropic compressibility K_s and deviation in isentropic compressibility ΔK_s , have been determined. The speeds of sound data have been analysed on the basis of Jouyban–Acree and Vandael–Vangeel models.

Corresponding Author*

Tel: +91 - 8976545095

Fax: 022 - 25337672

E-Mail: mvrathnam58@rediffmail.com

[a] Physical Chemistry Research Laboratory, B. N. Bandodkar College of Science, Thane-400601 - India., Tel.: +91 - 9819558695 Fax: 022 - 25337672, Email: DAMBAVADEKAR@yahoo.co.in

[b] Department of Chemistry, Dr. P.R.Ghogrey Science College, Deopur- Dhule-424005 - India, Tel.: +91. 2562.272562 Fax: +91.2562.271340, E-mail: m.nandinikumar@gmail.com

study of interaction of esters with ethers will throw light on designing, separation operations such as distillation etc.

In view of these above importance the present research has been undertaken with the objective of investigating the molecular interactions of the binary mixtures of butyl propionate with ethers. In continuation of our earlier work,¹¹⁻¹⁴ in this paper we report the density, viscosity and speed of sound of binary liquid mixtures of butyl propionate + tetrahydrofuran, butyl propionate + 1,4-dioxane, butyl propionate + anisole, and butyl propionate + butyl vinyl ether at (303.15, 308.15 and 313.15) K over the entire range of composition of n-butyl propionate.

From the experimental values excess volume V^E , deviation in viscosity $\Delta\eta$, deviation in speeds of sound Δu , isentropic compressibility K_s and deviation in isentropic compressibility ΔK_s , have been calculated. This work also provides a test of empirical equations proposed by Jouyban–Acree^{15,16} and Vandael–Vangeel¹⁷ to correlate speeds of sound data of the binary liquid mixtures in terms of pure component properties.

Introduction

A number of theories^{1,2} have been proposed to compute the useful thermodynamic properties of liquids and liquid mixtures. Parallel to this many experimental techniques have been developed. In liquid mixture studies attractive forces like dipole–dipole interactions, hydrogen bond type forces and dipole-induced dipole interactions lead to non ideal effects.³ However quantitative estimation of such interactions is important in order to achieve a fundamental understanding about the liquid state properties, which are useful in many specific disciplines like chemistry, physics, engineering, and biology. Numerous studies⁴⁻¹⁰ have been reported related to the interactions in binary liquid mixtures of esters with a variety of organic solvents. However no attempts have been made to study interactions in the binary mixtures containing butyl propionate as a common component.

Esters have found wide spread use in several industries and automotive applications due to their excellent performance characteristics such as solvency and evaporation rate. Butyl propionate is widely used for high solid coatings in automotive finishes, appliance coatings, cleaning fluids, enamels, lacquers, and printing inks. While ethers are commonly used as powerful non-polar solvents for both industrial applications and for chemical reactions. In medical applications ethers are used as a general anaesthetic for surgeries. Its use replaced chloroform which was extremely toxic. In automotive application an ether is added to the fuel in race cars for extra power. Therefore the

Experimental

Materials: Extra pure butyl propionate, tetrahydrofuran, 1,4-dioxane, anisole and butyl vinyl ether all Fluka AG were procured from the Aldrich company. The mass fraction purities as determined by gas chromatography (HP 8610) using FID were, butyl propionate (> 0.998), tetrahydrofuran (> 0.996), 1,4-dioxane (>0.997), anisole (> 0.998), and butyl vinyl ether (>0.996). Before use the pure chemicals were stored over 0.4 nm molecular sieves for 72 h to reduce water content if any and were degassed at low pressure.

Methods: The density of pure liquids and their binary mixtures were measured with Anton Paar DMA 4500 density meter with certified precision of better than $\pm 1 \times 10^{-5}$ g.cm⁻³ operated in the static mode and the cell was regulated to ± 0.01 K with solid state thermostat. The apparatus was calibrated once a day with dry air and double

distilled freshly degassed water. The uncertainty in the density measurements was found to be less than $\pm 0.0002 \text{ g cm}^{-3}$. Airtight stoppered bottles were used for the preparation of the mixtures. Mass measurements accurate to $\pm 0.01 \text{ mg}$ were made on a digital electronic balance (Mettler AE 240, Switzerland). Each mixture was immediately used after it was well mixed by shaking. The resulting mole fraction uncertainty was estimated to be less than ± 0.0001 . Viscosities were determined using an Ubbelohde viscometer with an uncertainty of $\pm 0.005 \text{ mPa s}$. The detailed method of measurement of viscosity has been described earlier.¹¹ The speeds of sound at frequency of 2 MHz were determined using single crystal variable path interferometer (F-8 Mittal Enterprises, New Delhi, India). The uncertainty in speed of sound was found to be $\pm 1 \text{ m s}^{-1}$.

Results and Discussion

The results of density ρ , excess volume V^E , viscosity η , and speed of sound u , isentropic compressibility K_S of the studied binary mixtures at (303.15, 308.15 and 313.15) K are given in Table 1. The excess volume V^E ($\text{cm}^3 \text{ mol}^{-1}$) was calculated using the relation

$$V^E = \frac{(x_1 M_1 + x_2 M_2)}{\rho_{12}} - \left(\frac{x_1 M_1}{\rho_1} + \frac{x_2 M_2}{\rho_2} \right) \quad (1)$$

where x , M and ρ are the mole fraction, molar mass, and density respectively of pure components 1 and 2. ρ_{12} is the density of the liquid mixture. The isentropic compressibility K_S was calculated using Newton-Laplace equation:

$$K_S = \frac{1}{u^2 \rho} \quad (2)$$

The deviations in viscosity $\Delta\eta$, speeds of sound Δu , and isentropic compressibility ΔK_S were calculated using the general equation

$$\Delta Y = Y_m - x_1 Y_1 - x_2 Y_2 \quad (3)$$

where ΔY is the deviation or excess property in question, Y_m refers to the property of the mixture, $x_1 Y_1$ and $x_2 Y_2$ refer to the mole fraction and specific property of the pure components 1 and 2 respectively. The results of V^E , $\Delta\eta$, Δu and ΔK_S , for the binary mixtures at (303.15, 308.15 and 313.15) K were graphically represented in Figures 1-4. Further these results were fitted to the Redlich-Kister¹⁸ polynomial equation by the method of least squares to derive the binary solution coefficients A_0 , A_1 , A_2 .

$$\Delta Y = x_1 x_2 \left[A_0 + A_1 (x_1 - x_2) + A_2 (x_1 - x_2)^2 \right] \quad (4)$$

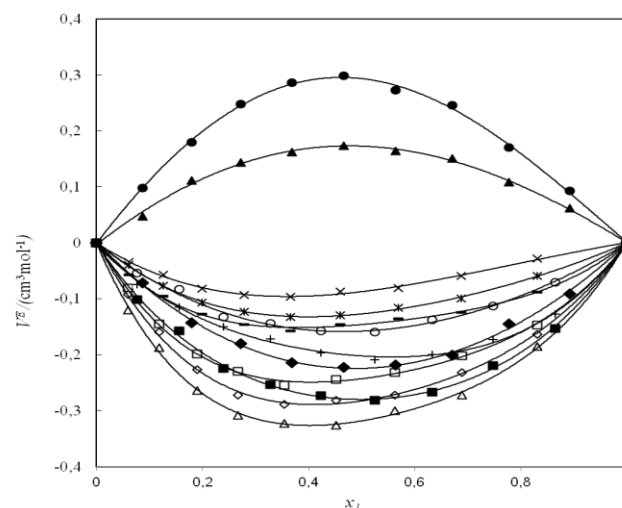


Figure 1. Curves of excess volumes (V^E) vs. mole fraction for the binary mixtures. Butyl propionate + Tetrahydrofuran at (\square , 303.15 K; \diamond , 308.15 K; Δ , 313.15 K; butyl propionate + 1,4-dioxane at (\times , 303.15 K; κ , 308.15 K; --- , 313.15 K; butyl propionate + anisole at \circ , 303.15 K; $+$, 308.15 K; \blacksquare , 313.15 K; butyl propionate + butyl vinyl ether \blacklozenge , 303.15 K; \blacktriangle , 308.15 K; \bullet , 313.15 K.

The standard deviations for V^E , $\Delta\eta$, Δu and ΔK_S were calculated using the relation

$$\sigma(Y) = \left[\frac{\sum (Y_{\text{exp}}^E - Y_{\text{cal}}^E)^2}{(D - N)} \right]^{0.5} \quad (5)$$

where D and N are the number of experimental data and equation parameters respectively. The coefficients of Eq.4 and the standard deviations of Eq.5 were presented in Table 2.

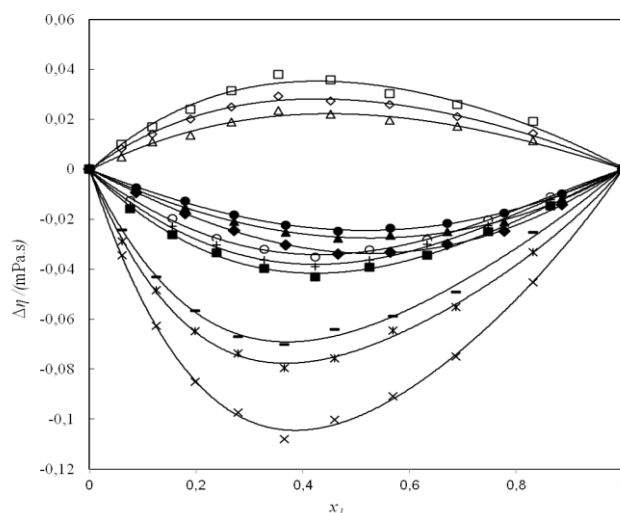


Figure 2. Curves of deviation in viscosity ($\Delta\eta$) Vs mole fraction for the binary mixtures. butyl propionate + tetrahydrofuran at (\square , 303.15 K; \diamond , 308.15 K; Δ , 313.15 K; butyl propionate + 1,4-dioxane at \times , 303.15 K; κ , 308.15 K; --- , 313.15 K; butyl propionate + anisole at \circ , 303.15 K; $+$, 308.15 K; \blacksquare , 313.15 K; butyl propionate + butyl vinyl ether \blacklozenge , 303.15 K; \blacktriangle , 308.15 K; \bullet , 313.15 K.

Table 1 Values of density ρ , excess volume V^E , viscosity η , speed of sound u , isentropic compressibility K_s , for the binary liquid mixtures.

x_1	$\rho, \text{g}\cdot\text{cm}^{-3}$	$V^E, \text{cm}^3\cdot\text{mol}^{-1}$	$\eta, \text{mPa}\cdot\text{s}$	$u, \text{m}\cdot\text{s}^{-1}$	K_s, Tpa^{-1}
Butyl propionate(1) + Tetrahydrofuran (2)					
$T=303.15 \text{ K}$					
0.0000	0.8787		0.439	1248	730.7
0.0596	0.8784	-0.080	0.465	1236	745.2
0.1176	0.8780	-0.145	0.487	1224	760.2
0.1900	0.8773	-0.199	0.513	1216	770.9
0.2667	0.8764	-0.230	0.540	1208	787.1
0.3539	0.8754	-0.255	0.570	1196	798.6
0.4521	0.8741	-0.244	0.593	1192	805.2
0.5628	0.8728	-0.231	0.616	1188	811.8
0.6893	0.8714	-0.202	0.645	1184	818.6
0.8314	0.8699	-0.147	0.675	1184	820.0
1.0000	0.8679		0.700	1188	816.4
$T=308.15 \text{ K}$					
0.0000	0.8730		0.429	1228	759.6
0.0596	0.8730	-0.093	0.450	1220	769.8
0.1176	0.8727	-0.160	0.469	1212	780.3
0.1900	0.8720	-0.227	0.491	1204	791.3
0.2667	0.8712	-0.272	0.513	1196	802.6
0.3539	0.8710	-0.289	0.537	1188	814.5
0.4521	0.8688	-0.282	0.557	1184	821.3
0.5628	0.8674	-0.272	0.581	1180	828.1
0.6893	0.8659	-0.231	0.604	1176	835.2
0.8314	0.8643	-0.163	0.629	1172	842.4
1.0000	0.8621		0.653	1172	844.5
$T=313.15 \text{ K}$					
0.0000	0.8669		0.394	1212	785.3
0.0596	0.8670	-0.120	0.409	1196	806.2
0.1176	0.8668	-0.187	0.427	1184	822.8
0.1900	0.8664	-0.264	0.445	1172	840.0
0.2667	0.8657	-0.308	0.467	1164	852.2
0.3539	0.8649	-0.323	0.491	1156	864.9
0.4521	0.8638	-0.326	0.511	1148	878.0
0.5628	0.8627	-0.301	0.532	1148	879.2
0.6893	0.8615	-0.272	0.557	1144	886.6
0.8314	0.8602	-0.186	0.582	1144	888.2
1.0000	0.8583		0.607	1156	871.9
Butyl propionate(1) + 1,4-Dioxane (2)					
$T=303.15 \text{ K}$					
0.0000	1.0228		1.090	1320	561.2
0.0612	1.0074	-0.035	1.031	1296	591.0
0.1261	0.9923	-0.057	0.978	1280	615.1
0.1987	0.9769	-0.082	0.927	1260	644.8
0.2785	0.9614	-0.093	0.882	1248	667.8
0.3653	0.9461	-0.096	0.840	1228	700.9
0.4599	0.9310	-0.088	0.810	1220	721.7
0.5687	0.9155	-0.081	0.777	1212	743.6
0.6873	0.9004	-0.059	0.747	1200	771.3
0.8318	0.8842	-0.029	0.721	1192	796.0
1.0000	0.8679		0.700	1188	816.4

Table 1. (contg.)

x_1	$T=308.15$ K				
0.0000	1.0173		0.999	1312	571.3
0.0612	1.0019	-0.040	0.949	1292	597.9
0.1261	0.9869	-0.076	0.907	1276	622.3
0.1987	0.9715	-0.107	0.865	1256	652.5
0.2785	0.9560	-0.124	0.829	1240	680.3
0.3653	0.9407	-0.133	0.793	1224	709.6
0.4599	0.9256	-0.130	0.764	1212	735.5
0.5687	0.910	-0.116	0.737	1200	763.1
0.6873	0.8949	-0.100	0.705	1188	791.8
0.8318	0.8786	-0.059	0.678	1180	817.4
1.0000	0.8621		0.653	1172	844.5
x_1	$T=313.15$ K				
0.0000	1.0116		0.946	1304	581.6
0.0612	0.9966	-0.058	0.901	1280	612.4
0.1261	0.9818	-0.096	0.860	1264	637.5
0.1987	0.9666	-0.127	0.822	1234	679.4
0.2785	0.9513	-0.146	0.786	1214	713.3
0.3653	0.9362	-0.158	0.752	1200	741.8
0.4599	0.9212	-0.146	0.726	1184	774.4
0.5687	0.9058	-0.135	0.695	1172	803.7
0.6873	0.8909	-0.125	0.664	1156	840.0
0.8318	0.8748	-0.089	0.639	1152	861.4
1.0000	0.8583		0.607	1156	871.9
Butyl propionate(1) + Anisole (2)					
x_1	$T=303.15$ K				
0.0000	0.9853		0.9227	1388	524.6
0.0760	0.9739	-0.054	0.8933	1356	558.4
0.1561	0.9623	-0.083	0.8683	1330	587.5
0.2390	0.9511	-0.133	0.8419	1304	618.3
0.3282	0.9394	-0.144	0.8175	1280	649.7
0.4230	0.9277	-0.1579	0.7935	1256	683.3
0.5248	0.9158	-0.159	0.7736	1240	710.2
0.6329	0.9038	-0.138	0.7538	1228	733.7
0.7474	0.8919	-0.113	0.7363	1212	763.3
0.8646	0.8804	-0.071	0.7192	1200	788.8
1.0000	0.8879		0.7002	1188	816.4
x_1	$T=308.15$ K				
0.0000	0.9792		0.8494	1368	542.7
0.0760	0.9680	-0.075	0.8200	1344	571.9
0.1561	0.9565	-0.115	0.7958	1324	596.4
0.2390	0.9452	-0.150	0.7720	1304	622.2
0.3282	0.9336	-0.172	0.7484	1276	657.9
0.4230	0.9220	-0.197	0.7271	1256	687.5
0.5248	0.9102	-0.210	0.7099	1238	716.8
0.6329	0.8983	-0.200	0.6948	1220	747.9
0.7474	0.8864	-0.173	0.6798	1204	778.2
0.8646	0.8741	-0.128	0.6672	1188	809.9
1.0000	0.8621		0.6528	1172	844.5

Table 1. (contg.)

x_1			$T=313.15\text{ K}$		
0.0000	0.9728		0.764	1348	561.6
0.0760	0.9621	-0.101	0.736	1324	592.9
0.1561	0.9510	-0.157	0.713	1296	626.1
0.2390	0.9402	-0.224	0.693	1276	653.2
0.3282	0.9289	-0.254	0.673	1252	686.8
0.4230	0.9175	-0.274	0.654	1228	722.8
0.5248	0.9059	-0.281	0.642	1212	751.5
0.6329	0.8942	-0.267	0.630	1196	781.8
0.7474	0.8824	-0.219	0.622	1184	808.4
0.8646	0.8710	-0.153	0.614	1168	841.6
1.0000	0.8583		0.607	1156	871.9
Butyl propionate(1) + Butyl Vinyl Ether (2)					
x_1			$T=303.15\text{ K}$		
0.0000	0.7741		0.387	1084	1099.4
0.0874	0.7839	-0.071	0.405	1104	1046.6
0.1792	0.7939	-0.143	0.425	1120	1004.1
0.2718	0.8035	-0.180	0.447	1132	971.2
0.3683	0.8132	-0.214	0.472	1144	939.6
0.4661	0.8226	-0.223	0.499	1160	905.6
0.5644	0.8317	-0.219	0.530	1168	881.3
0.6710	0.8412	-0.201	0.567	1176	859.6
0.7778	0.8502	-0.145	0.606	1184	839.0
0.8865	0.8591	-0.091	0.651	1188	824.8
1.0000	0.8679		0.700	1188	816.4
x_1			$T=308.15\text{ K}$		
0.0000	0.7682		0.374	1072	1132.8
0.0874	0.7773	0.047	0.391	1088	1086.8
0.1792	0.7865	0.111	0.409	1100	1050.8
0.2718	0.7957	0.144	0.429	1112	1016.3
0.3683	0.8051	0.163	0.452	1128	976.2
0.4661	0.8144	0.173	0.476	1140	944.8
0.5644	0.8236	0.164	0.505	1148	921.3
0.6710	0.8333	0.151	0.536	1156	898.0
0.7778	0.8429	0.108	0.570	1164	875.6
0.8865	0.8524	0.062	0.609	1168	859.9
1.0000	0.8621		0.653	1172	844.5
x_1			$T=313.15\text{ K}$		
0.0000	0.7633		0.354	1064	1157.2
0.0874	0.7721	0.098	0.369	1076	1118.5
0.1792	0.7875	0.180	0.387	1088	1081.1
0.2718	0.7905	0.248	0.405	1100	1045.5
0.3683	0.7999	0.286	0.425	1112	1011.0
0.4661	0.8093	0.298	0.447	1124	978.0
0.5644	0.8187	0.273	0.474	1132	953.2
0.6710	0.8286	0.246	0.502	1140	928.6
0.7778	0.8385	0.171	0.534	1148	904.9
0.8865	0.8483	0.093	0.569	1152	888.3
1.0000	0.8583		0.607	1156	871.9

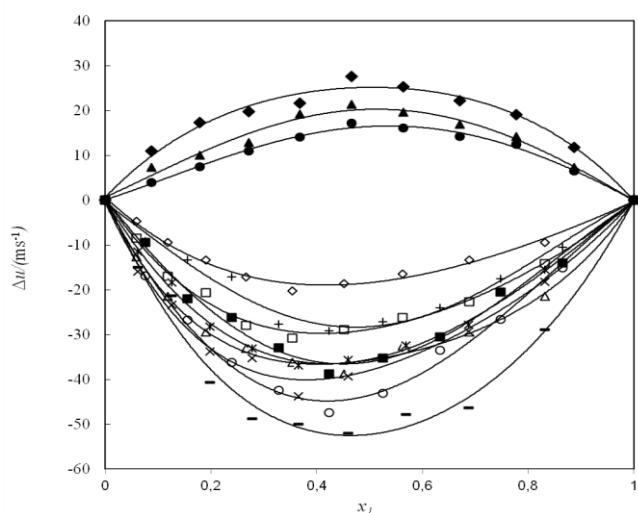


Figure 3. Curves of deviation in speed of sound (Δu) Vs mole fraction for the binary mixtures. Butyl propionate + Tetrahydrofuran at \square , 303.15 K; \diamond , 308.15 K; Δ , 313.15 K; Butyl propionate + 1,4-Dioxane at \times , 303.15 K; κ , 308.15 K; --- , 313.15 K; Butyl propionate + Anisole at \circ , 303.15 K; $+$, 308.15 K; \blacksquare , 313.15 K; Butyl propionate + Butyl vinyl ether \blacklozenge , 303.15 K; \blacktriangle , 308.15 K; \bullet , 313.15 K.

The excess molar volume V^E against mole fraction x_1 were graphically represented in Figure 1. The V^E values for butyl propionate with tetrahydrofuran, 1,4-dioxane, anisole are negative over the whole composition range at all studied temperatures. These negative values were found to increase with increase in temperature which suggest the increase in interactions between unlike molecules at high temperature. For the system butyl propionate + butyl vinyl ether the V^E values are negative at 303.15 K, but as the temperature is increased the V^E values change from negative to positive over the entire range of mole fraction. The negative values indicate the contraction in volume upon mixing butyl propionate with ethers due to association in dissimilar molecules¹⁹ while the positive V^E values indicate the weak interactions and may be due to dispersive forces involving between dissimilar molecules.

The plots of $\Delta\eta$ vs. mole fraction x_1 of butyl propionate at 303.15, 308.15 and 313.15 K are presented in Figure 2. The $\Delta\eta$ values for butyl propionate + tetrahydrofuran exhibits positive deviation at all studied temperatures. These positive $\Delta\eta$ values decrease with increase in temperature. For butyl propionate + 1,4-dioxane, butyl propionate + anisole and butyl propionate + butyl vinyl ether the $\Delta\eta$ values are negative over the entire range of composition at the studied temperature. The effect of temperature on $\Delta\eta$ values is significant as these values found to either decrease or increase systematically with rise in temperature. As suggested by Fort and Moore²⁰ the negative $\Delta\eta$ values in our present study indicate the presence of dispersion forces, while the positive values may be due to the presence of specific interactions between the unlike molecules in the mixtures.

Figure 3 shows that deviations in speeds of sound Δu , values are negative for butyl propionate + tetrahydrofuran, butyl propionate + 1,4-dioxane, butyl propionate + anisole, while for butyl propionate + butyl vinyl ether the Δu values are positive over the entire range of composition at the studied temperature.

Figure 4 shows deviations in isentropic compressibility ΔK_S . From the curves it was observed that for the systems butyl propionate with tetrahydrofuran, 1,4-dioxane and anisole the ΔK_S values are positive, while for butyl propionate + butyl vinyl ether the ΔK_S values are negative over the entire range of composition at the studied temperature. The negative values in case of butyl vinyl ether may be attributed to the weak dipolar interactions between unlike molecules which lead to decrease in the free length, and increase in the speed of sound with increase in composition of n-butyl propionate. The positive ΔK_S values may be due to the fact that the free length is not affected much.

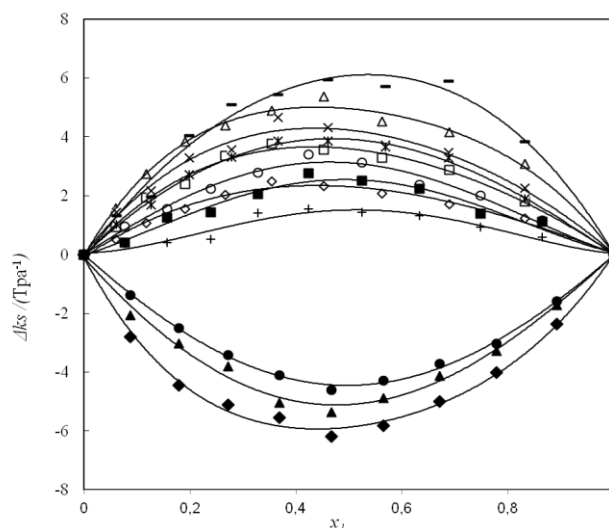


Figure 4. Curves of deviation in isentropic compressibility (ΔK_S) Vs mole fraction for the binary mixtures. Butyl propionate + Tetrahydrofuran at \square , 303.15 K; \diamond , 308.15 K; Δ , 313.15 K; Butyl propionate + 1,4-Dioxane at \times , 303.15 K; κ , 308.15 K; --- , 313.15 K; Butyl propionate + Anisole at \circ , 303.15 K; $+$, 308.15 K; \blacksquare , 313.15 K; Butyl propionate + Butyl vinyl ether \blacklozenge , 303.15 K; \blacktriangle , 308.15 K; \bullet , 313.15 K.

In this study an attempt has also been made to find the predictive ability of the empirical relations proposed by Jouyban–Acree¹⁵⁻¹⁶ and Vandael–Vangeel¹⁷ to correlate the speed of sound data of the studied binary mixtures in terms of pure components. The empirical relations used are as follows:

Jouyban–Acree¹⁵⁻¹⁶

$$\ln u = x_1 \ln u_1 + x_2 \ln u_2 + A_0 \left[\frac{x_1 x_2}{T} \right] + A_1 \left[\frac{x_1 x_2 (x_1 - x_2)}{T} \right] + A_2 \left[\frac{x_1 x_2 (x_1 - x_2)^2}{T} \right] \quad (6)$$

where

A_0 , A_1 , and A_2 are the model constants

u , u_1 and u_2 are the speed of sound of mixture and pure components 1 and 2 respectively.

T is the absolute temperature at which the data has been obtained.

Table 2. Derived parameters of excess functions and standard deviation of binary liquid mixtures

Function	T/K	A ₀	A ₁	A ₂	σ
Butyl propionate(1) + Tetrahydrofuran (2)					
V ^E	303.15	-0.9724	0.2282	-0.4587	0.005
	308.15	-1.1318	0.2745	-0.6654	0.005
	313.15	-1.2727	0.3136	-0.6254	0.005
Δη	303.15	0.1385	-0.0366	0.0128	0.002
	308.15	0.1100	-0.0300	0.0118	0.001
	313.15	0.0889	-0.0206	-0.0054	0.001
Δu	303.15	-115.39	37.97	-19.48	1.3
	308.15	-73.88	23.64	-3.77	1.0
	313.15	-142.75	35.23	-65.09	1.3
ΔKs	303.15	14.409	-3.602	1.312	0.17
	308.15	9.258	-2.223	-0.226	0.14
	313.15	19.845	-3.099	7.565	0.20
Butyl propionate(1) + 1,4-Dioxane (2)					
V ^E	303.15	-0.3496	0.2294	-0.0410	0.003
	308.15	-0.5094	0.1901	-0.9365	0.003
	313.15	-0.5849	0.1625	-0.3490	0.004
Δη	303.15	-0.3971	0.1712	-0.0849	0.002
	308.15	-0.2922	0.1422	-0.0858	0.002
	313.15	-0.2578	0.1355	-0.0551	0.002
Δu	303.15	-151.69	66.07	-45.26	2.40
	308.15	-141.97	47.43	-5.39	1.01
	313.15	-209.34	24.27	-32.35	3.34
ΔKs	303.15	16.917	-3.857	2.780	0.27
	308.15	15.685	-2.169	-1.136	0.11
	313.15	24.397	3.278	2.443	0.39
Butyl propionate(1) + Anisole (2)					
V ^E	303.15	-0.6322	0.0830	-0.0273	0.006
	308.15	-0.8079	-0.1180	-0.3271	0.006
	313.15	-1.1195	0.0052	-0.3022	0.006
Δη	303.15	-0.1325	0.0463	0.0102	0.001
	308.15	-0.1473	0.0513	0.0121	0.001
	313.15	-0.1624	0.0526	-0.0004	0.001
Δu	303.15	-173.83	64.54	13.53	1.84
	308.15	-112.69	16.72	35.95	2.01
	313.15	-144.35	34.95	32.73	1.97
ΔKs	303.15	12.460	-2.451	-3.504	0.20
	308.15	6.036	0.585	-4.467	0.20
	313.15	10.184	-0.394	-4.965	0.23
Butyl propionate(1) + Butyl Vinyl Ether (2)					
V ^E	303.15	-0.9004	0.0742	-0.0093	0.005
	308.15	0.6932	-0.0686	0.0582	0.006
	313.15	1.1762	-0.2137	-0.1678	0.005
Δη	303.15	-0.1341	-0.0167	0.0092	0.001
	308.15	-0.1107	-0.0123	-0.0012	0.001
	313.15	-0.1029	-0.0118	-0.0003	0.001
Δu	303.15	100.44	0.56	30.81	1.62
	308.15	80.84	4.43	-15.21	1.45
	313.15	65.63	11.95	-14.63	0.65
ΔKs	303.15	-23.512	4.393	-7.344	0.23
	308.15	-20.422	2.495	1.725	0.26
	313.15	-17.834	0.440	2.316	0.11

Table 3. Adjustable parameters and standard percentage deviations of models of speed of sound for binary liquid mixtures

T/K	Jouyban-Acree				Vandael-Vangeel
	A ₀	A ₁	A ₂	σ (%)	σ (%)
Butyl propionate(1) + Tetrahydrofuran (2)					
303.15	10.409	-16.836	31.300	0.698	0.091
308.15	10.463	-8.731	31.299	0.564	0.159
313.15	10.768	-8.302	31.299	0.516	0.040
Butyl propionate(1) + 1,4-Dioxane (2)					
303.15	-10.231	8.199	-30.700	0.821	0.156
308.15	-9.894	8.846	-30.699	0.601	0.130
313.15	-10.958	9.682	-30.700	0.591	0.245
Butyl propionate(1) + Anisole (2)					
303.15	-10.900	5.706	-27.656	0.190	0.219
308.15	-10.900	6.047	-29.106	0.280	0.119
313.15	-10.900	5.796	-30.664	0.575	0.174
Butyl propionate(1) + Butyl Vinyl Ether (2)					
303.15	-10.900	2.036	-18.439	0.086	0.307
308.15	-2.5064	-20.80	23.333	0.190	0.263
313.15	-10.900	3.135	-17.761	0.056	0.233

Vandael–Vangeel¹⁷

$$u = \left[\left(\frac{x_1}{M_1 u_1^2} + \frac{x_2}{M_2 u_2^2} \right) (x_1 M_1 + x_2 M_2) \right]^{-0.5} \quad (7)$$

where M_1 and M_2 are molecular weights of the pure components 1 and 2 respectively.

The speed of sound data correlated with the Eqs (6 and 7) were compared with the experimental data in terms of percentage standard deviation $\sigma(\%)$ as obtained by relation

$$\sigma(\%) = \left[\frac{1}{n-k} \frac{\sum \{100(u_{\text{exp}} - u_{\text{cal}})\}^2}{u_{\text{exp}}^2} \right]^{0.5} \quad (8)$$

where n represents the number of data points in each set and k the number of numerical coefficients of equation (6 and 7). u_{cal} has been obtained from model equation (6 and 7). The values of parameters of Equation 7 and the percentage standard deviations $\sigma(\%)$ of equation (8) are given in the Table 3. A perusal of Table 3 shows that the $\sigma(\%)$ values obtained by Vandael–Vangeel relation are very low for systems butyl propionate with tetrahydrofuran, 1,4-dioxane and anisole as compared to Jouyban–Acree model. However for butyl propionate + butyl vinyl ether the $\sigma(\%)$ values obtained by Jouyban–Acree model are very low as compared to Vandael–Vangeel relation. Finally it may be concluded that the Vandael–Vangeel model despite of having no interaction parameters has predicted the speeds of sound of the studied binary mixtures more satisfactorily as compared to Jouyban–Acree model.

Conclusions

Density, viscosity and speed of sound for the binary mixtures of butyl propionate with tetrahydrofuran, 1,4-dioxane, anisole and butyl vinyl ether have been determined at (303.15, 308.15 and 313.15) K over the entire range of composition. From the experimental data excess volume V^E , deviation in viscosities $\Delta\eta$, deviation in speeds of sound Δu and deviation in isentropic compressibilities ΔK_s , were evaluated. These excess or deviation functions found to exhibit both positive and negative deviations. Further the speeds of sound data were correlated using Jouyban–Acree and Vandael–Vangeel models to determine their predictive abilities. It was concluded that Vandael–Vangeel relation despite having no interaction parameters has predicted the speed of sound for the studied binary mixtures more satisfactorily as compared to Jouyban–Acree model.

Acknowledgement

Financial support from University Grants Commission, New Delhi India through Major Research Project (No. 38-24/2009 SR) to the corresponding author (MVR) is gratefully acknowledged. The authors also sincerely acknowledge the Hon'ble Editor and the reviewers for reviewing this paper.

References

- Frenkel, J., *Kinetic Theory of Liquids*, Dover Publications Inc, New York, **1955**, 488.
- Green, H. S., *The Molecular Theory of Fluids*, North Holland Publishing Co, Amsterdam, **1952**, 264.
- Chandler, D., *Ann. Rev. Phys. Chem.* **1978**, 29, 441.

- ⁴Rodriguez, A., Canosa, J., Dominguez, A., Tojo, J., *J.Chem.Eng.Data.*, **2003**, 48, 146
- ⁵Lopez, E. R., Logo, L., Comonas, M. J. P., *J. Chem. Thermodyn.*, **2000**, 32, 743.
- ⁶Iloukhani, H., Rostami, Z., Afshari, N., *J. Phys. Chem. Liq.*, **2009**, 47, 360.
- ⁷Fernando, E., Ortega, J., Penco, E., Wisniak, J., *Ind. Eng Chem. Res.*, **2010**, 49, 9548.
- ⁸Lien, P. J., Wu, S. T., Lee, M. J., Lin, H. M. *J. Chem. Eng. Data.*, **2003**, 48, 632
- ⁹Patwari, M. K., Bachu, R. K., Boodida, S., Nallani, S., *J. Chem. Eng. Data.*, **2009**, 54, 1069.
- ¹⁰Sheu, Y. W., Tu, C. H., *J. Chem. Eng. Data.*, **2006**, 57, 545.
- ¹¹Rathnam, M. V., Kavita, R. B., Reema, S. T., Kumar M. S. S., *Eur. Chem. Bull.*, **2013**, 2(7),434.
- ¹²Rathnam, M. V., Sudhir, M., Nandini, M., *J. Mol. Liq.*, **2013**, 177, 229.
- ¹³Rathnam, M. V., Sudhir, M., Kumar, M. S. S., *J. Serb. Chem. Soc.*, **2012**, 77(4), 507.
- ¹⁴Rathnam, M. V., Sharad, M., Kirti, J., Kumar, M. S. S., *J. Sol. Chem.* **2012**, 41, 475
- ¹⁵Jouyban, A. A., Fathi, A. A., Jafari, K. M., Acree, Jr., W. E., *Indian J. Chem.*, **2005**, 44A, 1553.
- ¹⁶Jouyban, A., Jafari, K. M., Vaez, G. Z., Fekari, Z., Acree Jr., W. E., *Chem. Pharm. Bull.*, **2005**, 53, 519
- ¹⁷Vadeal, W., Vangeel, E., *Proc. of 1st Int. Conf. Calor. Thermodyn., Warsaw*, **1969**, p. 556.
- ¹⁸Redlich, O., Kister, A. J., *Ind. Eng.Chem.* **1948**, 40, 345.
- ¹⁹Ali, A., Nain, A. K., *Pramana J. Phys.*, **2002**, 58, 695.
- ²⁰Fort, R. J., Moore, W. R., *Trans. Faraday Soc.*, **1966**, 62, 1112.

Received: 19. 03. 2013.

Accepted: 23. 04. 2013.



SYNTHESIS AND REACTIONS OF 2-(4-BROMOPHENYL)-4H-3,1-BENZOXAZINE-4-ONE

Maher A.El-Hashash and Dalal B.Guirguis

Keywords: Benzoxazin-4-one, 2,3-disubstituted quinazolin-4-one, glycine

A new series of 2,3-disubstituted quinazolin-4(3H)-one derivatives was synthesized via nucleophilic attack at C(2) of the corresponding key starting material 2-(4-bromophenyl)-4H-3,1-benzoxazin-4-one (Scheme 5). The reaction proceeded via amidinium salt formation (Scheme 3) rather than via an N-acyl anthranilamide. The structure of the prepared compounds were elucidated by physical and spectral data like FT-IR, ¹H-NMR, and mass spectroscopy.

Corresponding Authors

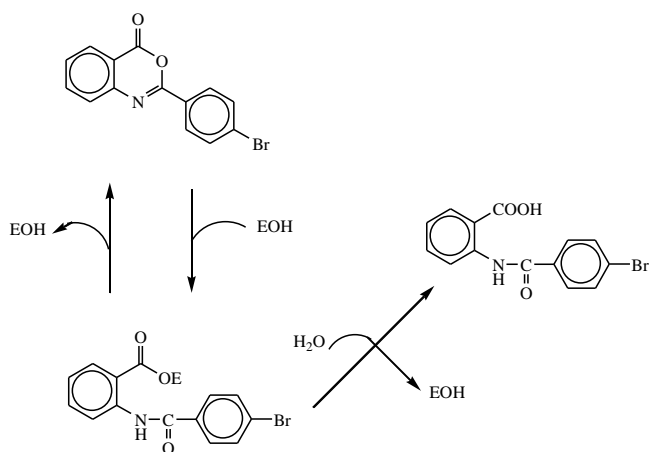
Tel:+201281033369

E-Mail: dalal.guirguis@hotmail.co.uk

[a] Department of Organic Chemistry, Faculty of Science, Ain Shams University, 11566 Abbseya, Cairo, Egypt

Introduction

Due to their interesting biological and other properties, 4H-3,1-benzoxazin-4-one derivatives are an important class of compounds.¹⁻⁴ Like other heterocyclic compounds, they are used directly or indirectly in many industrial research, and clinical applications. They can be used as starting material for different clinically used 4-quinazolone derivatives.⁵⁻⁹ Benzoxazinone derivatives are also used as antiphlogistic drugs.²⁻¹⁰ Anthalexine, another compound of this type, finds use as an antifungal and antibacterial agent.¹¹⁻¹⁴ Several 4H-3,1-benzoxazin-4-ones have been demonstrated to be alternate inhibitors of human leukocyte elastase (HLE), forming acyl-enzyme intermediate during catalysis. It was demonstrated that electron withdrawal at position 2 gives better inhibition because acylation rates are increased. 4H-3,1-Benzoxazin-4-ones was shown to be active in vivo after intracheal administration. Benzoxazinones temporarily inhibit the catalytic activity of serine protease by accumulation of a catalytically inactive acyl-enzyme intermediate (Scheme1). The rates of acylation and deacylation, as well as compound selectivity, are determined by substitution at the benzene ring unit and the 2-substituent.

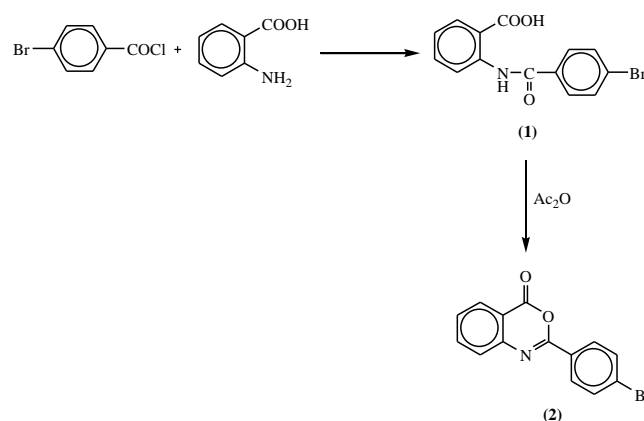


Scheme 1.

According to the reaction of 2-(4-bromophenyl)-4H-3,1-benzoxazin-4-one with serine protease (formation of acyl-enzyme, with a possible way of deacylation), prompted us to synthesis the 2-(4-bromophenyl)-4H-3,1-benzoxazin-4-one **2**, which posses an electron withdrawal group at position 2.

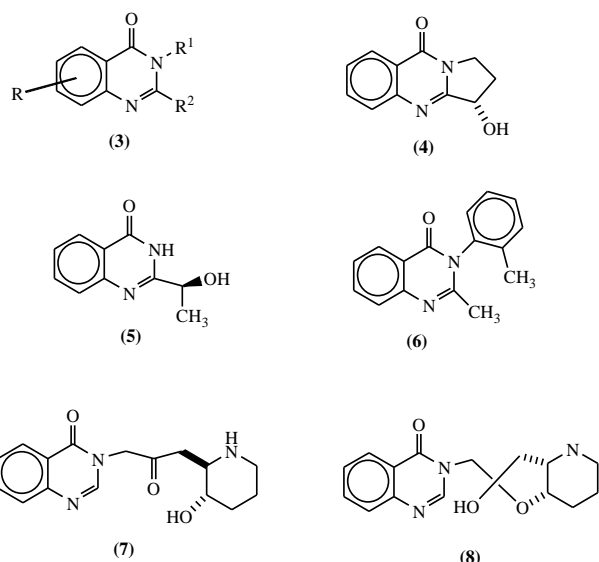
Results and discussion

The benzoxazinone derivative **1** was obtained via the interaction of 4-benzoyl chloride with anthranilic acid in pyridine, afforded the corresponding anthranil. The desired product **2** was obtained via ring closure of **1** with acetic anhydride (Scheme2).



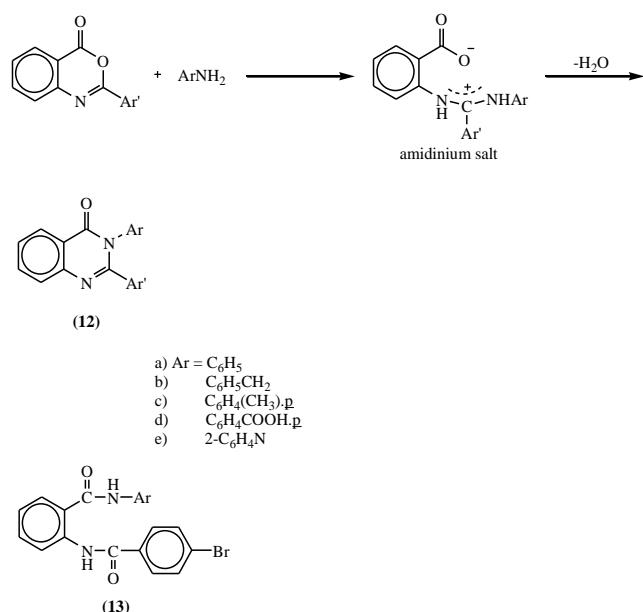
Scheme 2.

Considering the structure of 4-H-3,1-benzoxazin 4-one derivatives, there are two available sites for nucleophilic attack (C-2 and C-4), i.e. two different sites with partial positive charge that can lead to the opening of the oxazinone moiety by different nucleophiles. In most cases, reclosure of the heterocyclic part of the molecule is favored and provides a new compound with interesting biological properties.^{15,16} The **2** is considered as a key starting material for the synthesis of many heterocyclic systems. 3H-Quinazolin-4-one (**3**) is a frequently encountered unit in natural products such as L-vasicineone (**4**),^{17,18} chrysgine (**5**),¹⁹ and drugs as methqualone (**6**),²⁰ febrifungine (**7**), and isofebrifungine (**8**). The latter two compounds are potent but toxic antimalarial drugs. Molecules based on quinazoline and quinazolinone exhibit a multitude of interesting pharmacological,²¹ including anticonvulsant, antibacterial, and antidiabetic activity.^{22,23}



The aim of the present work is to synthesis quinazolin-4(3H)-one derivatives via interaction of benzoxazinone derivative **2** with nitrogen nucleophiles.

Thus, when **2** was submitted to react with formamide in boiling oil bath yielded 2-(4-bromo)-4(3H)-quinazolin-4-one (**9**). It was reported that 4H-3,1-benzoxazin-4-one derivatives react with semicarbazide (hydrazine-carboxamide) in boiling glacial acetic acid, afforded 2-propyl[1,2,4]triazolo[1,5-c]quinazolin-2(3H)-one.²⁴ Thus, upon treatment of **2** with hydrazine carboxamide in pyridine afforded 2-(4-bromophenyl)-[1,2,4]triazolo[1,5-c]quinazolin-2(3H)-one (**10**). The reaction took place via hetero ring opening at C-4 followed by double ring closure to yield the desired product.



Scheme 3.

Heating **2** in neat hydrazine hydrate afforded 3-amino-2-(4-bromophenyl)quinazolin-4(3H)-one (**11a**) while upon hydrazinolysis with phNHNH₂ provided the quinazolinone **11b**.

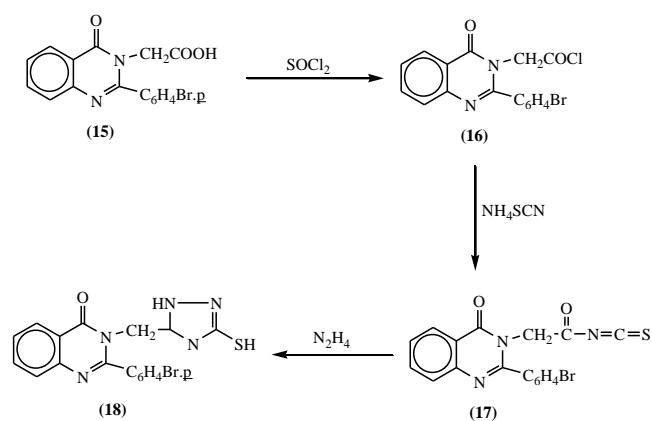
When aniline, benzylamine, and substituted aniline namely: 4-methylaniline (p-toluidine), 4-aminobenzoic acid, and 2-aminopyridine reacted with **2**, the 3-aryl-2-(4-bromophenyl)quinazolin-4(3H)-one derivatives **12a-e** were obtained (Scheme2). One can interpret these results as follows:

The N-nucleophile attack **2** in a fashion in which the amino group first undergoes H-bonding to the N-atom of the heterocyclic ring, then the amino group reacts by nucleophilic addition at the “azavinylic” C-2 forming an inner amidinium salt which subsequently dehydrated giving **12a-e** (Scheme 3).

The elemental analysis and spectroscopic datae for **12** are consistent with the assigned structures. No isolation of 2-(4-bromobenzoylamino)benzamide derivatives **13** ruled out the nucleophilic addition to C-4.

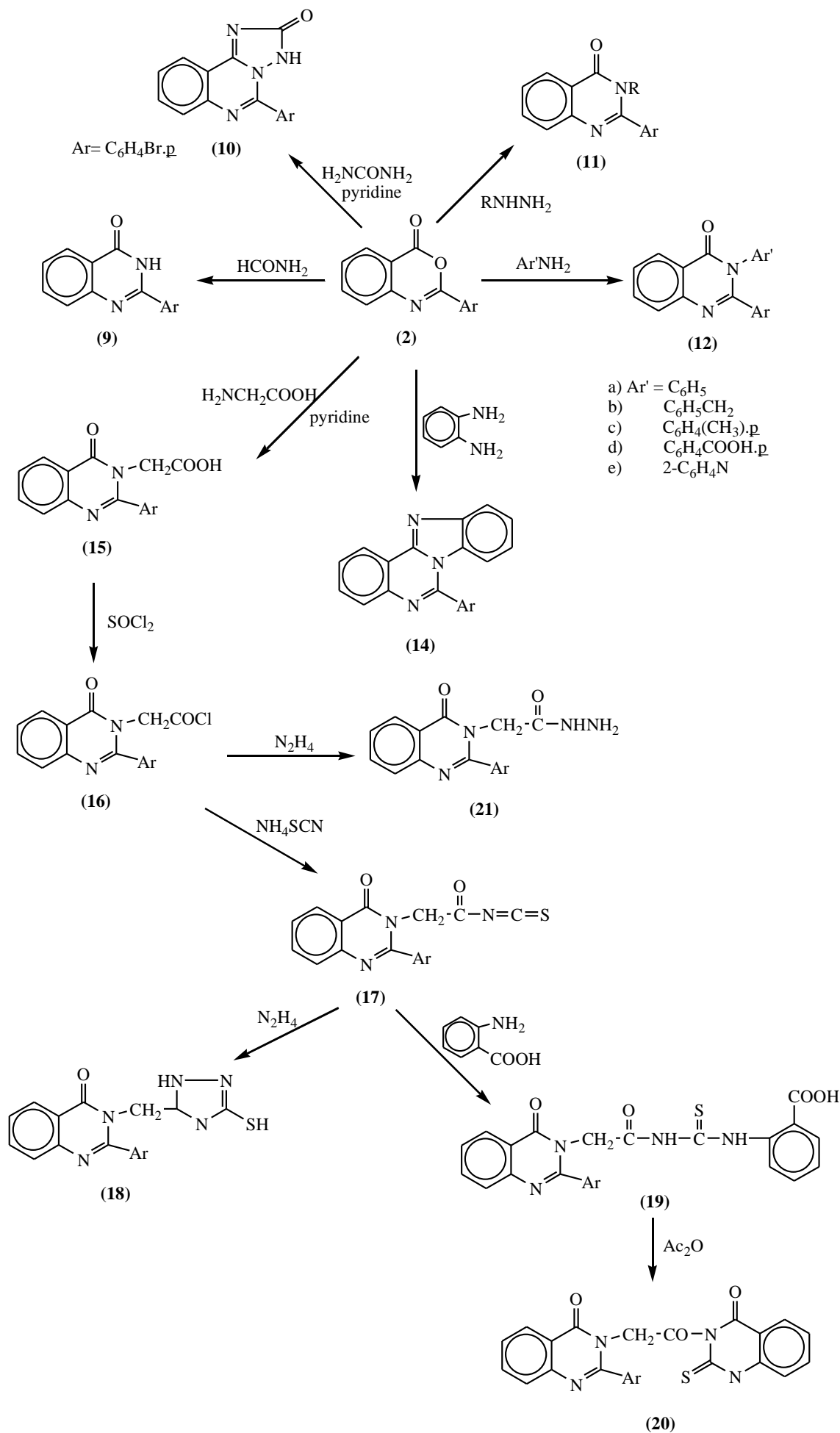
Fusion of **2** with o-phenylene diamine in an oil bath afforded 2-(4-bromophenyl)benzimidazolo[1,2-c]quinazolin (**14**), also when it was allowed to react with glycine in boiling pyridine, it gave [2-(4-bromophenyl)-4-oxoquinazolin-3-yl]acetic acid (**15**).

When **15** was treated with thionyl chloride on a heated water bath, yielded the corresponding acid chloride **16** as a fleeting (not isolated) intermediate, followed by a reaction with ammonium thiocyanate yielding the [2-(4-bromophenyl)-4-oxoquinazolin-3-yl]acetyl isothiocyanate (**17**) which on turn reacted with hydrazine hydrate giving 2-(4-bromophenyl)-3-[(3-mercapto-1H-1,2,4-triazolo-5-yl)methyl]-4(3H)-quinazolin-4-one (**18**).



Scheme 4.

Similarly, **17** reacted with anthranilic acid, yielded 2-[[2-(4-bromophenyl)-4-oxo-quinazolin-3-yl]acetyl thiocarbonyl amino benzoic acid (**19**). Treatment of **19** with boiling acetic anhydride afforded 2-(4-bromophenyl)-3-[2-oxo-2(4-oxo-2-thioxo-1,4-dihydroquinazolin-3(2H)-yl)ethyl]-4(3H)-quinazolin-4-one (**20**). Interaction of **16** with hydrazine hydrate in boiling toluene afforded 2-[2-(4-bromophenyl)-4-oxoquinazolin-3-yl]acetohydrazide (**21**).



Experimental Part

All melting points recorded are uncorrected and are determined on Gallen Kamp apparatus. The IR were recorded on Perkin Elmer 398 spectrophotometer, ¹H-NMR spectra were recorded on Varian Gemini, 300 MHz instrument. MS spectra were obtained on Shimadzu, GCMS QP 1000 Ex mass spectrophotometer (70 eV). Micro analytical data were obtained from the microanalytical center at Cairo University, Giza, Egypt.

2-(4-Bromobenzoyl)aminobenzoic acid (1)

A solution of o-aminobenzoic acid (1.37 g, 0.01 mol) in dry pyridine (3 ml) was treated with a solution of 4-bromobenzoyl chloride (0.01 mol) in dry pyridine (3 ml) drop by drop with stirring for 15 minutes. The reaction mixture was poured onto ice/HCl. The solution that separated was filtered off and recrystallized from ethanol: **1**, yield (80 %), colourless crystals, m.p. 190 °C. IR(KBr): 1660 (C=O amide), 1680 (C=O of acid), 3220 (NH), 3300, (OH, basin peak) cm⁻¹. ¹H-NMR (DMSO-d₆): 6.98-8.11 (m, 8H, Ar-H), 9.2 (s, 1H, NH, D₂O exchangeable) 12.11 (s, 1H, OH, D₂O exchangeable). MS (319, 321, M⁺, M⁺+2). Anal.: calcd for C₁₄H₁₀BrNO₃: C 52.32, H 3.34, N 4.37, Br 24.95; found: C 52.52, H 3.14, N 4.57, Br 24.57.

2-(4-Bromophenyl)-4H-3,1-benzoxa-4-one (2)

A suspension of aminobenzoic acid derivative **1** (3.2 g, 0.01 mol) in freshly distilled acetic anhydride (10 ml) was heated under reflux for 1 h, and then was concentrated. The solid that was separated was crystallized from benzene: **2**, yield (75 %), pale yellow crystals m.p. 166 °C. IR (KBr): 1617 (C=N), 1762 (C=O) cm⁻¹. ¹H-NMR (DMSO-d₆): 6.88-8.92 (m, 8H, Ar-H). MS: 301, 303 (M⁺, M⁺+2). Anal.: calcd for C₁₄H₈BrNO₂: C 55.62, H 2.68, N 4.55, Br 26.45; found: C 55.55, H 2.56, N 4.36, Br 26.64.

2-(4-Bromophenyl)-4(3H)-quinazolin-4-one (9)

A mixture of **2** (3.02 g, 0.01 mol) and formamide (10 ml) was heated under reflux for 2 h, after cooling, the reaction mixture was poured onto water. The precipitate that separated was filtered off and crystallized from ethanol: **9**, yield (70 %), m.p. 276 °C. IR(KBr): 1602 (C=N), 1676 (C=O), 3122 (NH) cm⁻¹. ¹H-NMR (DMSO-d₆): 6.99-8.11 (m, 8H, Ar-H), 10.89 (s, 1H, NH, D₂O exchangeable). Anal.: calcd for C₁₄H₉BrN₂O: C 55.81, H 2.95, N 9.03, Br 26.37; found: C 55.51, H 2.75, N 9.45, Br 26.37.

2-(4-Bromophenyl)[1,2,4]triazolo[1,5-c]quinazolin-2(3H)-one(10)

A mixture of **2** (3.02 g, 0.01 mol) and semicarbazide (0.01 mol) in pyridine (15 ml) was heated under reflux for 3 h. The reaction mixture after cooling was poured onto ice/HCl. The solid that separated was filtered off and crystallized from ethanol: **10**, yield (65 %) m.p. 128 °C. IR(KBr): 1599 (C=N), 1680 (C=O), 3321 (NH) cm⁻¹. ¹H-NMR (DMSO-d₆): 6.80-8.11 (m, 8H, Ar-H), 9.2 (s, 1H, NH, D₂O exchangeable). Anal.: calcd for C₁₅H₉BrN₄O: C 52.65, H 2.94, N 16.37, Br 23.35; found : C 52.55, H 2.74, N 16.57, Br 23.55.

3-Amino and 3-phenylamino-2(4-bromophenyl)quinazolin-4(3H)-one (11a and 11b)

A mixture of **2** (3.02 g, 0.01 mol) and hydrazine hydrate and/or phenylhydrazine (0.015 mol) in n-butanol (10 ml) was heated under reflux for 3 h. The solid that separated after cooling was filtered off and crystallized from butanol for **11a** and xylene for **11b**.

3-Amino-2-(4-bromophenyl)quinazolin-4(3H)-one (11a): yield (61 %), m.p. 188 °C. IR(KBr): 1637 (C=N), 1668 (C=O), 3217, 3311 (NH) cm⁻¹. M.S: 315, 317 (M⁺, M⁺+2). Anal.: calcd for C₁₄H₁₀BrN₃O: C 53.18, H 3.18, N 13.29, Br 25.27; found: C 53.28, H 3.18, N 3.18, Br 25.17.

3-Phenylamino-2-(4-bromophenyl)quinazolin-4(3H)-one (11b): yield (55%), m.p. 144 °C. IR(KBr): 1683 (C=O), 3249 (NH) cm⁻¹. Anal.: calcd for C₂₀H₁₄BrN₃O: C 61.24, H 3.59, N 10.71, Br 20.37; found: C 61.34, H 3.49, N 10.51, Br 20.37.

3-Aryl-2-(4-bromophenyl)quinazolin-4(3H)-ones, (12a-12e)

A solution of **2** (3.02 g, 0.01 mol) and aromatic amines namely; aniline, benzylamine, p-toluidine, p-aminobenzoic acid, and 2-aminopyridine (0.01 mol) in ethanol (40 ml) was heated under reflux for 3 h. The solids that separated after cooling were crystallized from toluene for **12a**, n-butanol for **12b** and **12c** ethanol for **12d** and xylene for **12e**.

3-Phenyl-2-(4-bromophenyl)quinazolin-4(3H)-one (12a): yield (60 %), m.p. 136 °C, IR(KBr): 1618(C=N), 1675 (C=O) cm⁻¹. Anal.: calcd for C₂₀H₁₃BrN₂: C 63.67, H 3.47, N 7.42, Br 21.18; found: C 63.47, H 3.37, N 7.42, Br 21.38.

3-Benzyl-2-(4-bromophenyl)quinazolin-4(3H)-one (12b): yield (65 %) m.p. 132 °C. IR(KBr): 1615 (C=N), 1680 (C=O) cm⁻¹. Anal.: calcd for C₂₁H₁₅BrN₂O: C 64.46, H 3.86, N 7.15, Br 20.24; found: C 64.56, H 3.66, N 7.13, Br 20.42.

3-(4-Methylphenyl)-2-(4-bromophenyl)quinazolin-4(3H)-one (12c) : yield (65%), m.p.148 °C. IR(KBr): 1615 (C=N), 1680 (C=O) cm⁻¹. Anal.: calcd for C₂₁H₁₅BrN₂O: C 64.46, H 3.86, N 7.15, Br 20.24; found: C 64.24, H 3.96, N 7.25, Br 20.44.

4-[4-Oxo-2-(4-bromophenyl)quinazolin-4(3H)-yl]benzoic acid (12d): yield (65%), m.p.186 °C. IR (KBr) γ : 1620 (C=N), 1680, 1687(C=O), 3200 (basin peak chelated OH) cm⁻¹. ¹H-NMR (d₆ DMSO): 7.11-8.99 (m, 12H, Ar-H), 12.5 (s, 1H, OH, D₂O exchangeable). Anal. Calcd C₂₁H₁₃BrN₂O₃: C 43.39, H 2.25, N 4.81, Br 13.75; found: C 43.59, H 2.45, N 4.61, Br 13.64.

3-(Pyridin-2-yl)-2-(4-bromophenyl)quinazolin-4(3H)-one (12e) : yield (55%). m.p. 140 °C, IR (KBr) γ : 1620 (C=N), 1687 (C=O) cm⁻¹. Anal. Calcd for C₁₉H₁₂BrN₃O: C 60.33, H 3.19, N 7.15, Br 21.12; found : C 60.13, H 3.29, N 11.42, Br 21.42.

2-(4-Bromophenyl)-benzimidazolo[1,2-C]quinazoline (14)

A mixture of **2** (3.02 g, 0.01 mol) and o-phenylene diamine (1.5 g, 0.01 mol) was heated in oil bath at 160 °C

for 2 h. The reaction product was treated with water and the solid that obtained was crystallized from ethanol. **14**: yield (77 %). m.p. 230 °C. IR(KBr): 1620 (C=N) cm^{-1} . MS. 373, 375 (M^+ , $\text{M}^+ + 2$). Anal.: calcd for $\text{C}_{20}\text{H}_{12}\text{BrN}_3$: C 64.81, H 3.23, N 11.22, Br 21.35; found: C 64.28, H 3.13, N 11.08, Br 21.15.

[2-(4-Bromophenyl)-4-oxoquinazolin-3-yl]acetic acid (**15**)

A mixture of **2** (3.02 g, 0.01 mol) and glycine (0.015 g, 0.01 mol) in pyridine (20 ml) was heated under reflux for 2 h. The reaction mixture was poured on ice/HCl, the solid that separated was filtered off and crystallized from methanol. **15**: yield (67 %) m.p. 174 °C. IR(KBr): 1610 (C=N), 1683 (C=O cyclic amide), 1722 (C=O of carboxylic), 3365 (broad peak chelated OH) cm^{-1} . $^1\text{H-NMR}$ (DMSO- d_6): 2.49 (s, 2H, methylene protons 7.18-8.66 (m, 8H, Ar-H), 12.26 (s, broad, 1H, OH, D_2O exchangeable). Anal.: calcd for $\text{C}_{16}\text{H}_{11}\text{BrN}_2\text{O}_3$: C 53.50, H 3.08, N 7.79, Br 27.25; found: C 53.40, H 3.18, N 7.59, Br 27.35.

[2-(4-Bromophenyl)-4-oxoquinazolin-3-yl]acetyl isothiocyanate(**17**)

A mixture of **8** (3.59 g, 0.01 mol) and thionyl chloride (10 ml) was heated on water bath for 2 h. Excess of thionyl chloride was removed by distillation under reduced pressure, a semisolid product was obtained treated with a solution of ammonium thiocyanate (1.5 g, 0.02 mol) in dry acetone (30 ml) with stirring for 30 min. The solid that separated after distillation of acetone was crystallized from dimethylformamide. **17**: yield (60 %), m.p. 150 °C. IR (KBr): 1620 (C=N), 1675 (C=O) cm^{-1} . Anal.: calcd for $\text{C}_{17}\text{H}_{10}\text{BrN}_3\text{O}_2\text{S}$: C 49.12, H 3.34, N 14.32, Br 20.42, S 8.06; found: C 49.22, H 3.34, N 14.11, S 7.85, Br 20.22

[2-(4-Bromophenyl)-3[(3-mercapto-1H-1,2,4-triazolo-5-yl)methyl]-3H]quinazolin-4-one(**18**)

A mixture of **17** (2 g, 0.005 mol) and hydrazine hydrate (0.01 mol) was refluxed in dry benzene (30 ml) for 3 h. The solid that separated after cooling was filtered off and crystallized from ethanol. **18**: yield (57 %), m.p. 167 °C. IR(KBr): 1671 (C=O), 2567 (SH), 3243 (NH) cm^{-1} . $^1\text{H-NMR}$ (DMSO- d_6): 4.22 (s, 2H, methylene protons), 5.53 (s, 1H, SH D_2O exchangeable), 9.88 (s, 1H, NH, D_2O exchangeable). Anal.: calcd for $\text{C}_{17}\text{H}_{12}\text{BrN}_5\text{OS}$: C 49.27, H 2.90, N 16.90, S 7.73, Br 19.10; found: C 49.67, H 2.71, N 16.55, S 7.93, Br 19.55.

2-{[2-(4-Bromophenyl)-4-oxoquinazolin-3-yl]acetylthio-carbamoyl}aminobenzoic acid (**19**)

A mixture of **17** (2 g, 0.005 mol) and anthranilic acid (1.37 g, 0.01 mol) in dry acetone (30 ml) was heated under reflux for 3 h. The solid that separated after distillation of acetone was diluted with water and filtered off and crystallized from benzene. **19**: yield (70 %), m.p. 183 °C. IR(KBr): 1665, (C=O), 3182 (NH), 3380 chelated (OH) cm^{-1} . Anal.: calcd for $\text{C}_{24}\text{H}_{17}\text{BrN}_4\text{O}_4\text{S}$: C 49.48, H 2.91, N 16.90, S 5.95, Br 19.28; found: C 49.84, H 2.71, N 16.70, S 5.53, Br 19.48.

2-(4-Bromophenyl)-3-[2-oxo-2(4-oxo-2thioxo-1,4-dihydroquinazolin-3(2H)-yl)ethyl]-4(3H)-quinazolin-4-one (**20**)

A solution of **19** (2.65 g, 0.005 mol) in freshly distilled acetic anhydride (10 ml) was heated on water bath for 2 h. The solid that separated after cooling was crystallized from ethanol: yield (52 %), m.p. 166 °C. IR(KBr): 1241 (C=S), 1630, 1680 (C=O), 3180 (NH) cm^{-1} . $^1\text{H-NMR}$ (DMSO- d_6): 2.8 (s, 2H, CH_2), 7.2-8.8 (m, 2H, Ar-H), (s, 1H, NH, D_2O exchangeable). Anal.: calcd. for $\text{C}_{24}\text{H}_{15}\text{BrN}_4\text{O}_3\text{S}$: C 53.64, H 3.18, N 10.42, S 6.16, Br 14.86; found: C 53.74, H 3.38, N 10.62, S 6.36, Br 14.76.

2-[2(4-Bromophenyl)-4-oxoquinazolin-3-yl]acetohydrazide (**21**)

A solution of the acid chloride (0.01 mol) and hydrazine hydrate (0.015 mol) in toluene (30 ml) was heated under reflux for 2 h.

The solid that separated after cooling was filtered off and crystallized from ethanol: **21** yield (63 %), m.p. 168 °C. IR(KBr): 1590 (C=N), 1683 (C=O), 3200, 3280 (NH) cm^{-1} . Anal.: calcd for $\text{C}_{16}\text{H}_{13}\text{BrN}_4\text{O}_2$: C 55.61, H 2.72, N 10.80, Br 15.41; found: C 55.34, H 2.52, N 10.75, Br 15.21.

REFERENCES

- Peet, N. P. and Sunder, N. P., *U. S. Patent*, **1983**, 4, 419, 357.
- Wilker, P. and Wilson, *J. Am. Chem. Soc.*, **1955**, 77, 5598.
- Drummond, G. I. and Severson, D. L., *Circ. Res.*, **1979**, 44, 1945.
- Belluci, C., Gualtieri, F. and Chiarine, A., *Eur. J. Med. Chem.* **1987**, 22, 473.
- Armarego, W. L. F., *Adv. Heterocyclic. Chem.*, **1979**, 24, 17.
- Amin, A. H., Mehta, D. R. and Samart, S. S., *Arzn. Forsch.*, **1970**, 14, 218.
- Ager, I. R., Harrison, D. R., Kennewel, P. D., and Taylor, J. B., *J. Med. Chem.* **1977**, 20, 379.
- Armarego, W. L. F., *Adv. Heterocyclic. Chem.* **1963**, 1, 304.
- Gupta, B. M., Agraval, U. and Khan, S. K., *Indian J. Exp. Biol.*, **1963**, 7, 61.
- Wikder, P. and Wilson, A., *J. Am. Chem. Soc.*, **1955**, 77, 5598.
- Bouillant, M. L., Farre-Bonvin, J. and Ricci, J. P., *Tetrahedron Lett.*, **1983**, 24, 51.
- Donchet, M., Martin-Tuguy, J., Marais, A. and Pupet, A., *Phytochem.*, **1981**, 23, 1901.
- Mayama, S., Tani, T., Uneo, T. and Hirabayashi, K., *Tetrahedron Lett.*, **1981**, 22, 2103.
- Mayama, S., Tani, T. and Matsura, Y., *J. Am. Oil Chem. Soc.*, **1981**, 5, 697.
- Krantz, A., Spencer, R. W., Tam, T. F., Thomas, E. M. and Rafferty, S. P., *J. Med. Chem.* **1990**, 33, 464.
- Mitsuhashi, H., Nonka, T., Hamumara, I., Kishimoto, T., Muratoni, E., Fujii, K. Br., *J. Pharmacol.*, **1999**, 126, 1147.
- Jone, S., *Prog. Chem. Org. Nat. Prod.*, **1984**, 46, 159-229.
- Eguchi, S., Suzuki, T., Okawa, T., Matsushita, Y., Yashima, E. and Okamoto, Y., *J. Org. Chem.* **1996**, 61, 7316-7319.
- Bergman, J. and Brynolf, A., *Tetrahedron*, **1990**, 46, 1295-1310.

²⁰ Kacker, I. K. and Zaheer, S. H., *J. Indian Chem. Soc.* **1951**, 28, 344-346.

²¹ Aramergo, W. L. F., *Adv. Heterocycl. Chem.* **1979**, 24, 1-62

²² Jiang, J. B., Hessian, D. P., Dusak, B. A., Dexter, D.L., Kang, G. J. and Hamel, *J. Med. Chem.*, **1990**, 33, 1721

²³ Meyer, J. F. and Wanger, E. C., *J. Org. Chem.* **1943**, 8, 239-252.

²⁴ El-Hashash, M. and El-Badry, Y. A., *Helv. Chim. Acta*, **2011**, 94, 389.

Received: 31.03.2013.

Accepted: 26.04.2013.



CYCLIC VOLTAMMETRIC STUDY OF PROTECTIVE FILM FORMED BY 2-CARBOXYETHYLPHOSPHONIC ACID - Ni²⁺ SYSTEM ON CARBON STEEL

K. Kavipriya^[a], J. Sathiyabama^[a] and S. Rajendran^{[a,b]*}

Keywords: corrosion inhibition; carbon steel; sea water; cyclic voltammetry; FTIR

The corrosion inhibition effect of carbon steel in sea water by 2-carboxyethylphosphonic acid (2-CEPA) and Ni²⁺ has been investigated using weight loss method and cyclic voltammetry. The results show that 73% inhibition efficiency is achieved with binary system consisting of 250 ppm of 2-CEPA and 50 ppm of Ni²⁺. Surface evaluation technique like FTIR is used to determine the nature of the protective film formed on the metal surface. The protective film consists of Fe²⁺ – 2-CEPA complex, Ni²⁺ – 2-CEPA complex and Ni(OH)₂. Cyclic voltammetry study reveals that the protective film is more compact and stable even in 3.5% NaCl environment.

Corresponding Authors

E-Mail: sennikavi@yahoo.co.in

[a] Corrosion Research Centre, PG and Research Department of Chemistry, GTN Arts College, Dindigul, India 624 005, E-mail: sennikavi@yahoo.co.in

[b] * RVS School of Engineering and Technology, Dindigul, India 624 005, E-mail: srmjoany@sify.com

INTRODUCTION

The corrosion in sea water is severe due to the presence of chloride ions and dissolved oxygen. Corrosion can cause great damages to marine steel infrastructures such as bridges, wharfs, platforms, and pipeline systems. It has been estimated that some 20% of the corrosion cost is due to microbial corrosion and degradation.¹ Metals obtain stability when their surfaces are separated from the normal terrestrial environment.² If this isolation is not achieved, they undergo a process of embrittlement, suffer fatigue, and transform into oxides, which peel off or just dissolve away. Metals become unstable when they contact moist atmosphere containing carbon-dioxide or sodium chloride suspension in marine atmosphere. The spontaneous corrosion of metal or its alloys results from the charged transfer reactions at their interface between the metal and its electrolytic environment.^{3,4} The goal of studying the processes of corrosion is to find methods of minimizing or preventing it. Inhibition of corrosion and scaling can be done by the application of inhibitors. Most of the organic inhibitors containing nitrogen, oxygen, sulfur atoms, and multiple bonds in their molecules facilitate adsorption on the metal surface.^{5,6} Several phosphonic acids have been used as corrosion inhibitor.⁷⁻¹¹ Phosphonic acids are organic compounds containing R-PO(OH)₂ or R-PO(OR)₂ groups. They are effective chelating agents that are used in cooling water and desalination systems to inhibit scale formation and corrosion. Phosphonic acids are extensively used now-a-days due to their complex forming abilities, high stability under harsh conditions, and low toxicity.^{12,13} The inhibition efficiency of phosphonates depends on the number of phosphono groups in a molecule and also on different substituents. Compounds with a phosphonic functional group are considered to be the most effective chemical for inhibiting

the corrosion process and it is well known that short-chain-substituted phosphonic acids are good corrosion inhibitors for iron and low-alloyed steels.¹⁴

An environmental friendly compound, 2-carboxyethylphosphonic acid, contains not only phosphono groups, but also carboxyl and ethyl groups, which can decrease corrosion. The present study aims **a**) to find out the corrosion inhibition effects of 2-CEPA and Ni²⁺ system on carbon steel in sea water medium using weight-loss method; their inhibitive action is due to coordination of the oxygen atom of the carboxylate anion to the metal ions to form metal-inhibitor complexes **b**) electrochemical techniques provide information on the corrosion rate, as well as on processes at interfaces affected by additives **c**) to analyze the protective film by Fourier Transform Infrared Spectroscopy (FTIR) **d**) to propose a suitable mechanism of corrosion inhibition based on the results from the above studies.

EXPERIMENTAL

Preparation of Specimen

Carbon steel specimen [0.0267 % S, 0.06 % P, 0.4 % Mn, 0.1 % C and the rest iron] of dimensions 1.0 cm x 4.0 cm x 0.2 cm were polished to a mirror finish and degreased with trichloroethylene.

Weight-Loss Method

Carbon steel specimens in triplicate were immersed in 100 mL of the solutions containing various concentrations of the inhibitor in the presence and absence of Ni²⁺ (as NiSO₄ · 6H₂O) for one day. The weight of the specimens before and after immersion was determined using a Shimadzu balance, model AY62. The corrosion products were cleaned with Clarke's solution.¹⁵ The inhibition efficiency (IE, %) was then calculated using the equation:

$$IE = 100 \left[1 - \frac{W_2}{W_1} \right] \quad (1)$$

where W_1 is the weight loss value in the absence of inhibitor and W_2 is the weight loss value in the presence of inhibitor.

Cyclic Voltammetry

Cyclic voltammograms were recorded in VersaSTAT MC electrochemical system. A three-electrode cell assembly was used. The working electrode was carbon steel. The exposed surface area was 1 cm². A saturated calomel electrode (SCE) was used as the reference electrode and a rectangular platinum foil was used as the counter electrode. The cyclic voltammetry curves were recorded in the scan range of -1.8 to -1.8 V (SCE) with a scan rate of 20 mV s⁻¹.

Fourier Transform Infrared Spectra (FTIR)

The FTIR spectra were recorded in a Perkin-Elmer-1600 spectrophotometer. The film formed on the metal surface was carefully removed and mixed thoroughly with KBr making the pellet.

RESULTS AND DISCUSSION

Weight-Loss Method

The physicochemical parameters of sea water are given in Table 1. Table 2 gives values of the corrosion inhibition efficiencies and the corresponding corrosion rates of 2-carboxyethyl phosphonic acid (2-CEPA) – Ni²⁺ in controlling corrosion of carbon steel in sea water for a period of 24 hours at room temperature. The 2-CEPA alone has high rate of corrosion. The inhibition efficiency of 2-CEPA is improved by adding various concentrations of Ni²⁺. Similar observations have been made by Abdallah et al.,¹⁶ who studied the inhibiting effect of 3-methylpyrazolone with Ni²⁺ cation for carbon steel in sulfuric acid solution. However, increasing the concentration of 2-CEPA as well as Ni²⁺, the maximum inhibition is achieved and the corrosion rate is decreased. It is found that 250 ppm of 2-CEPA and 50 ppm of Ni²⁺ has 73% inhibition efficiency. The inhibition efficiency increases with the increase of concentration of inhibitors. This behavior could be attributed to the increase of the surface area covered by the adsorbed molecules of phosphonic acid with the increase of its concentration. It is generally assumed that the adsorption of the inhibitor at the metal/solution interface is the first step in the mechanism of inhibition in aggressive media.

Cyclic Voltammetry

Cyclic voltammograms have been used to investigate the corrosion behaviour of metals.¹⁷⁻²⁰ Deyab and Keera²⁰ have analysed the influence of sulphide, sulphate, and bicarbonate anions on the pitting corrosion behaviour of carbon steel in formation water containing chloride ions by means of cyclic voltammetry technique. The cyclic voltammograms were recorded in the presence of

increasing amounts (0.1 to 0.3 M) of NaCl at a scan rate of 10 mV s⁻¹. The anodic response exhibits a well-defined anodic peak followed by a passive region. The anodic peak is due to active metal dissolution and formation of ferrous hydroxide.²¹ The cathodic sweep shows two cathodic peaks. The appearance of cathodic peak around -1.1 V is due to reduction of corrosion product, namely iron oxide to iron. The appearance of cathodic peak around -0.7 V is due to the reduction of pitting corrosion products precipitate on the electrode surface.

Table 1. The physicochemical parameters of natural sea water collected in Mandapam, Tamilnadu, India.

Parameter	Value
Total dissolved salts (mg L ⁻¹)	78136
Electrical conductivity (μΩ ⁻¹ cm ⁻¹)	70788
pH	7.82
Total Hardness (CaCO ₃ equivalent)	24500
Calcium as Ca ²⁺ (mg L ⁻¹)	2200
Magnesium as Mg ²⁺ (mg L ⁻¹)	1800
Sodium as Na ⁺ (mg L ⁻¹)	9600
Chloride as Cl ⁻ (mg L ⁻¹)	23100
Fluoride as F ⁻ (mg L ⁻¹)	1.2
Potassium (mg L ⁻¹)	900
Sulphate as SO ₄ ²⁻ (mg L ⁻¹)	2350

In the present study, cyclic voltammograms were recorded by measuring the working electrode, carbon steel, in 3.5% NaCl solution. The cyclic voltammogram of carbon steel immersed in 3.5% NaCl is shown in Fig.1a. It is observed that during anodic scan, no peak is observed but a passive state is noticed. This can be explained as follows: When the metal dissolves, ferrous hydroxide is formed. When the concentration of ferrous oxide at the anodic surface exceeds its solubility product, precipitation of solid oxide occurs on the electrode surface. When the surface is entirely covered with oxide passive film, anodic current density does not increase indicating onset of passivation.²⁰ In the passive state, the Cl⁻ ion can be adsorbed on the bare metal surface in competition with OH⁻ ions. As a result of high polarizability of the Cl⁻ ions, the Cl⁻ ions may adsorb preferentially.²²

The cathodic sweep shows only one peak at -1.12 V. This is due to the reduction of corrosion product, iron oxide to iron. The peak due to reduction of pitting corrosion product is absent.

The cyclic voltammogram of carbon steel, which has been immersed in sea water for one day and dried is shown in Fig.1b. (brown iron oxide is observed on the carbon steel electrode). It is observed that during anodic sweep, no peak appears, but a passive region is observed. During the cathodic sweep, the peak due to reduction of pitting corrosion product appears at -528 mV indicating that pitting corrosion takes place. However, the peak due to reduction of corrosion product, iron oxide, appears at -1.133 V. The current density increases from -1.148 x 10⁻³ A to -1.172 x 10⁻³ A.

Table 2. The inhibition efficiency (IE%) and the corrosion rate (mm y⁻¹) of 2-CEPA – Ni²⁺ system are determined by weight-loss method.

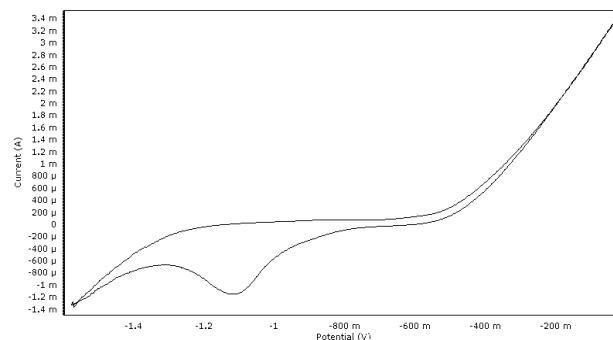
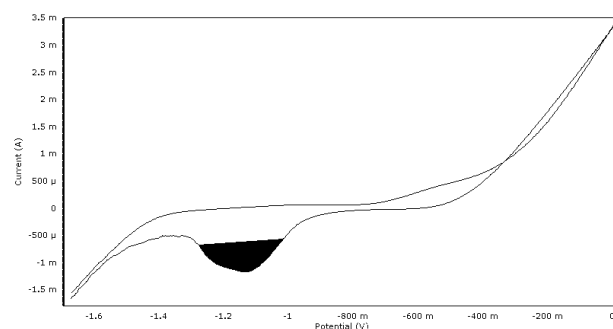
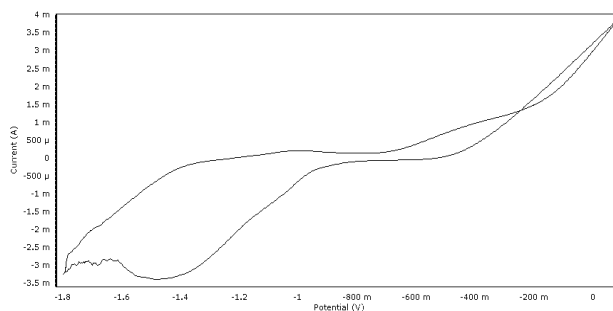
2-CEPA, ppm	Ni ²⁺ (ppm)					
	0		25		50	
	IE, %	CR, mm y ⁻¹	IE, %	CR, mm y ⁻¹	IE, %	CR, mm y ⁻¹
0	-	0.1858	8	0.1709	15	0.1579
50	15	0.1579	22	0.1449	51	0.0910
100	21	0.1468	28	0.1338	60	0.0743
150	26	0.1375	33	0.1245	65	0.0650
200	30	0.1301	39	0.1133	69	0.0576
250	35	0.1208	44	0.1040	73	0.0501

This indicates that when carbon steel electrode is immersed in sea water for one day, a protective film of iron oxide is formed on the electrode surface. It is stable in 3.5% NaCl solution. The increase in current density is explained as follows: Chloride ion is adsorbed on the passive film. The adsorbed chloride ion penetrates the oxide film especially at the flaws and defects in the oxide film.²³ When the penetrated chloride ion reaches the metal surface, they promote local corrosion.

When the carbon steel electrode is immersed in sea water containing 250 ppm of 2-CEPA and 50 ppm of Ni²⁺ for one day, a protective film is formed. It consists of Fe²⁺- 2-CEPA complex, Ni²⁺- 2-CEPA complex, and Ni(OH)₂ as revealed by FTIR spectroscopy. The cyclic voltammogram of carbon steel electrode deposited with the above protective film is shown in Fig.1c. It is observed that during anodic sweep, dissolution of metal does not take place. This indicates that the protective film is stable and compact. Electrons are not transferred from the metal surface, and a passive region is observed. During cathodic sweep, the peak corresponding to reduction of pitting corrosion product appears at -500 mV. However, the peak due to reduction of iron oxide to iron appears at -1.476 V. The current density increases from -1.148 x10⁻³ A to -3.388 x10⁻³ A. The increase in current density may be explained as above. It is observed from the Fig.1a, 1b, 1c that the pitting potentials for the three systems are at -644.4 mV, -755.5 mV, and -606.3 mV respectively. That is when carbon steel electrode is immersed in the sea water medium, the pitting potential is shifted to more negative side (active side, i.e., -755.5 mV). It accelerates corrosion because the protective film formed is porous and amorphous. When the electrode is immersed in the inhibitor medium, the pitting potential is shifted to the noble side, i.e., -606.3 mV. This indicates that the passive film found on the metal surface in the presence of inhibitors is compact and stable. It can withstand the attack of chloride ion present in 3.5 NaCl.

FTIR Spectra

FTIR spectra have been used to analyze the protective film found on the metal surface.^{24,25} The FTIR spectrum (KBr) of pure 2-CEPA is shown in Fig. 2a. The P-O stretching frequency appears at 1017 cm⁻¹ and the C=O stretching frequency of the carboxyl group appears at 1721 cm⁻¹. The FTIR spectrum of the film formed on the metal surface after immersion in sea water containing 250 ppm of 2-CEPA and 50 ppm of Ni²⁺ is shown in Fig. 2b.

**Figure 1a.** Cyclic voltammogram of carbon steel electrode immersed in 3.5% NaCl.**Figure 1b.** Cyclic voltammogram of carbon steel electrode submerged in 3.5% NaCl solution after its immersion in sea water for one day.**Figure 1c.** Cyclic voltammogram of carbon steel electrode submerged in 3.5% NaCl solution after its immersion in sea water containing 250 ppm of 2-CEPA and 50 ppm of Ni²⁺ for one day.

The P-O stretching frequency has shifted from 1017 to 1090 cm⁻¹ and the C=O stretching frequency has shifted from 1721 to 1701 cm⁻¹. It is inferred that oxygen atom of the carboxyl group has coordinated with Fe²⁺ resulting in the formation of Fe²⁺ – 2-CEPA complex formed on the anodic sites of the metal surface. The possibility of formation of Ni²⁺ – 2-CEPA complex, to some extent, on the metal surface cannot be ruled out. The peak at 3432 cm⁻¹ is due to –OH stretching. The band due to Ni-O appears at 1369 cm⁻¹. These results confirm the presence of Ni(OH)₂ deposited on the cathodic sites of the metal surface. Thus, FTIR spectral study leads to the conclusion that the protective film consists of Fe²⁺ – 2-CEPA complex, Ni²⁺ – 2-CEPA complex and Ni(OH)₂.

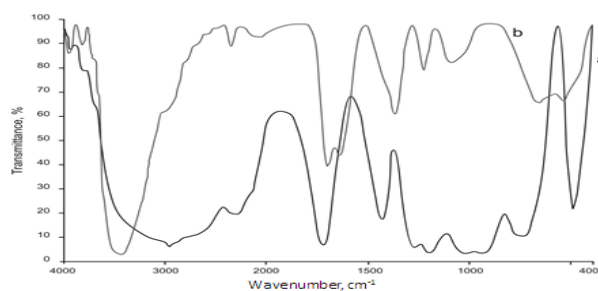


Figure 2. FTIR Spectra a) pure 2-CEPA b) film formed on metal surface after immersion in sea water containing 250 ppm of 2-CEPA and 50 ppm of Ni²⁺

Mechanism of Corrosion Inhibition

In order to explain the above results, the following mechanism of corrosion inhibition is proposed: When carbon steel is immersed in an aqueous solution, the anodic reaction is,

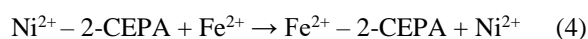


The corresponding cathodic reaction is reduction of oxygen to hydroxyl ions,



When the formulation consists of 250 ppm of 2-CEPA and 50 ppm Ni²⁺ in sea water, there is formation of 2-CEPA – Ni²⁺ complex in solution.

When carbon steel is immersed in this environment, the 2-CEPA – Ni²⁺ complex diffuses from the bulk of the solution to the metal surface. The 2-CEPA – Ni²⁺ complex is converted into 2-CEPA – Fe²⁺ complex on the anodic sites of the metal surface, the stability of Fe²⁺ – 2-CEPA complex is higher than the corresponding Ni complex.



The released Ni²⁺ combines with OH⁻ to form Ni(OH)₂ on the cathodic sites of the metal surface.



The possibility of formation of Ni²⁺ – 2-CEPA complex, to some extent, on the metal surface cannot be ruled out.

Thus, the protective film consists of Fe²⁺ – 2-CEPA complex, Ni²⁺ – 2-CEPA complex, and Ni(OH)₂.

CONCLUSIONS

The conclusions drawn from the results may be given

(1) The inhibition of corrosion of carbon steel in sea water has been evaluated in the absence and presence of 2-carboxyethylphosphonic acid and Ni²⁺.

(2) Weight-loss method and cyclic voltammetry have been used for this purpose.

(3) The formulation consisting of 250 ppm of 2-CEPA and 50 ppm of Ni²⁺ provides 73% inhibition efficiency.

(4) FTIR study reveals the protective film consists of Fe²⁺ – 2-CEPA complex, Ni²⁺ – 2-CEPA complex, and Ni(OH)₂.

(5) Cyclic voltammetry study reveals that the protective film is more compact and stable even in 3.5% NaCl environment.

REFERENCES

- Heitz, E., Flemming, H. C., Sand W., (Eds.), *Microbially Influenced Corrosion of Materials*, Springer-Verlag, Berlin, **1996**, 6.
- Bockris J. O. M., Reddy, A. K. N., *Modern Electrochemistry*, Plenum Press, New York, **1977**, 2, 861.
- Jeyaprabha, C., Sathiyarayanan, S., Venkatachari, G., *Appl. Surf. Sci.*, **2005**, 246, 108.
- Fontana, M. G., Greene, N. D., *Corrosion Engineering*, McGraw Hill, New York, **1978**.
- Badr, G. E., *Corros. Sci.*, **2009**, 51, 2529.
- Gao, G., Liang, C. H., and Wang, H., *Corros. Sci.*, **2007**, 49, 1833.
- Amar, H., Benzakour, J., Derja, A., Villemin, D., Moreau, B., *J. Electroanal. Chem.*, **2003**, 558, 131.
- Amar, H., Benzakour, J., Derja, A., Villemin, D., Moreau, B., Braisaz, T., Tounsi, A., *Corros. Sci.*, **2008**, 50, 124.
- Gopi, D., Manimozhi, S., Govindaraju, K. M., *J. Appl. Electrochem.*, **2007**, 37, 439
- Apparao, B. V., Christina, K., *Indian J. Chem. Technol.*, **2006**, 13, 275.
- Labjar, N., Lebrini, M., Bentiss, F., Chihib, N. E., El Hajjaji, S., Jama, C., *Mater. Chem. Phys.*, **2010**, 119, 330.
- Ochoa, N., Basil, G., Moran, F., Pebere, N., *J. Appl. Electrochem.*, **2002**, 32, 497.
- Horvath, T., Kalman, E., *Russ. J. Electrochem.*, **2000**, 36, 1085.

- ¹⁴Fang, J. L., Li, Y., Ye, X. R., Wang, Z. W., Liu, Q., *Corrosion*, **1993**, 49, 266.
- ¹⁵Wranglen, G., *Introduction to corrosion and protection of Metals*, London: Chapman & Hall., **1985**, 236.
- ¹⁶ Abdallah, M., Meghed, H. E., Sobhi, M., *Mater. Chem. Phys.*, **2009**, 118, 111.
- ¹⁷Dutra, C. A. M., Codaro, E. N., Nakazato, R. Z., *Mater. Sci. Appl.*, **2012**, 3, 348.
- ¹⁸Feng, L., Yang, H., Wang, F., *Electrochim. Acta.*, 2011, 58, 427.
- ¹⁹Li, Y., Kumar, P., Shi, X., Nguyen, T. A., Xiao, Z., Wu, J., *Int. J. Electrochem. Sci.*, **2012**, 7, 8151.
- ²⁰Deyab, M. A., Keera, S. T., *Egypt. J. Petrol.*, **2012**, 21, 31.
- ²¹Gouda, V. K., in: *Proc. 12th Int. Corrosion Cong., Houston, TX, USA*, **1993**, 19.
- ²²Refaey, S. A. M., Abd El-Rehim, S. S., Taha, F., Saleh, M. B., Ahmed, R.A., *Appl. Surf. Sci.*, **2000**, 158, 190.
- ²³Kannagara, D. C. W., Conway, B. E., *J. Electrochem. Soc.*, **1987**, 134, 894.
- ²⁴Rajendran, S., Anuradha, K., Kavipriya, K., Krishnaveni, A., Angelin Thangakani, J., *Eur. Chem. Bull.*, **2012**, 1, 503.
- ²⁵Rajendran, S., Apparao, B. V ., Palaniswamy, N., Periasamy, V., Karthikeyan, G., *Corros. Sci.*, **2001**, 43, 1345.

Received: 25.03.2013.

Accepted: 29.04.2013.



SYNTHESIS AND SPECTRAL STUDIES OF NOVEL PYRIDINE, PYRIDO[2,3-d]PYRIMIDINE AND PYRIDO[2,3-d]-3,1-OXAZINE DERIVATIVES

Mahmoud R. Mahmoud^{[a]*}, Hamed A. Derbala^[a], Hassan M. F. Madkour^[a], Mohamed M. Habashy^[a] and Mohamed H. Nassar^[a]

Keywords: pyrido[2,3-d]pyrimidines, pyrido[2,3-d]-3,1-oxazines, one carbon donors.

Several novel pyridine, pyrido[2,3-d]pyrimidine and pyrido[2,3-d] 3,1-oxazine derivatives were prepared using the readily obtainable starting material 2-amino-6-aryl-4-(3,4,5-trimethoxyphenyl) pyridine-3-carbonitrile **1a,b** via the reaction with one carbon donors such as phenylisothiocyanate, carbon disulphide and formic acid. The IR, ¹H-NMR and mass spectra for the new synthesized compounds were discussed.

* Corresponding Authors

E-Mail: mrefaee2000@yahoo.com

[a] Chemistry Department, Faculty of Science, Ain Shams University, Abbassia 11566, Cairo, Egypt

Introduction

Within the framework of our research program¹⁻⁶ concerning the utility of activated nitriles, we turned our interest to 2-amino-4,6-diaryl pyridine-3-carbonitrile **1** as an example for heterocyclic compounds whose structure represents β-enaminonitrile incorporated with heterocyclic ring.

It has been reported a series of publications reflecting the importance and synthetic applications of aminonitriles bearing various heterocyclic nuclei.⁷⁻¹¹ Among those reports, there has been found different investigation concerning 2-amino-3-cyanofurans^{12,13} and pyrroles.¹⁴ On the other hand, few reports dealing with similar two bifunctional pyridines were submitted.¹⁵

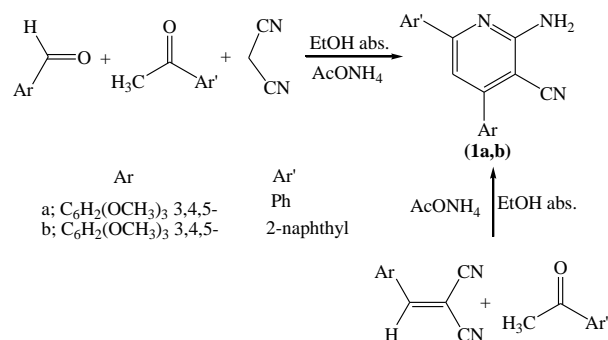
Results and Discussions

The titled compounds **1a, b** were successfully prepared by the following two attractive synthetic strategies. First, by the application of the reported one pot methodology used for the preparation of 2-aminopyridine-3-carbonitriles.¹⁶ Thus a mixture of equimolar amounts of 3,4,5-trimethoxybenzaldehyde, acetophenone (2-acetylnaphthalene), malononitrile and ammonium acetate in absolute ethanol was heated under reflux for 2 hrs. Second, by refluxing the arylidenmalononitrile, namely, 3,4,5-trimethoxybenzylidenemalononitrile with the coreactant ketone and ammonium acetate on molar ratios in absolute ethanol. The reaction readily proceeded to afford in each case an excellent yield of pyridine derivatives **1a, b**. (Scheme 1)

The structure of the products obtained was inferred from microanalytical and spectral data. Thus, the IR spectra of both compound showed two sharp absorption frequencies at 3496 and 3372 cm⁻¹ standing for the –NH₂ group absorption,

in addition to the vibrational frequency at 2207 cm⁻¹ indicating the presence of nitrile functionality.

Furthermore, the ¹H-NMR spectrum of compound **1a** in DMSO-d₆ exhibited signals from low to high field which were in agreement with the concerned structure. The aromatic protons of 6-substituted phenyl moiety displayed two multiplets at δ 8.8-8.40 ppm and 7.48-7.46 ppm integrating to two and three protons, respectively. However, the absorption singlet exhibited at δ 7.3 ppm integrating to one proton refers to the aromatic hydrogen located at C-5. Two magnetically equivalent protons at 2' and 6' positions of trimethoxyphenyl moiety displayed a singlet at δ 6.97 ppm. The amino group protons showed a singlet at δ 6.92 ppm (exch. in D₂O).

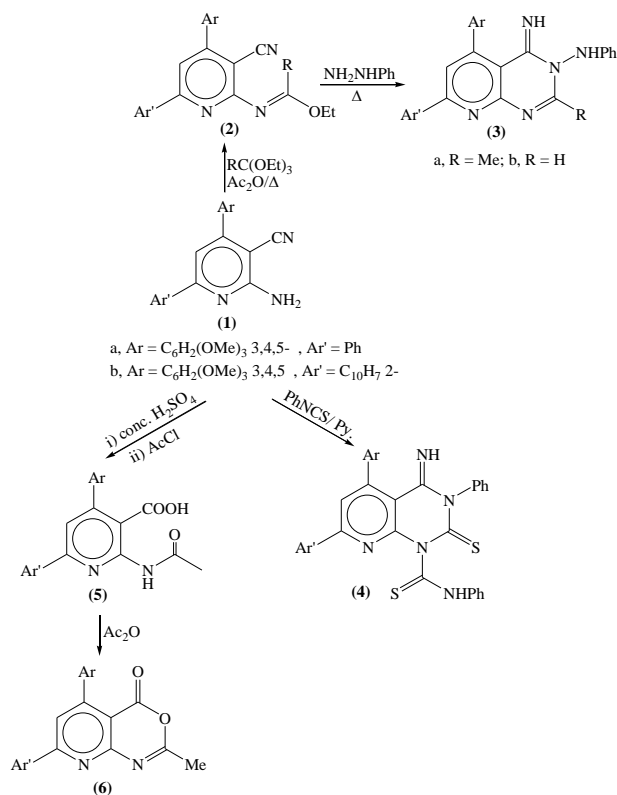


Scheme 1

Moreover, the 3,4,5-trimethoxy groups showed two singlets at δ 3.84 and 3.72 ppm, integrating to six and three protons of two magnetically equivalent –OCH₃ groups at 3'- and 5'- positions, while the latter corresponding to that one located at position 4'. Furthermore, structures **1a** and **1b** received a satisfactory support from the study of their mass spectra which were in full agreement with their assigned structure (c.f. Exp.).

It has been reported that the amino group bearing a heterocyclic ring readily reacts with triethylorthoformate or acetate to afford the corresponding ethoxyimine

derivatives.¹⁷ Thus, when conducting compound **1a** with triethylorthoacetate and/or compound **1b** with triethylorthoformate in refluxing acetic anhydride for 6 hrs. resulted in the formation of 4,6-diethoxymethyleneaminopyridine-3-carbo-nitriles **2a,b** in moderate yields. (Scheme 2)

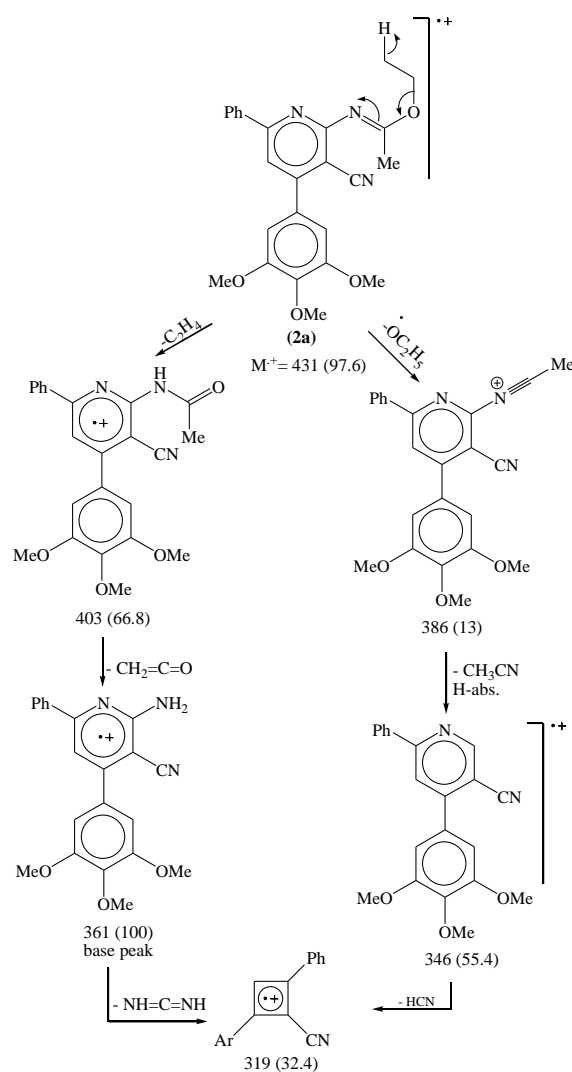


Scheme 2

The structure of products **2a,b** was inferred from microanalytical and spectral data. Thus, they lacked the coupling absorption bands characteristic to the -NH_2 group and acclaimed only the appearance of absorption frequencies of the nitrile and imino -C=N groups at 2209 cm^{-1} and 1626 cm^{-1} .

Moreover, the structural features of both compounds **2a,b** received further support by a study of their mass spectra.

Furthermore, the mass spectrum of **2b** show a fragmentation pattern which very close to **2a** with the correct molecular ion at $m/z = 467$ (100%) which is the base peak (c.f. Exp.). Because of the presence of two almost similar electrophilic sites, the nitrile and its orthoethoxyisnitrile functionalities, it would be suitable to attempt its condensation with binucleophilic centers reagent e.g., phenylhydrazine. Thus, compounds **2a,b** were allowed to react with the latter reagent in refluxing ethanol for two hrs. It was proposed that the reaction proceeded via nucleophilic addition on the ethoxyisnitrile group followed by cyclization on the nitrile functionality to afford 5,7-diaryl-3-phenylamino-4-iminopyrido-[2,3-d](3H)pyrimidine derivatives **3a,b** in good yields. (Scheme 2)

Figure 1. EI fragmentation pattern of compound **2a**

The $^1\text{H-NMR}$ spectrum of compound **3a** in DMSO-d_6 clearly showed the absorption signals corresponding to each proton type in the assigned structure. Thus, the imino -NH proton displayed a singlet at $\delta 9.11$ ppm integrating to one proton, however, the aromatic proton exhibited three multiplets in the range of $\delta 8.04\text{-}6.6$ ppm integrating all thirteen protons, along with the anilino -NH proton appeared as abroad signal at $\delta 5.034$ ppm. The trimethoxy group protons showed their absorption signal as two singlets at $\delta 4.03$ ppm and 3.97 ppm integrating for six and three protons, respectively. In addition the two methyl proton type displayed a singlet at $\delta 2.30$ ppm.

Moreover, the mass fragmentation pattern of compound **3b** presented a satisfactory support which was in full accordance with the proposed structure. It showed the fragment 529 (14.96%) corresponding to the parent peak.

When we devoted our efforts to the reactions **1a,b** with bifunctional reagents we thought that its treatment with phenyl isothiocyanate in refluxing pyridine would occur via initial attack of amino group followed by cyclization leading to addition of one molecule of the reagent.

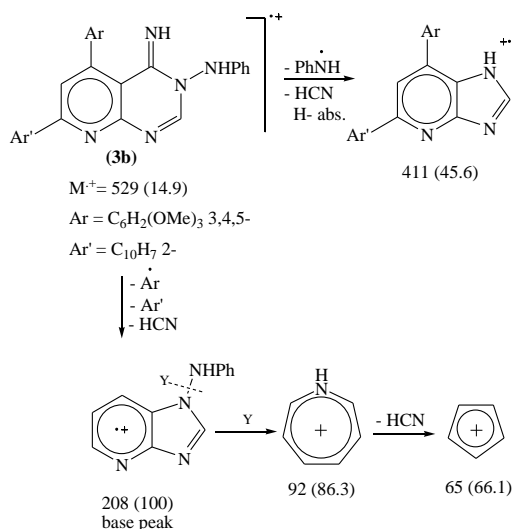


Figure 2. EI- fragmentation pattern of **3b**

By the study of their mass spectra it has been found that the molecular weight determination indicated the incorporation of two molecules of phenyl isothiocyanate in the formation of reaction product. It was proposed that the reaction involved the formation of 7-aryl-4-imino-3-phenyl-1-(N-phenylthiocarbox-amido)-5-(3,4,5-trimethoxyphenyl)-pyrido[2,3-d] pyrimidin-2-thione **4a,b**.

Examination of 1H -NMR spectrum of **4b** in DMSO- d_6 revealed two singlets, the former at δ 9.57 ppm integrating for one proton attributable to the exocyclic imino C=NH proton and the latter at δ 8.3 ppm stands for the thiocarboxamide proton absorption. The aromatic protons displayed signals in the range of δ 8.09-6.96 ppm, integrating totally for 20 protons of five aromatic rings existing in the concerned structure. Moreover, the three methoxy group protons located at 3', 4' and 5'-positions of the 5-substituted phenyl rings showed two singlets integrating to nine protons at δ 3.81 ppm and 3.78 ppm. The mass spectra of **4a** and **4b** were completely in accord with the proposed structures (C.F. Fig. 3,4).

Fused oxazinones are among the most important heterocycles which are required as synthons and their wide scope of biological activity.¹⁸⁻²⁵ Thus, the author intended to synthesize pyrido[2,3-d][3,1]oxazinone derivative **6** via two steps reaction involving hydrolysis of **1b** with the aid of concentrated sulphuric acid followed by refluxing in acetyl chloride to give 2-acetamidonicotinic acid derivative **5** which underwent cyclodehydration by treatment with acetic anhydride to afford 2-methyl-7-(2-naphthyl)-5-(3,4,5-trimethoxyphenyl)pyrido[2,3-d][3,1]oxazin-4-one **6** in a moderate yield (Scheme 2).

The structure of the acetamidonicotinic acid derivative **5** was proven by solubility in aqueous sodium carbonate solution and its IR spectrum showed two broad vibrational bands at 3405 cm^{-1} and 3227 cm^{-1} attributable to the open amide -NH group and the carboxylic functionality existing in H-bonding that causes broadening of their absorption frequencies. Two strong absorption bands appeared at 1705 and 1662 cm^{-1} referring to the presence of carbonyl functionalities of both the carboxy and the open amide groups, respectively.

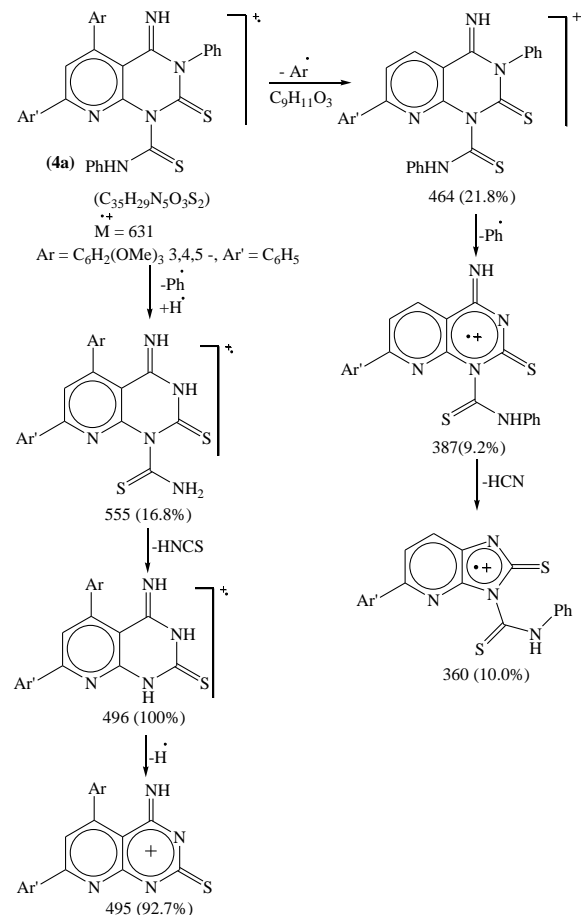


Figure 3. EI fragmentation pattern of compound **4a**

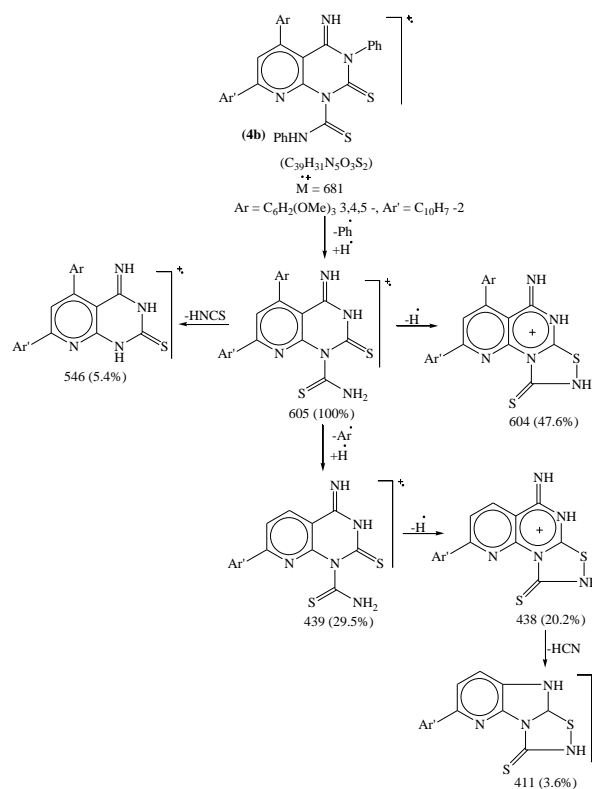


Figure 4. EI fragmentation pattern of compound **4b**

On the other hand, the structure of the product **6** was established from microanalytical and spectral data. Thus, its IR spectrum showed the lack of absorption bands of the amide –NH and acidic –OH groups that refers to their involvement in the cyclization process. The 6 μ m region revealed a stretching absorption frequency of 6-membered lactone at 1767 cm⁻¹ with the band appearing at 1663 cm⁻¹ which indicated the existence of C=N.

¹H-NMR of compound **6** in DMSO-d₆ show from low to high field signals characteristic for aromatic protons at δ ppm 8.1-7.5 (m, 10H), two singlet at δ 4.0, 3.8 ppm for the three methoxy protons in the ratio 6:3 and singlet at δ 2.3 for the three methyl protons.

Moreover, a full support of the proposed structure was provided by quantitative investigation of its mass fragmentation pattern (Fig. 5).

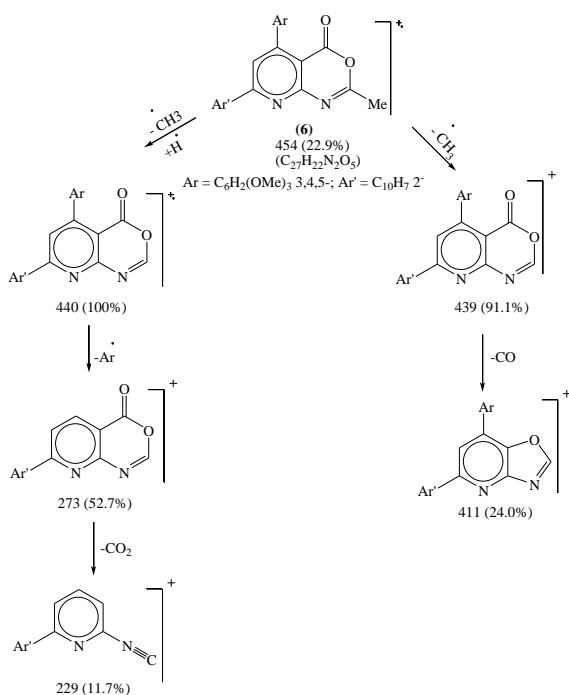
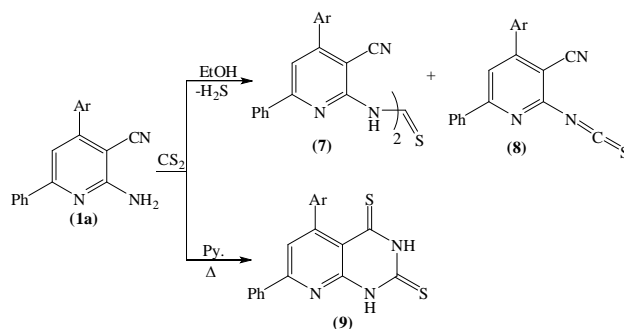


Figure 5. EI fragmentation of compound **6**

It has been reported that heterocyclic o-amino carbonitriles including furans, pyrimidines and quinazolines^{26,27} reacted with carbon disulphide under different reactions conditions to afford biologically interest fused thiazines and/or pyrimidinedithione. However, when compound **1a** was treated with the reagent in ethanolic solution of KOH at refluxing temperature for 6hrs. The reaction fails to give the fused pyridine compound. Instead a semisolid product was separated out (two spots in TLC) and subjected to fractional crystallization, non of these products could be isolated in a pure state. Meanwhile, it was possible to detect in the crude reaction mixture by GC-MS technique two different compounds. The EI fragmentation pattern of one of them is completely in accord with N,N'-bis[4-aryl-3-cyano-6-phenyl pyridine-2-yl]thiourea **7** and the second showed completely different pattern whose highest m/z (relative intensity) peak is recorded at 403 (45.6) which is attributable to the isothiocyanate derivative **8** (Scheme 3). Tentative fragmentation which are in a good compatible with the proposed structures.



Scheme 3

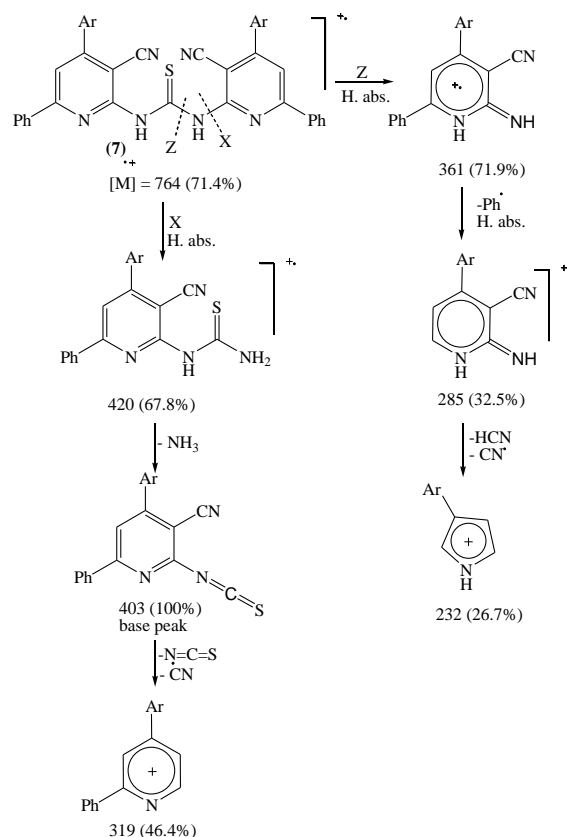
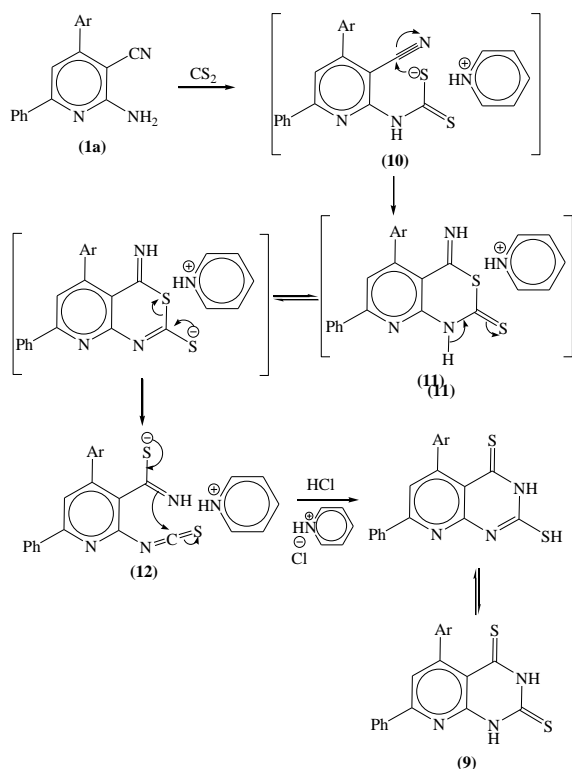


Figure 6. The main fragmentation pattern for **7**

Moreover, the highest recorded peak in the mass spectrum of **8** at m/z = 403 (45.6) represent the correct molecular ion peak which upon loss of methyl and cyanide radical afforded the radical cation at m/z = 362(100%) which represent the base peak.(c.f. Exp.).

By repeating the above reaction in pyridine under the same previous reaction conditions resulted in the formation of fused compound **9** whose structure was described as 5-aryl-7-phenylpyrido[2,3-d]pyrimidine-2,4-(1H,3H) dithione (Scheme 3). Now, it is postulated that the utility of pyridine is responsible for the existence of thiocarbamate intermediate **10** which in turn attacks the nitrile group to give the pyrimidine salt of 2-thioxo-1,3-thiazine derivative **11** which undergo rearrangement to the isothiocyanate derivative²⁸ **12** which underwent cyclization to give pyrido pyrimidine dithione derivative **9** (Scheme 4).

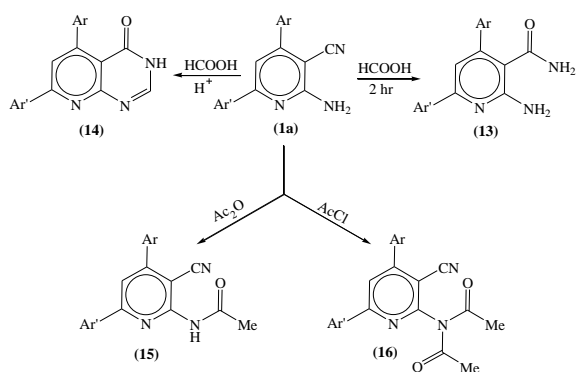


Scheme 4

The structure **9** was substantiated from the analytical and spectroscopic data. Moreover, its mass fragmentation pattern was in full harmony with the assigned structure. (c.f. Exp.).

Recently, there has been found a number of publications^{29,30} reported that the formation of fused pyrimidinones via condensation of variety of substituted 2-aminobenzonitriles and/or 2-aminopyrrolonitriles with formic acid is either an acid catalyzed or time dependent reaction.

We were able in our lab to obtain the intermediate substituted 2-aminopyridine-3-carboxamide derivative **13** by refluxing **1a** with formic acid on water bath for 2 hr. in absence of acid catalysis. Whereas, the reaction of **1a** with formic acid in the presence of concentrated sulphuric acid as acatalyst, afforded the cyclized product 5-aryl-7-phenylpyrido[2,3-d]pyrimidine-4(3H)one **14** in good yield (Scheme 5).



Scheme 5

The structure of pyridopyrimidinone **14** was proven on the basis of microanalytical and spectral data. Thus, their IR spectra revealed a broad band in the $3 \mu\text{m}$ region standing for stretching vibration of $\nu_{\text{NH,OH}}$, of the cyclic amide group. In addition, the $6 \mu\text{m}$ region exhibited the carbonyl vibrational band at 1680 cm^{-1} and/or 1659 cm^{-1} of cyclic 6-membered lactam ring.

Furthermore, the assigned structure of compound **14** received satisfactory support by the study of its mass fragmentation pattern which showed the correct molecular ion peak at 389 (45.7%).

The $^1\text{H-NMR}$ spectra of compound **14** in DMSO-d_6 revealed to doublets at $\delta 8.14 \text{ ppm}$ standing for the ring $-\text{NH}$ proton. However, the pyridyl H-2 proton displayed a singlet at $\delta 7.33 \text{ ppm}$ along with the phenyl group protons absorption shown as multiplet at $\delta 7.49 \text{ ppm}$ integrating to five protons, a singlet at $\delta 7.1 \text{ ppm}$ integrated for one proton (C6-H). The two protons at m-positions of 5-substituted 3,4,5-trimethoxyphenyl ring exhibited a singlet at $\delta 6.88 \text{ ppm}$, meanwhile the three methoxy group of the same ring displayed their absorption signals as two singlets at $\delta 3.84 \text{ ppm}$, and 3.75 ppm integrating for six and three protons located at 3'- and 5'- positions along with those substituted at 4'-position.

One of the historical beneficial roles of the amino group in organic chemistry is its susceptibility to be acylated upon treatment with various number of acylating agents, in easy going reactions. Of these reactions, the concerned compound **1a** was treated with acetyl chloride and/or acetic anhydride at the reflux temperature of the reagent. The reaction readily occurred via nucleophilic addition of the amino group on electronically deficient carbonyl carbon atom of the acetyl segment that led finally to the formation of monoacetyl derivative **15** in the first case and the diacetyl derivative **16** in the latter one (Scheme 5). The IR spectrum of **15** displayed ν_{NH} (sharp) at 3347 cm^{-1} , ν_{CN} at 2220 cm^{-1} and $\nu_{\text{CO(amide)}}$ at 1658 cm^{-1} . On the other hand, the latter product **16** exhibited vibrational coupling bands for a carbonyl groups at 1730 and 1700 cm^{-1} and show the absence of absorption bands for NH group.

Moreover, the $^1\text{H-NMR}$ spectrum of compound **16** in CDCl_3 displayed a singlet at $\delta 2.42 \text{ ppm}$ integrating to six protons indicates the presence of two symmetrical acetyl groups.

On the other hand, compound **16** received further support to its structure assignment from the study of its mass spectrum whose fragmentation pattern was in full agreement with the proposed structure.(c.f. Exp.)

Experimental

All melting points were taken on Griffin and Geory melting point apparatus and are uncorrected. IR spectra were recorded on Pye Unicam SP1200 spectrophotometer using KBr Wafer technique. $^1\text{H-NMR}$ spectra were determined on a Varian Gemini 200 MHz, Bruker AC-200 MHz using TMS as internal standard (chemical shifts in δ -scale). EI-MS were measured on a Shimadzu-GC-MS instrument operating at 70 eV. Microanalysis measurements were carried out at Ain Shams University laboratory and satisfactory analytical data (± 0.4) were obtained for all compounds. $^1\text{H-NMR}$ spectra and EI-MS were run at Cairo University labs.

Condensation of 3,4,5-trimethoxybenzaldehyde, acetophenone, malononitrile and ammonium acetate; Formation of 2-amino-6-phenyl-4-(3,4,5-trimethoxy-phenyl)pyridine-3-carbonitrile (1a)

A mixture of malononitrile (0.66 g; 0.01 mol), acetophenone (1.2 g; 0.01 mol), 3,4,5-trimethoxybenzaldehyde (1.96 g; 0.01 mol) and ammonium acetate (1.15 g; 0.015 mol) in dry benzene (50 ml) was heated under reflux using water separator for 4 hrs, cooled and the crude solid was triturated with ethanol. The solid product so formed was collected by filtration, dried and recrystallized from ethanol giving **1a** as yellow crystals, 2.8 g (78%), mp 161-163°C, ir: NH₂ 3496, 3372, C≡N 2207, C=N 1630 cm⁻¹. ¹H nmr (DMSO-d₆) δ 8.8-7.4 (m, 5H_{arom.}), 7.3 (s, 1H, C₅-H), 6.97 (s, 2H_{arom.}), 6.9 (br.s, 2H, NH₂, exchangeable with D₂O), 3.84 (s, 6H, 2OMe), 3.72 (s, 3H, OMe). ms: m/z: 362 (M+1, 100), 347 (43), 319 (24.2), 286 (13.6), 234 (16.2). Anal. Calcd. for C₂₁H₁₉N₃O₃ (361): C, 69.8; H, 5.26; N, 11.63. Found: C, 69.73; H, 5.42; N, 11.46.

Condensation of 3,4,5-trimethoxybenzaldehyde, 2-acetylnaphthalene, malononitrile and ammonium acetate; Formation of 2-amino-6-(2-naphthyl)-4-(3,4,5-trimethoxyphenyl) pyridine-3-carbonitrile (1b)

A mixture of malononitrile (0.66 g; 0.01 mol), 2-acetylnaphthalene (1.7 g; 0.01 mol), 3,4,5-trimethoxybenzaldehyde (1.96 g; 0.01 mol) and ammonium acetate (1.15 g; 0.015 mol) in dry benzene (50 ml) was heated under reflux using water separator for 4 hrs, cooled and triturated with ethanol. The solid product so formed was collected by filtration, dried and recrystallized from ethanol giving **1b** as yellow crystals, 3.5 g (87%), mp 173-175°C, ir: NH₂ 3476, 3296, C≡N 2207, C=N 1642 cm⁻¹. ms: m/z: 412 (M+1, 100), 397 (19), 381 (12), 286 (13.6), 288 (12), 244 (13.3). Anal. Calcd. for C₂₅H₂₁N₃O₃ (411): C, 72.99; H, 5.1; N, 10.21. Found: C, 73.09; H, 5.32; N, 10.0.

Reaction of 1a with triethylorthoacetate; Formation of 2-ethoxyethylenamino- 6-phenyl-4-(3,4,5-trimethoxyphenyl)-pyridine-3-carbonitrile (2a)

A mixture of compound **1a** (3.61 g; 0.01 mol), triethylorthoacetate (5 ml) in freshly distilled acetic anhydride (5 ml) refluxed for 5 hrs. The solvent was removed under reduced pressure and the resulted solid was triturated with ether and recrystallized from ethanol giving **2a** as glassy yellow crystals, 2.28 g (53%), mp 158-160°C, ir: C≡N 2209 cm⁻¹. ms: m/z: 431 (M⁺, 97.6), 403 (66.8), 386 (13), 373 (30), 361 (100), 346 (55.4), 319 (32.4). Anal. Calcd. for C₂₅H₂₅N₃O₄ (431): C, 69.6; H, 5.8; N, 9.74. Found: C, 69.92; H, 5.66; N, 9.72.

Synthesis of 2-ethoxymethylenamino- 6-(2-naphthyl)-4-(3,4,5-trimethoxy-phenyl) pyridine-3-carbonitrile (2b)

A mixture of compound **1b** (4.11 g; 0.01 mol), triethylorthoacetate (10 ml) in acetic anhydride (5 ml) was refluxed for 5 hrs. The solvent was removed under reduced pressure and the resulted solid was triturated with ether and recrystallized from ethanol giving **2b** as buff crystals, 2.8 g

(61%), mp 143-145°C, ir: C≡N 2207 cm⁻¹. ms: m/z: 467 (M⁺, 100), 340 (M-C₁₀H₇, 22.8), 300 (M-Ar, 70.3), 421 (7.6), 395 (46.2), 167 (32.6), 77 (18.9). Anal. Calcd. for C₂₈H₂₅N₃O₄ (467): C, 71.94; H, 5.35; N, 8.99. Found: C, 72.08; H, 5.3; N, 8.73.

Reaction of 2 with phenyl hydrazine; Formation of 2-methyl-7-aryl-5-(3,4,5-trimethoxyphenyl)-3-phenylamino-4-imino-pyrido[2,3-d](3H)pyrimidine (3a) and (3b)

A mixture of compound **2** (0.01 mol) and phenyl hydrazine in ethanol (20 ml) was heated under reflux for 8 hrs. The reaction mixture was left to cool, poured into dilute hydrochloric acid; the solid product so formed was filtered off, dried and recrystallized from methanol giving **3a** as light brown crystals, 2.8 g (58%), mp 197 °C decomp., ir: NH 3383, C=N 1661 cm⁻¹. ¹H nmr (DMSO-d₆) δ 9.11 (s, 1H, =NH), 8.04-7.5 (m, 10H_{arom.}), 7.1 (s, 1H, C₆-H), 6.66 (s, 2H_{arom.}), 5.03 (br.s, 1H, NH, exchangeable with D₂O), 4.03 (s, 6H, 2OMe), 3.9 (s, 3H, OMe), 2.3 (s, 3H, Me). ms: m/z: 493 (M⁺, 100), 479 (22.8), 402 (70.3), 319 (44.8), 92 (83.6), 65 (33.6). Anal. Calcd. for C₂₉H₂₇N₅O₃ (493): C, 70.58; H, 5.47; N, 14.19. Found: C, 70.68; H, 5.34; N, 13.89.

3b: crystallized from dioxane to give buff crystals, 2.4 g (46%), mp 206-208°C, ir: NH 3376, C=N 1652 cm⁻¹. ms: m/z: 529 (M⁺, 4.9), 487 (17.8), 411 (45.6), 396 (15.5), 380 (8.1), 351 (14), 224 (12.6), 208 (100), 93 (33.6), 77 (44.1). Anal. Calcd. for C₃₂H₂₇N₅O₃ (529): C, 72.58; H, 5.10; N, 13.23. Found: C, 72.73; H, 5.0; N, 13.09.

Reaction of 1a,b with phenyl isothiocyanate; Formation of 7-aryl-4-imino-3-phenyl-1-[N-phenylthiocarboxamido]-5-(3,4,5-trimethoxy phenyl)pyrido[2,3-d]pyrimidine-2-thione (4a,b)

A mixture of compound **1a** (3.61 g; 0.01 mol) or **1b** (4.1 g; 0.01 mol) and excess phenyl isothiocyanate in pyridine (20 ml) was refluxed for 6 hrs. The reaction mixture was left to cool, acidified with dilute hydrochloric acid; the solid product so formed was filtered off, dried and recrystallized from the proper solvent to give **4a** and **4b**, respectively.

3,7-Diphenyl-5-(3,4,5-trimethoxyphenyl)-1-[N-phenylthiocarboxamido]-pyrido[2,3-d]pyrimidine-2-thione (4a)

Recrystallized from benzene as yellow crystals, 5.1 g (92%), mp 280-282°C, ir: NH 3357, 3376, C=N 1631, C=S 1259 cm⁻¹. ¹H nmr (DMSO-d₆) δ : 9.57 (s, 1H, =NH), 8.3 (s, 1H, NH), 8.09-6.96 (m, 15H_{arom.}), 7.2 (s, 1H, C₆-H), 6.7 (s, 2H_{arom.}), 3.81 (s, 6H, 2OMe), 3.78 (s, 3H, OMe). ms: m/z: 555 (M-Ph, 16.8), 497 (94.2), 496 (100), 466 (42.2), 387 (9.2), 360 (10). Anal. Calcd. for C₃₅H₂₉N₅O₃S₂ (631): C, 66.56; H, 4.59; N, 11.09; S, 10.14. Found: C, 66.91; H, 4.32; N, 10.88; S, 10.0.

7-(2-Naphthyl)-3-phenyl-5-(3,4,5-trimethoxyphenyl)-1-[N-phenylthio-carboxamido]pyrido[2,3-d]pyrimidine-2-thione (4b)

Recrystallized from benzene as greenish-yellow crystals, 5.9 g (87%), mp 236-238°C, ir: NH 3386, 3346, C=N 1644, C=S 1287 cm⁻¹. ms: m/z: 605 (M-Ph, 100), 546 (5.4), 439 (29.5), 411 (3.6), 304 (15.7), 135 (60.3), 92 (30.2), 65 (22.8).

Anal. Calcd. for $C_{39}H_{31}N_5O_3S_2$ (681): C, 68.72; H, 4.55; N, 10.27; S, 9.39. Found: C, 68.61; H, 4.4; N, 10.0; S, 9.23.

Formation of 2-acetylamino-6-(2-naphthyl)-4-(3,4,5-trimethoxyphenyl)pyridine-3-carboxylic acid (5)

A mixture of **1b** (4.11 g; 0.01 mol) in concentrated sulphuric acid (5 ml) was heated for 2 hrs, left to cool, neutralized by 5N sodium hydroxide solution and filtered. The clear filtrate was then acidified depositing an orange solid which was filtered off, dried then dissolved in acetyl chloride (5ml), refluxed for only 1 hr, left to cool, and poured into ice water. The separated solid was collected by filtration and dissolved in aqueous solution of sodium bicarbonate, filtered and the alkaline filtrate then acidified with dilute acetic acid. The deposited solid was filtered off, dried and recrystallized from methanol to give **5** as yellow crystals, 2.1 g (46%), mp 214-216°C, ir: NH 3405, 3227, CO acid 1705, CO amide 1662 cm^{-1} . ms: m/z: 472 (M^+ , 33.4), 454 (M-H₂O, 30.1), 430 (M-CH₂=C=O, 27.6), 384 (60.3), 181 (12.8). Anal. Calcd. for $C_{27}H_{24}N_2O_6$ (472): C, 68.64; H, 5.08; N, 5.93. Found: C, 68.83; H, 4.8; N, 5.77.

Synthesis of 2-methyl-7-(2-naphthyl)-5-(3,4,5-trimethoxyphenyl) pyrido [2,3-d]3,1-oxazin-one (6)

A solution of compound **5** (1 g) in freshly distilled acetic anhydride (5 ml) was heated under reflux for one hour, then left to cool and poured into ice water with stirring. The separated solid was collected by filtration, dried and recrystallized from light petroleum ether (b.p. 100-120°C) to give **6** as orange crystals, 2.08 g (46%), mp 98°C (decomp.), ir: CO oxazinone 1767, C=N 1663 cm^{-1} . ¹H nmr (DMSO-d₆) δ: 8.1-7.5 (m, 7H_{arom.}), 7.1 (s, 1H, C₆-H), 6.7 (s, 2H_{arom.}), 4.0 (s, 6H, 2OMe), 3.8 (s, 3H, OMe), 2.3 (s, 3H, C₂-Me). ms :m/z: 454 (22.9), 440 (M-Me, 100), 410 (12.4), 411 (24.0), 312 (11.9), 273 (52.7), 229 (11.7). Anal. Calcd. for $C_{27}H_{22}N_2O_5$ (454): C, 71.36; H, 4.84; N, 6.16. Found: C, 71.61; H, 4.9; N, 5.86.

Reaction of 1a with CS₂ / KOH; Formation of N,N-bis[4-aryl-3-cyano-6-phenylpyridin-2-yl]thiourea (7) & isothiocyanate derivative (8)

A mixture of compound **1a** (3.61 g; 0.01 mol), carbon disulphide (5 ml) in ethanolic KOH solution (20 ml) was refluxed for 5 hrs. The excess ethanol was evaporated, then reaction mixture was left to cool, acidified with dilute hydrochloric acid giving a semisolid paste which was triturated with ether, recrystallized by DMF to afford a non isolable mixture of two compounds which were identified by GC-MS as **7** and **8**.

Reaction of 1a with CS₂ / pyridine; Formation of 7-phenyl-5-(3,4,5-trimethoxyphenyl)-1H,3H-pyrido[2,3-d]pyrimidin-2,4-dithione (9)

A mixture of compound **1a** (3.61 g; 0.01 mol), carbon disulphide (10 ml) in pyridine (20 ml) was refluxed for 6 hrs. The reaction mixture was left to cool, acidified with dilute hydrochloric acid. The solid product so formed was filtered off, dried and recrystallized from acetic acid giving **9** as buff

crystals, 2.6 g (61%) mp 164-166°C, ir: NH 3424, 3329, C=S 1241 cm^{-1} . ms :m/z: 437 (M^+ , 17.6), 422 (M-Me, 100), 406 (M-OMe, 44.2), 363 (36.2), 348 (22.7), 319 (16.1), 182 (80.7). Anal. Calcd. for $C_{22}H_{19}N_3O_3S_2$ (437): C, 60.41; H, 4.34; N, 9.61; S, 14.64. Found: C, 60.78; H, 4.18; N, 9.37; S, 14.33.

Reaction of 1a with formic acid i) in absence of catalyst; Formation of 2-amino-3-carboxamide-6-phenyl-4-(3,4,5-trimethoxyphenyl)pyridine (13)

A solution of **1a** (3.61 g, 0.01 mol) in formic acid (10 ml) was refluxed for 2 hrs, cooled, diluted with cold water. The solid product so formed was then filtered off, washed with water, dried and recrystallized from DMF affording **13** as light brown crystals, 2.1 g (57%), mp 223-225°C, ir: NH₂ 3412, 3380, 3240, C=O amide 1659 cm^{-1} . ms: m/z: 379 (M, 78.1), 365 (70), 349 (33.1), 304 (22.8), 291 (20.2). Anal. Calcd. for $C_{21}H_{21}N_3O_4$ (379): C, 66.49; H, 5.54; N, 11.08. Found: C, 66.71; H, 5.32; N, 10.84.

ii) In presence of Conc. H₂SO₄; Formation of 7-phenyl-5-(3,4,5-trimethoxyphenyl)-3H-pyrido[2,3-d]pyrimidin-4(3H)one (14)

A solution of **1a** (3.61 g, 0.01 mol) in formic acid (10 ml) was refluxed in the presence of Conc. H₂SO₄ (1 ml) for 10 hrs. The reaction mixture was then cooled, neutralized by 1N NaOH. The solid product so formed was filtered off, washed with water, dried and recrystallized from DMF affording **14** as brown crystals, 1.59 g (41%); mp 211-213°C, ir: (br) NH.OH 3271, C=O 1680 cm^{-1} . ¹H nmr (CDCl₃) δ: 8.14 (d, 1H, NH), 7.49 (m, 5H_{arom.}), 7.33 (s, 1H, C₂-H), 7.1 (s, 1H, C₆-H), 6.88 (s, 2H_{arom.}), 3.84 (s, 6H, 2OMe), 3.75 (s, 3H, OMe). ms :m/z: 389 (45.7), 388 (100), 374 (40.6), 357 (18.9), 299 (16). Anal. Calcd. for $C_{22}H_{19}N_3O_4$ (389): C, 67.86; H, 4.88; N, 10.79. Found: C, 67.67; H, 5.0; N, 10.66.

Formation of 2-acetylamino-6-phenyl-4-(3,4,5-trimethoxyphenyl)-pyridin-3-carbonitrile (15)

A mixture of compound **1a** (3.61 g, 0.01 mol) and acetyl chloride (10 ml) was heated on a water bath for one hour. The reaction mixture left to cool then poured drop wisely into ice-water with fast stirring. The solid formed was collected by filtration, washed several times with water, dried and recrystallized from chloroform affording **15** as yellow crystals, 3.38 g (84%), mp 218-220°C, ir: NH 3347, C≡N 2220, CO amide 1658 cm^{-1} . ms :m/z: 403 (100), 361 (90.3), 195 (21.7), 181 (16.2), 91 (30.3). Anal. Calcd. for $C_{23}H_{21}N_3O_4$ (403): C, 68.48; H, 5.21; N, 10.42. Found: C, 68.71; H, 5.0; N, 10.37.

Formation of 2-(N,N-diacetylamino)-6-phenyl-4-(3,4,5-trimethoxyphenyl)-pyridin-3-carbonitrile (16)

A mixture of compound **1a** (3.61 g, 0.01 mol) in freshly distilled acetic anhydride (10 ml) was refluxed for two hours, then left to cool, poured into ice cold water with stirring. The separated solid was filtered off, dried and recrystallized from light petroleum ether (b.p. 80-100°C) to give **16** as glassy pale brown crystals, 2.51 g (58%), mp 128-130°C, ir: CO coupling bands 1730, 1700 cm^{-1} . ¹H nmr (CDCl₃) δ:

8.10-8.05 (m, 5H_{arom.}), 7.01 (s, 1H, C5-H), 6.88 (s, 2H_{arom.}), 3.96 (s, 9H, 3OMe), 2.42 (s, 6H, 2MeCO). ms :m/z: 446 (M⁺+1, 70.1), 389 (100), 373 (82.6), 372 (82.5), 346 (22.6). Anal. Calcd. for C₂₅H₂₃N₃O₅ (445): C, 67.41; H, 5.16; N, 9.43. Found: C, 67.72; H, 5.0; N, 9.22.

References

- ¹Mahmoud, M. R.; Abou El-magd, W. S. I.; Derbala, H. A.; Hekal, M. H.; *Chinese J. Chem.*, **2011**, 29(7), 1446.
- ²Mahmoud, M. R.; Abou El-magd, W. S. I.; Derbala, H. A.; Hekal, M. H.; *J. Chem. Res.*, **2012**, 75.
- ³Mahmoud, M. R.; Abu El-azm, F. S. M.; *Eur. Chem. Bull.*, **2013**, 2(6), 335.
- ⁴Mahmoud, M. R.; Abou El-magd, W. S. I.; Abd El-Wahab, S. S.; Soliman, S.A.; *J. chem. Res.*, **2012**, 66.
- ⁵Mahmoud, M. R.; Madkour, H. M. F.; Habashy, M. M.; El-Shwaf, A. M.; *Am. J. Org. Chem.*, **2012**, 2(1), 39.
- ⁶Abdel Rahman, R. M.; Seada, M.; Fawzy, M. H.; El-Baz, I.; *Pharmazie* **1994**, 49, 811.
- ⁷Abdel Galil, M. F.; Riad, B. Y.; Sherif, S. M.; El-Nagdi, M. H.; *Chem. Lett.*, **1982**, 1123.
- ⁸Abdel Galil, M. F.; Sherif, S. M.; El-Nagdi, M. H.; *Heterocycles* **1986**, 24, 2023.
- ⁹Soto, J. L.; Perandones, F.; *J. Heterocyclic Chem.*, **1998**, 35, 413.
- ¹⁰Soliman, H. A.; Kalafallah, A. K.; Abdel-Zaher, H. M.; *J. Chinese Chem. Soc.*, **2000**, 47(6), 1267 [C.A. 134(19), 266269Y, 2001].
- ¹¹Nasser, A. H.; *Molecules* **2000**, 5, 826.
- ¹²Feng, X.; Lancelot, J. C.; Gillard, A. C.; Landelle, H.; Rault, S.; *J. Heterocyclic Chem.*, **1998**, 35, 413.
- ¹³Dave, C. G.; Saha, R. D.; *J. Heterocyclic Chem.*, **1998**, 35, 1295.
- ¹⁴Mohareb, R. M.; Habashi, A.; Shams, H. Z.; Fahmy, S. M.; *Arch. Pharm.*, **1987**, 320(7), 599.
- ¹⁵Mona, M. H.; Nadia, S. S.; El-Nagdi, M. H.; *Heterocycles* **1987**, 26, 4.
- ¹⁶Álvarez-Pérez, M.; Marco-Contelles, J.; *Arkivoc*, **2011**, (ii), 283.
- ¹⁷Mahmoud, M. R.; El-Bordany, E. A. A.; Hassan, N. F.; Abu El-Azm, F. S. M.; *Phosphorus, Sulfur, and Silicon and the Related Elements*, **2007**, 182, 2507.
- ¹⁸Mahmoud, M. R.; El-Bordany, E. A. A.; Hassan, N. F.; Abu El-Azm, F. S. M.; *J. Chem. Res.*, **2007**, 541.
- ¹⁹El-Hashash, M. A.; Hassan, M. A. and Sayed, M. A.; *Pakistan J. Sci. Ind. Res.*, **1977**, 20(6), 336.
- ²⁰El-Hashash, M. A.; Kaddah, M. A.; El-Kady, M.; Amer, M. M.; *Pakistan J. Sci. Ind. Res.*, **1982**, 25(4), 104.
- ²¹Mitsuhashi, H.; Nonaka, T.; Hamamura, I.; Kishimoto, T.; Muratani, E.; Fujii, K.; *Pharmacol. J.*, **1999**, 126, 1147.
- ²²Neumann, U.; Schechter, N.; Gütschow, M.; *Bioorg. Med. Chem.*, **2001**, 9, 947.
- ²³Mohamed, M. M.; El-Hashash, M. A.; El-Gendy, A. M.; Hamed, M. M.; *Ind. J. Chem.*, **1982**, 21B, 593.
- ²⁴Krantz, A.; Spencer, R. W.; Tam, T. F.; Liak, T. J.; Copp, I. J.; Thomas, E. M.; Rafferty, S. P.; *J. Med. Chem.*, **1990**, 33, 464.
- ²⁵Fahmy, A. M.; El-Hashash, M. A.; Habishy, M. A.; Nassar, S.; *J. Revue Roumaine de Chimie*, **1978**, 23, 11.
- ²⁶Eddy, S.; Nuria, B. C.; Jordi, R.; Enrique, R.; *Tetrahedron* **2002**, 58, 2389.
- ²⁷El-Meligie, S.; El-Ansary, A. K.; Said, M. M.; Hussein, M. M.; *Ind. J. Chem.*, **2001**, 40B, 62.
- ²⁸Said, S. A.; *World J. Chem.*, **2009**, 4(2), 92.
- ²⁹Roth, G. A.; Tai, J. J.; *J. Heterocycl. Chem.*, **1996**, 33(6), 2051.
- ³⁰Mohamed, M. S.; El-Domany, R. A.; Abd El-Hameed, R. H.; *Acta Pharm.*, **2009**, 59, 145.

Received: 27.03.2013.

Accepted: 03.05.2013.



SYNTHESIS AND CHARACTERIZATION OF BIODEGRADABLE CLAY- POLYMER NANOCOMPOSITES FOR ORAL SUSTAINED RELEASE OF ANTI-INFLAMMATORY DRUG

Manpreet Kaur^[a] and Monika Datta^{[b]*}

Keywords: diclofenac sodium, montmorillonite, PLGA nanocomposite, sustained release

In this paper, a clay based drug delivery system comprising of [poly(D,L-lactide-co-glycolide)] (PLGA)/montmorillonite (MMT) nanocomposite has been explored for the oral sustained release of diclofenac sodium (DS) using double emulsion solvent evaporation technique. Encapsulation of diclofenac sodium in PLGA matrix and clay matrix was also undertaken to assess the role of clay and PLGA in drug encapsulation and its subsequent release from the respective formulations. A drug encapsulation efficiency of 98 % was obtained for the synthesized PLGA/MMT nanocomposite system. The drug was found to be intercalated in the PLGA/MMT nanocomposite as confirmed by the X-Ray diffraction studies. The thermal analysis shows the crystalline nature of the encapsulated drug in the nanocomposite. The particle size of the drug loaded PLGA/MMT nanocomposite was found to be in the range of 10-20 nm as analysed by high resolution transmission electron microscopic (HRTEM) technique. The in vitro drug release studies of the drug encapsulated PLGA/MMT nanocomposite under simulated gastric fluid (phosphate buffer saline, PBS 1.2) shows no drug release while a sustained release was seen under simulated intestinal condition (phosphate buffer saline, PBS 7.4) releasing 51% drug in 8 hours.

*Corresponding Author

E-Mail: monikadatta_chem@yahoo.co.in

[a] Department of Chemistry, University of Delhi, Delhi-110007, India. E-mail: manpreetkaur.chem@gmail.com

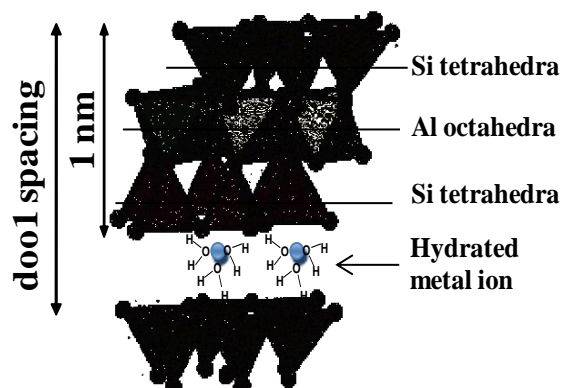
[b] Department of Chemistry, University of Delhi, Delhi-110007, India

INTRODUCTION

Polymer/clay nanocomposites are a class of hybrid systems in which clay/organo-clay nanoparticles (often montmorillonite) are dispersed in a polymer matrix. With small amount of the clay, they exhibit high thermal stability, enhanced mechanical¹⁻⁶ and rheological properties etc.⁷ These benefits along with the good intercalation capacity offered by the clay mineral have been used to develop new sustained release systems, as documented by a number of patents.⁸⁻¹⁰ A number of polymers have been investigated for designing the nanoparticulate delivery systems, but PLGA [copolymer of poly (lactide), (PLA) and poly (glycolide), (PGA)] has been most extensively used because of its biocompatibility, biodegradability, and versatile degradation kinetics. It is an FDA approved biodegradable and biocompatible polymer which has been in use for years.¹¹⁻¹³ Also, its final degradation products (lactic and glycolic acids) are completely safe, as they are either excreted by the kidneys or enter the Krebs' cycle to be eventually eliminated as carbon dioxide and water.

Of all the clays, montmorillonite (MMT) has been extensively used in the pharmaceutical formulations. It is a FDA approved excipient and belongs to the 2:1 smectite group (general formula $M^{x+y}(Al_{2-x})(OH)_2(Si_{4-y}Al_y)O_{10}$) of clay minerals. It is a naturally occurring layered silicate having a unit thickness of 1 nm which makes it suitable for the synthesis of nano structured materials. It has rich interlayer chemistry, possesses high potential for ion exchange, is stable under acidic conditions and has high

chemical resistance. It is associated with good hydration and swelling properties and acts as a potent detoxifier.¹⁴

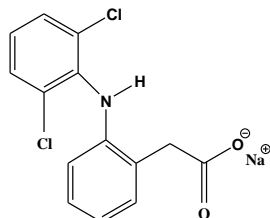


Structure of montmorillonite

Besides it has large specific surface area and exhibits stand out mucoadhesive ability to cross the GI barrier. As a result, MMT is a common ingredient both as an excipient and active substance in pharmaceutical products.^{15,16} Diclofenac is currently the eighth largest-selling drug and the most frequently used nonsteroidal anti-inflammatory drug (NSAID) in the world, since its introduction in Japan in 1974. Diclofenac is among the better tolerated NSAIDs and is widely used in the long term treatment of degenerative diseases such as rheumatoid arthritis, osteoarthritis. Diclofenac sodium (DS) has analgesic and antipyretic actions and is one of the few NSAIDs used to treat ocular inflammatory conditions. But it has short biological half life of 1-2 hours¹⁷ therefore requires frequent dosing leads to adverse gastrointestinal disturbances, peptic ulceration and gastrointestinal bleeding. The most common route of administration of this drug is oral.^{18,19} Thus in order to achieve improved therapeutic efficacy and patient

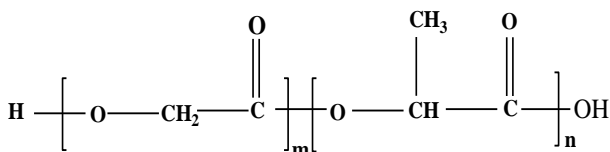
compliance, development of oral sustained-release formulations of this drug is highly desirable. To minimize the side effects, particularly to avoid gastric ulcers, diclofenac sodium is marketed as enteric coated and sustained release tablets. But even these formulations have shown GI toxicity in clinical studies.²⁰

In this work, we propose novel formulation- diclofenac sodium encapsulated biodegradable PLGA/MMT nanocomposites, synthesized for the oral sustained delivery of diclofenac sodium.



Chemical structure of diclofenac sodium

The double emulsion solvent evaporation technique was used to synthesize these nanocomposites. Poloxamer 188 [polyoxyethylene-polyoxy-propylene-polyoxyethylene (PEO-PPO-PEO) block polymer], a non-ionic stabilizing surfactant, suitable for oral administration and widely used as wetting and solubilising agent was employed in the synthesis.



Chemical structure of poly(lactic-co-glycolic acid) (PLGA), m =poly(glycolic acid) (PGA), n =poly(lactic acid) (PLA)

For comparative study, the drug loaded samples were synthesized in the absence of MMT and PLGA to investigate the effect of the two on the encapsulation efficiency and subsequent release kinetics of the drug under simulated intestinal conditions (PBS 7.4).

MATERIALS AND METHODS

Materials

The PLGA used in the present study was obtained from Sigma Aldrich, St. Louis MO USA and was used without any further purification. Poloxamer 188 (F68) having more than 98% purity was obtained from Fluka, Switzerland. The clay used in the present study, montmorillonite was obtained from Sigma Aldrich, St. Louis USA. The drugs - diclofenac sodium (DS) and diclofenac acid (DH) were obtained from Sigma Aldrich, St. Louis MO USA and were used without any further purification.

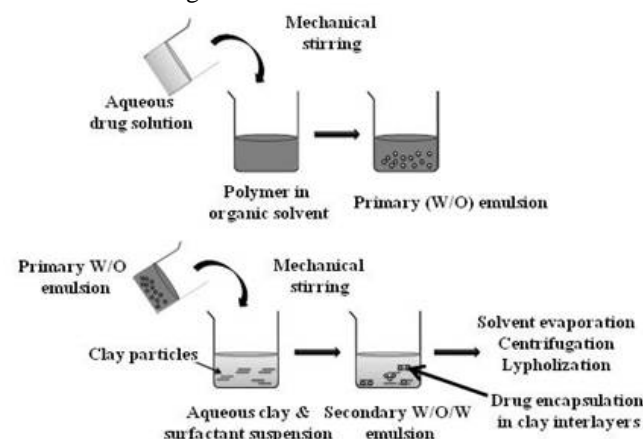
HPLC grade ethyl acetate having 99.8% assay was obtained from Research laboratories Ltd., Mumbai. HPLC grade dichloromethane (DCM) and methanol having 99.5% and 99.7% assay, respectively, were obtained from Merck,

Mumbai. NaOH and KH_2PO_4 used for making PBS 7.4 buffer were obtained from Merck, Mumbai.

Encapsulation of diclofenac sodium in PLGA/MMT composite

The double emulsion (w/o/w) solvent evaporation method was employed for the encapsulation of diclofenac sodium in PLGA/MMT nanocomposite. The multiple emulsions were prepared by using two step emulsification procedures. In the first step, the primary (w/o) emulsion was prepared by incorporating the aqueous drug (20 mg) phase into the oily phase containing PLGA (40 mg) dissolved in ethyl acetate and the resulting emulsion was sonicated for a minute at 25 °C using ultrasonics sonicator.

In the second step, the primary emulsion was added slowly into the aqueous phase containing a given amount of MMT and F-68 (at critical micelle concentration) to encapsulate the (w/o) emulsion. The resulting double emulsion, (w/o/w) was stirred at 700 rpm and the organic solvent was evaporated at 37 °C leaving behind diclofenac sodium encapsulated PLGA-MMT composite. The contents were then centrifuged at 20,000 rpm for 30 minutes at 20 °C using Sartorius 3K30 centrifuge. The filtrate was preserved and the residue was lyophilized for further characterizations (Scheme 1). A number of formulations were tried by varying different parameters before arriving at the optimized formulation designated as 002.



Scheme1. Schematic representation of synthesis of drug encapsulated clay polymer nanocomposite by w/o/w double emulsion solvent evaporation method

To investigate the effect of MMT on the drug encapsulation and its subsequent release from the synthesised formulation, diclofenac sodium was encapsulated in PLGA matrix using w/o/w double emulsion solvent evaporation technique. All the parameters and processing conditions were kept the same as in optimized formulation - 002 except for MMT, which was not added. The sample thus synthesised was designated as 010.

To see the effect of PLGA on the encapsulation of diclofenac sodium in the clay, the aqueous drug was added slowly under the same conditions to the aqueous suspension of MMT containing F-68. All the parameters and processing conditions were kept the same as in optimized formulation - 002 except that PLGA was not used. The sample thus synthesised was designated as 012.

Quantitative estimation of diclofenac sodium in the synthesized formulations using high performance liquid chromatographic (HPLC) method

Method development and analysis of formulations

The amount of diclofenac sodium encapsulated in the synthesized formulations was determined by HPLC technique using a reversed phase C18 column (250 × 460 mm, Phenomex, USA) and UV-VIS photo-diode array. The samples were separated using an isocratic mobile phase consisting of CH₃OH: PBS 6.8 (13:7 v/v) at a flow rate of 1 mL min⁻¹.

The drug was extracted from the PLGA-MMT composite system and PLGA matrix using a mixture of dichloromethane (DCM) and PBS 7.4 in 1:1 ratio. The aqueous phase containing the drug was quantitatively analysed by HPLC using a calibration curve and the % drug encapsulation efficiency (% EE) and % drug content (% DC) were determined using equations (1) and (2).

$$\% EE = \frac{m_1}{m_2} 100 \quad (1)$$

$$\% DC = \frac{m_1}{m_3} 100 \quad (2)$$

where

m_1 – mass of the drug loaded in sample

m_2 – mass of the total drug added

m_3 – mass of the drug loaded sample

Characterizations of the optimal formulations

X-Ray diffraction (XRD) studies

The X-Ray diffraction (XRD) patterns of MMT, diclofenac sodium, F-68 and the synthesized formulations- 002, 010 and 012 were recorded using Cu K α radiation ($n = 1 \text{ \AA}$) on a Philips X' Pert-PRO MRD system operating at 50 kV and 100 mA in continuous scan mode with a scanning speed of 0.008°sec⁻¹.

Differential scanning calorimetric (DSC) analysis

The differential scanning calorimetric (DSC) analyses of MMT, F-68, pristine diclofenac sodium, diclofenac acid and synthesized formulations- 002, 010 and 012 was performed using Perkin Elmer Q200 (V23.10 build 79) system operating at a heating rate of 20 °C min⁻¹. The samples were purged with nitrogen at a flow rate of 50.0 ml min⁻¹.

Fourier Transformed Infrared (FT-IR) studies

The IR transmission spectra (4000–400 cm⁻¹) were recorded in a KBr matrix at 25 °C using a Perkin-Elmer FT-IR spectrum BX.

Scanning electron microscopic studies (SEM) with EDAX (energy dispersive X-ray analysis)

All the samples were sputter coated with gold (used as a conductive material) and the surface morphology of the samples was then examined using Zeiss EVO MA15 (Oxford instruments).

High resolution transmission electron microscopic (HRTEM) studies

The samples were prepared by depositing the aqueous suspensions of the samples on carbon film attached to a 400 mesh Cu grid. The images were recorded using TECNAI G2T30 FEI Instrument operated at 120 kV.

In vitro drug release kinetics

The study of in vitro drug release behaviour of pure diclofenac sodium and the synthesized formulations was carried out in simulated gastric (PBS 1.2) and intestinal fluid (PBS 7.4) using dialysis bag method for a period of 8 hours. A known amount of the formulation was dispersed in the dialysis bag and was immersed in 100 ml of dissolution media maintained at 37° ± 0.5°C with constant stirring at 300 rpm. After every one hour interval, 5.0 ml of the dissolution medium was withdrawn for the estimation of the drug content and at the same time 5 mL of the fresh solution was added to maintain the constant volume of the dissolution medium.²¹ The obtained 5 mL of the solution was filtered through a membrane with a pore diameter of 0.45µm. The concentration of the drug released was determined by UV spectrophotometer at 277 nm, and then the cumulative percentage of DS released was calculated.

RESULTS AND DISCUSSION

Quantitative estimation of drug in the synthesized formulations by HPLC method

The % encapsulation efficiency and drug content of synthesised formulations as estimated using HPLC are tabulated in Table 1.

Table 1. Encapsulation efficiency and drug content in synthesised formulations

Sample	Amounts, in mg			% EE	% DC
	clay	polymer	drug		
002a	60	40	20	15.31	2.98
002b	40	40	20	29.8	7.13
002	20	40	20	98.01	36.30
002c	10	40	20	45.25	24.14
002d	20	55	20	41.83	6.83
002e	20	86	20	1.72	3.47
010	-	40	20	93.94	41.48
012	20	-	20	66.41	58.80

%EE= % encapsulation efficiency; %DC= % drug content

Keeping the amount of clay and the drug content constant, the effect of the polymer concentration on encapsulation efficiency was investigated. As can be seen (table1), the %

encapsulation efficiency decreases from 98.01% to 1.72% with increase in the concentration of the polymer. To study the effect of the clay amount on % encapsulation efficiency, the amount of the clay was decreased from 60 mg to 10 mg, keeping the amount of the drug and the polymer constant. The encapsulation efficiency increased from 15.31% to 98.01% with decrease in the clay content upto 20mg, a further decrease in the clay content to 10 mg resulted in a decrease in the % encapsulation efficiency and drug content.

In case of 010 formulation (synthesized under the same set of experimental conditions and with same amount of the excipients as in 002 but minus MMT), an encapsulation efficiency of 93.94% was obtained. An encapsulation efficiency of 66.41% was achieved in case of 012 formulation (synthesized under the same set of experimental conditions and with same amount of the excipients as in 002 but minus PLGA).

Altogether, these results suggest that the highest encapsulation efficiency was achievable under the present experimental conditions with 002 formulation.

Characterizations of the optimal formulations

X-Ray diffraction (XRD) studies

The XRD pattern of 002 and 012 formulations show a shift in the peak in the lower angle region in the 001 plane from $2\theta = 6.8^\circ$ in the pristine MMT to 4.4° and 4.7° in 002 and 012 respectively, resulting in an increase in the corresponding d spacing from 13.4 Å to 20 Å and 18.6 Å respectively (Fig.1a and b). This increase in d spacing suggests that the drug has been intercalated within the clay interlayers²¹. Moreover, the diffractogram of 002 and 012 shows characteristic peaks of the drug²² which indicates that the drug is present in crystalline state in the synthesized formulations.

Differential scanning calorimetric (DSC) analysis

To investigate the physical state of diclofenac sodium in the synthesized formulations (002, 010 and 012) and to confirm the interaction of the drug with the excipients, DSC studies were performed. In the DSC curve of pure drug, the melting endothermic peak appears at 292 °C. This is followed by complex endothermic – exothermic phenomenon indicating decomposition of the drug.²³

The small broad endotherm at 65 °C in the DSC trace of 012 formulation (Fig.2a) corresponds to the loss of surfaced adsorbed water followed by another sharp endothermic peak at 176 °C corresponding to the melting endothermic peak of diclofenac acid which indicates the conversion of diclofenac sodium into diclofenac acid in the clay matrix.²⁴ The broad endothermic peak at 303 °C (encircled) which is absent in pristine MMT and F-68 corresponds to the melting of the drug thus suggesting its presence in the crystalline state in the synthesized formulation-012.²⁵ However, the temperature at which this peak appears (303 °C) is lower than the melting endothermic peak of pure diclofenac acid (323 °C). This suggests that there may be certain interaction between the drug and the excipients.

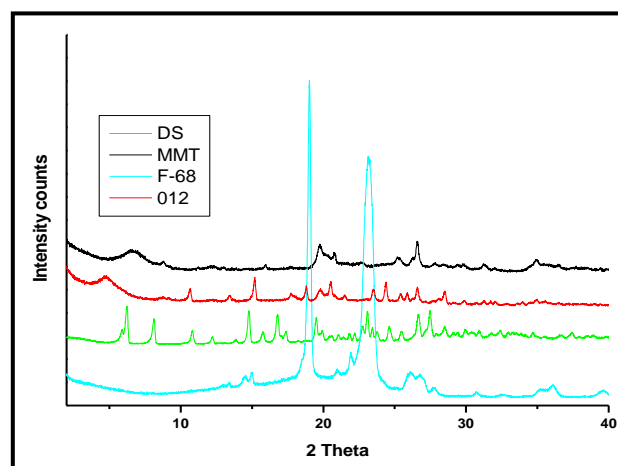


Figure 1a. XRD pattern of formulation 012, MMT, DS and F-68

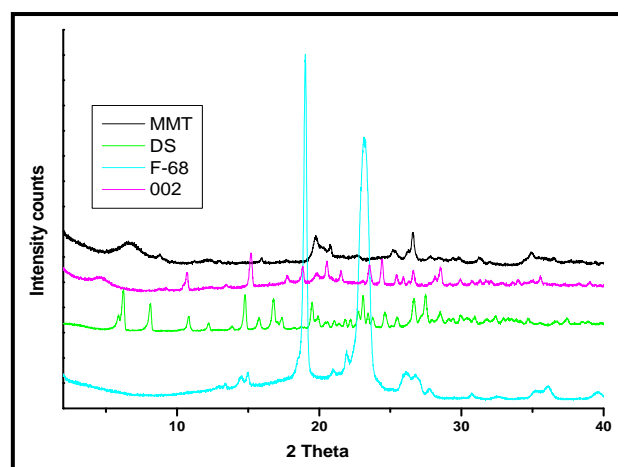


Figure 1b. XRD pattern of formulation 002, MMT, DS and F-68

In case of 010 formulation (Fig.2b), the small endotherm at 50 °C corresponds to the glass transition temperature of PLGA.²⁶ The decomposition temperature of PLGA and the melting endotherm of the pure drug fall in the similar temperature range, therefore it is difficult to observe a clear well defined melting endothermic peak corresponding to the drug in this formulation. However a small endotherm (encircled) can be seen in the DSC curve of 010 formulation at 308 °C which is absent in the DSC curve of pure PLGA and F-68 which could be due to the melting endotherm peak of the diclofenac sodium. A big endotherm peak at 361 °C corresponds to the decomposition of PLGA.²⁷

In the DSC curve of 002 formulation (Fig. 2c), the very small endotherm at 50 °C correspond to the glass transition temperature of PLGA. This is followed by another small endotherm c.a 158 °C which could be due to the loss of interlayer water in MMT.²⁸ The sharp endothermic peak at 280 °C (encircled) corresponds to the melting of the diclofenac sodium as this peak is found to be absent in the DSC curve of pure F-68 and MMT while pure PLGA decomposes at 361 °C thus suggesting the presence of crystalline form of the drug in the formulation. However, this melting endothermic peak appears at slightly lower temperature as compared to the pure drug which may be because of certain possible interaction between the drug and the excipients.

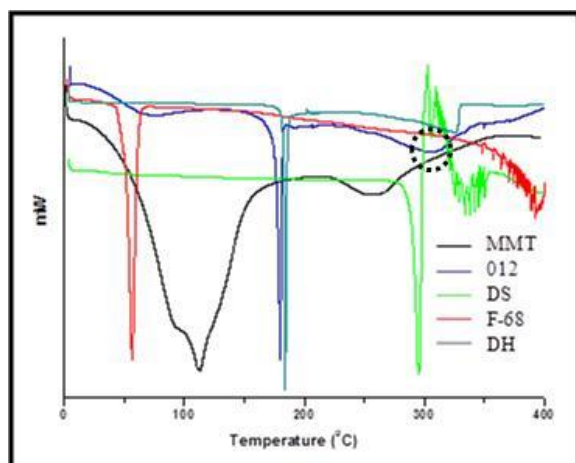


Figure 2a. DSC curves of formulation 012, MMT, DS, DH and F-68

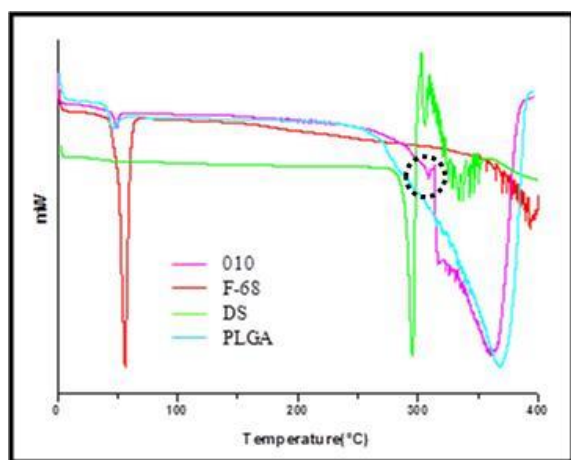


Figure 2b. DSC curves of formulation 010, PLGA, DS and F-68

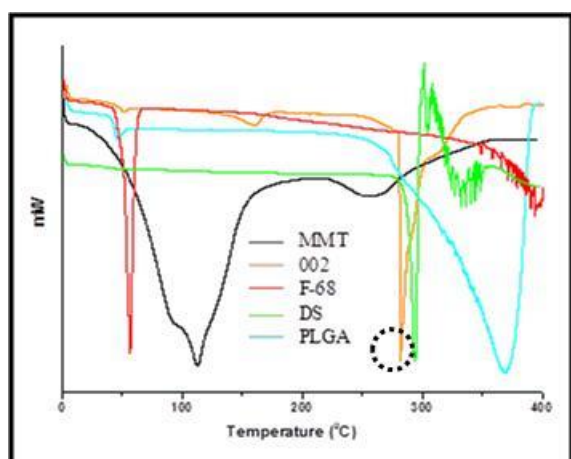


Figure 2c. DSC curves of formulation 002, PLGA, DS, MMT and F-68

Fourier-transformed infrared (FT-IR) spectroscopic studies

The FT-IR spectral studies were carried out to confirm the presence of drug and to investigate the possible interaction between the drug and the excipients. In the 012 synthesized formulation (Fig.3a and 3a1), the band at 3622 cm^{-1} corresponds to the O-H stretching vibrations from the

structural water in the clay. The presence of characteristic vibrational band at 1044 cm^{-1} corresponding to Si-O stretching indicates the presence of clay matrix.²⁹ The vibrational band at 3324 cm^{-1} corresponds to the N-H stretching while the intense band at 1694 cm^{-1} has been assigned to C=O stretching from the -COOH group in the drug.²⁴ The presence of these two bands (at 3324 cm^{-1} and 1694 cm^{-1}) suggests the conversion of diclofenac sodium into diclofenac acid^{30,31} as is evident from the DSC results of this formulation. The vibrational bands at 1508 cm^{-1} corresponds C-N-H in plane bending respectively from the drug molecule. The vibrational band at 1454 cm^{-1} has been assigned to -CH₂ bending from disubstituted benzene ring from the drug molecule. The bands at 766 cm^{-1} and 742 cm^{-1} correspond to out of plane C-H ring bending and in plane ring deformation respectively in the drug.^{32,33}

In the 010 formulation (Fig.3b and 3b1), the broad vibrational band at 3449 cm^{-1} corresponds to the O-H stretching vibration from F-68.³⁴ The weak vibrational band at 2995 cm^{-1} corresponds to -CH, -CH₂ stretching while the one at 1761 cm^{-1} corresponds to -C=O stretching from PLGA.³⁵ The vibrational band at 1454 cm^{-1} corresponds to -CH₂ bending from disubstituted benzene ring from the drug molecule while the bands at 766 cm^{-1} and 742 cm^{-1} correspond to out of plane C-H ring bending and in plane ring deformation respectively from the drug molecule.

In the 002 formulation (Fig.3c and c1), the vibrational band at 1760 cm^{-1} corresponds to the -C=O stretching in PLGA. The bands at 766 cm^{-1} and 742 cm^{-1} correspond to out of plane C-H ring bending and in plane ring deformation respectively from the drug molecule. The shifting of the band from 3622 cm^{-1} in pristine MMT corresponding to the O-H stretching vibrations from the structural water [(Al, Mg-) OH] in the clay to 3651 cm^{-1} in 002 sample suggests the interaction of the structural hydroxyl groups in MMT with the polar groups of F-68.

The presence of characteristic absorption bands of the drug in the synthesized formulations confirms presence of the drug in these synthesized formulations. No significant shifting of the absorption bands of drug was observed in the synthesized formulations suggesting that there is no strong chemical interaction between the drug and the excipients. The characteristic absorption band at 1760 cm^{-1} in PLGA corresponding to the C=O vibrational stretching was not shifted in 002 and 010 formulations suggesting that there is no strong chemical interaction of PLGA either with the encapsulated drug, F-68 or MMT.

Scanning electron microscopic studies (SEM) with EDAX (energy dispersive X-ray analysis)

The morphology of 012 formulation seems to have become agglomerated as compared to pristine MMT (Fig. 4). The agglomeration may have taken place because of the presence of small amount of non- intercalated drug (free drug) and /or F-68 on the clay surface. The EDAX data (S1, Supplementary material) shows the presence of drug as indicated by chlorine content.

The 010 formulation has rod like structures as clearly seen in the SEM images. The surface morphology of 002 formulation is different from that of pristine montmorillonite.

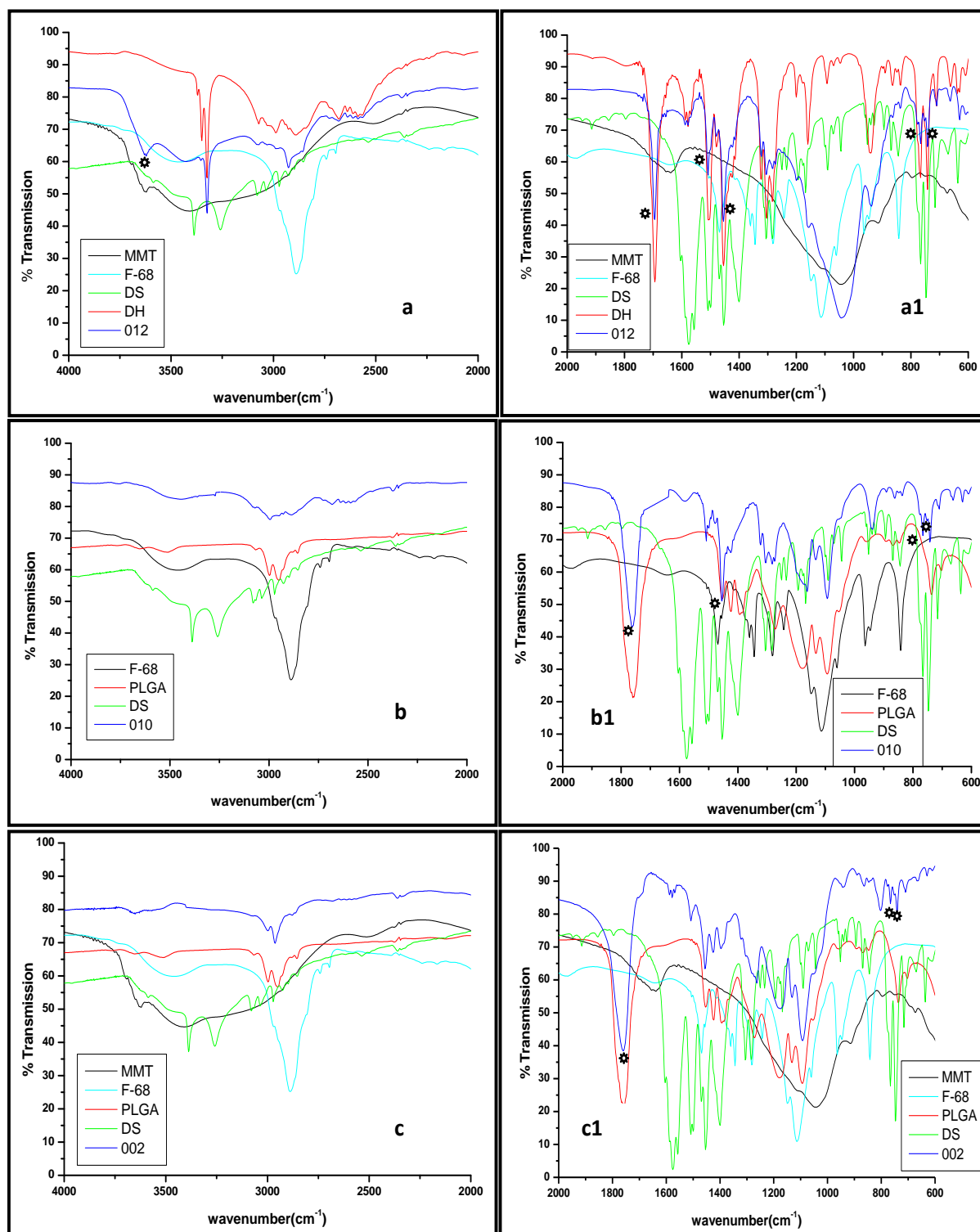


Figure 3. FTIR spectra a) 012 in 4000-2000 cm⁻¹ range, a1) 012 in 2000-600 cm⁻¹ range; b) 010 in 4000-2000 cm⁻¹ range, b1) 010 in 2000-600 cm⁻¹ range; c) 002 in 4000-2000 cm⁻¹ range, c1) 002 in 2000-600 cm⁻¹ range along with MMT, DS, DH, F-68

The structure seems to have become more porous. The EDAX data of 002 formulation shows the presence of drug as suggested by the presence of chlorine. It is clear from the EDAX data that the % composition by weight of this formulation shows highest chlorine content as compared to 012 and 010 formulations. The EDAX figures can be seen in the supplementary material (S1). This is supported by

the fact that this formulation shows highest encapsulation efficiency of all the three formulations. This shows that it is clay which plays an important role in the entrapment of the drug in the PLGA/MMT composite as the composition of the 010 formulation is just the same but without clay and this formulation shows comparatively lower encapsulation efficiency.

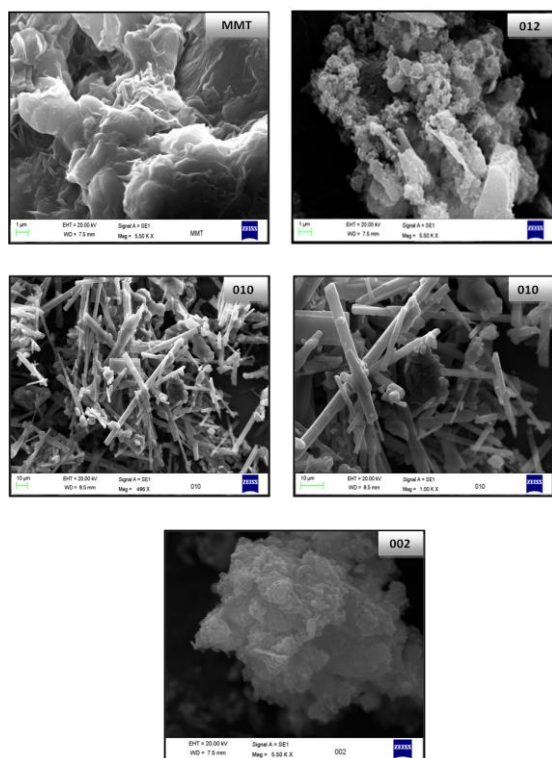


Figure 4. SEM images of MMT and drug encapsulated formulations-012, 010 and 002

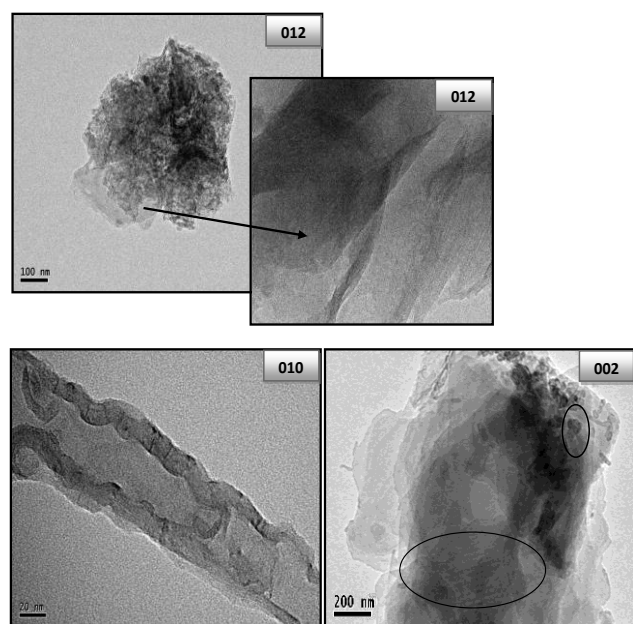


Figure 5. TEM images of drug encapsulated formulations-012, 010 and 002

High resolution transmission electron microscopic (HRTEM) studies

The particle size of the encapsulated drug in the 012 formulation was found to be in the range of 5 nm to 10 nm from the HRTEM image (Fig.5. image 012a). The well defined layered structure of clay observed in this case (image 012b) excludes the possibility of exfoliation and supports the XRD results which suggest intercalation. The HRTEM images of 010 formulation show rod like structures (also seen in the scanning electron micrographs) with a thickness of around 15 nm. In the HRTEM image of 002

formulation, the drug encapsulated PLGA particles can be seen entrapped in the clay layers (small circled) with a particle size in the range 10 nm to 20 nm. The characteristic Moiré fringes can be seen in the 002 micrograph (big circled) indicating misaligned stacking of the nanoplatelets in MMT. The misaligned stacking of the nanoplatelets for 002 formulation was believed to associated with their lamellar structure.³⁶ The interplanar distance of 25 Å in the Moiré fringes confirms the intercalation of the PLGA encapsulated drug in the clay in accordance with the XRD results, however the d spacing value obtained is slightly on the higher side as compared to the corresponding XRD results. Taking into account the d spacing of MMT (1.34 nm), PLGA/MMT nanocomposite (2.0 nm) and average particle size of the PLGA encapsulated drug particles (15 nm) in PLGA/MMT nanocomposite, it can be concluded that the entrapped drug particles are arranged at an angle and not in an absolute anti conformation in the clay interlayer in the synthesized PLGA/MMT nanocomposite.

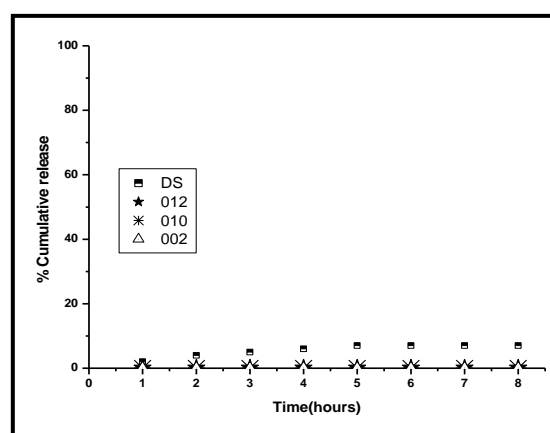


Figure 6a. In vitro cumulative release profiles of pure DS and drug encapsulated formulations- 012, 010 and 002 in PBS 1.2.

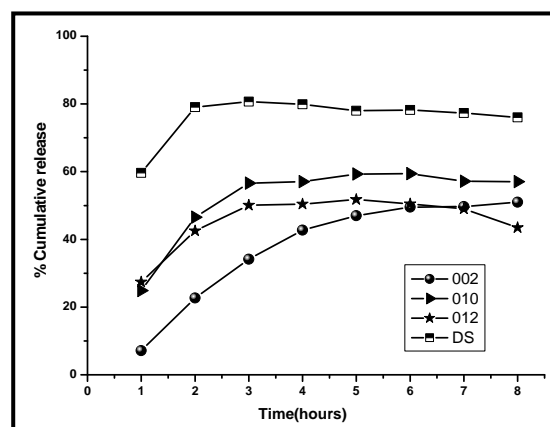


Figure 6b. In vitro cumulative release profiles of pure DS and drug encapsulated formulations- 012, 010 and 002 in PBS 7.4.

In vitro drug release kinetics

From (Fig.6a), it is evident that no drug release takes place from any of the three formulations synthesized, in simulated gastric fluid (PBS 1.2). However, 4 % release was seen in the second hour and a total of 7 % release was observed in 8 hours in case of pure drug. It was observed that 60% of the pure diclofenac sodium was released in the first hour in simulated intestinal fluid (PBS 7.4) which rose

to 80% in the second hour after which no drug release was seen (Fig. 6b). Whereas in the case of 012 formulation, 25 % of the drug was released in the first hour after which slow release was found to occur releasing up to 51 % of the drug by 5th hour after which no drug release was found to occur. In the case of 010 formulation, 24.9 % of the drug was released in the first hour releasing up to 59.42 % of the drug up to 6th hour. After 6th hour no drug release was found to take place. In the 002 formulation, 7 % of the drug was released in the first hour exhibiting sustained release afterwards, releasing 51 % of the drug by the 8th hour.

A sustained release was seen in all the formulations synthesized as compared to the pure drug. The 010 formulation exhibited more sustained release than 012 formulation and also a higher amount of the drug release was seen as compared to rest of the formulations synthesized. However, out of all, the most sustained release behaviour was seen in 002 formulation, with no burst release implying that the outer covering of the clay plays an important role in the sustained release of the drug encapsulated in the polymer.

Infact the drug encapsulated PLGA/MMT nanocomposite shows more sustained release as compared to the commercial sustained release Voltaren tablet which is known to release ~85 % of the drug by the 8th hour.³⁷ The almost no release of DS in pH 1.2 PBS and a sustained release in pH 7.4 PBS makes the PLGA/MMT nanocomposite an excellent pH-sensitive matrix for sustained drug release, which could be used for the fabrication of pharmaceutical formulation for oral intake.

Surface morphology of 002 formulation after drug release

There is a clear change in the morphology of 002 formulation after drug release (Fig.7). The SEM image of the 002 formulation show swelled clay particles with perforations (encircled region in the image) indicating the release of the encapsulated drug from the clay interlayers.

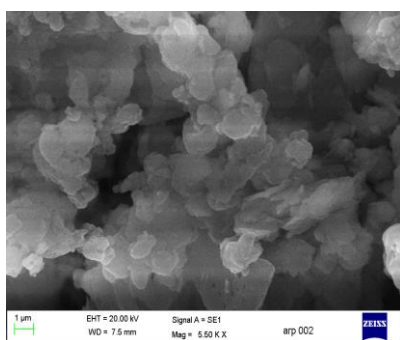


Figure 7. SEM image of 002 formulation after drug release

Mechanism of drug encapsulation in PLGA/ montmorillonite nanocomposite

The poloxamer 188 is supposed to form micelles in the clay interlayers (as critical micellar concentration of it has been used) (Fig. 8a) and intercalates through polar interactions with the structural hydroxyl groups in the clay.

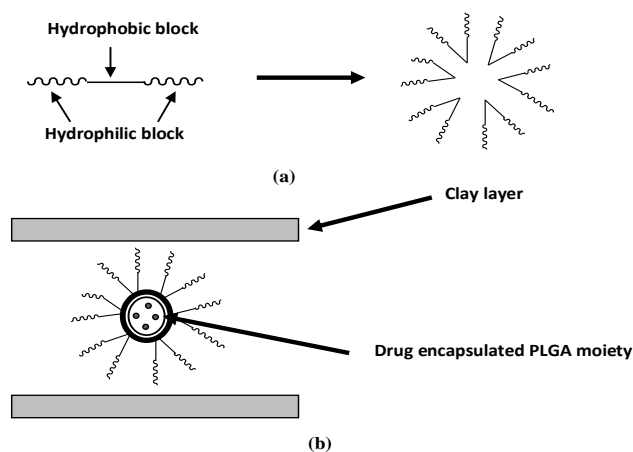


Figure 8. a) Micellization of poloxamer 188, b) Encapsulation of drug encapsulated PLGA moiety in clay interlayers

This is evident from the FTIR spectral results of drug encapsulated PLGA/montmorillonite nanocomposite sample (002 formulation) wherein a shift in the vibrational band corresponding to the structural hydroxyl group in MMT was seen towards higher wavenumber from 3622 cm^{-1} in pristine MMT to 3651 cm^{-1} in the drug encapsulated PLGA/montmorillonite nanocomposite. The PLGA encapsulate the drug through interaction of its polar groups with the polar groups of the drug. This drug encapsulated PLGA moiety then intercalates into the clay layers by encapsulation into the hydrophobic cavity of poloxamer 188 micelles through hydrophobic interactions with non polar groups of poloxamer 188 (Fig.8b).

CONCLUSION

Diclofenac sodium loaded PLGA/MMT nanocomposite was prepared by double emulsion solvent evaporation process. The XRD results confirmed the intercalation of the drug encapsulated PLGA moiety in the clay interlayers. The DSC results indicate the presence of the crystalline form of drug in PLGA/MMT nanocomposite. The FTIR results suggest that there is no strong chemical interaction between the drug and the excipients. The particle size of the encapsulated drug in the nanocomposite was found to be in the range 10 nm to 20 nm. The presence of MMT resulted in high drug encapsulation efficiency (98.01 %) as confirmed by the comparative studies performed to evaluate the role of clay. However, the presence of PLGA is also necessary as in its absence the drug encapsulation efficiency drastically decreases (66.41 %, formulation 012). No drug release was found to occur in simulated gastric fluid (PBS 1.2) in any of the formulations synthesized, indicating the stability of the formulations under strong acidic conditions prevailing in the stomach. The drug loaded PLGA/MMT nanocomposite (002 formulation) demonstrated the most sustained release behaviour in simulated intestinal conditions (PBS 7.4) as compared to the other formulations, releasing 51 % of the drug in the 8th hour. No burst release was seen during the initial hour implying that the clay plays an important role in the sustained release of the drug encapsulated in the polymer as evident from the comparative in vitro release studies results (formulation 010).

In fact the drug loaded PLGA/MMT nanocomposite is found to show more sustained release in comparison to the commercial Voltaren tablet in simulated intestinal fluid (PBS 7.4). Thus on the basis of the present results, it can be concluded that PLGA/MMT nanocomposite may function as a suitable drug delivery vehicle for oral sustained release of diclofenac sodium.

ACKNOWLEDGEMENT

The authors are grateful to the Head, Department of Chemistry, Department of Geology and the Director of the University Science Instrumentation Centre of the University of Delhi for providing the Instrumentation facilities. We are also thankful for the financial assistance received from the University of Delhi in the form of annual research grant for carrying out the research work.

REFERENCES

- ¹Chang, J. H., Ana, Y. U., Choa, D., Giannelis, E. P., *Polymer*, **2003**, *44*, 3715–3720.
- ²Cypes, S. H. W., Saltzman, M., Giannelis, E. P., *J. Control. Release*, **2003**, *90*, 163–169.
- ³Lee, W. F., Fu, Y. T., *J. Appl. Polym. Sci.*, **2003**, *89*, 3652–3660.
- ⁴Kiersnowski, A., Pigłowski, J., *Eur. Polym. J.*, **2004**, *40*, 1199–1207.
- ⁵Lee, W. F., Chen, Y. C., *J. Appl. Polym. Sci.*, **2004**, *91*, 2934–2941.
- ⁶Puttipipatkachorn, S., Pongjanyakul, T., Priprem, A., *Int. J. Pharm.*, **2005**, *293*, 51–62.
- ⁷Pongjanyakul, T., Priprem, A., Puttipipatkachorn, S., *J. Pharm. Pharmacol.*, **2005a**, *57*, 429–434.
- ⁸Greenblatt, G. D., Hughes, L. D., Whitman, W., Patent number EP1470823, **2004**.
- ⁹Nagasaki, Y., Takahashi, T., Kataoka, K., Yamada, Y., *PCT Int. Appl.*, WO 2005005548, **2005**.
- ¹⁰Zhong, S., U.S. Pat. Appl. Publ. US 2005181015, **2005**.
- ¹¹Jiang, W. L., Gupta, R. K., Deshpande, M. C., Schwendeman, S. P., *Adv. Drug Deliv. Rev.*, **2005**, *57*, 391–410.
- ¹²Zweers Mielche, L. T., Engbers Gerard, H. M., Grijpma Dirk, W., Jan, F. J., *J. Control. Release*, **2004**, *100*, 347–356.
- ¹³Jain, R.A., *Biomaterials*, **2000**, *21*, 2475–2490.
- ¹⁴Aguzzi, P.C., Viseras, C., Caramella, C., *Appl. Clay Sci.*, **2007**, *36*, 22.
- ¹⁵Dong, Y., Feng, S. S., *Biomaterials*, **2005**, *26*, 6068.
- ¹⁶Takahashi, T., Yamada, Y., Kataoka, K., Nagasaki, Y., *J. Control. Release*, **2005**, *107*, 408.
- ¹⁷Saravanan, M., Bhaskar, K., Maharajan, G., Pillai, K. S., *Int. J. Pharm.*, **2004**, *283*, 71–82.
- ¹⁸Arias, J. L., López-Viota, M., Sáez-Fernández, E., Ruiz, M. A., *Colloids Surf.*, **2010**, *75*, 204–208.
- ¹⁹Bertocchi, P., Antoniella, E., Valvo, L., Alimontia, S., Memoli, A., *J. Pharm. Biomed. Anal.*, **2005**, *37*, 679–685.
- ²⁰Davies, N. M., *J. Pharm. Pharm. Sci.*, **1999**, *2*, 5–14.
- ²¹Joshi, G. V., Kevadiya, B. D., Patel, H. A., Bajaj, H. C., Jasra, R. V., *Int. J. Pharm.*, **2009**, *374*, 53–57.
- ²²Kenawi, I. M., Barsoum, B. N., Youssef, M. A., *J. Pharm. Biomed. Anal.*, **2005**, *37*, 655–661.
- ²³Tudja, P., Khan, M. Z. I., Mestrovic, E., Horvat, M., Golja, P., *Chem. Pharm. Bull.*, **2001**, *49*, 1245–1250.
- ²⁴Durairaj, C., Kim, S. J., Edelhauser, H. F., Shah, J. C., Kompella, U. B., *Invest. Ophthalmol. Vis. Sci.*, **2009**, *50*, 4887–4889.
- ²⁵Dixit, M., Kulkarni, P. K., Panner, S., *Int. Res. J. Pharm.*, **2011**, *2*, 207–210.
- ²⁶Mukerjee, A., Vishwanatha, J. K., *Anticancer Res.*, **2009**, *29*, 3867–3876.
- ²⁷Mainardes, R. M., Gremião, M. P. D., Evangelista, R. C., *Brazil. J. Pharm. Sci.*, **2006**, *42*, 528.
- ²⁸Del Hoyo, C., Rives, V., Vicente, M. A., *Thermochim. Acta*, **1996**, *286*, 89–103.
- ²⁹Davarcioğlu, B., Ciftci, E., *Int. J. Nat. Eng. Sci.*, **2009**, *3*, 154–161.
- ³⁰Jubert, A., Massa, N. E., Tevez, L. L., Okulik, N. B., *Vibrat. Spectros.*, **2005**, *37*, 161–178.
- ³¹Beck, R. C. R., Lionzo, M. I. Z., Costa, T. M. H., Benvenuti, E. V., Ré, M. I., Gallas, M. R., Pohlmann, A. R., Guterres, S. S., *Brazil. J. Chem. Eng.*, **2008**, *25*, 389–398.
- ³²Kenawi, I. M., Barsoum, B. N., Youssef, M. A., *J. Pharm. Biomed. Anal.*, **2005**, *37*, 655–661.
- ³³Iliescu, T., Baia, M., Kiefer, W., *Chem. Phys.*, **2004**, *298*, 167–174.
- ³⁴Patil, S. B., Shete, D. K., Narade, S. B., Surve, S. S., Khan, Z. K., Bhise, S. B., Pore, Y. V., *Drug Discov. Therap.*, **2010**, *4*, 435–441.
- ³⁵Dey, S. K., Mandal, B., Bhowmik, M., Ghosh, L. K., *Brazil. J. Pharm. Sci.*, **2009**, *45*, 589.
- ³⁶Lin, K-J., Jeng, U-S., Lin, K-F., *Mater. Chem. Phys.*, **2011**, *131*, 120–126.
- ³⁷Korkiatithaweechai, S., Umsarika, P., Praphairaksit, N., Muangsin, N., *Mar. Drugs*, **2011**, *9*, 1660.

Received: 30.03.2013.
Accepted: 03.05.2013.



MICROWAVE ASSISTED EXPEDITIOUS SYNTHESIS OF BIOACTIVE POLYHYDROQUINOLINE DERIVATIVES

Vijaykumar M. Joshi^[a] and Rajendra P. Pawar^{[b]*}

Keywords: polyhydroquinolines, Hantzsch's condensation, $\text{ZnFe}_{0.2}\text{Al}_{1.8}\text{O}_4$ nanocomposite catalyst, microwave irradiation.

A facile and green one pot four component synthesis of polyhydroquinoline derivatives from aldehydes, dimedone, ethyl acetoacetate and ammonium acetate in the presence of a spinel ($\text{ZnFe}_{0.2}\text{Al}_{1.8}\text{O}_4$) composite catalyst has been reported under microwave irradiation. The method offers excellent yield of products in short reaction time.

Corresponding Author

Fax: +91-240-2334430.

Email: rppawar@yahoo.com

[a] Shri Jagdishprasad Jhabarmal Tibrewala University, Rajasthan, India

[b] Department of Chemistry, Deogiri College, Aurangabad-431 005, (MS) India.

Introduction

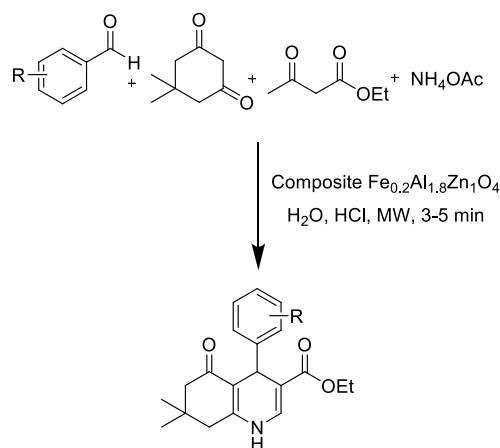
Recently, the class of polyhydroquinoline heterocycles has emerged as one of the most important class of drugs used in the treatment of cardiovascular diseases, including hypertension.¹ Certain cardiovascular agents nifedipine, nicardipine, amlodipine and other dihydropyridyl compounds, are also used effectively in hypertension treatment.² These compounds are also known for a wide range of biological activity.³ Polyhydroquinoline derivatives are found to be analogs of NADH co-enzymes, which are explored for calcium channel activity. The heterocyclic rings present in such compounds are also employed as bronchodilators, geroprotective and hepatoprotective agents.⁴ Overall, these compounds exhibit different medicinal functions, acting as neuroprotectants, antiplatelet aggregators, cerebral antiischemic agents and chemosensitizers.⁵ Thus, polyhydroquinoline compounds have attracted the attention of chemists to synthesize these compounds.

In view of the importance of polyhydroquinoline derivatives, many classical methods for the synthesis of these heterocycles are reported⁶⁻¹¹ using conventional heating and refluxing approaches in presence of an organic solvent. These methods, however, involves long reaction times, harsh reaction conditions, use of a large quantity of volatile organic solvents and low yields.

Non-conventional microwave irradiation (MW) processes have also attracted the attention of synthetic organic chemists due to fast reaction rate. Better results can be obtained by employing MW heating under similar reaction conditions.¹² Thus, the development of an efficient and versatile method for the preparation of polyhydroquinoline derivatives is necessary. Progress in this field is including the recent promotion of microwave irradiation, TMSCl , ionic liquids, polymers and $\text{Yb}(\text{OTf})_3$.¹³

Heterogeneous catalysts are being explored rapidly in organic synthesis due to their wide range of advantages over

homogenous catalysts.¹⁴⁻¹⁵ In continuation of our efforts in the development of new routes for the synthesis of heterocyclic compounds using composite materials,¹⁶ herein we report a one pot synthesis of Hantzsch's polyhydroquinoline derivatives in aqueous medium and spinel composites (**Scheme-1**).



Scheme 1

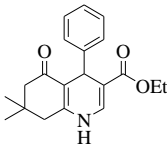
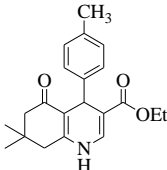
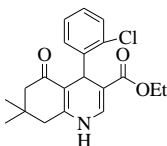
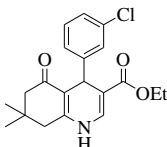
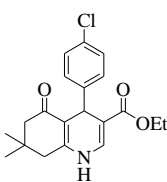
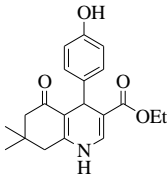
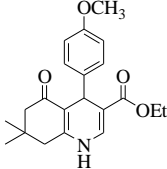
Experimental Section

All the chemicals were purchased from SD fine chemicals Ltd and used without further purification. Melting points of the products were in open capillaries and were uncorrected. NMR spectra were recorded 400 MHz Varian NMR spectrophotometer using tetramethylsilane (TMS) as the internal standard. All solvents were AR grade and used as received. IR spectra of the samples were recorded on Perkin IR spectrophotometer using KBr discs and samples were analyzed for mass on Shimadzu mass analyzer. The catalyst was synthesized by reported sol-gel method.¹⁷

General procedure for the synthesis of Hantzsch's polyhydroquinoline derivatives:

A mixture of aldehyde (1 mmol), dimedone (1mmol), ethyl acetoacetate (1 mmol), ammonium acetate (1.5 mmol) and composite-A ($\text{ZnFe}_{0.2}\text{Al}_{1.8}\text{O}_4$) (50 mg) in 5 mL of water and 2 drops of HCl was irradiated under microwave for 3-5 minutes in a scientific oven (RAGA'S Electromagnetic

Table 1. Synthesis of polyhydroquinoline by using composite-A under microwave irradiation.

Sr. No.	Ar	Product	Time, min	Yield, %	M.P., °C
1	C ₆ H ₅		3	96	205-207
2	4-CH ₃ -C ₆ H ₄		4	95	261-263
3	2-Cl-C ₆ H ₄		5	94	209-211
4	3-Cl-C ₆ H ₄		4	96	230-232
5	4-Cl-C ₆ H ₄		4	95	242-244
6	4-OH-C ₆ H ₄		5	94	235-238
7	4-OCH ₃ -C ₆ H ₄		5	90	258-260

8	4-NO ₂ -C ₆ H ₄		5	94	240-242
9	4-OH-3-NO ₂ -C ₆ H ₃		5	90	236-238
10	2-OCH ₃ -C ₆ H ₄		3	90	248-250
11	4-Br-C ₆ H ₄		4	93	250-253
12	4-F-C ₆ H ₄		4	95	182-185

System). After completion of reaction, the mixture was allowed to cool at room temperature. The reaction mixture was treated with ice-cold water; separated solid product was filtered and recrystallized from ethanol to obtain the pure product.

Using the same procedure a series of different polyhydroquinoline derivatives were prepared (**Table 1**). All the synthesized compounds are reported and characterized by IR, ¹H NMR, mass and comparison of their physical constants as reported in the literature. The spectral data of the representative compounds is described below:

Ethyl 1,4,5,6,7,8-hexahydro-4-(phenyl)-7,7-dimethyl-5-oxoquinoline-3-carboxylate (1): M.P. 205-207°C, IR (KBr, cm⁻¹): 3289, 3080, 2959, 1698, 1610; ¹H NMR (DMSO) δ ppm 0.91 (s, 3H), 1.05 (s, 3H), 1.17 (t, 2H), 2.14-2.20 (m, 4H), 2.28 (s, 3H), 4.03 (q, 3H), 5.02 (s, 1H) 5.96 (s, 1H), 7.04-7.09 (m, 1H), 7.14-7.19 (m, 2H), 7.23-7.26 (m, 2H).

Ethyl 1,4,7,8-tetrahydro-2,7,7-trimethyl-4-(2-chlorophenyl)-5(6H)-oxoquinolin-3-carboxylate (3): M.P. 209-211°C, IR (KBr, cm⁻¹): 3063, 2956, 1721, 1640, 1611, 1467, 1384, 1227, 1021, 745; ¹H NMR (200 MHz, DMSO-d₆): δ 0.95 (s, 3H, CH₃), 1.05 (s, 3H, CH₃), 1.20 (t, 3H, CH₃),

2.01-2.21 (m, 4H, 2-CH₂), 2.40 (s, 3H, CH₃), 4.05 (q, 2H, CH₂), 4.60 (s, 1H, CH), 7.10-7.30 (m, 4H, ArH), 7.60 (s, 1H, NH).

Ethyl-1,4,7,8-tetrahydro-2,7,7-trimethyl-4-(4-methoxyphenyl)-5(6H)-oxoquinolin-3-carboxylate (7):

M.P. 258-260 °C, IR (KBr, cm⁻¹): 3276, 2956, 1703, 1648, 1606, 1496, 1381, 1215, 1031, 765; ¹H NMR (200 MHz, DMSO-d₆): δ ppm 0.95 (s, 3H, CH₃), 1.09 (s, 3H, CH₃), 1.21 (t, 7.2 Hz, 3H, CH₃), 2.01-2.10 (m, 4H, 2-CH₂), 2.30 (s, 3H, CH₃), 3.70 (s, 3H, OCH₃), 4.00 (q, 2H, CH₂), 4.80 (s, 1H, CH), 6.65 (d, 2H, ArH), 7.10 (d, 2H, ArH), 8.65 (s, 1H, NH).

Conclusion

In summary the present work explores a green approach for the one pot four component Hantzsch's polyhydroquinoline derivatives using nano composite ZnFe_{0.2}Al_{1.8}O₄ as a catalyst under microwave irradiation. This protocol has several advantages such as shorter reaction time, green synthetic method with clean reaction profile.

References

- ¹(a) Bossert, F., Meyer, H., Wehinger, E. *Angew. Chem. Int. Ed. Engl.* **1981**, *20*, 762-769 (b) Nakayama, H., Kasoaka, Y. *Heterocycles* **1996**, *42*, 901-909.
- ²(a) Buhler, F. R., Kiowski, W. *J. Hypertens.* **1987**, *5*, S3-10 (b) Reid, J. L., Meredith, P. A., Pasanisi, F. *J. Cardiovasc. Pharmacol.* **1985**, *7*, S18-20.
- ³(a) Mauzeral, D., Westheimer, F. H. *J. Am. Chem. Soc.* **1955**, *77*, 2261-2264 (b) Baraldi, P. G., Bu-driesi, R., Cacciari, B., Chairini, A., Garuti, L., Giovanninetti, G., Leoni, A., Roberti, M. *Collect. Czech. Chem. Commun.* **1992**, *57*, 169-178 (c) DiStilo, A., Visentin, S., Clara, C., Gasco, A. M., Ermondi, G., Gasco, A. *J. Med. Chem.* **1998**, *41*, 5393-5401 (d) Kawase, M., Shah, A., Gaveriya, H., Motohashi, N., Sakagami, H., Varga, A., Molnar, J. *J. Bioorg. Chem.* **2002**, *10*, 1051-1055. (e) Suarez, M., Verdecia, Y., Illescas, B., Martinez-Alvarez, R., Avarez, A., Ochoa, E., Seoane, C., Kayali, N., Martin, N. *Tetrahedron* **2003**, *59*, 9179-9186 (f) Shan, R., Velazquez, C., Knaus, E. E. *J. Med. Chem.* **2004**, *47*, 254-261 (g) Sawada, Y., Kayakiri, H., Abe, Y., Mizutani, T., Inamura, N., Asano, M., Hatori, C., Arsmori, I., Oku, T., Tanaka, H. *J. Med. Chem.* **2004**, *47*, 2853-2863.
- ⁴(a) Godfraid, T., Miller, R., Wibo, M. *Pharmacol. Rev.* **1986**, *38*, 321-416 (b) Sausins, A., Duburs, G. *Heterocycles* **1988**, *27*, 269-289 (c) Mager, P. P., Coburn, R. A., Solo, A. J., Triggle, D. J., Rothe, H. *Drug Des. Discov.* **1992**, *8*, 273-289 (d) Mannhold, R., Jablonka, B., Voigdt, W., Schoenafinger, K., SchraVan, K. *Eur. J. Med. Chem.* **1992**, *27*, 229-235.
- ⁵(a) Klusa, V. *Drugs Future* **1995**, *20*, 135-138 (b) Bretzen, R. G., Bollen, C. C., Maeser, E., Federlin, K. F. *Am. J. Kidney Dis.* **1993**, *21*, 53-64 (c) Boer, R., Gekeler, V. *Drugs Future* **1995**, *20*, 499-509.
- ⁶ Hantzsch, A. *Ann. Chem.* **1882**, *215*, 1-82.
- ⁷ Sainani, J. B., Shah, A. C., Arya, V. P. *Indian J. Chem. Sect B* **1994**, *33*, 526-531.
- ⁸ Ahluwalia, V. K., Goyal, B., Das, U. *J. Chem. Res. Synop.* **1997**, 266.
- ⁹ Margarita, S., Estael, O., Yamila, V., Beatriz, P., Lourdes, M., Nazario, M., Margarita, Q., Carlos, S., Jose, L. S., Hector, N., Norbert, B., Oswald, M. P. *Tetrahedron* **1999**, *55*, 875-884.
- ¹⁰ Ahluwalia, V. K., Goyal, B., Das, U. *J. Chem. Res. Miniprint.* **1997**, *7*, 1501.
- ¹¹ Ahluwalia, V. K., Goyal, B. *Indian J. Chem. Sect. B* **1996**, *35*, 1021-1025.
- ¹³(a) Khadikar, B. M., Gaikar, V. G., Chitnavis, A. A. *Tetrahedron Lett.* **1995**, *36*, 8083-8086. (b) Ohberg, L., Westman, J. *Synlett* **2001**, 1296-1298. (c) Tu, S.-J., Zhou, J.-F., Deng, X., Cai, P.-J., Wang, H. Feng, J.-C. *Chin. J. Org. Chem.* **2001**, *21*, 313-316. (d) Agarwal, A., Chauhan, P. M. S. *Tetrahedron Lett.* **2005**, *46*, 1345-1348. (e) X-L. Zhang, S-R. Sheng, X-L. Liu, X-L. Liu, *ARKIVOC* **2007**, (xiii), 79-86.
- ¹⁴ Dalko, P. I., Moisan, L. *Angew. Chem. Int. Ed.*, 2004, *43*, 5138-5175;
- ¹⁵(a) List, B., Lerner, R. A., Barbas, C. F. III, *J. Am. Chem. Soc.* **2000**, *122*, 2395-2396 (b) W. Notz, B. List *J. Am. Chem. Soc.* **2000**, *122*, 7386-7387 (c) List, B., Porjarliev, P., Castello, C. *Org. Lett.*, **2001**, *3*, 573-575 (d) Cordova, A., Notz, W., Barbas, C. F. III, *Chem. Commun.* **2002**, 3024-3025 (e) A. Cordova, W. Notz, C. F. Barbas, III *J. Org. Chem.* **2002**, *67*, 301-303 (f) A. B. Northrup and D. W. C. MacMillan *J. Am. Chem. Soc.* **2002**, *124*, 6798-6799 (g) Bøgevig, A., Kumaragurubaran, N., Jørgensen, K. A. *Chem. Commun.* **2002**, 620-621 (h) H. Torii, M. Nakadai, K. Ishihara, S. Saito and H. Yamamoto, *Angew. Chem. Int. Ed.* **2004**, *43*, 1983-1986 (i) A. Berkessel, B. Koch and J. Lex, *Adv. Synth. Catal.* **2004**, *346*, 1141-1146 (j) A. J. A. Cobb, D.M. Shaw, D. A. Longbottom, J. B. Gold and S. V. Ley, *Org. Biomol. Chem.* **2005**, *3*, 84-96.
- ¹⁶ Joshi, V. M., Vyawahare, S. K., Tekale, S. U., Shinde, S. B., Fareesuddin, M., Dake, S. A., Shisodia, S. U., Pawar, R. P. *Eur. Chem. Bull.* **2013**, *2*, 481-484.
- ¹⁷ Mircea, S., Stoia, O., Stefanescu, P., Barvinschi, J. *Therm. Anal. Calorim.*, **2010**, *99*, 459-464.

Received: 10.04.2013.

Accepted: 03.05.2013.



A GREEN REGIO- AND DIASTEREOSELECTIVE SYNTHESIS OF NOVEL TRISPIROHETEROCYCLES IN 2,2,2-TRIFLUOROETHANOL

Anshu Dandia^{[a]*}, Ruby Singh^[a], Jyoti Joshi^[b] and Sukhbeer Kumari^[b]

Keywords: Spiroheterocycles; cycloaddition; azomethine ylides; 2,2,2-trifluoroethanol; trispiropyrrolidine and thiapyrrrolizidine derivatives

A new regio- and diastereoselective 1,3-dipolar cycloaddition reaction of 7,9-bis[(E)-arylidene]-1,4-dioxaspiro[4,5]decane-8-ones, sarcosine/1,3-thiazolane-4-carboxylic acid and acenapthequinone has been developed for the synthesis of trispiropyrrolidine/thiapyrrrolizidine derivatives using 2,2,2-trifluoroethanol as a green solvent. The solvent (TFE) can be readily separated from reaction products and recovered in excellent purity for direct reuse. A regio- and stereochemical outcome of the cycloaddition reaction was ascertained by X-ray crystallographic study.

Corresponding Author*

Tel: +91-9414073436; (0141) 2520301

Fax: 0091-141-2523637

E-Mail: dranshudandia@yahoo.co.in

[a] Department of Chemistry, University of Rajasthan, Jaipur, India

[b] Department of Chemistry, Malaviya National Institute of Technology, Jaipur, India

INTRODUCTION

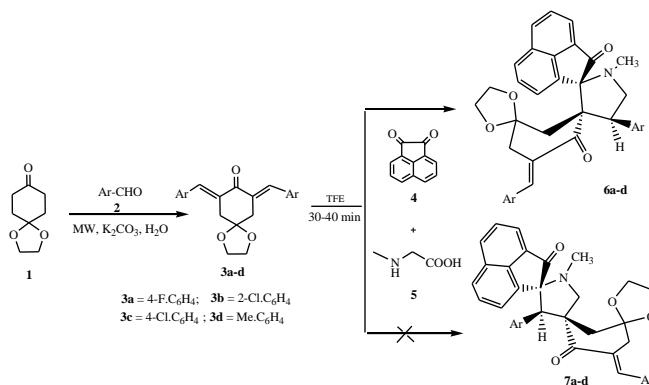
Nitrogen-containing five membered heterocycles are an important class of compounds, not only because of their natural abundance, but also for their chemical and pharmacological significance.¹ Functionalized pyrrolidines are important targets in synthetic chemistry and form the central skeletons of numerous alkaloids and are classes of compounds with significant biological activity.²⁻⁴ On the other hand, spiro-pyrrolidines have gained significant attention due to their interesting biological activities, such as antimicrobial, antitumor and antibiotic properties.⁵⁻⁷ Some spiro-pyrrolidines are potential antileukemic and anticonvulsant agents and antiviral and local anaesthetic activities. Therefore, the synthesis of these compounds has become an important target in recent years.⁸⁻¹⁰

The most developed procedure for construction of spiro-containing compounds depends mainly on cycloaddition reactions, especially 1,3-dipolar cycloaddition to exocyclic double bonds.¹¹ Azomethine ylides are considered as one of the most important dipole systems which are used intensively for preparation of spiro-pyrrolidine compounds where, great attention was directed towards their reactions due to their high regio- as well as stereoselective properties.¹²⁻¹⁴

Development of eco-friendly synthetic protocols for the assembly of new chemical entities is of great importance in recent years.¹⁵ In this context, fluorinated alcohols have emerged as new 'green' solvents to replace the conventional volatile organic solvents.¹⁶

They exhibit a booster effect as a reaction medium and thus, they promote various reactions by pure solvent effect.^{17,18} Further, their unique and promising physicochemical properties, such as high selectivity, low nucleophilicity, high hydrogen bonding donor ability, nonvolatility, nonflammability, high ionizing power and recyclability by simple distillation made them well known polar solvent in green synthesis.¹⁹⁻²²

Recently, our research group has been largely involved in the synthesis of dispiropyrrolidine/pyrrolizidine derivatives via 1,3-cycloaddition reaction.^{23,24} Encouraged by these studies and our research program aims to develop new selective and environmental friendly methodologies for synthesis of spiroheterocycles,²⁵⁻³⁰ herein we report an expeditious and facile protocol for the synthesis of novel trispiropyrrolidines derivatives through 1,3-dipolar addition reaction of 7,9-bis[(E)-arylidene]-1,4-dioxaspiro[4,5]-decane-8-ones (**3**), acenapthequinone (**4**) and sarcosine (**5**) using 2,2,2-trifluoroethanol as a reusable solvent for the first time (Scheme 1). To the best of our knowledge, there is no report for the synthesis of novel trispiropyrrolidine derivatives using acenapthequinone, sarcosine and bis-(arylidene substituted)-spiro[4,5]decan-8-ones so far.



Scheme 1. Synthesis of trispiroacenaphthylenepyrrolidines (**6a-d**)

RESULT AND DISCUSSION

The required dipolarophiles 7,9-bis[(E)-arylidene]-1,4-dioxaspiro[4,5]decane-8-ones (**3a-d**) were prepared by green approach using water and mild base K₂CO₃ under microwaves by the reaction of spiro[4,5]decane-8-one (**1**) with various substituted benzaldehydes **2** in shorter reaction time and in excellent yield as compared to conventional method.³¹ The geometry of the olefinic double bond was found to be *E* as evidenced by ¹H NMR spectra wherein the olefinic protons appeared at δ 7.64-7.67 (s, 2H) and is found to be identical with those of authentic samples prepared by reported method.

A mixture of 7,9-bis[(E)-4-fluoro-benzylidene]-1,4-dioxaspiro[4,5]decane-8-one (**3a**), acenapthequinone (**4**) and sarcosine (**5**) was refluxed for 30-40 minutes in trifluoroethanol to furnish a yellow solid, to be characterized 1-N-methylspiro[2,2]acenaphthylene-spiro[3,9"]-7"--(4-fluorophenylmethylidene)-1,4-dioxaspiro[4",5"]decan-4-(4-fluorophenyl)-pyrrolidine-8",2'-dione (**6a**). The product is isolable simply by filtration with reasonable purity. Initially to study the effect of solvent on present cycloaddition reaction, the reaction was also carried out in different solvents and among them, trifluoroethanol was found to be the best to get a maximum yield of product (Table 1).

Table 1 Preparation of **6a** in different solvents for optimization of reaction conditions^a

Entry	Solvent	Temp., °C	Time, h	Yield ^b , %
1	ethanol	Reflux	8	78
2	methanol	Reflux	6	75
3	acetonitrile	Reflux	5	69
4	1,4-dioxane	Reflux	6	71
5	THF	Reflux	7	68
6	TFE	Reflux	0.5	92

^a Reaction conditions: 1mmol of **3a**, **4** and **5**; ^b Isolated yields

Encouraged by these results, the rest of compounds as listed in Table 2 were similarly synthesized using trifluoroethanol as solvent. The reaction gave a single product in all cases as evidenced by thin layer chromatography (TLC). This cycloaddition is also regioselective with the electron rich carbon of the dipole adding to the β-carbon of the α, β-unsaturated moiety of **3** and stereoselective affording only one diastereomer is obtain exclusively, despite the presence of three stereo center in the product **6**. In this cycloaddition only one C=C of **3** is involved, ascribable to steric hindrance encountered for the second cycloaddition resulting in chemoselectivity. The stereochemical information was obtained from an X-ray crystallographic study of a single crystal of **6a** (Fig. 1).³² The cyclohexanone and the pyrrolidine rings of **6a** are in half chair and envelop forms, respectively. The structures and the regiochemistry of the cycloadducts were also confirmed by spectral analysis. The IR spectrum of **6a** showed two peaks at 1710 and 1680 cm⁻¹ due to carbonyl groups of the acenapthequinone and bis (arylidene)-1,4-dioxaspiro[4,5]decane-8-ones. The ¹H NMR spectrum of compound **6a** the three *N*-CH₃ hydrogens of the pyrrolidine ring appear as a singlet at δ 1.89 ppm. The -NCH₂ protons and benzylic proton of pyrrolidine ring appeared at δ 3.23 (m, 1H), δ 3.71 (t, 1H, J = 7.2 Hz), δ 4.95 (t, 1H, J = 7.2 Hz)

which explained the regiochemistry of the cycloadduct. The ¹³C NMR spectrum of **6a** showed two signals at δ 163.83, and δ 187.20 for the carbonyl groups.

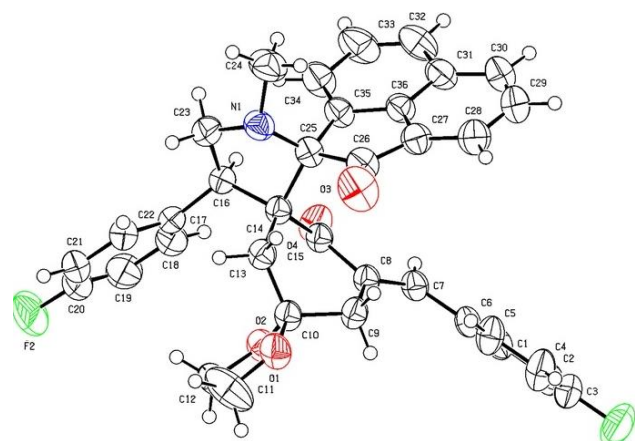
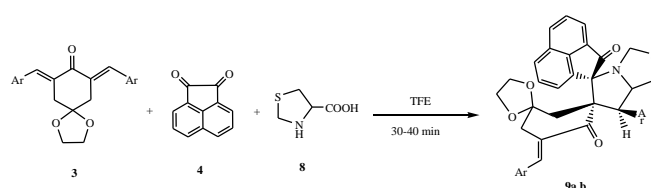


Figure 1. ORTEP diagram of compound **6a**

To further explore the potential of this cycloaddition reaction for synthesis of other spiro-heterocycles, we have investigated the present reaction with thiazolidine-4-carboxylic acid (**8**) in place of sarcosine (**5**) to obtained novel trispirothiapyrrolizidine derivatives listed in table 2 (Scheme 2). The structures of all products were characterized by IR, ¹H NMR and ¹³C NMR spectral analysis.



Scheme 2. Synthesis of trispiroacenaphthylene-thiapyrrolizidines **9a, b**

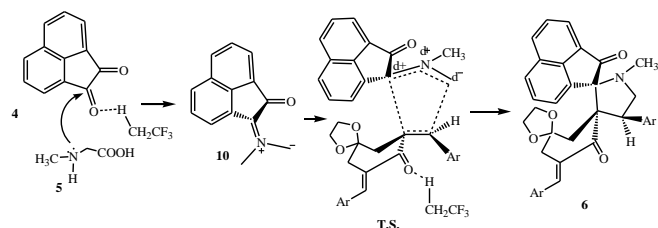
Table 2 Synthetic results of trispiroacenaphthylene-pyrrolidine/thiapyrrolizidines (**6a-d/9a-b**)

No.	Ar	Yield, %	Mp, °C	R _f ^a
6a	4-FC ₆ H ₄	92	228-230	0.85
6b	2-ClC ₆ H ₄	93	234-236	0.81
6c	4-ClC ₆ H ₄	94	188-190	0.87
6d	4-MeC ₆ H ₄	92	196-198	0.83
9a	4-FC ₆ H ₄	89	220-222	0.79
9b	4-MeC ₆ H ₄	90	190-192	0.83

^a(C₆H₆:EtOAc=8:2)

A plausible mechanism for the formation of the cycloadducts is proposed in Scheme 3. It is known that due to the Bronsted acidity (pK_a =12.4) and strong ionizing power 2,2,2-trifluoroethanol play unique behavior in organic transformations.³³ In the present cycloaddition reaction the reaction of acenapthequinone (**4**) with sarcosine (**5**) leads to the "in situ" formation of an azomethine ylide (**10**). Subsequent 1,3-dipolar cycloaddition reaction of dipolarophile **3** and **10** afford trispiropyrrrolidine derivative **6**. The hydrogen atom of TFE being electron-deficient and could form hydrogen bonds with carbonyl groups of both acenapthequinone and dipolarophile **3** thereby catalyses

reaction. Further, the polar transition state of the reaction could be stabilized well by high ionizing solvent TFE. These catalysis presumably expedites the reaction in TFE relative to other solvents.



Scheme 3. Plausible mechanism for synthesis of trispiropyrrolidine derivatives

EXPERIMENTAL SECTION

The melting points of all compounds were determined on a Toshniwal apparatus. The purity of compounds was checked on thin layers of silica Gel-G coated glass plates and n-hexane: ethyl acetate (8:2) as eluent. IR spectra were recorded on a Shimadzu FT IR-8400S spectrophotometer using KBr pellets. ¹H and ¹³C NMR spectra were recorded in DMSO-d₆ and CDCl₃ using TMS as an internal standard on a Bruker Avance spectrophotometer at 300 and 75 MHz, respectively. Mass spectra of representative compounds were recorded on JEOL SX-102 spectrometer at 70 eV. Elemental analyses were carried out on a Carlo-Erba 1108 CHN analyzer. X-ray intensity data were collected on Bruker Kappa Apex II instrument.

General procedure for the synthesis of trispiro-pyrrolidine/thiapyrrolizidines 6/9

An equimolar mixture of appropriate 7,9-bis[(E)-arylidene]-1,4-dioxo-spiro[4,5]decane-8-ones (**3**) (1 mmol), acenapthequinone (**4**) (1 mmol) and sarcosine (**5**)/thiazolidine-4-carboxylic acid (**8**) (1 mmol) in 2,2,2-trifluoroethanol (2-3 ml) was refluxed for the appropriate time (30-40 min). After completion of the reaction as indicated by (TLC), the solid precipitate was filtered and washed with TFE to furnish pure trispiropyrrolidine/thiapyrrolizidine derivatives. The TFE was distilled off (to recover for the next run).

Synthesis of 6a. Yellow Solid; Yield: 92%; IR (KBr, ν cm⁻¹): 3030 (arom-CH), 1710 (>C=O), 1680 (>C=O); ¹H NMR (300 MHz, DMSO-d₆): δ 1.65(d, 1H, J = 13.8 Hz), 1.89 (s, 3H, N-CH₃), 2.31-2.48 (m, 2H), 2.90 (m, 1H), 3.23 (m, 1H), 3.29-3.43 (m, 4H, OCH₂)₂, 3.71 (t, 1H, J = 7.2 Hz), 4.95 (t, 1H, J = 7.2 Hz), 6.62-8.14 (m, 15H, Ar-H and =CH-Ar); ¹³C NMR (75 MHz, DMSO-d₆) 35.09, 37.78, 40.33, 47.63, 56.71, 63.18, 63.06, 64.22, 80.54, 105.37, 114.78, 115.06, 115.31, 115.59, 115.90, 119.96, 124.38, 125.16, 127.99, 128.42, 129.73, 130.89, 131.92, 132.04, 132.57, 133.42, 135.30, 135.69, 141.51, 159.58, 198.58, 204.79; Anal.: Calcd for C₃₆H₂₉F₂NO₄ C, 74.86; H, 5.06; N, 2.42. Found: C, 74.71; H, 5.02; N, 2.38; Mass (m/z): 578 [M⁺].

Synthesis of 6b. Yellow Solid; Yield: 93 %; IR (KBr, ν cm⁻¹): 3020 (arom-CH), 1711 (>C=O), 1685 (>C=O); ¹H NMR (300 MHz, DMSO-d₆): δ 1.23 (d, 1H, J = 13.8 Hz), 1.78 (s, 3H, N-CH₃), 1.85-1.97 (m, 2H), 2.73-2.79 (m, 1H), 3.02-3.29 (m, 4H, OCH₂)₂, 3.43 (t, 1H, J = 8.6 Hz), 3.75 (t,

1H, J = 8.7 Hz), 5.11 (t, 1H, J = 8.7 Hz), 7.01-8.07 (m, 15H, Ar-H and =CH-Ar); ¹³C NMR (75 MHz, DMSO-d₆) 35.112, 35.89, 37.78, 40.36, 48.61, 57.21, 64.12, 65.18, 80.34, 105.27, 110.10, 122.52, 123.45, 124.69, 125.56, 126.38, 126.71, 126.98, 128.42, 129.14, 130.15, 130.62, 132.65, 133.57, 134.86, 135.08, 136.18, 136.28, 137.26, 137.98, 198.68, 203.42. Anal.: Calcd for C₃₆H₂₉Cl₂NO₄ C, 70.82; H, 4.76; N, 2.29. Found: C, 70.98; H, 4.72; N, 2.34; Mass (m/z): 610 [M⁺].

Synthesis of 6c. Yellow solid; Yield: 94%; IR (KBr, ν cm⁻¹): 3045 (arom-CH), 1708 (>C=O), 1687 (>C=O); ¹H NMR (300 MHz, DMSO-d₆): δ 1.25 (d, 1H, J = 13.7 Hz), 1.84 (s, 3H, N-CH₃), 2.56-2.65 (m, 2H), 2.95 (m, 1H), 3.09-3.34 (m, 4H, OCH₂)₂, 3.46 (m, 1H), 3.78 (t, 1H, J = 8.7 Hz), 5.12 (t, 1H, J = 8.7 Hz), 7.04-8.23 (m, 15H, Ar-H and =CH-Ar); ¹³C NMR (75 MHz, DMSO-d₆) 35.06, 35.89, 36.28, 42.35, 47.83, 56.61, 63.48, 64.89, 80.14, 105.27, 109.21, 121.51, 121.22, 123.41, 125.35, 126.51, 127.98, 128.99, 129.53, 129.85, 131.42, 132.73, 133.53, 134.46, 135.18, 135.48, 135.97, 136.21, 140.24, 142.54, 198.34, 203.19. Anal.: Calcd for C₃₆H₂₉Cl₂NO₄ C, 70.82; H, 4.76; N, 2.29. Found: 70.68; H, 4.72; N, 2.23; Mass (m/z): 610 [M⁺].

Synthesis of 6d. Yellow Solid; Yield: 92%; IR (KBr, ν cm⁻¹): 3060 (arom-CH), 1710 (>C=O), 1688 (>C=O); ¹H NMR (300 MHz, DMSO-d₆): δ 1.45 (d, 1H, J = 13.8 Hz), 1.78 (s, 3H, N-CH₃), 2.14 (s, 3H, CH₃), 2.18 (s, 3H, CH₃) 2.32-2.42 (m, 2H), 2.82 (m, 1H), 3.25-3.43 (m, 4H, OCH₂)₂, 3.70 (t, 1H, J = 7.3 Hz), 4.92 (t, 1H, J = 7.3 Hz), 6.65-8.24 (m, 15H, Ar-H and =CH-Ar); ¹³C NMR (75 MHz, DMSO-d₆) 34.41, 35.55, 37.44, 47.66, 57.29, 61.36, 64.39, 65.18, 76.97, 105.34, 109.21, 115.35, 115.54, 116.26, 116.67, 122.16, 125.17, 127.53, 130.27, 132.76, 133.16, 133.37, 135.87, 138.21, 139.76, 143.32, 134.08, 134.58, 135.28, 137.26, 198.58, 204.79. Anal.: Calcd for C₃₈H₃₅NO₄: C, 80.12; H, 6.19; N, 2.46. Found: C, 80.26; H, 6.23; N, 2.41; Mass (m/z): 570 [M⁺].

Synthesis of 9a. Yellow Solid, Yield: 89%; IR (KBr, ν cm⁻¹): 3070 (arom-CH), 1710 (>C=O), 1685 (>C=O); ¹H NMR (300 MHz, DMSO-d₆): δ 1.66 (d, 1H, J = 13.8 Hz), 2.56-2.76 (m, 3H), 2.81 (dd, 2H), 3.08 (dd, 1H, J = 6.9 Hz), 3.45 (dd, 1H, J = 7.4 Hz), 3.61-3.72 (m, 4H, OCH₂)₂, 4.32 (d, 1H, J = 10.5 Hz), 4.54 (m, 1H), 6.28-7.49 (m, 15H, Ar-H and =CH-Ar), 10.63 (s, 1H, NH); ¹³C NMR (75 MHz, DMSO-d₆) 31.13, 35.85, 37.46, 48.21, 52.10, 53.01, 63.33, 64.84, 66.60, 76.77, 105.96, 109.59, 114.98, 115.26, 115.94, 116.23, 121.11, 124.23, 129.74, 129.97, 131.38, 132.30, 132.41, 132.60, 132.70, 133.33, 133.52, 133.92, 142.75, 177.93, 197.61. Anal.: Calcd for C₃₇H₂₉F₂NO₄S: C, 71.48; H, 4.70; N, 2.25. Found: C, 71.42; H, 4.66; N, 2.21; Mass (m/z): 622 [M⁺].

Synthesis of 9b. Yellow Solid, Yield: 90%; IR (KBr, ν cm⁻¹): 3055 (arom-CH), 1710 (>C=O), 1684 (>C=O); ¹H NMR (300 MHz, DMSO-d₆): δ 1.98 (d, 1H, J = 13.8 Hz), 2.05 (s, 3H, CH₃), 2.20 (s, 3H, CH₃), 2.24-2.50 (m, 3H), 2.91 (m, 2H), 3.13 (m, 1H), 3.44 (dd, 1H), 3.56-3.69 (m, 4H, OCH₂)₂, 4.41 (d, 1H, J = 10.6 Hz), 4.71 (m, 1H), 6.68-8.04 (m, 15H, Ar-H and =CH-Ar); ¹³C NMR (75 MHz, DMSO-d₆) 19.16, 19.41, 33.77, 35.82, 36.07, 39.00, 50.71, 51.35, 61.28, 62.74, 65.43, 77.42, 103.91, 118.90, 123.70, 124.26, 125.91, 125.91, 126.21, 127.05, 128.00, 128.55, 129.62, 129.81, 130.74, 130.18, 130.63, 131.91, 133.89, 134.62, 136.12, 137.20, 179.50, 196.23. MS (m/z): 611[M⁺]

1]. Anal.: Calcd for C₃₉H₃₅NO₄S: C, 76.32; H, 5.75; N, 2.28. Found: C, 76.20; H, 5.70; N, 2.22; Mass (m/z): 614 [M⁺].

CONCLUSION

In conclusion, we have developed an efficient and regioselective three-component 1,3-dipolar cycloaddition reaction for the synthesis of novel trispiro-pyrrolidine and thiapyrrolizidines that incorporate in their structures a 1,3-dioxalane moiety. This method has the advantages of good yield, mild reaction condition, low cost and simplicity in process and handling. The recovered TFE of this method for other useful reactions are currently underway.

ACKNOWLEDGEMENTS

Financial assistance from the C.S.I.R. (02(0143)/13/EMR-II), New Delhi is gratefully acknowledged and two of authors also thankful for providing SRA and JRF. We are also thankful to the Central Drug Research Institute (CDRI), Lucknow and SAIF, Cochi for the spectral analyses and elemental analyses.

REFERENCES

- ¹Vidhya Lakshmi, N., Tamilisai, R., Perumal, P. T., *Tetrahedron Lett.* **2011**, 52, 5301.
- ²Augustine, T., Kanakam, C. C., Vithiya, S. M., Ramkumar, V., *Tetrahedron Lett.* **2009**, 50, 5906.
- ³Luibineau, A., Bouchain, G., Queneau, Y., *J. Chem. Soc., Perkin Trans 1*, **1995**, 2433.
- ⁴Deshong, P., Leginus, J. M., *J. Am. Chem. Soc.* **1983**, 105, 1686.
- ⁵Kozikowski, A. P., *Acc. Chem. Res.* **1984**, 17, 410.
- ⁶Chande, M. S., Verma, R. S., Barve, P. A., Khanwelkar, R. R., *Eur. J. Med. Chem.* **2005**, 40, 1143.
- ⁷Ban, Y., Taga, N., Oishi, T., *Chem. Pharm. Bull.* **1976**, 24, 736.
- ⁸Kornet, M. J., Thio, A. P., *J. Med. Chem.* **1976**, 19, 892.
- ⁹Bridges, R. J., Lovering, F. E., Humphery, J. M., Stanley, M. S., Blakely, T. N., Cristofaro, M. F., Chamberlin, A. R., *Bioorg. Med. Chem. Lett.* **1993**, 3, 115.
- ¹⁰Rathna, D., Manian, R. S., Jayadevan, J., Kumar, S. S., Raghavachary, R., *Tetrahedron Lett.* **2006**, 47, 829.
- ¹¹Padwa, A., *In 1,3-Dipolar Cycloaddition Chemistry*; Padwa, A., Ed.; John Wiley & Sons: New York **1984**, 2, 277.
- ¹²Grigg, R., Sridharan, V., Curran D. P., (Eds.) *Advance in Cycloaddition*, Jai Press, London **1993**, 161.
- ¹³Coldham, L., Hufton, R., *Chem. Rev.* **2005**, 105, 2765.
- ¹⁴Lashgari, N., Ziarani, G. M., *ARKIVOC* **2012**, (i), 277.
- ¹⁵Rajesh, R., Raghunathan, R., *Tetrahedron Lett.* **2010**, 51, 5845.
- ¹⁶Khaksar, S., Rouhollahpour, A., Talesh, S. M., *J. Fluorine Chem.* **2012**, 141, 11.
- ¹⁷Vuluga, D., Legros, J., Crousse, B., Slawin, A. M. Z., Laurence, C., Nicolet, P., Bonnet-Delpon, D., *J. Org. Chem.* **2011**, 76, 1126.
- ¹⁸Berkessel, A., Adrio, J. A., Huttenhain, D., Neudorfl, J. M., *J. Am. Chem. Soc.* **2006**, 128, 8421.
- ¹⁹Khaksar, S., Heydari, A., Tajbakhsh, M., Bijanzadeh, H. R., *J. Fluorine Chem.* **2010**, 131, 106.
- ²⁰Qiao, R. Z., Xu, B. L., Wang, Y. H., *Chinese Chem. Lett.* **2007**, 18, 656.
- ²¹Begue, J.P., Bonnet-Delpon, D., Crousse, B., *Synlett* **2004**, 18.
- ²²Shuklov, I.A., Dubrovina, N.V., Borner, A., *Synthesis* **2007**, 2925.
- ²³Dandia, A., Jain, A. K., Bhati, D. S., *Tetrahedron Lett.* **2011**, 52, 5333.
- ²⁴Dandia, A., Jain, A. K., Sharma, S., *Tetrahedron Lett.* **2012**, 53, 5859.
- ²⁵Dandia, A., Laxkar, A. K., Singh, R., *Tetrahedron Lett.* **2012**, 53, 3012.
- ²⁶Dandia, A., Singh, R., Bhaskaran, S., *Green Chem.* **2011**, 13, 1852.
- ²⁷Dandia, A., Singh, R., Bhaskaran, S., *Ultrason. Sonochem.* **2010**, 17, 399.
- ²⁸Dandia, A., Singh, R., Khaturia, S., *J. Fluorine Chem.* **2007**, 128, 524.
- ²⁹Dandia, A., Gautam, S., Jain, A. K., *J. Fluorine Chem.* **2007**, 128, 1454.
- ³⁰Dandia, A., Singh, R., Sachdeva, H., Arya K., *J. Fluorine Chem.* **2001**, 111, 61.
- ³¹Dimmock, J. R., Padmanilayam, M. P., Zello, G. A., Nienaber, K. H., Allen, T. M., Santos, C. L., DeClerq, E., Balzarini, J., Manavathu, E. K., Stables, J. P., *Eur. J. Med. Chem.* **2003**, 38, 169.
- ³²Crystallographic data (excluding structure factors) for trispiroderivative **6a** in this letter have been deposited with the Cambridge Crystallographic Data Centre as supplementary publication numbers CCDC 874669. Copy of the data can be obtained, free of charge, on application to CCDC, 12 Union Road, Cambridge CB2 1EZ, UK [fax:+44 (0)1223-336033 or e-mail: deposit@ccdc.cam.ac.uk].
- ³³Fustero, S., Roman, R., Sanz-Cervera, J. F., Simon-Fuentes, A., Cunat, A. C., Villanova, S., Murgua, M., *J. Org. Chem.* **2008**, 73, 3523.

Received: 16.04.2013.

Accepted: 03.05.2013.



MINIATURIZED POTENTIOMETRIC SENSORS BASED ON PbS NANOPARTICLES AND A NEWLY SYNTHESIZED IONOPHORE AND THEIR APPLICATION FOR STATIC AND HYDRODYNAMIC MONITORING OF LEAD AS A HAZARDOUS WASTE

Ayman H. Kamel^{[a,b]*}, Fahad M. Al Romian^[a], Abdel-Galil E. Amr^[c]

Keywords: Potentiometric sensors; PbS nanoparticles; FIA; Hazardous waste.

New membrane sensors for lead (II) ions are described based on the use of a newly synthesized pyridine carboximide derivatives as neutral ionophore in plasticized PVC membranes (sensor 1) and PbS nanoparticles (NPs) capped in polyvinyl alcohol (PVA) (sensor 2). The sensors exhibited significantly enhanced response towards lead (II) ions over the concentration range 1.0×10^{-7} - 1.0×10^{-3} mol L⁻¹ at pH 3.0 - /6.5 with a lower detection limit of 7.0-10.0 ng mL⁻¹. The sensors displayed near-Nernstian slope of 28.2-33.5 mV per decade for Pb(II) ions. The sensors showed long life span, good selectivity for Pb(II) over a wide variety of other metal ions, long term stability, high reproducibility, and fast response. Validation of the method by measuring the lower detection limit, range, accuracy, precision, repeatability and between-day-variability revealed good performance characteristics of the proposed sensors. Membrane incorporating the neutral ionophore in a flow detector was used in a two channels flow injection set up for continuous monitoring of Pb²⁺ at a frequency of ca. 48-50 samples h⁻¹. Direct determination of lead in water samples as well as in biological fluids gives results in good agreement with data obtained using standard AAS method.

*Corresponding Authors

Tel.: +201000743328

E-Mail: ahkamel76@yahoo.com

[a] Chemistry Department, College of Science, Qassim University, Burayida, KSA.

[b] Chemistry Department, Faculty of Science, Ain Shams University, Abbasia, Cairo, Egypt.

[c] Pharmaceutical Chemistry Department, College of Pharmacy, King Saud University, Riyadh 11451, KSA.

health risk to animals and humans. On the other hand, the presence of trace amounts of lead in many industrial streams is also undesirable, mainly because it may eventually enter the food chain or other products used by people. Hence, the development of analytical methods for the selective and low-level determination of lead ions in natural waterways, potable water, soil, and air is still a challenging task.

Introduction

Monitoring air, soil and water for hazardous pollutants is important and based on the need to protect the environment and public health from possible distribution of natural and industrial inorganic and organic contaminants. There is a constantly increasing need for online monitoring of contaminants in our environment, driven by new legislation and new technologies.¹ Heavy metals occur naturally in the environment, but, due to industrialization, large amounts of heavy metals bound in fossil fuels and mineral materials have been released into the environment and deposited in trace amounts in nearly every part of the planet. Elevated levels of heavy metals in natural water may have a detrimental effect on both human health and the environment.^{1,2}

Lead is the most widely used heavy metal with a number of properties that have made its industrial use increase during recent decades. Lead is an environmental toxicant that affects virtually every system in the body.³ It is a general metabolic poison and enzyme inhibitor which can cause mental retardation and semi-permanent brain damage with learning and behavior disorders in young children⁴. Moreover, lead has the ability to replace the calcium in bone to form sites for long-term release⁵. Therefore, environmental lead results in a serious and well-known

In recent years, various techniques for the determination of lead such as spectrophotometric methods,⁶ atomic absorption and emission spectroscopy,⁷⁻¹⁰ mass spectrometry,¹¹ and electrochemistry¹²⁻¹⁴ have been developed. However, these methods required expensive instruments, well-controlled experimental conditions, frequent maintenance and calibration, and some sample pretreatment. Compared with other analytical methods, potentiometry is an easy and inexpensive technique that has found applications in many clinical, environmental, and toxicological analyses. Most of the reported lead ion-selective electrodes were polymeric membrane electrodes containing neutral carrier ionophores.¹⁵⁻³³

Nanoparticles (NPs) are attracting attention due to their low cost and unique size-dependent properties. The incorporation of NPs into a variety of matrices to form nanocomposite films is attracting much attention. NPs have been used in many electrochemical, electroanalytical and bioelectrochemical applications. The uniqueness of NPs is due to their mechanical, electrical, optical, catalytic and magnetic properties as well as their extremely high surface area per mass. In addition to novel properties, nanomaterials and nanotechnology open up new approaches to manufacture electrodes cost effectively by minimizing the materials needed and waste generation.³⁴⁻³⁶ This is especially relevant to expensive materials (e.g., gold and platinum). For example, inexpensive materials (e.g., carbon

coated by NPs) result in a large ratio of surface area to volume for low-cost sensing electrodes. In recent studies, it was demonstrated that NP electrodes could be obtained with high sensitivity and even with individual NPs giving responses.^{37,38} The combination of nanotechnology with modern electrochemical techniques allows the introduction of powerful, reliable electrical devices for effective process and pollution control.

Herein, we investigate the use of a newly synthesized pyridine carboximide derivative (i.e. 2,6-bis((1-(methoxycarbonyl)-N-ethyl)carboxamide)pyridine) as neutral ionophore in plasticized PVC membranes (sensor 1) and PbS nanoparticles (NPs) capped in polyvinyl alcohol (PVA) (sensor 2). The feasibility of employing the above pyridine carboximide derivative as carrier for lead and PbS nanoparticles is examined and their response in terms of detection limit, slope, response time and selectivity over other cations are described. The selectivity behavior, response mechanism, response time and signal stability were evaluated, and found to be superior than most of those previously described. The sensitivity and stability offered by this simple electrode configuration are highly enough to allow accurate determination of low levels of lead in water and biological fluids and the data were compared with atomic absorption spectrometry.

Experimental

Chemicals and reagents

All reagents were of analytical grade and used without further purification. High molecular weight poly(vinyl chloride) (PVC), potassium tetrakis (4-chlorophenylborate) (KTpClPB), *o*-nitrophenyl octyl ether (*o*-NPOE), polyvinyl alcohol (PVA) and dioctyl phthalate (DOP) were obtained from Fluka (Switzerland), dioctyl sebacate (DOS) from BDH Chemical LTD (England) and metal nitrates and tetrahydrofuran (THF) was purchased from Merck (Germany). The ionophore 2,6-bis((1-(methoxycarbonyl)-N-ethyl)carboxamide)pyridine derivative (Fig. 1) was synthesized as described before.³⁹

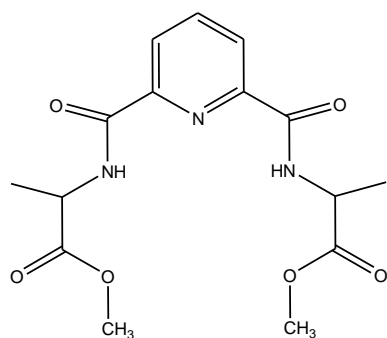


Figure 1. Chemical structure of 2,6-bis((1-(methoxycarbonyl)-N-ethyl)carboxamide)pyridine ionophore

All solutions were prepared with doubly distilled water. A 0.1 mol L⁻¹ Pb(NO₃)₂ stock solution was prepared and the working solutions of different concentrations were prepared daily by dilution of the stock solution and then by adjusting the ionic strength with 1 mol L⁻¹ LiNO₃.

Equipments

All potentiometric measurements were made at 25±0.1 °C with an Orion pH/mV meter (model SA 720) and Pb²⁺ ion-PVC membrane sensors in conjunction with an Orion Ag/AgCl double junction reference electrode (model 90-02) with 10% (w/v) KNO₃ in the outer compartment. A combination Ross glass pH electrode (Orion 81-02) was used for all pH measurements.

The FIA system consisted of an Ismatech MS-REGLO pump and an Omnifit injection valve (Omnifit, Cambridge, UK) with sample of 100 µL sample. The potential measurements were obtained with a high resolution data logger [Pico Technology limited] (model ADC-16). The flow Tygon tubes were obtained from (AIKEM) (P/N A00349 and P/N A000355), the pump tubes were red/red 0.71 "ID and blue/blue 0.065" ID. The distance between the injection valve and the detector was 40 cm. The end of the tube was placed in a petri dish where a double-junction Ag/AgCl reference electrode was placed downstream from the indicator sensor just before the solution went to waste.

Preparation of PbS nanoparticles

The PbS nanoparticles is prepared by the method proposed by Badr and Mahmoud.⁴⁰ Lead acetate (Pb(CH₃COO)₂·2H₂O), 50 mmol L⁻¹, with different volumes (1, 4, 8, 12, and 16 mL) was added to 2.2 g PVA (13,000 g/mol) and the volume of each solution was completed to 50 mL by bidistilled water. Each solution was left for 24 h at room temperature to swell, and then the solutions were warmed up to 60 °C and stirred for 4 h until viscous transparent solutions were obtained. One milliliter Na₂S (50 mmol L⁻¹) was dropped to each solution with gentle stirring. Each solution was cast on flat glass plate dishes. After the solvent evaporation, a thin film containing PVA-capped PbS NPs was obtained. The films were washed with deionized water to remove other soluble salts.

Sensors fabrication

The membrane cocktail was prepared by adding three milligrams of 2,6-bis((1-(methoxycarbonyl)-N-ethyl)carboxamide)pyridine derivative ionophore to 124 mg of *o*-NPOE plasticizer, 66 mg PVC and 1mg KTpClPB. All are dissolved in ca. 3 mL of THF.

A planar gold base electrode (3mm×5 mm) was sputtered on a (13.5mm×3.5 mm) flexible polyimide (Kapton®, DuPont) substrate (125 µm thick), as shown in Fig. 2; single site electrode (area = 0.06 cm²) (used for all the optimization and characterization studies), and used as previously described.⁴¹ An electrical wire was connected to the electrode by means of Ag-epoxy (Epoxy Technology). Insulation of the electrical contact was made using silicon rubber coating seal (Dow Corning 3140 RTV).

The membrane cocktail mixture was directly coated to the sputtered gold layer using micro-syringe to apply few microliters of the sensing solution (typically 10µL of membrane cocktail is dispersed), left to dry in the air for 1 min before repeating further addition (i.e. four times of the sensing solution).

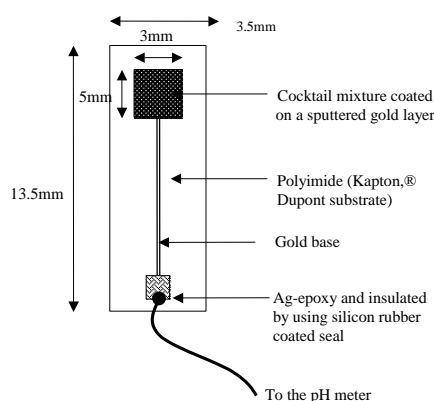


Figure 2. Planar-chip sensor

For sensors based on PbS NPs, the resulting membrane containing PVA-capped PbS NPs was peeled off from the glass mould and disks of 9-mm i.d. were cut out and glued onto a 7-mm i.d. PVC body (2 cm long) using THF. The tube was filled with 1×10^{-3} mol L $^{-1}$ Pb $^{2+}$ solution of pH 4.5. An Ag/AgCl coated wire was used as an internal reference electrode.

Potentiometric procedures

All electrodes were placed in a convenient support over a magnetic stirrer with an Ag/AgCl double junction reference electrode into a 25 mL beaker containing 9.0 mL of 10^{-2} mol L $^{-1}$ acetate buffer solution pH 4. Portions (1.0 mL) of 10^{-6} to 10^{-1} mol L $^{-1}$ standard pb $^{2+}$ solutions were successively added and the potential response of stirred solutions was measured after stabilization to ± 0.2 mV. A calibration graph was constructed by plotting the emf readings against the logarithm of Pb $^{2+}$ concentrations. The plot was used for subsequent determination of unknown pb $^{2+}$ ions.

The influence of pH on the electrode potential response of was investigated using 1×10^{-3} and 1×10^{-4} mol L $^{-1}$ of Pb $^{2+}$ solution over the pH range 2–8. Adjustment of pH was carried out using nitric acid or sodium hydroxide solution.

For FIA measurements, a series of 100 μ L portions of Pb $^{2+}$ test solutions spanning the concentration range from 1.0×10^{-2} to 1.0×10^{-6} mol L $^{-1}$ were injected into a flow stream of 1.0×10^{-2} mol L $^{-1}$ acetate buffer of pH 4.5, flowing at a rate of 3.5 mL min $^{-1}$. The lead sensor was used as a working sensor against Ag/AgCl double junction reference electrode. Each solution was measured in triplicate. The average potentials at maximum heights were plotted against log [Pb $^{2+}$].

Analytical applications

Water samples were spiked by Pb $^{2+}$ at a concentration of 0.5, 1.0, 2.0 and 5.0 μ g mL $^{-1}$. These samples do not need pretreatment before potentiometric determination of Pb $^{2+}$ ions by these sensors using the calibration curve method.

For the determination of lead in human serum, aliquots of human blood were obtained from some volunteers and analyzed within 3 h of extraction. Blood was collected in tubes and then 9 mL portion of absolute ethyl alcohol was added, thoroughly mixed and left for 10 min before being centrifuged at 4000 rpm. The supernatant liquid was without removal of any particulate matter to a 20 mL beaker and then evaporated at 50 °C on a hot plate till dryness before being reconstituted in de-ionized water. A 9 mL of 10^{-2} mol L $^{-1}$ acetate buffer solution of pH 4.5 was added. The extracts were transferred to 25 mL measuring flask and complete to the mark. A 10 mL aliquot of the sample solution was transferred to a 25 mL beaker. The working and reference electrode were immersed, and the potential readings were recorded after reaching the equilibrium response (10–20s). The concentration of lead, expressed as [Pb $^{2+}$], was calculated using a calibration graph.

For flow injection analysis (FIA), a flow stream of the carrier solution (10^{-2} mol L $^{-1}$ acetate buffer of pH 4.5) was allowed to pass through the flow cell at a flow rate 3.5 mL min $^{-1}$. Successive 100 μ L aliquots of standard 10^{-2} to 10^{-6} mol L $^{-1}$ Pb $^{2+}$ and unknown test sample solutions were injected into the flowing stream. The corresponding potential change was measured and recorded versus time. A typical calibration plot was made used to determine the concentration of the unknown samples.

Result and discussion

Potentiometric characteristics of sensors incorporating 2,6-bis((1-(methoxycarbonyl)-N-ethyl)carboxamide)pyridine derivative ionophore and PbS NPs revealed strong response for Pb $^{2+}$ ions. Results from replicate studies indicated near-Nernstian slope of 22.1 ± 0.6 , and 33.5 ± 0.3 mV per decade, with lower detection limits of 0.05 and 0.007 μ g mL $^{-1}$ for sensors based on the neutral ionophore and PbS NPs, respectively. Addition of 0.5 wt. % KTpCIPB to the ionophore significantly improved the sub-Nernstian calibration slope from 22.1 ± 0.6 to 28.2 ± 0.2 mV per decade and decreased the limit of detection from 0.05 to 0.01 μ g mL $^{-1}$. Typical calibration curves of these sensors are shown in Fig. 3 and their general response characteristics are presented in Table 1.

Replicate measurements (n=10) of an internal quality control (IQS) sample (2.0 μ g mL $^{-1}$, 9.66×10^{-6} mol L $^{-1}$ of certified reference Pb $^{2+}$) gave an average results of 1.8 ± 0.2 μ g mL $^{-1}$. Calculation of the student's (*t*) value at 95% confidence level was made using Eqn 1:

$$t_{\text{exp}} = \frac{(\mu - x)n^{0.5}}{s} \quad (1)$$

where

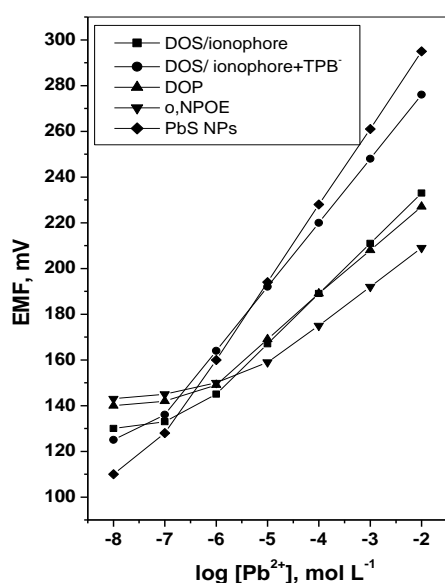
μ is the concentration of the initial internal quality control sample,

x is the average concentration found, n is the number of replicates analyzed and s is the standard deviation of measurements.

Table 1. Response characteristics of lead membrane sensors in 0.01 mol L⁻¹ acetate buffer of pH 4.5.

Parameter	Ionophore DOS	Ionophore DOS+TPB ⁻	Ionophore DOP	Ionophore o,NPOE	PbS NPs
Slope (mV decade ⁻¹)	22.1±0.6	28.2±0.2	19.5±0.6	16.7±0.9	33.5±0.3
Correlation coefficient, <i>r</i> (<i>n</i> =5)	0.999	0.999	0.998	0.998	0.999
Linear range, mol L ⁻¹	1.0x10 ⁻⁶	1.0x10 ⁻⁷	1.0x10 ⁻⁶	1.0x10 ⁻⁵	1.0x10 ⁻⁷
Detection limit, µg mL ⁻¹	0.05	0.01	0.16	0.65	0.007
Working range, (pH)	3.5-6.0	3.5-6.0	3.5-6.0	3.5-6.0	3.0-6.5
Response time, (s)	<10	<10	<10	<10	<20
Standard deviation σ _v (mv)	2.1	1.6	1.4	1.7	1.5
Repeatability, C _v w (%)	1.3	0.8	0.9	1.1	0.9
Accuracy (%)	99.1	98.6	99.3	99.6	99.4

No statistical difference was detected between the practically obtained ($t_{exp}=1.63$) and the theoretically tabulated ($t_{tab}=1.833$) values. Thus the null hypothesis is retained and the method accuracy is acceptable.

**Figure 3.** Potentiometric response of lead membrane sensors using 0.01 mol L⁻¹ acetate buffer of pH 4.5.

Effect of plasticizer

Potentiometric response of sensor based on the neutral ionophore was greatly influenced by the polarity of the membrane medium. Lead PVC matrix membrane sensor incorporating the ionophore with (DOS), (DOP) and (o,NPOE) plasticizers were prepared and tested. The calibration slope and lower limit of detection were declined from 22.1±0.6 to 19.5±0.6 and 16.7±0.9 mV decade⁻¹ and from 0.05 to 0.16 and 0.65 mg mL⁻¹ upon using DOS instead of DOP and o,NPOE, respectively. It can be seen that membranes incorporating DOP plasticizer gave more favorable slope than those containing o,NPOE plasticizer. Table 2 shows the selectivity coefficients of membrane sensor incorporating the ionophore with DOS, DOP and

o,NPOE plasticizers. Selectivity for Pb²⁺ in the presence of many common cations such as Ni²⁺, Co²⁺, Mg²⁺, Zn²⁺, Cd²⁺, Ba²⁺ and Hg²⁺ was significantly improved with sensor incorporating DOS. All subsequent measurements were made with membranes plasticized with DOS.

Table 2. Selectivity coefficient values using lead based membrane sensors

Interferent	Ionophore				PbS NPs
	DOS	DOS+TPB ⁻	DOP	o,NPOE	
Pb ²⁺	0	0	0	0	0
Hg ²⁺	-2.6	-2.7	-2.5	-1.9	-3.1
Zn ²⁺	-3.1	-3.2	-3.1	-2.5	-0.9
Mg ²⁺	-4.1	-4.2	-4.0	-4.0	-4.1
Ca ²⁺	-3.8	-3.9	-3.9	-3.7	-4.0
Cu ²⁺	-0.05	-0.03	-0.05	-0.02	-0.5
Co ²⁺	-3.0	-2.9	-2.9	-2.8	-3.4
Ni ²⁺	-3.1	-3.0	-3.2	-2.9	-1.1
Cd ²⁺	-1.8	-1.9	-1.7	-1.6	-2.6
Ba ²⁺	-4.2	-4.05	-4.0	-3.9	-1.3
K ⁺	-4.5	-3.9	-4.3	-4.4	-0.8
I ⁻	-4.6	-4.5	-4.3	-4.4	-1.3
SCN ⁻	-4.5	-4.6	-4.3	-4.5	-1.1
S ²⁻	-4.3	-4.4	-4.2	-4.2	0

Effect of pH and response time

The effect of pH on the response of the sensors based on either the ionophore (sensor 1) or PbS nanoparticles (sensor 2) were studied over the pH range of 2 to 8 at 10⁻⁴ and 10⁻³ mol L⁻¹ of Pb²⁺ solution. The pH of solutions was adjusted with either HNO₃ or NaOH solutions. The potential remained constant at pH range of 3 to 6.5 and 4 to 6 for both sensors 1 and 2, respectively. Below pH 3, the change in the potential is due to co fluxing of hydrogen ions and above pH 6.5, the variation of potential may be due to formation of some hydroxyl complex of the Pb²⁺ ions in the solution. The response time of the sensors, tested by measuring the time required to achieve a steady potential (within ±3 mV), was less than 10 s for sensor 1 but exceeds to be less than 20 s for sensor 2. The detection system was very stable, and after a period of 8 weeks, calibration sensitivity decreased about 1.5 mV without any considerable change in its linear range.

The reproducibility of the slope of calibration graphs was within ± 1.5 mV per decade over a period of 8 weeks ($n=6$).

The ruggedness of the potentiometric method was also evaluated by carrying out the analysis using four different sensors and two different instruments on different days. A relative standard deviation (RSD) of less than 1.0 % was observed for repetitive measurements during three different days ($n=10$). The results indicate that the method is capable of producing results with high precision and stability.

Effect of diverse ions

The influences of different cation and anion ions on the response of Pb^{2+} sensors were investigated. The selectivity coefficients $K^{\text{pot}}_{\text{Pb}^{2+},J}$ were evaluated according to IUPAC recommendations using the matched potential method (MPM)⁴² in 0.01 mol L^{-1} acetate buffer at pH 4.5. In this method, the potentiometric selectivity coefficient is defined as the activity ratio of primary ion and interfering ions that give the same potential under identical conditions. At first, a known activity (a_A) of the primary ion solution is added into a reference solution that contains a fixed activity ($a_A = 10^{-4} \text{ mol L}^{-1}$) of primary ions, and the corresponding potential change (ΔE) is recorded. Next, a solution of an interfering ion (a_B) is added to the reference solution until the same potential change (ΔE) is recorded. The change in potential produced at the constant background of the primary ion must be the same in both cases. The selectivity coefficient is calculated from the Eqn. (2):

$$K_{A,B}^{\text{POT}} = \frac{(a_A - a_A')}{a_B} \quad (2)$$

The results given in Table 2 revealed reasonable selectivity for lead ion in presence of many related substances.

Flow Injection Set Up

A planar-chip detector incorporating the ionophore+TPB-/DOS based membrane sensor was prepared and used under hydrodynamic mode of operation for continuous Pb^{+2} quantification. A linear relationship between Pb^{+2} concentrations and FIA signals was obtained over a concentration range of 10^{-5} to $10^{-3} \text{ mol L}^{-1}$ using $10^{-2} \text{ mol L}^{-1}$ acetate buffer, pH 4.7. The flow rate was chosen to be 3.5 mL min^{-1} (Fig. 4). The slope of the calibration plot was near Nernstian ($28.2 \pm 0.2 \text{ mV decade}^{-1}$). The limit of detection was $8.0 \times 10^{-6} \text{ mol L}^{-1}$. The sampling frequency is ca. 48-50 samples per hour.

Lead assessment

Lead(II) was determined in drinking as well as in biological fluids under both the static and the hydrodynamic mode of operations. The use of the sensors in a FIA mode of operation shorten the assay time, allow the use of little sample quantities for lead detection. The samples analyzed by the proposed method using both the ionophore and PbS

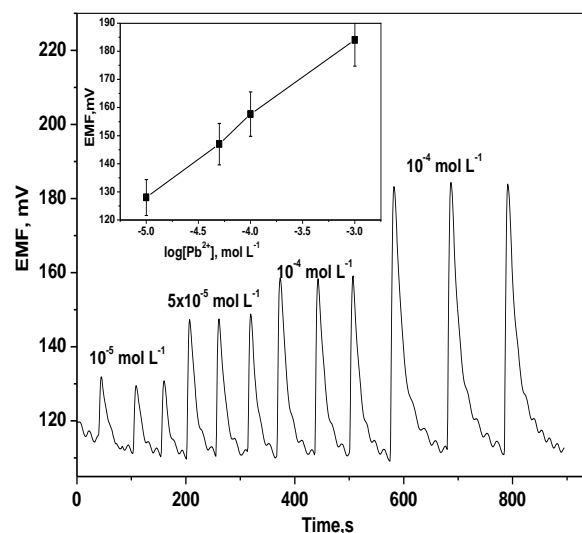


Figure 4. Typical FIA signal obtained by injecting Pb^{2+} standard solutions using ionophore I membrane based sensor.

nanoparticles membrane based sensors. Their content in lead is presented in Table 3.

A blank sample was used to control and ascertain the accuracy of the analytical results. This blank sample was marketed bottled water that had no lead on its content. Standard additions were carried out over this sample. For this, the blank sample was spiked with 0.5, 1.0, 2.0 and $5.0 \mu\text{g mL}^{-1}$; the lead found was $0.47 (\pm 0.05)$; $0.95 (\pm 0.04)$, $1.94 (\pm 0.06)$ and $4.82 (\pm 0.03) \mu\text{g mL}^{-1}$. The corresponding coefficient variation was 6.0%, 5.0%, 3% and 3.6%, respectively, attesting for the precision of the flow-potentiometric method. Thus, the analytical data support the application of the proposed potentiometric method for the routine control of lead.

Another application of the present method for determining Pb^{2+} in biological fluids was tested by spiking aliquots of human plasma samples with a known concentration of standard Pb^{2+} in $10^{-2} \text{ mol L}^{-1}$ acetate buffer of pH 4.5. Internal QC samples containing $0.5\text{--}5 \mu\text{g mL}^{-1} \text{ Pb}^{+2}$ were spiked into human plasma test solutions to evaluate the effect of matrix and the method recovery (φ , %) were using Eqn 3.

$$\varphi = \frac{X_s - X}{X_{\text{add}}} 100 \quad (3)$$

where

X_s , X and X_{add} are the results of spiked sample, mean results of un-spiked sample and of added (spiked) reference, respectively.

The results show average recoveries (accuracy) of $97.4 \pm 1.1\%$ and $98.2 \pm 1.5\%$ and $96.5 \pm 1.8\%$ and $96.4 \pm 1.4\%$ in plasma samples using batch and FIA techniques, respectively (Table 3). This confirms the applicability of the method for accurate routine analysis of Pb^{2+} in biological fluids.

Table 3. Potentiometric determination of Pb²⁺ in spiked water and human plasma samples using lead based membrane sensors.

Matrix	Spiked concentration, (µg mL ⁻¹)	Recovery found* (%)				
		Sensor (I)		Sensor (II)		AAS
		Batch	FIA	Batch	FIA	
Water	0.5	0.47±0.002	0.45±0.003	0.48±0.002	0.46±0.002	0.48±0.003
	1.0	0.95±0.007	0.93±0.006	0.97±0.004	0.95±0.003	0.97±0.002
	2.0	1.94±0.06	1.91±0.03	1.97±0.07	1.93±0.08	1.97±0.02
	5.0	4.82±0.08	4.77±0.07	4.79±0.03	4.69±0.05	4.81±0.01
Human serum	0.5	0.48±0.003	0.46±0.005	0.47±0.01	0.46±0.007	0.45±0.001
	1.0	0.98±0.005	0.97±0.004	0.95±0.008	0.93±0.007	0.94±0.004
	2.0	1.93±0.07	1.91±0.04	1.91±0.09	1.88±0.06	1.93±0.03
	5.0	4.82±0.06	4.75±0.02	4.77±0.07	4.73±0.09	4.76±0.02

*Average of 5 measurements

Conclusion

New lead sensors based on synthesized 2,6-bis((1-(methoxycarbonyl)-N-ethyl)carboxamide)pyridine as neutral ionophore in plasticized PVC membranes and PbS nanoparticles (NPs) capped in polyvinyl alcohol (PVA) were prepared, characterized and used for Pb²⁺ measurements. The sensors offered the advantages of fast response, reasonable selectivity, low cost and possible interfacing with computerized and automated systems. Interfacing the sensors in a FIA system offers adequate analysis speed, good reproducibility, high sample throughputs and excellent response characteristics. The sensors were useful to perform the analysis of lead in water and biological fluids samples. The potentiometric devices are simple, of low cost and easy to manipulate. The overall procedure is precise, accurate and inexpensive regarding reagent consumption and equipment involved.

Acknowledgements

The authors acknowledge the financial support from Deanship of scientific research, Qassim University, by means of project 1074/2012.

References

- Huang, X., Sillanpaa, M., Gjessing, E. T., Peraniemi, S., Vogt, R. D., *River Res. Appl.*, **2011**, *27*, 113-121.
- Huang, X., Sillanpaa, M., Gjessing, E. T., Vogt, R. D., *Sci. Total Environ.* **2009**, *407*, 6242-6254.
- Needleman, H. L., Gatsonis, C. A., *J. Am. Med. Assoc.*, **1990**, *263*, 673-678.
- McMichael, A. J., Baghurst, P. A., Wigg, N. R., Vimpani, G. V., Robertson, E. F., Roberts, R. J., *N. Engl. J. Med.*, **1988**, *319*, 468-475.
- Volesky, B., *Biosorption of heavy metals*, CRC, Boca Raton, **1990**.
- Klamtet, J., Sanguthai, S., Sriprang, *NU Sci J.*, **2007**, *4*, 122.
- Chen, J., Xiao, S., Wu, X., Fang, K., Liu, W., *Talanta*, **2005**, *67*, 992-996.
- Talebi, S. M., Safigholi, H., *J. Serb. Chem. Soc.*, **2007**, *72*, 585-590.
- Mattos, J. C. P. D., Nunes, A. M., Martins, A. F., Dressler, V. L., Flores, E. M. D. M., *Spectrochim Acta*, **2005**, *60*, 687-692.
- Campos, R. C. D., Santos, H. R. D., Grinberg, P., *Spectrochim Acta B*, **2002**, *57*, 15-28.
- Bhandari, S. A., Amarasiriwardena, D., *Microchim. J.*, **2000**, *64*, 73-84.
- Kamel, A. H., *Electroanalysis*, **2007**, *19*, 2419-2427.
- Li, G., Ji, Z., Wu, K., *Anal. Chim. Acta*, **2006**, *577*, 178-182.
- Mhammedi, M. A. E., Achak, M., Bakasse, M., Chtaini, A., *Chemosphere*, **2009**, *76*, 1130-1134.
- Mousavi, M. F., Sahari, S., Alizadeh, N., Shamsipur, M., *Anal. Chim. Acta*, **2000**, *414*, 189-194.
- Ganjali, M. R., Rouhollahi, A., Mardan, A. R., Hamzeloo, M., Mogimi, A., Shamsipur, M., *Microchem. J.*, **1998**, *60*, 122-133.
- Ganjali, M. R., Hosseini, M., Basiripour, F., Javanbakht, M., Hashemi, O. R., Rastegar, M. F., Shamsipur, M., Buchanen, G. W., *Anal. Chim. Acta*, **2002**, *464*, 181-186.
- Chen, L., Zhang, J., Zhao, W., He, X., Liu, Y., *J. Electroanal. Chem.* **2006**, *589*, 106-111.
- Bhat, V. S., Ijeri, V. S., Srivastava, A. K., *Sens. Actuators B*, **2004**, *99*, 98-105.
- Bochenska, M., Guzinski, M., Kulesza, J., *Electroanalysis*, **2009**, *21*, 2054-2060.
- Vassilev, V., K. Tomova, K., Boycheva, S., *J. Non-Cryst. Solids*, **2007**, *353*, 2779-2784.
- Ardakani, M. M., Kashani, M. K., Niasari, S. M., Enasfi, A. A., *Sens. Actu. B*, **2005**, *107*, 438-445.
- Jeong, T., Lee, H. K., Jeong, D. C., Jeon, S., *Talanta*, **2005**, *65*, 543-548.
- Lee, H. K., Song, K., Seo, H. R., Choi, Y. K., Jeon, S., *Sens. Actu. B*, **2004**, *99*, 323-329.
- Barzegar, M., Mousavi, M. F., Khajehsharifi, H., Shamsipur, M., Sharghi, H., *IEEE Sens. J.*, **2005**, *5*, 392-397.
- Xu, D. F., Katsu, T., *Anal. Chim. Acta*, **1999**, *401*, 111-115.
- Hassan, S. S. M., Ghalia, M. H. A., Amr, A. G. E., Mohamed, A. H. K., *Talanta*, **2003**, *60*, 81-91.
- Abbaspour, A., Tavakol, F., *Anal. Chim. Acta*, **1999**, *378*, 145-149.
- Sadeghi, S., Dashti, G. R., Shamsipur, M., *Sens. Actu. B*, **2002**, *81*, 223-228.

- ³⁰Xu, D. F., Katsu, T., *Talanta*, **2000**, *51*, 365–371.
- ³¹Mousavi, M. F., Barzegar, M. B., Sahari, S., *Sens. Actu. B*, **2001**, *73*, 199–204.
- ³²Lu, X. Q., Chen, Z. L., Hall, S. B., Yang, X. H., *Anal. Chim. Acta*, **2000**, *418*, 205–212.
- ³³Wilson, D., Arada, M. D., Alegret, S., del Valle, D., *J. Hazard. Mater.*, **2010**, *181*, 140–146.
- ³⁴Welch, C.M., Compton, R.G., *Anal. Bioanal. Chem.*, **2006**, *384*, 601.
- ³⁵Campbell, F. W., Compton, R.G., *Anal. Bioanal. Chem.*, **2010**, *396*, 241.
- ³⁶Ward Jones, S. E., Compton, R. G., *Curr. Anal. Chem.*, **2008**, *4*, 177.
- ³⁷Belding, S. R., Dickinson, E. J. F., Compton, R. G., *J. Phys. Chem. C*, **2009**, *113*, 11149.
- ³⁸Zhou, H. J., Fan, F. R. F., Bard, A. J., *J. Phys. Lett.*, **2010**, *1*, 2671.
- ³⁹Abounassif, M. A., Al-Omar, M. A., Amr A.G. E., Mostafa, G. A. E., *Drug Test. Analysis*, **2011**, *3*, 373–379.
- ⁴⁰Badr, Y., Mahmoud, M. A., *Physica B*, **2005**, *369*, 278–286.
- ⁴¹Kamel, A. H., *J. Pharm. & Biomed. Anal.*, **2007**, *45*, 341–348.
- ⁴²Umezawa, Y., Batlmann, P., K. Umezawa, K., Tohda, K., Amemiya, S., *Pure Appl. Chem.*, **2000**, *72*, 1851.

Received: 18.04.2013.

Accepted: 04.05.2013.



CATALYTIC PERFORMANCE OF SiO₂-SUPPORTED Fe(ClO₄)₃·6H₂O IN SYNTHESIS OF 2-SUBSTITUTED BENZIMIDAZOLES

Farahnaz K. Behbahani^{[a]*}, and Azam Lotfi^[a]

Keywords: benzimidazole, Fe(ClO₄)₃/SiO₂, heterogeneous, synthesis, catalyst

Benzimidazole derivatives have been synthesized using a catalytic amount of Fe(ClO₄)₃/SiO₂ at room temperature with excellent yields under solvent-free conditions. The solid phase conditions and use of a heterogeneous, and inexpensive catalyst are attractive features of this method.

Corresponding Authors*

Tel: +98 0261 4418145

Fax: 0261 4418156

E-Mail: Farahnazkargar@yahoo.com

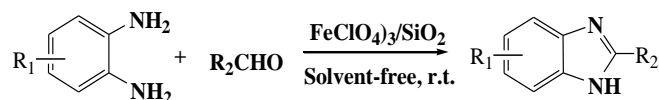
[a] Department of Chemistry, Karaj Branch, Islamic Azad University, Karaj, Iran

Introduction

Various pharmaceutical agents with a wide range of biological applications have benzimidazole derivatives.^{1,2} Owing to their significant biological activity has prompted a very wide study for their synthesis. Benzimidazoles have been prepared by *o*-phenylenediamine (OPD) and carboxylic acids or their derivatives such as nitriles, chlorides, or orthoesters³⁻⁶ under strong acidic conditions, and sometimes at high temperatures using polyphosphoric acid or by microwave irradiation and the oxidative cyclodehydration of OPD and aldehydes by using various reagents.⁷⁻²⁰ Although a variety of reagents/catalysts have been recently developed but unfortunately, many of these methods suffer from one or more limitations such as requiring harsh reaction conditions, low to moderate yields, long reaction times, tedious work-up procedures, and co-occurrence of several side products. The main disadvantage of most of these methods is that the catalysts are destroyed in the work-up procedure and cannot be recovered and reused. Therefore, there is still a demand for a simple, green and general procedure for the synthesis of tetrahydroquinolines under catalytic conditions. Additionally, Fe(ClO₄)₃/SiO₂ has been employed for various transformations in organic synthesis.²¹ Ferric perchlorate adsorbed on silica gel has also been found to be effective for the rapid organic functional group transformations such as dimerization of alkynes, aromatic hydrocarbons, selective oxidation of thiols to disulfides, and transannular reaction in 1,5-cyclooctadienes on grinding using pestle and mortar in the solid state²² and alumina-supported iron (III) perchlorate [Fe(ClO₄)₃·Al₂O₃] have been effectively used as a Lewis acid catalyst for Nazarov cyclization/Michael addition of pyrrole derivatives.²³

We have also reported a variety of organic transformations.²⁴⁻²⁶ In this communication, we wish to introduce a worth catalyst, Fe(ClO₄)₃/SiO₂, for the

preparation of 2-substituted benzimidazoles in terms of operational simplicity, reusability and economic viability



Scheme 1. Synthesis of 2-substituted benzimidazoles

Experimental

General procedure for synthesis of benzimidazole derivatives

A mixture of *o*-phenyldiamine (1 mmol), benzaldehyde (1 mmol), and Fe(ClO₄)₃/SiO₂ (0.15 g) was stirred magnetically at room temperature, and the progress of the reaction was monitored by thin layer chromatography (TLC) till completing of the reaction. Then, the reaction mixture was diluted with ethyl acetate (20 ml), the catalyst was filtered off. The organic phase was dried with Na₂SO₄ and concentrated under reduced pressure. In all the cases, the product obtained after the usual workup gave satisfactory spectral data.

Recyclability of the catalyst

The reusability of the catalyst was also studied. At the end of the reaction, the catalyst was removed by filtration and washed with dichloromethane. The recycled catalyst could be subjected to a second or even another reaction. In the case of the model reaction, after four runs the catalytic activity of the catalyst was almost the same as those of the freshly used catalyst (Table 3).

Data

2-Phenyl-1H-benzimidazole (1): m.p. 290-293 °C (ref.³⁰ m.p. 290-292 °C). IR (KBr, cm⁻¹): 3435.55, 3059.40, 1602.27, 1493.62, 1276.30, 742.84. ¹H NMR ([D₆]DMSO,

400 MHz, δ ppm): 7.17-7.24 (m, 2H, Ar-H), 7.49-7.57 (m, 4H, Ar-H), 7.66 (d, 1H, Ar-H) 8.17 (d, 2H, Ar-H), 12.90. (s, 1H, N-H).

2-(2-Hydroxyphenyl)-1H-benzimidazole (2): m.p. 240-242 °C (ref³⁶ m.p. 242 °C IR (KBr, cm⁻¹): 3325.40, 3043.47, 1604.26, 1530.30, 1489.42, 1279.88, 1118.68, 753.12. ¹H NMR ([D₆]CDCl₃, 300 MHz, δ ppm): 5.79 (s, 1H), 6.94-7.06 (m, 2H), 7.13-7.25(m, 3H), 7.39-7.44(m, 2H), 7.13-7.25 (m, 2H) 8.68(s, 1H), 12.26 (s, 1H).

2-(2-Chlorophenyl)-1H-benzimidazole (3): m.p. 232-235 °C (ref³⁰ m.p. 233-234 °C) IR (KBr, cm⁻¹): 3413.04, 1620, 1589, 1440.54, 1274.17, 1047.25, 743.29. ¹H NMR ([D₆]DMSO, 250 MHz, δ ppm): 7.20-7.24 (m, 2H), 7.48-7.51 (m, 2H), 7.54-7.68 (m, 3H), 7.89-7.93 (m, 1H), 12.74 (s, 1H).

2-(3-Methoxyphenyl)-1H-benzimidazole (4): m.p. 223-227 °C (ref³² m.p. 205-206 °C) IR (KBr, cm⁻¹): 3430.28, 2930.75, 1602.95, 1456.20, 1264.06, 872.81, 788.93, 690.92. ¹H NMR ([D₆]DMSO, 250 MHz, δ ppm):

2-(2,4-Dichlorophenyl)-1H-benzimidazole (5): m.p. 220-223 °C (ref³⁷ m.p. 218-219 °C), IR (KBr, cm⁻¹): 3435.87, 3101.44, 1620.65, 1593.61, 1489.08, 1283.76, 783.54, 741.39. ¹H NMR ([D₆]DMSO, 300 MHz, δ ppm): 3.78 (s, 3H), 7.10 (d, J=8.8, 2H), 7.16 (q, J=3.01, 2H), 7.50 (m, 2H), 8.12(d, J=8.8, 2H), 12.76 (s, 1H).

2-(4-Methoxyphenyl)-1H-benzimidazole (6): m.p. 224-225 °C (ref³¹ m.p. 222-224 °C, IR (KBr, cm⁻¹): 3421.39, 3051.09, 2986.46, 1609.99, 1585.73, 1510.89, 1245.48, 1177.78, 744.06. ¹H NMR ([D₆]DMSO, 300 MHz, δ ppm): 3.78 (s, 3H), 7.10 (d, J=8.8, 2H), 7.16 (q, J=3.01, 2H), 7.50 (m, 2H), 8.12 (d, J=8.8, 2H), 12.76 (s, 1H).

2-(4-Bromophenyl)-1H-benzimidazole (7): m.p. 280-281 °C (ref³⁶ m.p. 283-284 °C, IR (KBr, cm⁻¹): 3435.87, 2928.57, 1593.98, 1446.34, 1399.20, 1270.26, 828.58. ¹H NMR ([D₆]CDCl₃, 300 MHz, δ ppm): 7.18-7.21 (m, 2H), 7.59 (m, 4H), 7.85-7.87 (d, 1H), 5.37 (s, 1H).

2-(4-Methylphenyl)-1H-benzimidazole (8): m.p. 269-273 °C (ref³⁰ m.p. 270-272 °C, IR (KBr, cm⁻¹): 3025.18, 2917.47, 1614.79, 1515.56, 1481.56, 1456.72, 821.30. ¹H NMR ([D₆]DMSO, 250 MHz, δ ppm): 2.35 (s, 3H), 7.15-7.2 (m, 2H), 7.33 (d, J=8.1, 2H), 7.46-7.56 (m, 2H), 8.07 (d, J=8.1, 2H), 12.84 (s, 1H).

2-(2-Pyridylphenyl)-1H-benzimidazole (9): m.p. 217-218 °C (ref³⁰ m.p. 218 °C, IR (KBr, cm⁻¹): 3435.97, 1603.21, 1591.82, 1441.75, 1279.38, 742.97. ¹H NMR ([D₆]DMSO, 250 MHz, δ ppm): 7.16-7.24 (m, 2H), 7.47-7.71 (m, 3H), 7.98 (dd, J₁ 7.7, J₂=1.7, 1H) 8.3-8.34 (m, 1H) 8.71 (d, J=6.9, 1H), 13.01 (s, 1H).

2-(2-Furylphenyl)-1H-benzimidazole (10): m.p. 287-288 °C (ref³⁶ m.p. 288 °C, IR (KBr, cm⁻¹): 3435.92, 3120.87, 2923.7, 1614.58, 1508.93, 1456.81, 1100.17, 1013.07, 745.66, 593.50. ¹H NMR ([D₆]DMSO, 250 MHz, δ ppm):

6.69 (dd, J₁=3.4, J₂=1.7, 1H), 7.16-7.20 (m, 4H), 7.53 (d, J=3.1, 1H), 7.56 (d, J= 3.1, 1H), 7.89 (s, 1H).

5-Nitro-2-phenyl-1H-benzimidazole (11): m.p. 206-209 °C (ref³⁴ m.p. 207-208 °C, IR (KBr, cm⁻¹): 3377.57, 1625.56, 1519.21, 1335.77, 694.57, 735.32. ¹H NMR ([D₆]DMSO, 300 MHz, δ ppm): 7.57 (m, 2H), 7.59 (m, 1H), 7.74 (d, 1H), 8.09-8.12 (m, 1H), 8.18-8.2 (m, 2H), 8.45 (s, 1H), 13.60 (s, 1H).

5-Methyl-2-phenyl-1H-benzimidazole (12): m.p. 240-242 °C (ref⁹ m.p. 242-243 °C, IR (KBr, cm⁻¹): 3412.81, 1603.91, 1453.77, 1101.52, 806.88, 698.23. ¹H NMR ([D₆]DMSO, 400 MHz, δ ppm): 2.41 (s, 3H), 6.97-7.03 (m, 1H), 7.38 (d, 2H), 7.43-7.46 (m, 2H), 7.49-7.53 (m, 2H), 8.12 (d, 1H) 12.69 (s, 1H).

2-(2,4-Dichlorophenyl)-5-methylbenzimidazole (13): m.p. 103-106 °C (ref³⁸ m.p. 104-106 °C, IR (KBr, cm⁻¹): 3444.39, 3053.83, 2912.08, 1604.95, 1594.99, 1558.56, 1234.60, 754.51, 702.52. ¹H NMR ([D₆]DMSO, 400 MHz, δ ppm): 2.42 (s, 3H), 7.05 (d, 1H), 7.40 ((s, 1H) 7.50 (d, 1H), 7.59-7.62 (m, 1H), 7.79 (d, 1H), 12.63 (s, 1H).

6-Methyl-2-(4-methylphenyl)-1H-benzimidazole (14): m.p. 100-104 °C (ref³⁹ m.p. 101-102 °C, IR (KBr, cm⁻¹): 3421.53, 2919.35, 1615.03, 1448.01, 804.87, 827.88. ¹H NMR ([D₆]CDCl₃, 250MHz, δ ppm): 2.21 (s, 3H), 2.34 (s, 3H), 6.99-7.08 (m,3H), 7.48 (s, 1H), 7.54 (d, J=1.8, 1H), 8.15 (d, J=8.1, 2H), 12.65 (s, 1H).

Results and discussion

To establish the optimum condition for this reaction, various ratios of anhydrous Fe(ClO₄)₃/SiO₂ were examined using *o*-phenylenediamine and benzaldehyde under solvent-free at room temperature in 5.0 minutes as a model reaction (Table 1). We observed that very little of the desired products were obtained in the absence of Fe(ClO₄)₃/SiO₂. The best yields were obtained with 0.15 gr (2.0 mol% of the catalyst loading) of Fe(ClO₄)₃/SiO₂. Thus the catalyst is efficient component for the synthesis of 2-substituted benzimidazoles.

Table 1. Optimization of the catalyst amount

Entry	Catalyst, g	Yield, %
1	Free	5
2	0.05	10
3	0.1	60
4	0.15	92

To evaluate the scope and limitations of this work, we focused our attempts on the synthesis of the benzimidazoles using differently substituted *o*-phenylenediamine and aldehydes. A wide variety of compounds were applied under optimal reaction conditions to prepare benzimidazoles. The results are summarized in Table 2. A variety of aldehydes aromatic compounds possessing both electron-donating and electron-withdrawing groups were employed for benzimidazole formation, and in all cases, the yields were excellent (Table 2).

Table 2 Synthesis of benzimidazoles by Fe(ClO₄)₃/SiO₂ at room temperature.

Entry	R ₁	R ₂	Time, min	Yield, %	M.p(°C)	
					Found	Reported
1	H	C ₆ H ₅ -	10	92	290-293	290-292 ³⁰
2	H	2-HOC ₆ H ₄ -	40	85	240-242	242 ³⁶
3	H	2-ClC ₆ H ₄ -	40	90	232-235	233-234 ³⁰
4	H	3-MeOC ₆ H ₄ -	25	91	223-227	205-206 ³²
5	H	2,4-Cl ₂ C ₆ H ₃ -	20	90	220-223	218-219 ³⁷
6	H	4-MeOC ₆ H ₄ -	45	87	224-225	222-224 ³¹
7	H	4-BrC ₆ H ₄ -	30	92	280-281	283-284 ³⁶
8	H	4-MeC ₆ H ₄ -	60	95	269-273	270-272 ³⁰
9	H	2-pyridil	180	85	217-218	218 ³⁶
10	H	2-Furyl	120	85	287-288	288 ³⁶
11	4-Nitro	C ₆ H ₅ -	30	40	206-209	207-208 ³⁴
12	4-Me	C ₆ H ₅ -	15	87	240-242	242-24 ³⁹
13	4-Me	2,4-Cl ₂ C ₆ H ₃ -	20	95	103-106	104-106 ³⁸
14	4-Me	4Me	45	93	100-104	101-102 ³⁹

Table 3. Synthesis of 2-phenyl-1*H*-benzimidazole was catalyzed using anhydrous Fe(ClO₄)₃/SiO₂ (0.15 g)/air in the presence of benzaldehyde and *o*-phenylene diamine.

Entry	Catalyst	Conditions	Time, min	Yield, %	Ref.
1	Fe(NO ₃) ₃ ·9H ₂ O (10 mol%)/ H ₂ O ₂ (0.4 ml)	Solvent-free/50°C	2.0	98	27
2	FeBr ₃ (5.0 mol %)	DMF/60 °C	25	88	28
3	Fe(NO ₃) ₃ ·9H ₂ O(10 mol%)	DMF/60 °C	25	85	28
4 ^a	FeCl ₃ /PANI	EtOH/r.t.	30	90	29
5 ^b	T(<i>o</i> -Cl)PPFe ^{III} Cl (5.0 mol%)	EtOH/r.t.	30	97	30
6 ^b	T(<i>o</i> -Cl)PPFe ^{III} -SiO ₂ (5.0 mol%)	EtOH/r.t.	90	95	30
7	Fe(ClO ₄) ₃ /SiO ₂ (2.0 mol %)	Solvent free/r.t	10	92	This work

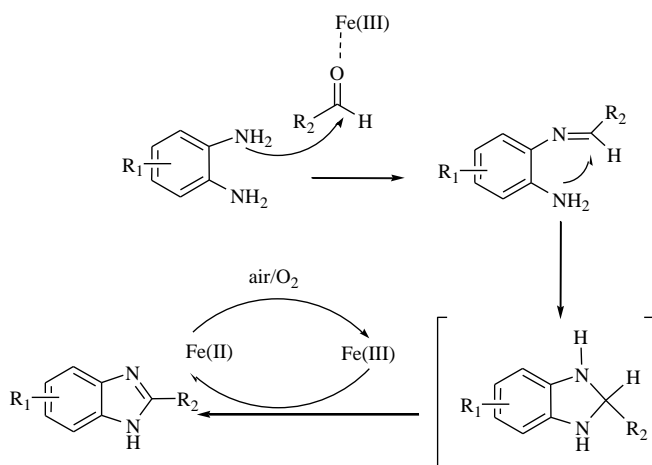
a) FeCl₃ /PANI = FeCl₃-doped polyaniline; b) T(*o*-Cl)PPFe^{III}Cl= *meso*-tetrakis(*o*-chlorophenyl)porphyrin-Fe^{III}Cl

To show the merits of this catalytic method in comparison with those of reported protocols, we compiled the results of the formation of 2-phenyl-1*H*- benzimidazoles in the presence of a variety of catalysts, especially iron (III) salts and complexes. From the results given in [Table 3](#), the advantages of our method are evident, regarding the catalyst amounts which are very important in chemical industry especially when it is combined with easy separation.

The proposed mechanism for Fe(III)-catalyzed synthesis of 2-substituted benzimidazoles may be visualized to occur via a sequence of reactions as depicted in Scheme 2.

Table 3 Reusability of the catalyst was survived for the model reaction(entry 1, Table 2).

Entry	Runs	Yield, %
1	First	92
2	2th	90
3	3th	90
4	4th	85

**Scheme 2.** Mechanism of the 2-substituted benzimidazoles formation

Conclusion

In conclusion, Fe(ClO₄)₃/SiO₂ has been employed as a novel and efficient catalyst for the synthesis of benzimidazoles in good yields from *o*-phenylenediamine and a wide variety of aldehydes. All the reactions were carried out at room temperature, while using Fe(ClO₄)₃/SiO₂. The reaction conditions were very mild, and the isolation of products was very easy and the catalyst was reusable.

References

- ¹Craig, W. A., Lesueur, B. W., Skibo, E. B., *J. Med. Chem.*, **1999**, *42*, 3324
- ²Gudmundsson, K. S., Tidwell, J., Lipka, N., Koszalka, G. W., Van Dranen, N., Ptak, R. G., Drach, J. C., Townsend, L. B., *J. Med. Chem.*, **2000**, *43*, 2464.
- ³Czarny, A., Wilson, W. D., Boykin, D. W., *J. Heterocycl. Chem.*, **1996**, *33*, 1393.
- ⁴Tidwell, R. R., Geratz, J. D., Dann, O., Volz, G., Zeh, D., Loewe, H., *J. Med. Chem.*, **1978**, *21*, 613.
- ⁵Fairley, T. A., Tidwell, R. R., Donkor, I., Naiman, N. A., Ohemeng, K. A., Lombardy, R. J., Bentley, J. A., Cory, M., *J. Med. Chem.*, **1993**, *36*, 1746.
- ⁶Foks, H., Pancechowska-Ksepko, D., Kuzmierkiewicz, W., Zwolska, Z., Augustynowicz-Kopec, E., Janowiec, M., *Chem. Heterocycl. Compd.*, **2006**, *42*, 611.
- ⁷Tagawa, Y., Yamagata, K., Sumoto, K., *Heterocycles*, **2008**, *75*, 415.
- ⁸Bahrami, K., Khodaei, M. M., Kavianinia, I., *Synthesis*, **2007**, 547.
- ⁹Du, L. H., Wang, Y. G., *Synthesis*, **2007**, 675
- ¹⁰Das, B., Holla, H., Srinivas, Y., *Tetrahedron Lett.*, **2007**, *48*, 61
- ¹¹Varala, R., Nasreen, A., Enugala, R., Adapa, S. R., *Tetrahedron Lett.*, **2007**, *48*, 69.
- ¹²Ma, H., Wang, Y., Li, J., Wang, J., *Heterocycles*, **2007**, *71*, 135.
- ¹³Nagawade, R. R. Shinde, D. B., *Indian J. Chem.*, **2007**, *46B*, 349.
- ¹⁴Ramachary, D. B., Reddy, G. B., *Org. Biomol. Chem.*, **2006**, *4*, 4463.
- ¹⁵Ma, H., Wang, Y., Wang, J., *Heterocycles*, **2006**, *68*, 1669.
- ¹⁶Lin, S., Yang, L., *Tetrahedron Lett.*, **2005**, *46*, 4315.
- ¹⁷Curini, M., Epifano, F., Montanari, F., Rosati, O., Taccone, S., *Synlett*, **2004**, 1832.
- ¹⁸Itoh, T., Nagata, K., Ishikawa, H., Ohsawa, A., *Heterocycles*, **2004**, *63*, 2769
- ¹⁹Nagata, K., Itoh, T., Ishikawa, H., Ohsawa, A., *Heterocycles*, **2003**, *61*, 93.
- ²⁰Beaulieu, P. L., Hache, B., Von Moos, E., *Synthesis*, **2003**, 1683
- ²¹Heravi, M. M. and Behbahani, F. K., *J. Iran. Chem. Soc.*, **2007**, *4*, 375-392.
- ²²Parmar, A., Kumar, H., *Synth. Commun.* **2007**, *37*, 2301-2308.
- ²³Fujiwara, M., Kawatsura, M., Hayase, S., Nanjo, M., Itoh, T., *Adv. Synth. Catal.* **2009**, *351*, 123-128.
- ²⁴Behbahani, F. K., Farahani, M., Oskooie, H. A., *Korean J. Chem. Soc.*, **2011**, *55*, 1.
- ²⁵Behbahani, F. K., Farahani, M. *Lett. Org. Chem.*, **2011**, *81*, 436 (2011).
- ²⁶Behbahani, F. K., Ziaei, P., Fakhroueian, Z. Doragi, N., *Monatsh. Chem.*, **2011**, *142*, 901.
- ²⁷Bahrami, K., Khodaei, M. M., Naalia, F., *Synlett*, 2009, 569.
- ²⁸Ma, H., Han, X., Wang, Y., Wang, J., *Heterocycles*, **2007**, *71*, 1821.
- ²⁹Abdollahi-Alibeik, M., Moosavifard, M., *Synth. Commun.*, **2010**, *40*, 2686.
- ³⁰Sharghi, H., Beyzavi, M. H., Doroodmand, M. M., *Eur. J. Org. Chem.*, **2008**, 4126.
- ³¹Farahnaz K., Behbahani, F. K., Parisa Ziaei, *Chemistry of Heterocyclic Compounds*, **2012**, inpress.
- ³²Gadekar, L. S., Arbad, B. R., Lande, M. K., *Chin. Chem. Lett.*, **2010**, *21*, 1053.
- ³³Das Sharma, S., Konwar, D. *Synth. Commun.*, **2009**, *39*, 980.
- ³⁴Raju, B. C., Theja, N. D., Kumar, J. A., *Synth. Commun.*, **2009**, *39*, 175.
- ³⁵Du, L. H. Wang, Y. G., *Synthesis*, **2007**, 675.
- ³⁶Abdelkrim, B. A., *Tetrahedron Lett.*, **2003**, *44*, 5935.
- ³⁷Heravi, M. M., Tajbakhsh, M. M., Ahmadi, A. N., Mohajerani, B., *Monatsh. Chem.* **2006**, *137*, 175-179.
- ³⁸Rao, N. V. S. *Proc. Ind. Acad. Sci., Sect. A*, **1957**, *45A*, 253-259.
- ³⁹Mobinikhaledi, A., Zendehtdel, A., Hasanvand, M., Jamshidi, F., *Synth. React. Inorg. Met.-Org. Chem.*, 2007, *37*, 175.

Received: 07.04.2013.

Accepted: 05.05.2013.